

The Role of Mitochondrial Survivin in Phospholipid Biosynthesis

Thesis submitted to the University of Nottingham for the Degree of Doctor of Philosophy

Lucia Dunajova, BSc

July, 2016

ABSTRACT

Survivin is an essential protein that is highly overexpressed in most human cancers and is known to be involved in many cellular processes by virtue of its different locations and interacting partners in the cell. At mitosis it is part of the chromosomal passenger complex, which ensures correct temporal and spatial regulation of chromosome movements and cytokinesis. Survivin also acts in apoptosis suppression via distinct mechanisms many of which have been ascribed to the mitochondrial pool of survivin. However, it is still unclear precisely how survivin gains access to this organelle, its other possible functions while there and its effect on mitochondrial morphology. Though mitochondria play an essential role in apoptosis induction and execution, they also provide phospholipids for incorporation into membranes. Of particular interest to this study, they synthesise phosphatidylethanolamine (PE), by decarboxylation of phosphatidylserine, which is catalysed by phosphatidylserine decarboxylase (PSD). The purpose of this thesis was to test the hypothesis that mitochondrial survivin regulates PSD-mediated conversion of PS to PE in the mitochondria. This thesis shows PSD is a novel partner of survivin which interacts with it both *in vivo* and *in vitro*. The interaction was mapped to the N-terminal BIR domain of survivin. Furthermore, only mature catalytically active PSD could interact with survivin, suggesting that survivin regulates PSD activity, and thereby could regulate PE availability to the cell. In addition to discovering that survivin is a novel regulator of PSD activity, this thesis also identified a second isoform of human PSD, and discovered that the NH2 terminal ten amino acids of survivin are a non-canonical mitochondrial targeting sequence. As PE is an essential phospholipid which is required for maintenance of mitochondrial integrity, successful cytokinesis and lipidation of autophagosomes during autophagy, the identification of mitochondrial survivin as a regulator of PSD activity can be expected to have a significant impact on cellular health. Therefore, this thesis identified a completely novel mechanism by which mitochondrial survivin could be further fuelling tumorigenesis *in vivo*.

Keywords: survivin, mitochondria, phosphatidylserine decarboxylase (PSD), phosphatidylethanolamine (PE)

ACKNOWLEDGMENTS

I would like to thank my supervisor Dr Sally P. Wheatley for her help and support throughout this project, particularly during the very stressful submission time. I have really appreciated her approachability and I hope her positive attitude will stay with me. I would also like to thank the past members of our laboratory, Jamie Webster and Aysha Aljaberi, and also current members Sophie Rochette and Nicola Humphry who have never hesitated to assist me. I also feel indebted to the members of the Life Sciences department: academic, research staff and postgraduate students alike for assistance during this project. In particular, I would like to highlight Dr Boyan Bonev who has granted me free access to his laboratory equipment and Dr Andy Bennett and his PhD student Richard Maclennan who have provided me with human hepatocytes. I am grateful to all my friends, in particular Veronika Majcher, Simon Cass, Andrea Loreto, Carolyn Palmer, Nicola Portolano and Matt Hardcastle, and also my family who have supported me throughout this period and without whom I would not have been able to complete this thesis. Finally, I thank BBSRC for funding this project.

ABSTRACT ..... **II**

ACKNOWLEDGMENTS ..... **III**

1 INTRODUCTION **1**

1.1 OVERVIEW 1
1.2 CELL DIVISION 1
1.2.1 The cell cycle *1*
1.2.2 Regulation of the cell cycle *5*
1.2.3 Chromosomal passenger complex (CPC) *6*
1.3 PROGRAMMED CELL DEATH 11
1.3.1 Apoptosis *11*
1.3.2 Autophagy *18*
1.3.3 Additional modes of PCD *20*
1.4 SURVIVIN 21
1.4.1 Transcriptional regulation *22*
1.4.2 Structure *23*
1.4.3 Localization *24*
1.4.4 The different roles of survivin *25*
1.4.5 Post-translational regulation of survivin *29*
1.5 PHOSPHOLIPID SYNTHESIS 33
1.5.1 Phospholipid synthesis pathways *35*
1.5.2 The physiological roles of PS and PE in mammalian cells *39*
1.6 HYPOTHESIS AND AIMS 43

2 MATERIALS AND METHODS **44**

2.1 MOLECULAR BIOLOGY TECHNIQUES 44
2.1.1 Preparation of E. coli competent cells *44*
2.1.2 Transformation of E. coli with plasmid DNA *44*
2.1.3 Purification of plasmid DNA *44*
2.1.4 Polymerase Chain Reaction (PCR) *45*
2.1.5 Site directed mutagenesis *45*
2.1.6 DNA agarose gel electrophoresis *46*
2.1.7 PCR purification *46*
2.1.8 Restriction digestions of DNA *46*
2.1.9 Phosphatase treatment of vector DNA *46*
2.1.10 Ligations *47*
2.1.11 RNA extraction and cDNA synthesis *47*
2.1.12 Reverse transcription polymerase chain reaction (RT-PCR) *47*
CLONING STRATEGIES FOR INDIVIDUAL PLASMID CONSTRUCTS 48
Cloning of mitochondrially targeted survivin constructs *48*
Cloning of FLAG-tagged survivin expression constructs *48*
Cloning of His-tagged survivin expression construct *49*
Cloning of Phosphatidylserine decarboxylase (PSD) expression constructs *49*
Cloning of inactive PSD with the point mutation S378A *49*
Epitope tagging of PSD (FLAG and 8xHis) *49*
2.2 MAMMALIAN CELL CULTURE TECHNIQUES 50
2.2.1 Cell culture *50*
2.2.2 Cell transfections *50*
2.2.3 Cell counting *51*

2.2.4 Preparation of whole cell extracts *51*
2.2.5 Cell treatments *52*
2.3 BIOCHEMICAL ASSAYS 53
2.3.1 Subcellular fractionation *53*
2.3.2 Discontinuous sucrose density gradient *54*
2.3.3 Experiments with isolated mitochondria *55*
2.4 SDS POLYACRYLAMIDE GEL ELECTROPHORESIS (SDS-PAGE) AND IMMUNOBLOTTING 56
2.4.1 SDS-PAGE *56*
2.4.2 Immunoblotting *56*
2.5 PROTEIN PURIFICATION 58
2.5.1 Bacterial protein overexpression *58*
2.5.2 Mammalian protein overexpression/His purification *59*
2.6 BINDING STUDIES 59
2.6.1 Co-immunoprecipitations *59*
2.6.2 Glutathione S-Transferase Pull-down Assays *60*
2.7 LIPID TECHNIQUES 61
2.7.1 PSD conversion assay and lipid extraction *61*
2.7.2 Lipid extraction from cells *61*
2.7.3 Thin layer chromatography (TLC) *62*
2.7.4 Lipid quantitation *62*
2.8 IMAGING TECHNIQUES 63
2.8.1 Live cell fluorescence imaging *63*
2.8.2 Fixed cell fluorescence imaging *63*
2.8.3 Electron microscopy *64*

3 MITOCHONDRIAL TARGETING OF SURVIVIN 65

3.1 PROTEIN IMPORT INTO MITOCHONDRIA 65
3.2 MITOCHONDRIAL TARGETING SEQUENCES 67
3.3 MITOCHONDRIAL LOCALIZATION OF PSD AND SURVIVIN 70
3.4 RESULTS 71
3.4.1 Mitochondrial survivin at different stages of cell cycle *71*
3.4.2 Mitochondrial survivin in normal versus cancer cells *73*
3.4.3 Computational analysis of PSD and survivin subcellular distribution *74*
3.4.4 Subcellular localization of ectopically expressed Survivin and PSD in HeLa cells *77*
3.4.5 Mitochondrial import of survivin and PSD *78*
3.4.6 Submitochondrial localization of survivin and PSD *82*
3.4.7 Overexpression of survivin does not affect mitochondrial morphology *85*
3.5 DISCUSSION 87
3.5.1 Circumstances of survivin mitochondrial localization *88*
3.5.2 Mitochondrial import of survivin *89*
3.5.3 Effect of ectopic survivin expression at the level of mitochondria in different cell types *91*

4 DOES SURVIVIN HAVE A ROLE IN AMINOPHOSPHOLIPID SYNTHESIS? 93

4.1 MITOCHONDRIAL SURVIVIN IN CYTOPROTECTION 93
4.2 AMINOPHOSPHOLIPID SYNTHESIS IN THE MITOCHONDRIA 94
4.3 RESULTS 96
4.3.1 Survivin interacts with PSD in vivo and in vitro *96*
4.3.2 Probing for functional significance of survivin – PSD interaction *100*
4.3.3 Assessment of cell behaviour after Survivin and PSD depletion *110*

4.4 DISCUSSION 118
4.4.1 Survivin interacts with PSD in vitro and in vivo 118
4.4.2 Recombinant expression systems for PSD 119
4.4.3 Assay systems for measurement of PSD activity 120
4.4.4 Effect of Survivin and PSD silencing on cell growth 121
4.4.5 Mitochondrial morphology in PSD silenced cells 122
4.4.6 Survivin as PE regulator in autophagy and mitochondrial bioenergetics 123

5 INVESTIGATION OF A PUTATIVE PSD SPLICE VARIANT 126

5.1 TYPES OF PSD 126
5.2 RESULTS 130
5.2.1 Analysis of the putative PSD isoform 2 130
5.2.2 Transcriptional expression of PSD isoform 1 and putative isoform 2 in different tumour cell lines 132
5.2.3 Generation of a PSD isoform 2 specific antibody 133
5.2.4 Ectopically expressed PSD isoform 2 localizes in the mitochondria 136
5.2.5 PSD isoform 2 binds directly to survivin in vitro 137
5.3 DISCUSSION 137

6 FINAL CONCLUSIONS AND OUTLOOK 141

7 REFERENCES 144

8 APPENDIX 173

ABBREVIATIONS 177

1 INTRODUCTION

1.1 OVERVIEW

Since its discovery in 1997 (Ambrosini et al.), survivin has emerged as a key regulator of cell division with additional anti-apoptotic activities. Both these processes need to be tightly regulated to ensure the health of the organism. Indeed, unlimited replicative potential coupled with successful evasion of apoptosis can contribute to oncogenic transformation of a cell. Perhaps unsurprisingly, survivin upregulation has been associated with many human cancers. However, in recent years it has become apparent that survivin might play roles in multiple others process including autophagy and mitochondrial bioenergetics. The aim of this project was to investigate yet another possible aspect of survivin function, namely its involvement in phospholipid synthesis in the mitochondria via association with the enzyme phosphatidylserine decarboxylase (PSD). Therefore, to provide adequate background, this chapter will give an overview of cell division and its regulation followed by different modes of programmed cell death, encompassing the aforementioned apoptosis and autophagy with a brief account of other modes of cell death. Next, survivin will be introduced and its function in these processes discussed with what is known to date about their regulation. Finally, the chapter will end with an overview of phospholipid synthesis pathways with particular focus on aminophospholipids as this is the possible link with survivin that is being explored.

1.2 CELL DIVISION

1.2.1 THE CELL CYCLE

The ability of cells to divide is of paramount importance for continued survival of all organisms. However, as opposed to unicellular organisms such as bacteria and yeast, which require cell division for propagation of the species, in

multicellular organisms, it underlies the development and regeneration of all the organism tissues. In order to proliferate, cells undergo a sequence of highly coordinated and regulated events known as the cell cycle, during which the genetic material, as well as other cell organelles and components, is duplicated and separated into two genetically identical daughter cells. In eukaryotes, the cycle initiates with interphase which encompasses, in temporal order, G1 (gap 1), S (synthesis) and G2 (gap 2) phases during which the cell prepares for cell division at M (mitosis) phase. At G1/S and G2/M transitions progression into the next cycle phase is halted in case of DNA damage, unsatisfactory cell preparation for division or a change in the external conditions. Such organisation allows time for repair of any errors that have arisen, particularly during DNA replication, before the cycle can proceed to cell division at M phase. However, in order to ensure the integrity of the multicellular organism, if errors cannot be resolved, programmed cell death should follow. M-phase is the culmination of the cycle when the cell undergoes major cytoskeletal rearrangements to segregate the replicated chromosomes (mitosis) and divide the cytoplasm (cytokinesis) (Figure 1-1). Following successful cell division the cell can then re-enter the cell cycle or remain in G0 phase indefinitely.

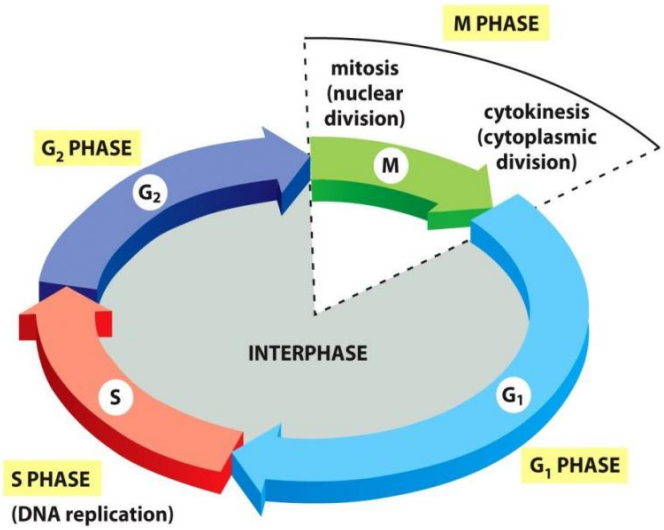


Figure 1-1. Schematic overview of the cell cycle. The cycle initiates with interphase which encompasses, in temporal order, G1 (gap 1), S (synthesis) and G2 (gap 2) phases during which the cell prepares for cell division at M (mitosis) phase. At M-phase the replicated chromosomes are segregated (mitosis) and the cytoplasm is divided (cytokinesis). (Figure adapted from Alberts et al. 2013).

M-phase is characterized by a set of distinct events which take place in six stages: prophase, prometaphase, metaphase, anaphase and telophase, collectively termed mitosis, and cytokinesis, summarized in Figure 1-2. Mitosis initiates with prophase when the duplicated chromosomes condense to form compact structures, consisting of two sister chromatids joined together via the centromere. Simultaneously, duplicated centrosomes begin to move apart to opposite poles of the cell and nucleate microtubules to assemble a bipolar mitotic spindle. Once the nuclear membrane is disassembled at prophase, the cell proceeds to the prometaphase where spindle microtubules emanating from the two centrosomes at opposite poles of the cell attach to specialized multi-protein mitotic structures, the kinetochores, which assemble on the centromeres of sister chromatids such that each sister chromatid pair can achieve a bipolar attachment. This creates tension across the spindle and forces the chromosomes to align halfway through the cell between the two poles, perpendicular to the spindle, a stage known as metaphase. Onset of anaphase follows the activation of the anaphase promoting complex/cyclosome (APC/C), a multi-subunit E3 ubiquitin ligase, which ubiquitinates and so directs the proteasomal degradation of securin, releasing the otherwise sequestered protease separase (Peters, 2006). Separase can then cleave the Scc1 subunit of cohesin, a multimeric protein complex ensuring sister chromatid cohesion (Uhlmann et al., 2000). Hence sister chromatid separation is initiated, which is aided by the shortening of spindle microtubules and the increasing separation of the spindle poles. Additionally, a contractile ring consisting of actin and myosin fibres starts to assemble at the cell equator initiating cytokinesis or cleavage of the cytoplasm. Finally with telophase, the chromosomal segregation is complete, the nuclear envelope reforms and chromosomes decondense. Concurrently, the contractile ring creates a cleavage furrow where the plasma membrane is progressively drawn inward, leaving a so-called midbody connecting the two cells which is eventually cleaved by abscission, giving rise to two separate cells.

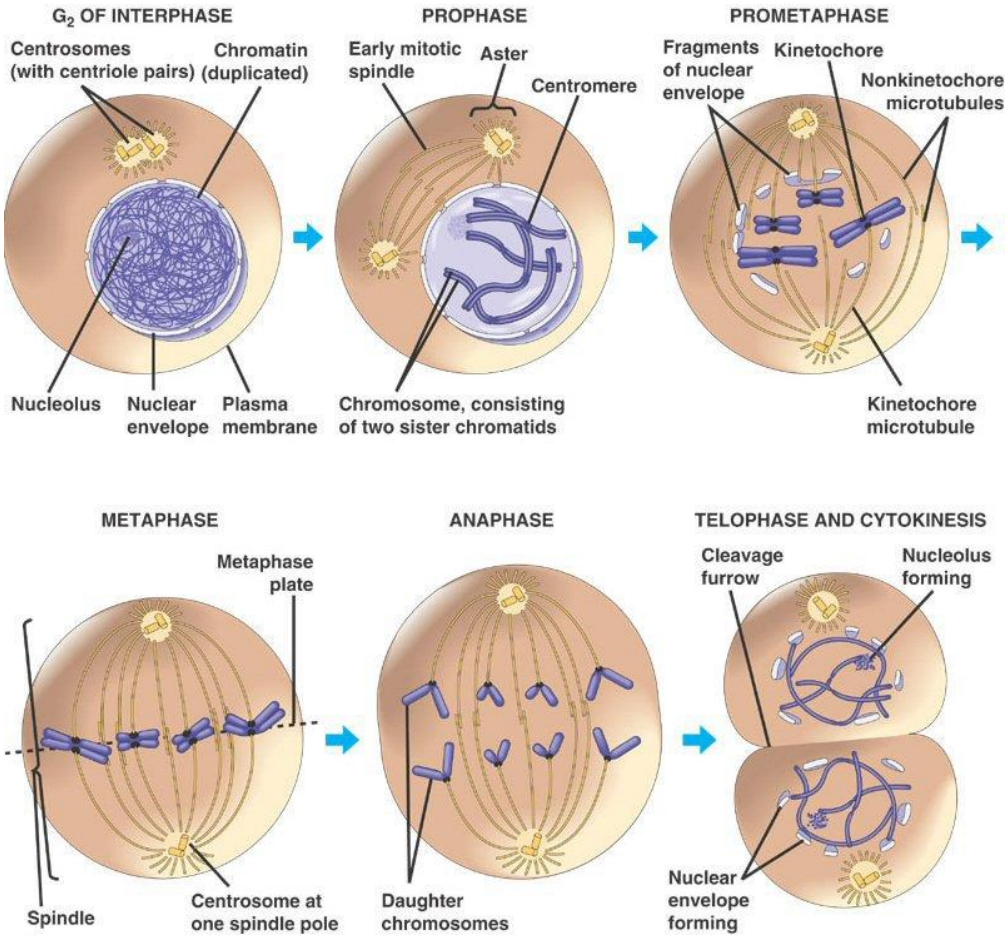


Figure 1-2. Schematic overview of mitosis. Towards the end of G2 phase the cell is ready to enter mitosis. Mitosis can be divided into distinct stages: prophase, prometaphase, metaphase, anaphase, and telophase with simultaneous cytokinesis. At prophase chromosomes condense, and centrosomes start to move to opposite poles of the cell nucleating a microtubule spindle. Next, at prometaphase the nuclear envelope breaks down and microtubules from the mitotic spindle start to attach to the kinetochores of condensed chromosomes. During metaphase, chromosomes align in the centre of the cell perpendicular to the spindle which if followed by the separation of sister chromatids at anaphase. Finally at telophase and cytokinesis, a cleavage furrow forms across the cell which pinches the cell in two accompanied by reformation of the nuclear envelope. (Figure adapted from http://dedunn.edublogs.org/2011/06/08/cell-cycle/).

1.2.2 REGULATION OF THE CELL CYCLE

As mentioned, rather than systematically proceeding through the cycle, the cell has an inbuilt checkpoint system to ensure all processes have been completed successfully before continuing. Detection systems verify the integrity of DNA and its faithful replication (DNA damage checkpoint), as well as whether all chromosomes have been properly attached to the spindle microtubules and aligned at the metaphase plate (mitotic spindle checkpoint). If problems are encountered, the cell cycle is arrested to give time for correction of encountered errors. Failure of this surveillance mechanism can directly contribute to the generation of aneuploidies due to chromosome mis-segregation as well as to the development of cancer as a result of accumulating mutations, which further highlights the importance of tight control over the cell cycle (Hanahan & Weinberg, 2011).

The task of successful separation of duplicated sister chromatids, such that both daughter cells receive the correct complement of chromosomes, strongly relies on the mitotic spindle checkpoint or spindle assembly checkpoint (SAC). At the onset of mitosis, SAC remains active and does not allow progression into anaphase until all chromosomes have attained correct bipolar orientation, generating tensile force across the mitotic spindle (Lara-Gonzalez et al., 2012). SAC is activated in response to unattached kinetochores of both sister chromatids or where only one of the chromatids has succeeded to attach (monotelic attachment). Incorrect kinetochore-microtubule attachments where both sister chromatids are attached to the same pole (syntelic attachment) or one or both of the chromatids are attached to the same pole (merotelic attachment) fail to produce sufficient tension which triggers mechanisms to destabilize and eliminate such attachments. This in turn again produces unattached kinetochores which can sustain SAC signalling and provide another chance for attaining correct bipolar attachment. SAC activation promotes the recruitment of various components including kinases Mps1, Bub1, BubR1 and non-kinases Bub3, Mad1, Mad2 and Cdc20 to the kinetochore and their assembly into complexes such as the mitotic checkpoint

complex (MCC) which together delay the onset of anaphase until all chromosomes have successfully bi-oriented at the metaphase plate (Lara-Gonzalez et al., 2012).

1.2.3 CHROMOSOMAL PASSENGER COMPLEX (CPC)

Successful cell division requires coordinated segregation of chromosomes prior to the separation of two daughter cells at cytokinesis. These events are overseen by 'chromosomal passenger proteins' (CPPs) which dynamically relocate from chromosomes at the onset of mitosis to the mitotic spindle midzone at late mitosis, and the midbody at cytokinesis. The CPPs are the highly conserved proteins Survivin, INCENP, Borealin and Aurora B kinase which together form a complex known as the 'Chromosomal Passenger Complex' (CPC) (Figure 1-3). Within this complex, Aurora-B provides the enzymatic activity, and the remaining three proteins act as regulatory and targeting modules which deliver Aurora B to its substrates and control its activity. The main roles of the CPC is to ensure correct kinetochore-microtubules attachments are formed to allow faithful chromosome segregation, activation of the SAC and timely coordination of nuclear envelope reformation and cytokinesis. Another CPP, the guanine nucleotide exchange factor TD-60, also shares the dynamic pattern of localization of the CPC members, though it does not physically associate with the complex (Mollinari et al., 2003; Gassmann et al., 2004). Nonetheless, there is strong interdependence between TD-60 and the

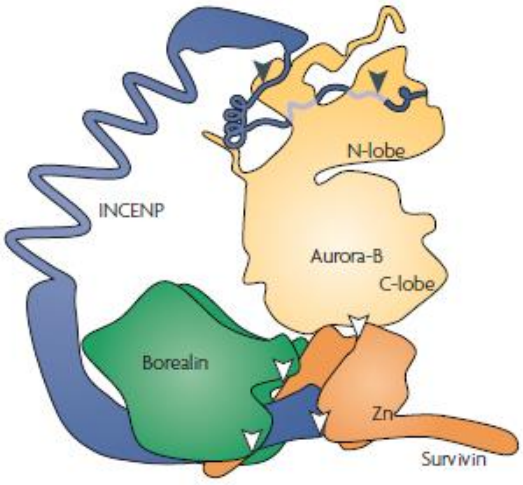


Figure 1-3. Chromosomal passenger complex. A schematic representation of the structural organization of the CPC complex. INCENP forms the core scaffold on which the remaining complex members, Survivin, Borealin and the enzymatic component Aurora B kinase assemble. (Figure adapted from Ruchaud et al., 2007)

core CPC, as knockdown of TD-60 perturbs CPC localization and affects Aurora B kinase activity and conversely, interference with the CPC causes TD-60 mislocalization (Mollinari et al., 2003; Gassmann et al., 2004; Papini et al., 2015).

Structural studies show INCENP forms the scaffold core of the CPC with its C-terminal highly conserved IN box docking Aurora B and its N-terminal α-helix (residues 1-58) stacking in parallel with the extended C-terminal α-helix of survivin and N-terminal α-helix of borealin forming a three helix bundle (Adams et al., 2000; Jeyaprakash et al., 2007). Moreover, some studies report Aurora B can also directly interact with survivin (Wheatley et al., 2001a; Bolton et al., 2002). The C-terminus of borealin and the N-terminal BIR domain of survivin remain exposed in this complex and mediate the centromere CPC localization (Jeyaprakash et al., 2007). In turn, the triple helical bundle is important for anaphase spindle midzone and telophase midbody targeting as demonstrated by mutational analysis (Jeyaprakash et al., 2007). The stability of the whole complex strongly depends on the protein-protein interactions among the individual members to the extent that perturbation of either member by depletion/knockdown or use of a dominant negative mutant causes mislocalization and also destabilizes all others (Adams et al., 2001; Carvalho et al., 2003; Gassmann et al., 2004; Honda et al., 2003). Such CPC disturbance leads to mitotic defects such as failure to correctly biorient and segregate all chromosomes or to complete cytokinesis leading to polyploidy and eventually cell death or senescence. Indeed, phenotypes observed through CPC interference together with its pattern of localization provided important clues towards its function at cell division.

Towards late S-phase, the CPC starts to decorate the pericentromeric heterochromatin via INCENP binding to heterochromatin protein 1 (HP1) (Wheatley et al., 2001b; Hayashi-Takanaka et al., 2009; Kang et al., 2011b). The CPC is then released from the chromosome arms via Aurora B mediated phosphorylation of histone 3(H3) at Ser10 (H3pS10) which disrupts HP1-chromatin association allowing it to become enriched at the inner centromeres of condensing chromosomes at prometaphase (Fischle et al., 2005). The inner centromere is “labelled” for CPC

docking through an intersection of two mitosis specific phosphorylation events on histone H3 and histone H2A recognized by survivin and borealin, respectively (Tsukahara et al., 2010; Yamagishi et al., 2010). However, the activity of both Aurora B and Mps1 is also required for successful centromere targeting but not maintenance at that site (Bekier et al., 2015). Recent evidence also found CPC dimerizes via the borealin C-terminal dimerization domain which allows for a more stable association with the centromeres than monomeric CPC (Bekier et al., 2015). Indeed, CPC comprising borealin lacking this domain exchanged on the centromeres more rapidly.

When at centromeres, the CPC directed Aurora B is essential for sensing defective tension across the spindle caused by maloriented chromosomes and subsequently, for resolving erroneous attachments to prevent chromosome missegregation (Cimini et al., 2006). Inhibition of Aurora B is accompanied by an increased number of merotelic and syntelic attachments leading to chromosome segregation failure (Hauf et al., 2003; Cimini et al., 2006). Similarly, survivin knockdown cells with diminished CPC fail to arrest mitosis in response to taxol, which causes loss of tension via microtubule stabilization (Carvalho et al., 2003). The underlying mechanism of CPC achieving chromosome biorientation is thought to entail removing incorrect kinetochore-microtubule attachments to generate unattached kinetochores which activates the SAC (Tanaka et al., 2002; Pinsky et al., 2006). The kinetochore is able to mediate dynamic microtubule attachments via distinct interacting protein components, namely the KMN network, which comprises cooperating KNL1, Mis12 complex and Ndc80 complex, and the spindle and kinetochore-associated (SKA) complex, consisting of SKA1-3 (Varma & Salmon, 2012). Aurora B directly phosphorylates Ndc80 reducing its affinity for microtubule binding and also components of the SKA complex preventing their recruitment to the kinetochore and so negatively regulating stabilization of kinetochore-microtubule attachments (Cheeseman et al., 2006; Chan et al., 2012). The proposed mode of Aurora B-dependent phosphorylation of its kinetochore substrates relies on their physical proximity when there is lack of tension across the

centromere (syntelic attachment) or defective tension such that the kinetochore Is being pulled toward the inner centromere (Cimini et al., 2006). However, once correct biorientation of the sister chromatids is achieved, the inner centromere located Aurora B becomes spatially separated from the kinetochores as they are pulled away from the centromere towards the opposing poles. This then not only reduces Aurora B-mediated phosphorylation of these substrates but also enhances their dephosphorylation by phosphatase PP1 at the kinetochore, which effectively stabilizes the bipolar microtubule attachments (Tanaka et al., 2002; Liu et al., 2009; Pinsky et al., 2009). Indeed, artificially placing Aurora B closer to the kinetochore allowed chromosome congression but failed to stabilize correctly oriented chromosomes (Liu et al., 2009). Given the number of Aurora B substrates, and the spatial and temporal importance of individual phosphorylation events, it is unsurprising its activity needs to be tightly regulated. As highlighted previously, direct inhibition of Aurora B activity or mislocalization of the CPC causes pronounced mitotic defects. Similarly, high Aurora B activity also results in defects due to persistent destabilization of kinetochore-microtubule attachments, once correct biorientation has been achieved (Munoz-Barrera & Monje-Casas, 2014). This in turns sustains SAC signalling and results in failure to complete cytokinesis even though chromosome segregation eventually takes place (Munoz-Barrera & Monje-Casas, 2014). The other CPC members modulate Aurora B activity and particularly INCENP is essential for its activation. Binding of Aurora B to INCENP provides sufficient activity for it to phosphorylate the C-terminal IN box of INCENP which further stimulates its activity leading to its autophosphorylation and full activation (Bishop & Schumacher, 2002; Yasui et al., 2004; Wang et al., 2011a). Whereas borealin does not seem to affect Aurora B kinase activity, evidence for its stimulation by survivin appears to be contentious (Bolton et al., 2002; Honda et al., 2003; Gassmann et al., 2004). Further correct CPC localization requires dynamic microtubules in concert with modulation through TD-60 (Wheatley et al., 2001b; Rosasco-Nitcher et al., 2008).

Successful chromosome alignment and segregation also requires MCAK, kinesin 13 family member with microtubule depolymerase activity. Aurora B kinase phosphorylates MCAK and in this manner directs its localization to the inner centromeres, and also negatively regulates its affinity for microtubule ends and activity (Andrews et al., 2004; Lan et al., 2004; Ems-Mcclung et al., 2013). Conversely, Aurora B mediated phosphorylation of Plk-1 enhances Plk-1 activity causing it to phosphorylate MCAK and so increase its microtubule binding affinity and depolymerase activity (Shao et al., 2015). Therefore, the two kinases act in concert to remove aberrant kinetochore attachments via MCAK.

In addition to indirectly invoking mitotic spindle checkpoint through establishing unattached kinetochores, the CPC plays a part in directly activating SAC upon mitotic entry. Aurora B kinase activity is required for efficient recruitment of SAC components Mad1, Mad2, Bub1, BubR1, Mps1 and CENP-E to the kinetochore (Ditchfield et al., 2003; Hauf et al., 2003; Saurin et al., 2011). Indeed, pharmacological Aurora B inhibition was associated with reduced SAC functionality (Ditchfield et al., 2003; Hauf et al., 2003). Specifically, Aurora B is required for recruitment and timely activation of Mps1, which in turn mediates the recruitment of the other SAC components. Artificial tethering of Mps1 to the kinetochores could reverse the effects of Aurora B inhibition (Saurin et al., 2011).

At the metaphase-anaphase transition, following the CPC release from the centromeres, the CPC is targeted to the spindle midzone via Aurora B and INCENP binding with the mitotic kinesin Mklp2 in a mutually dependent manner, which is negatively regulated by cyclin-dependent kinase 1 (Cdk1) (Gruneberg et al., 2004; Hümmer & Mayer, 2009). The CPC relocates from the chromosomes to the cell equator, the spindle midzone, and also the cell cortex with the intention of assembling the cleavage furrow for subsequent cytokinesis (Carmena et al., 2012). The main function of the CPC at this stage becomes stabilization of the spindle midzone followed by directing the formation of the equatorial contractile ring. The site and the timing of cell constriction at the cleavage furrow is critical and needs to be coordinated with chromosome segregation and migration to the opposite poles

of the cell to prevent chromosome breakage at the cleavage plane, all processes overseen by the CPC (Carmena et al., 2012). A so called NoCut pathway can delay cytokinesis in response to segregation defects via recruitment of abcission inhibitors to the site of cleavage in Aurora B dependent manner (Norden et al., 2006).

1.3 PROGRAMMED CELL DEATH

Programmed cell death (PCD) represents a set of defined molecular pathways which actively cause cell death in response to various cytotoxic stimuli. PCD is not only required for maintenance of tissue homeostasis of multicellular organisms but it is also an essential component of normal embryonic development. Moreover, it serves as a defence mechanism against neoplastic or infected cells preventing malignant transformation and persistent infections. Since the initial characterization of PCD (Kerr et al., 1972), used synonymously with 'apoptosis', two other pathways featuring biochemical events different from those of apoptosis have now been described, known as autophagic cell death and regulated necrosis, though a degree of cross-talk between them occurs . The type of cell death inducing stimulus (e.g. DNA damage, excessive starvation, infection) and other physiological conditions determine which PCD the cell is instructed to initiate. However, tight regulation of PCD is vital to maintain the integrity of the organism as inappropriate PCD responses have been shown to contribute to the pathogenesis of various conditions such as autoimmune or neurodegenerative diseases, immunodeficiency or cancer (Danial et al., 2004). The three types of PCD will be described in greater detail in the following sections.

1.3.1 APOPTOSIS

Apoptosis is the best characterized form of PCD. The most prominent morphological features of cells undergoing apoptosis are shrinkage due to systematic breakdown of cytoskeletal components, plasma membrane blebbing,

chromatin condensation and nuclear fragmentation (Hotchkiss et al., 2009). Importantly, in multicellular organisms, apoptotic cells are rapidly cleared by phagocytes or neighbouring cells precluding any damage to the healthy surrounding tissue and minimizing the onset of inflammation.

The apoptotic demolition machinery comprises a family of cysteine aspartate proteases - caspases with a wide substrate specificity that cleaves essential cellular components and activates DNases (Danial et al., 2004). In order to prevent any collateral damage, caspases are produced in the form of largely inactive zymogens or procaspases which are held in an inactive conformation by virtue of an N-terminal prodomain. They have a large and a small subunit which are released in a series of cleavage events facilitated either by proximal active caspases or by an autocatalysis mechanism (Ramage et al., 1995; Yamin et al., 1996). Following the onset of apoptosis, initiation caspases (caspase-2, 8, 9, 10 and 12) activated in response to death inducing stimuli can facilitate the activation of downstream effector/executioner caspases (caspases – 3,6,7) and so amplify the proteolytic cascade. In initiator caspases, the prodomain is large and contains protein interaction motifs such as the death effector domain (DED) and the caspase activation and recruitment domain (CARD) which once engaged by upstream apoptosis signalling molecules trigger autocatalysis of initiator caspases (Degterev et al., 2003). In contrast, effector caspases possess only a short prodomain which is cleaved by initiator caspases (Meergans et al., 2000).

The cell can be instructed to undergo apoptotic cell death via two major pathways - the extrinsic/death receptor pathway or the intrinsic/mitochondrial pathway, converging on the activation of effector caspases (summarized in Figure 1-4). The extrinsic branch of apoptosis relies on signalling from the cell surface located death receptors belonging to the Tumour necrosis factor (TNF) receptor superfamily such as TNF receptor 1 and 2 (TNFR1 and TNFR2), Fas (CD95) or DR 4 and 5 which direct the assembly of the Death-Inducing Signalling Complex (DISC) (Ashkenazi & Dixit, 2015). Upon binding of its respective ligand (e.g. TNF-α for TNF receptors, Fas ligand for Fas) at the extracellular face of the receptor, a

conformational change causes clustering of the death domains (DD) located in its intracellular portion prompting the recruitment of specific adaptor proteins via their own homologous DDs (Itoh & Nagata, 1993; Tartaglia et al., 1993). One such protein is FADD which once mobilized by Fas signalling, recruits pro-caspase-8 through interactions of DED domains present in both proteins (Chinnaiyan et al., 1995; Muzio et al., 1996). This brings high number of pro-caspase-8 molecules in close proximity promoting their autoactivation (Muzio et al., 1996). Activated caspase-8 can then cleave and so activate effector caspases-3 and -7, committing the cell to apoptosis. On the other hand, TNFα mediated TNFR1 activation recruits TRADD (TNFR-associated death domain protein) which can then mobilize FADD, promoting apoptosis through DISC, but also additional adaptor molecules TRAF2 and RIP activating NF-κB signalling which can counteract apoptosis (Hsu et al., 1996b, 1996a).

The intrinsic pathway is triggered by a variety of stress signals such as DNA damage, growth factor withdrawal or xenobiotics converging at the mitochondria. This leads to the mitochondrial outer membrane permeabilization (MOMP) causing the release of cytochrome c and other pro-apoptotic proteins such as Smac/DIABLO, HtrA2 (also referred to as Omi) and catabolic hydrolases endonuclease G and apoptosis-inducing factor (AIF) from the mitochondrial intermembrane space into the cytosol (Susin et al., 1999; Du et al., 2000; Li et al., 2001; Suzuki et al., 2001). Once in the cytosol, cytochrome c binds to Apoptotic protease activating factor 1 (Apaf-1) in the presence of ATP, triggering a conformational change that causes Apaf-1 to oligomerize into a heptamer known as the apoptosome (Li et al., 1997; Srinivasula et al., 1998). In this wheel-like structure, Apaf-1 exposed CARD domains can be readily bound by CARD domains of initiator pro-caspase-9 molecules allowing their dimerization and subsequent self-processing (Srinivasula et al., 1998). Here instead of caspase-8, activated caspase-9 can then also cleave and release active forms of effector caspases -3 and 7 which will ensure ensuing destruction of the cell. Moreover, concomitant with

cytochrome c release, mitochondria suffer overall respiratory dysfunction which contributes to cell demise (Mootha et al., 2001).

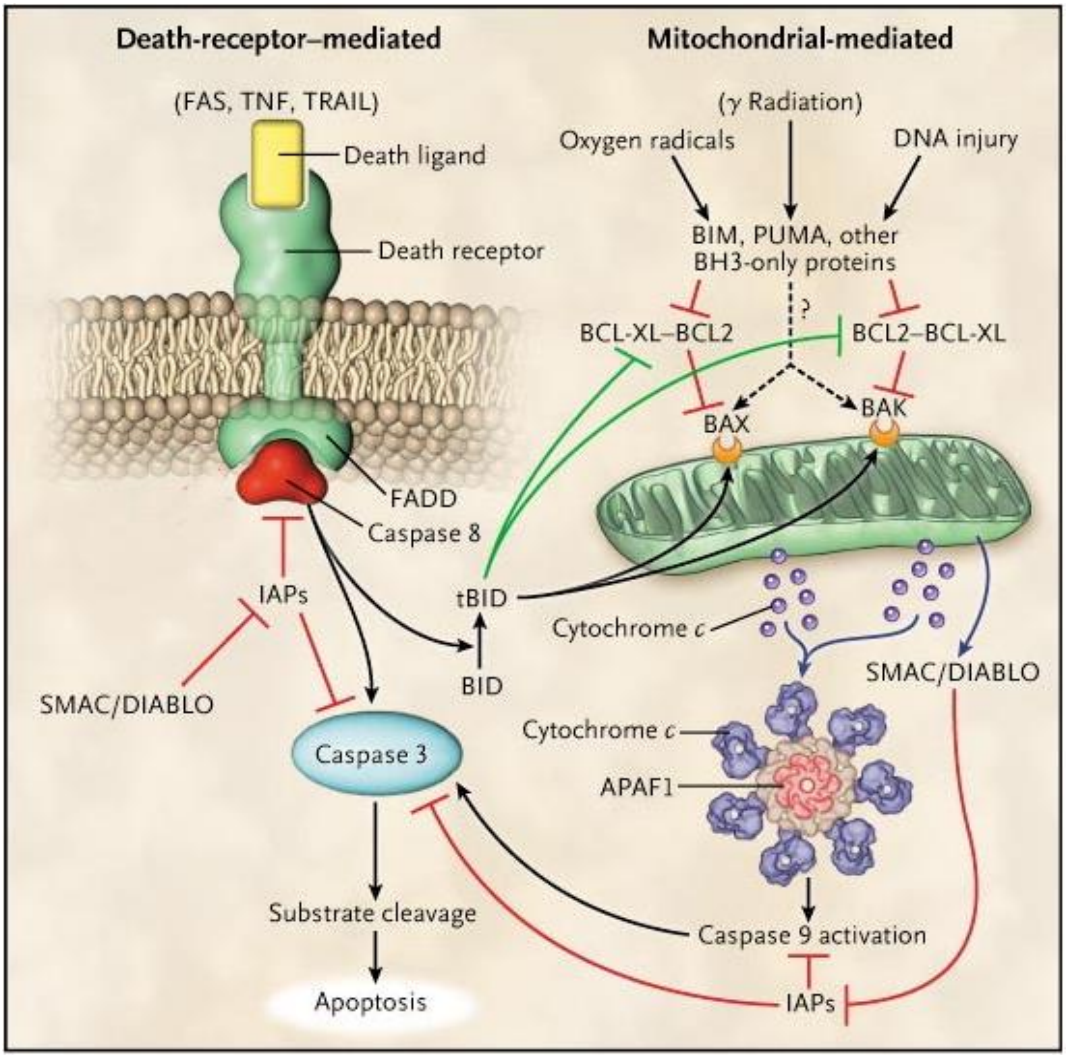


Figure 1-4. Overview of pathways for apoptosis induction and execution: death-receptor-mediated/extrinsic and mitochondria-mediated/intrinsic pathways. In the death-receptor mediated pathway ligand binding stimulates receptor oligomerization and recruitment of the adaptor protein FAS-associated death domain (FADD), which acts as a scaffold for pro-caspase 8 binding and activation. Active caspase-8 activates effector caspase-3 (and -7 – not shown). The mitochondrial-mediated pathway responds to harmful stimuli such as reactive oxygen species, irradiation or DNA damage, activating proapoptotic Bcl-2 BH3-only members which directly inhibit the anti-apoptotic Bcl-2 members. Interplay between the extrinsic and intrinsic pathway occurs at this point as active caspase-8 can cleave another BH3-only protein BID into its truncated form (tBID), capable of inhibiting the anti-apoptotic Bcl-2 proteins. This allows the pro-apoptotic Bax and Bak insert into the outer mitochondrial membrane causing its permeabilizaton and release of cytochrome c. Cytochrome c then binds to Apaf-1 in a large complex, recruiting and activating pro-caspase 9 which can also cleave and so activate effector caspases. Cytosolic Inhibitor of Apoptosis (IAP) proteins can directly inhibit caspases, however, SMAC/DIABLO released from the permeabilized mitochondria counteracts this inhibition. (Figure adapted from Hotchkiss et al., 2009)

Though the precise mechanism of MOMP remains elusive, it is known to be mediated by oligomerized Bax and Bak, members of the Bcl-2 family. Indeed, double Bax/Bak deficient cells fail to induce apoptosis in response to a range of stress signals known to initiate the mitochondrial pathway including staurosporine (kinase inhibitor), etoposide (topoisomerase II inhibitor) and ultraviolet radiation (UVC), whereas single Bax and Bak deletions have no effect on apoptosis onset (Wei et al., 2001). Bcl-2 members all share sequence similarities in a Bcl-2 homology (BH) domain and can be subdivided into three main classes based on their structural similarity and role in the apoptotic process. The anti-apoptotic Bcl-2 members contain four BH domains: Bcl-2 (first protein identified), Bcl-X_L, Mcl-1, Bcl-W and Bcl-B , similarly to the pro-apoptotic effector proteins BAX and BAK (Czabotar et al., 2014). A distinct group are the pro-apoptotic BH3-only proteins such as Bid, Bad, Bim, Noxa and Puma which only possess the BH3 domain (Czabotar et al., 2014). Whereas the pro-survival Bcl-2 proteins and pro-apoptotic effectors act at the level of mitochondria, BH3-only members act upstream of the former two groups to convey stress signals. Indeed, BH3-only protein Bid provides an important link between the extrinsic pathway and MOMP. Fas or TNFα activated caspase-8 cleaves Bid into a truncated form (tBid) which can translocate from the cytosol into the mitochondrial outer membrane where it activates Bax and Bak oligomerization and subsequent cytochrome c release, a process which can be blocked by pro-survival Bcl-2 protein overexpression (Li et al., 1998b; Luo et al., 1998; Eskes et al., 2000; Wei et al., 2000). The mitochondrial pathway of apoptosis induction is particularly important in selected cell types, “type II cells” where Fas stimulation causes only limited DISC formation, but which is sufficient to trigger MOMP and so undergo cell death efficiently via the mitochondrial pathway, which can again be inhibited by Bcl-2 (Scaffidi et al., 1998, 1999). Therefore, such cells cannot undergo apoptosis if mitochondria-mediated apoptosis is inhibited, highlighting the important role of mitochondria in the apoptotic process. This is in contrast to “type I cells” which strongly induce DISC and do not depend on MOMP for apoptosis execution. Indeed, Fas-stimulated hepatocytes from Bid-deficient mice essentially fail to induce apoptosis with none to moderate effector caspase activation and no cytochrome c

release, but respond normally to intrinsic death stimuli such as DNA damage or replicative stress (Yin et al., 1999; Kaufmann et al., 2007). Therefore, this highlights the dependence of some cells on MOMP for apoptosis induction.

Though long debated, a consensus on how the three groups of Bcl-2 family regulate apoptosis has been reached. In healthy cells, pro-survival proteins such as Bcl-2 or Mcl-1 sequester effector proteins (Bax, Bak) but also the pro-apoptotic BH3-only proteins (Bad, Bim, Bid) (Willis et al., 2005). However, upon receipt of an intrinsic stress stimulus, BH3-only proteins, many of which become transcriptionally upregulated or switched on by post-translational modification, can displace anti-apoptotic Bcl-2 members from Bax and Bak, leaving them free to oligomerize. Whereas some BH3-only proteins (Bad) can only neutralize pro-survival proteins, termed “sensitizers” or “derepressors”, others known as “activators” (Bid, Bim) can directly activate Bax and Bak once freed from pro-survival proteins, allowing them to oligomerize and induce MOMP (Kuwana et al., 2005; Certo et al., 2006).

Further control over apoptosis induction is ensured by the Inhibitor of Apoptosis Protein (IAP) family mostly localizing in the cytosol, originally described in baculoviruses where IAPs acted to suppress apoptosis of the infected host cell (Crook et al., 1993). Eight lAPs have been identified in humans: Neuronal apoptosis inhibitory protein (NAIP), cellular IAP 1 (cIAP1) and 2 (cIAP2), X-linked inhibitor of apoptosis (XIAP), Survivin, Apollon/BRUCE, Livin/ML-IAP and IAP-like protein 2 (ILP-2). Members of the IAP family characteristically feature one to three copies of a Baculovirus Inhibitor of Apoptosis Repeat (BIR) domain at their N-terminus which are essential for mediating protein interactions but also for their anti-apoptotic activity. The BIR domain consists of a ~70 amino acid segment folded into four α-helices and three-stranded β- sheet which coordinate a zinc atom in the interior via highly conserved motif comprising three cysteines and a histidine (Verdecia et al., 2000). Interestingly, in addition to the BIR domain/s, different IAPs have one or more distinct conserved domains at their C-terminus which provide them with additional functionalities and also expand IAP roles beyond apoptosis regulation (Srinivasula & Ashwell, 2008). XIAP, cIAP1, cIAP2, Livin and ILP-2 all contain a RING

domain at their C-terminus allowing them to act as an E3 ubiquitin ligase and so target others proteins for proteasomal degradation (Wang & Lin, 2013). Similarly, Apollon has an ubiquitin conjugating enzyme domain (UBC) which mediates ubiquitination of BIR-bound Smac, discussed later, and caspase-9 (Hao et al., 2004). NAIP has a nucleotide-binding and oligomerization domain (NOD) and a carboxyl-terminal leucine-rich repeat (LRR) domain which mediate its assembly into a tetramer, that undergoes a conformational change upon ATP binding allowing BIR3-dependent caspase-9 binding and inhibition (Davoodi et al., 2004). Moreover, cIAP1 and cIAP2 also contain a CARD domain important for protein-protein interactions (Choi et al., 2014).

In addition to the aforementioned modes of apoptosis inhibition, at least some IAPs suppress apoptosis by inhibiting caspase substrate cleavage. Indeed, XIAP, c-IAP-1 and 2 have been shown to directly bind to and prevent pro-caspase 9 activation and in this manner block the proteolytic processing of pro-caspases -3, -6 and -7 (Deveraux et al., 1998). However, they can also inhibit already active effector caspases-3 and 7 (Deveraux et al., 1997; Roy et al., 1997; Sun et al., 1999; Huang et al., 2001; Riedl et al., 2001). Whereas caspase-9 inhibition requires binding to BIR3 domain, the linker region between BIR1 and BIR2 together with BIR2 domain itself are necessary for binding to caspase-3 and 7 (Huang et al., 2001; Riedl et al., 2001; Shiozaki et al., 2003). Though the survivin BIR domain most resembles the BIR2 domain of XIAP, it lacks the necessary linker region shown to be required for XIAP-mediated caspase-3 and 7 targeting. Nonetheless, its potential to directly inhibit caspases has been long debated, with evidence both in favour (Tamm et al., 1998; Conway et al., 2000; Shin et al., 2001) and against (Banks et al., 2000; Li et al., 2008) being presented. Additional modes of survivin apoptosis control have been explored and are described in chapter 4. The anti-apoptotic activity of IAPs is counteracted by pro-apoptotic mediators released into the cytosol following MOMP such as Smac and the serine protease Omi/HtrA2 (Du et al., 2000; Suzuki et al., 2001). Whereas Smac binds to IAPs to destabilize caspase/IAP interactions and to repress the E3 ubiquitin ligase activity, Omi/HtrA2 proteolytically cleaves IAPs

such as XIAP, c-IAPs 1 and 2, directly prohibiting their anti-apoptotic activity (Huang et al., 2001; Yang et al., 2003; Creagh et al., 2004).

1.3.2 AUTOPHAGY

Autophagy (from Greek meaning 'self-eating') is a conserved mechanism of self- preservation that involves the lysosomal degradation of damaged or redundant proteins, entire organelles and even larger portions of the cytoplasm in response to stress conditions, including starvation, hypoxia and mitochondrial damage. Such breakdown of cellular components permits the recycling of the resulting macromolecules and promotes cell survival. Thus, this process is vital for cell homeostasis as it maintains continuous turnover of cellular content. Unsurprisingly, its malfunction is associated with the pathogenesis of a range of diseases including cancer, neurodegenerative and inflammatory diseases (Levine & Kroemer, 2008). Though induced as a pro-survival mechanism, excessive or prolonged periods of autophagy can also result in cell death which led to its recognition as a second type of PCD (Denton et al., 2012). Morphologically it is accompanied by large vacuoles filling the cytoplasm. However, it is disputable whether what follows is autophagic cell death *per se* or simply other modes of cell death due to overall failure of the cell life machinery caused by degradation of indispensable parts of the cell (Liu & Levine, 2014).

There are three distinct pathways of autophagy in eukaryotic cells, namely, macroautophagy, microautophagy and chaperone-mediated autophagy. Macroautophagy (hereafter referred to as autophagy) entails engulfment of parts of cytosol, including intact organelles into *de novo* formed double-membrane vesicles known as autophagosomes. These eventually fuse with lysosomes giving rise to autolysosomes where digestive enzymes complete degradation of the engulfed material. During microautophagy the formation of autophagosome is omitted with the direct budding of the lysosomal membrane enveloping the cytoplasm, whereas chaperone-mediated autophagy enables the direct transport of target proteins across the lysosomal membrane (Yang & Klionsky, 2010).

The key players involved in autophagy orchestration have been identified in yeast, and are known as the products of autophagy-related genes (Atg), with mammalian homologs identified soon after (Yang & Klionsky, 2010). However, the precise molecular mechanism of autophagosome formation is still unclear. The core molecular machinery mediating this process comprises the unc-51-like kinase 1 (ULK1) and 2 complex, Vps34 (mammalian class III phosphatidylinositol 3-kinase (PI3K)) complex, two ubiquitin-like conjugation systems Atg12 and LC3 (Atg8 in yeast) and the transmembrane proteins mAtg9 and vacuole membrane protein 1(VMP1) (Yang & Klionsky, 2010). Activation of this machinery relies on signalling from sensors of the cell growth factors and energy and nutrient status which converges on the main regulator of autophagy; mammalian-target of rapamycin complex 1 (mTORC1), a serine/threonine protein kinase. Energy depletion detected as low ATP/AMP ratio elicits AMP-activated protein kinase (AMPK) signalling which shuts down mTORC1 allowing autophagy to initiate (Gleason et al., 2007). On the other hand, the presence of growth factors stimulates the Akt (class I PI3K also known as protein kinase B (PKB)) pathway which in turn activates mTORC1, thus inhibiting autophagy (Sengupta et al., 2010).

The process of autophagosome formation begins with the initial organization of phagophore assembly sites/pre-autophagosomal structures (PAS) for which the lipid kinase vacuolar protein sorting 34 (Vps34) complex is required (Figure 1-5) (Yang & Klionsky, 2010). Amino acid starvation induces the protein kinase ULK to directly phosphorylate Beclin-1 activating the Vps34 which in turn phosphorylates phosphatidylinositol to produce phosphatidylinositol 3-phosphate (PI3P) on the nascent PAS membranes (Russell et al., 2013). The core complex includes hVps34, Beclin-1 and p150 to which additional proteins bind in specific combinations forming distinct complexes which either promote (Atg14-like protein (Atg14L or Barkor), UVRAG, Ambra1) or inhibit (Rubicon) autophagy, presumably at specific points of autophagosome formation (Fimia et al., 2007; Itakura et al., 2008; Matsunaga et al., 2009; Zhong et al., 2009). Autophagy can also be regulated by mitochondrial anti-apoptotic Bcl-2 proteins which sequester Beclin-1 preventing its

association with the Vps34 complex and so arresting autophagy which can be counteracted by pro-apoptotic BH3-only protein Bad (Maiuri et al., 2007; Pattingre et al., 2005). Next, PAS successively elongates and bends starting to envelop its cargo until it is fully sealed inside a double-membrane vesicle, the autophagosome which is promoted by the two interdigitated conjugation systems.

In the second ubiquitin-like system, LC3 undergoes cleavage by Atg4 to expose a C-terminal glycine residue (LC3-I), becomes activated by Atg7 (E1-like enzyme) and is passed on to Atg3 (E2-like enzyme) to be conjugated to phosphatidylethanolamine (PE) (LC3-II) with the aid of the Atg16L complex (E3-like enzyme) which acts as a scaffold for pinpointing the site of lipidation (Kirisako et al., 2000; Fujita et al., 2008). Such modified LC3-PE becomes associated with the phagophore membrane and possibly participates in membrane expansion, but also needs to be eventually removed prior to lysosome fusion (Geng & Klionsky, 2008). The autophagosome formation in autophagy is summarized in Figure 1-5.

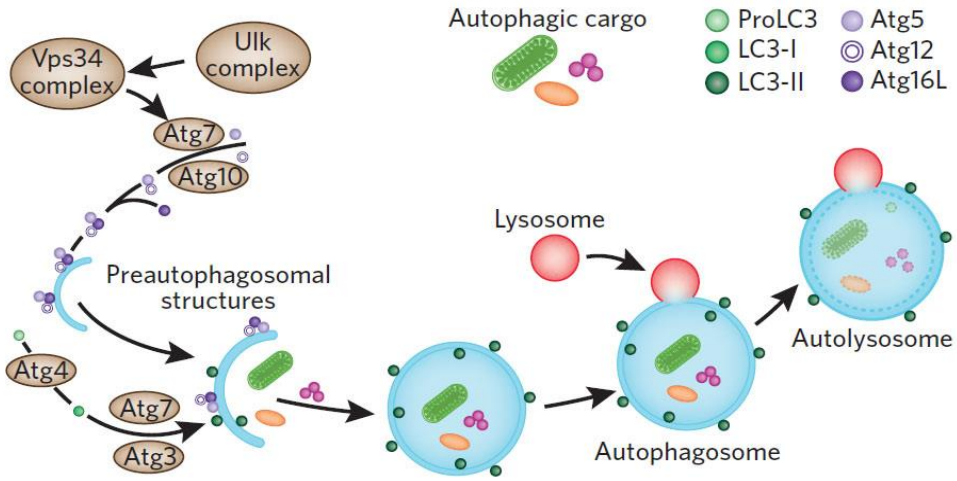


Figure 1-5. Overview of autophagy in mammalian cells. Upon stimulation of autophagy, the Ulk complex signals the initiation of autophagosome formation to the Vps34 complex. This class III phosphoinositide 3-kinase (PI3K) phosphorylates phosphatidylinositol to produce phosphatidylinositol 3-phosphate (PI3P) which is required for PAS (phagophore assembly site) initiation - a double-membrane pre-autophagosomal structure. The phagophore membrane then expands though the activity of two ubiquitin-like systems - Atg12-Atg5-Atg16L assembled via the action of Atg7 and Atg10, and the LC3 system comprising LC3 covalently modified with a PE molecule (LC3-II). Eventually the autophagosomal membrane closes, enveloping its cargo. Finally, the autophagosome fuses with a lysosome which causes the degradation of enclosed material by lysosomal hydrolases and the release of macromolecules back into the cytosol for recycling. (Figure adapted from Fleming et al., 2011).

1.3.3 ADDITIONAL MODES OF PCD

In contrast to the neat course of apoptosis or autophagy, necrotic cell death has been deemed a passive unregulated process during which the cytoplasmic organelles and the cell itself swell and due to loss of plasma membrane integrity spills all of its contents into its surroundings in response to acute cell injury, therefore potentially alerting the immune response. However, it has recently been shown also this type of death can be triggered by specific signalling pathways and so be considered "programmed". Indeed, several active necrosis pathways have been described including necroptosis, parthanatos, ferroptosis or oxytosis, mitochondrial permeability transition (MPT)-dependent necrosis, pyroptosis and pyronecrosis, each with distinct regulatory and effector factors mediating the process (Pasparakis & Vandenabeele, 2015). These processes also play important roles during development, adult tissue homeostasis and in disease pathogenesis and occur in caspase-independent fashion (Pasparakis & Vandenabeele, 2015). For example, necroptosis can be induced by some of the same stimuli which induce apoptosis such as TNF-α dependent TNFR1 activation, activation of other death receptors by their respective ligands (e.g. FasL to Fas, TRAIL to TRAILR1/DR4) and cellular stress, damage and infection sensed by a variety of receptors including Toll-like receptors, under conditions when apoptotic cell death has been prevented (Pasparakis & Vandenabeele, 2015).

1.4 SURVIVIN

Survivin is indispensable for cell survival; homozygous deletion of survivin in mice manifests with embryonic lethality at day 4.5 post coitum (Uren et al., 2000). Survivin expression is cell cycle-regulated with peaking protein levels at G2 and M phase (Li et al., 1998a). Therefore, its detection in tissues is limited to cells dividing at a high rate, characteristic of developing embryo and malignant tumours, with virtually no expression seen in adult normal differentiated tissues which has inspired novel anti-cancer therapies targeting survivin (Ambrosini et al., 1997).

Regulation occurs on transcriptional (negative regulation by p53) but also posttranslational level whereby survivin is ubiquitinated, phosphorylated and acetylated, which will be discussed below.

The human survivin gene additionally allows the generation of four alternatively spliced isoforms: Survivin-2α, Survivin-2B, Survivin-3B and Survivin-ΔEx3 each with distinct localization and characteristics. Survivin-2α (74 amino acids) and Survivin-3B (120 amino acids) both result from incorporation of an intron which introduces a premature stop codon yielding truncated protein products (Badran et al., 2004; Caldas et al., 2005). Survivin-2B (165 amino acids) results from retaining part of intron 2 as a cryptic exon termed exon 2B (Mahotka et al., 1999). Though this does not cause a frameshift, 23 amino acids are introduced within the BIR domain which is predicted to cause some structural changes of the domain and so affect its anti-apoptotic activity. The same rings true for the Survivin-ΔEx3 isoform (137 amino acids), which lacks exon 3 and so also suffers truncation of its BIR domain at the same position as 2B followed by a frameshift giving rise to a unique 63 amino acid C-terminal tail with no homology to wild type survivin (Mahotka et al., 1999). Therefore, obvious structural differences of the four isoforms as compared to the wild type survivin mean their functional properties might differ as well.

1.4.1 TRANSCRIPTIONAL REGULATION

The human survivin gene, also known as birc5, comprises 4 exons interspaced by 3 introns on chromosome 17q25 (Ambrosini et al., 1997). The promoter of the gene contains a CpG island and several Sp1 sites but lacks a TATA box. Additionally, there are three Cell-cycle Dependent Elements (CDE) and one Cell-cycle gene Homology Region (CHR) sequence which are responsible for the periodical cell-cycle dependent increase of survivin expression at G2/M (Li et al., 1998a). Over the years increasing numbers of different transcription factors interacting with specific regions of survivin promoter have surfaced which can either upregulate or repress survivin expression. For instance, survivin is induced

by NFκB, GATA-1 but also phosphorylated STAT-3 (Boidot et al., 2014). Moreover, the promoter also has two E2F binding sites which upon E2F1, E2F2, and E2F3 transcriptional activators binding induces survivin expression (Jiang et al., 2004). Given the tumour-promoting potential of survivin, its expression needs to be also negatively regulated, a feat achieved by the master tumour-suppressor p53 (Hoffman et al., 2002). Since the p53 binding site in survivin promoter overlaps with E2F binding site, it was reported that p53 could be repressing the survivin gene in part by preventing E2F-mediated survivin transactivation via directly interacting with the promoter binding site or by recruitment of Sin-3 (a corepressor factor) and histone deacetylases (HDACs) to the promoter (Hoffman et al., 2002).

1.4.2 STRUCTURE

Survivin is a small 16.5 kDa protein comprising 142 residues, which forms a bow tie-shaped homodimer in solution (Verdecia et al., 2000). The N-terminus comprises a globular zinc finger domain (M1-S88), structurally akin to the BIR domain of the IAP family, and is connected via a short linker (V89-T97) to a long extended α-helix at the C-terminus (L98-D142) which can be seen in crystal structure of survivin in Figure 1-6 (Chantalat et al., 2000; Muchmore et al., 2000; Verdecia et al., 2000). The C-terminus is required for protein-protein interactions. Superimposition of survivin and XIAP structures revealed the BIR domain of survivin was in highest agreement with the BIR2 domain of XIAP (Muchmore et al., 2000; Verdecia et al., 2000). The zinc atom within the BIR domain is coordinated by highly conserved residues C57, C60, H77 and C84 which are essential for the overall stability of the domain (Chantalat et al., 2000). The dimerization of survivin occurs predominantly via hydrophobic interactions and involves the N-terminal residues L6-W10 and a longer stretch encompassing the linker region and the very beginning of the C-terminal α-helix, V89-L102 (Verdecia et al., 2000). Survivin exists in either monomeric or dimeric form in cells which has important functional implications that will be discussed below. Furthermore, as shown in Figure 1-6, survivin has a nuclear export sequence (NES) at its dimerization interface. Also highlighted in

Figure 1-6 are the residues at which survivin is post-translationally modified and will be discussed below in greater detail.

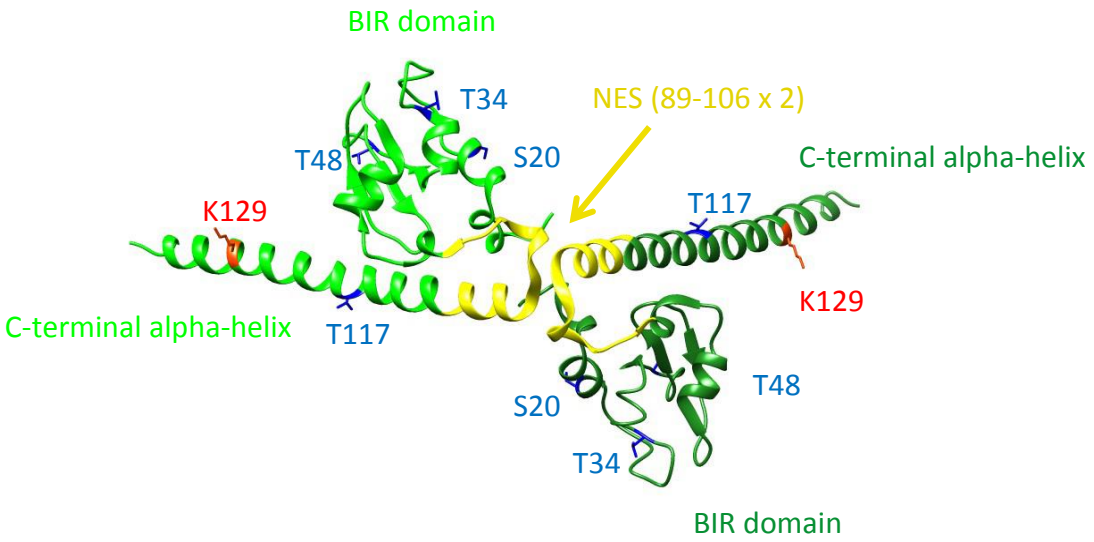


Figure 1-6. Crystal structure of the survivin dimer. The two survivin monomers are in light green and dark green, each with their respective N-terminal BIR domain and C-terminal α-helix. Residues S20, T34, T48 and T117 which are subject to phosphorylation are highlighted in blue, while the acetylation site K129 is shown in red. The nuclear export sequence (NES) is shown in yellow. Model constructed from structure 1F3H using the UCSF Chimera package (http://www.cgl.ucsf.edu/chimera).

1.4.3 LOCALIZATION

At mitosis, survivin behaves as a chromosomal passenger, localizing at centromeres of condensed chromosomes at prometaphase and metaphase, spindle midzone at anaphase until being eventually discarded in the midbody in late telophase (Skoufias et al., 2000; Uren et al., 2000; Wheatley et al., 2001a) as can be seen in Figure 1-7. Though endogenous survivin is absent from cells at interphase, when overexpressed it can be seen in the cytoplasm, with limited levels also in the nucleus (Skoufias et al., 2000; Wheatley et al., 2001a; Colnaghi et al., 2006). Such cytoplasmic distribution is achieved by an active nuclear export via the CRM1-dependent pathway (Rodríguez et al., 2002; Colnaghi et al., 2006). Though initially conflicting, the nuclear export sequences (NES) mediating shuttling from the nucleus to the cytoplasm were identified within a region encompassing the central

linker (residues 84-109) and portion of the C-terminus (119-142) (Rodríguez et al., 2002; Stauber et al., 2006; Colnaghi et al., 2006; Engelsma et al., 2007). Mutation of residues L101A and L102A within the linker NES which coincidentally constitutes survivin dimerization interface, restricted survivin in its monomeric form (Engelsma et al., 2007). This significantly enhanced CRM1 binding and export from the nucleus, suggesting survivin nuclear export via this central NES is monomer dependent and so could regulated by survivin dimerization (Engelsma et al., 2007). Moreover, survivin cytoplasm-nucleus shuttling appears central to survivin anti-apoptotic activity as nuclear accumulation of survivin fails to protect against chemo- and radiotherapy-induced apoptosis (Colnaghi et al., 2006; Knauer et al., 2007). Additionally, a small pool of survivin localizes in the mitochondria and is the prime subject of this thesis (Dohi et al., 2004a).

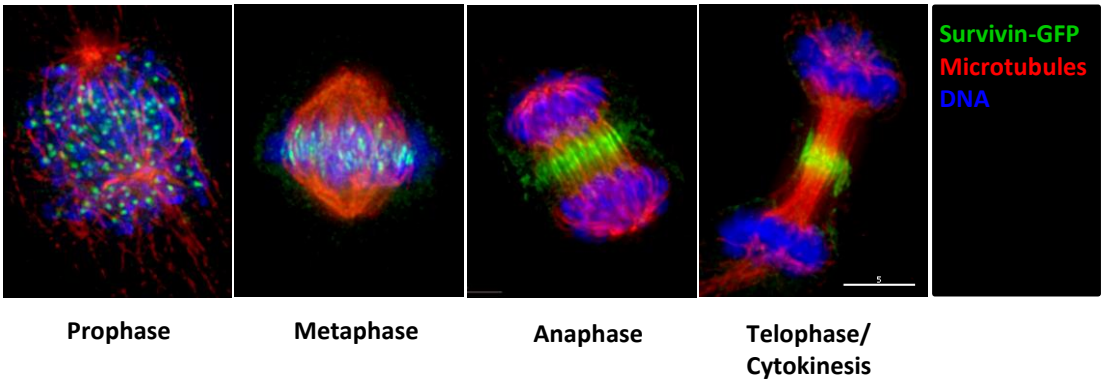


Figure 1-7. Localization of survivin at mitosis. Dynamic localization of survivin and members of the CPC at mitosis. Survivin accumulates at centromeres of condensed chromosomes at prophase and (pro)metaphase, followed by transfer to the spindle midzone at anaphase. Finally, at telophase/cytokinesis, survivin concentrates in the midbody. (Figure images courtesy of Sally P. Wheatley.)

1.4.4 The different roles of survivin

1.4.4.1 Survivin as part of the CPC

As mentioned previously, CPC localization is dynamic throughout mitosis to ensure Aurora B proximity to its substrates at the right time and at the right place. Survivin is necessary for directing the CPC members to centromeres at the onset of

prometaphase where the CPC oversees correction of faulty kinetochore-microtubule attachments. This is thought to be achieved by survivin and borealin cooperatively recognizing specific mitotic phosphorylation marks on histones within the centromeric chromatin. The cohesin-associated kinase Haspin phosphorylates histone 3 on threonine 3 (H3pT3) which can then be directly bound by the survivin BIR domain, recruiting all the other CPC members including Aurora B to the centromere (Kelly et al., 2010; Wang et al., 2010a; Yamagishi et al., 2010). Disruption of Haspin activity or introduction of survivin BIR domain mutants unable to bind to H3pT3 into cells causes mislocalization of Aurora B and delay spindle checkpoint arrest in response to taxol (Wang et al., 2010a; Yamagishi et al., 2010). The kinetochore-associated kinase Bub1 phosphorylates threonine 120 of histone H2A (H2ApT120), necessary for the recruitment of the adaptor protein Shugoshin 2 (Sgo2) to the centromere during prometaphase and metaphase which can then associate with Cdk1 phosphorylated borealin, together with the remaining CPC members (Kawashima et al., 2007, 2010; Tsukahara et al., 2010). Bub1 silencing also negatively impacts positioning of CPC members at the centromere (Yamagishi et al., 2010). Therefore, both Haspin-H3 and Bub1-H2A-Sgo2 pathways are important for targeting CPC members at the centromere.

1.4.4.2 SURVIVIN AND MICROTUBULE DYNAMICS REGULATION

In addition to CPC centromeric targeting, early studies pointed to a possible involvement of survivin in the regulation of microtubule stability and mitotic spindle assembly independently of the CPC, as it was shown to associate with the centrosomes and spindle microtubules (Li et al., 1999; Giodini et al., 2002). Indeed, Liu et al. (1999) found antisense directed degradation of survivin was accompanied by spontaneous induction of apoptosis, multinucleation and formation of multipolar mitotic spindles. Conversely, survivin overexpression repressed microtubule dynamics and centrosomal microtubule nucleation (Rosa et al., 2006). However, it is not known exactly how survivin is involved in these processes.

1.4.4.3 SURVIVIN IN APOPTOSIS

The prominent feature of survivin structure which sparked a lot of debate is the BIR domain which assigned it, through homology, to a protein family known as Inhibitor of Apoptosis Proteins (IAPs). IAP family members such as XIAP, cIAP1 and cIAP2 have been shown to directly bind to and inhibit caspases, hence preventing the onset of the programmed cell death (Deveraux et al., 1997, 1998). Though survivin is also capable of inhibiting apoptosis, its potential to directly inhibit caspases similarly to the IAP representative member XIAP has been long debated. Evidence both in favour (Tamm et al., 1998; Conway et al., 2000; Shin et al., 2001) and against (Banks et al., 2000; Li et al., 2008) direct caspase inhibition has been presented, current view suggests that survivin suppresses apoptosis via different mechanisms (Altieri, 2010). Indeed, structural studies indicate survivin lacks the linker segment N-terminal of the XIAP BIR2 domain precluding direct inhibition of caspase-3 in the manner pertaining to XIAP at least (Verdecia et al., 2000). Several alternative modes of apoptosis inhibition by survivin have been proposed whereby survivin contributes to cytoprotection via its interacting partners. Survivin forms a complex with XIAP, enhancing its stability, protecting it from proteasomal degradation and synergistically inhibiting caspase-9 following apoptosis induction (Dohi et al., 2004b). Next, survivin can also sequester Smac/DIABLO preventing it from inhibiting XIAP, which can then mediate caspase inhibition (Song et al., 2003). Moreover, following UVB treatment of melanocytes, survivin could partially block the release of AIF, Smac and cytochrome c from the mitochondria, hence conferring cytoprotection (Liu et al., 2006). Finally, caspase-9 activation and recruitment to oligomerized Apaf-1 can be inhibited by survivin when in complex with hepatitis B X-interacting protein (HBXIP) (Marusawa et al., 2003). Formation of survivin- HBXIP complex is positively regulated by Cdk1 phosphorylation of threonine 34 (Marusawa et al., 2003). Interestingly, switching between monomeric and dimeric form of survivin seems to be particularly relevant with regards to its anti-apoptotic function. Whereas association with Smac can occur irrespective of survivin being a dimer or a monomer, only monomeric form can associate with XIAP (Pavlyukov et al., 2011). Given that mitochondria mediate the intrinsic pathway of apoptosis,

survivin localizing in the mitochondria has also been specifically implicated in apoptosis suppression. Studies highlighting its effects when present in this organelle will be discussed further in chapter 4. Therefore, survivin functions in cytoprotection via multiple mechanisms, and additional ones are possibly still waiting to be addressed.

1.4.4.4 SURVIVIN IN AUTOPHAGY

Evidence for survivin involvement in autophagy is scarce and mainly comes from studies with a novel survivin suppressant YM155 aimed at tumour elimination, which induces autophagy-dependent cell death in both prostate cancer cells and adenoid cystic carcinoma cells (Wang et al., 2011b, 2014). siRNA silencing of survivin also induced autophagy recapitulating the effects of YM155 and so further suggesting that survivin is a negative regulator of autophagy (Wang et al., 2011b) However, overexpression of survivin was only able to only partially repress YM155 mediated onset of apoptosis suggesting YM155 has additional off-target effects and induces apoptosis also via another mechanism. Similarly, the survival of serum starved prostate cancer cells was enhanced by treatment with CCL2, a chemokine known to induce prostate cancer cell proliferation. Molecularly, CCL2 caused upregulation of survivin expression in a PI3K/Akt dependent manner and had an inhibitory effect on autophagy induction and autophagy-dependent cell death (Roca et al., 2008). Conversely, silencing of survivin abolished the CCL2-dependent protection from cell death. This study reported survivin association with the lipidated form of LC3 (LC3-II) suggesting a possible mechanism of survivin regulation of autophagy (Roca et al., 2008). Survivin has been also reported as an interacting partner of Beclin-1 (Niu et al., 2010). Knockdown of Beclin-1 caused downregulation of survivin sensitizing human glioma cells to TRAIL-induced apoptosis which was rescued by reexpression of survivin (Niu et al., 2010).

Interestingly, Jurkat T cells subjected to sublethal doses of DNA damaging drugs such as etoposide and cisplatin upregulated autophagy and Atg5, an essential autophagy mediator, and caused it to translocate to the nucleus (Maskey et al.,

2013). Here, Atg5 bound to nuclear survivin and triggered the appearance of cells with multipolar spindles with up to several large irregular nuclei, features characteristic of mitotic catastrophe. In this manner Atg5 outcompeted Aurora B for survivin binding, causing its mislocalization and so failure to engage as part of CPC which lead to gross mitotic defects seen. At the same time, survivin remained stably associated with the centromeres throughout mitosis and failed to transfer to the central spindle at anaphase. Interestingly, ectopic expression of wild-type or mutant K130R Atg5, unable to be conjugated to Atg12 for the purpose of LC3 lipidation and autophagosome formation, both led to the onset of mitotic catastrophe (Maskey et al., 2013). Therefore, though in this scenario autophagy induction was necessary for continued survival of drug treated cells, it was not the mechanism by which Atg5 in complex with survivin mediated mitotic catastrophe.

1.4.5 POST-TRANSLATIONAL REGULATION OF SURVIVIN

Survivin is also regulated via different post-translational modifications which fine tune its function and allow it to participate in a number of different processes. Here, the different ways survivin can be modified and their functional significance is summarized.

1.4.5.1 UBIQUITINATION

Protein ubiquitination involves reversible covalent attachment of the small protein ubiquitin to a lysine residue/s within the substrate protein (monoubiquitination), with the possibility of further ubiquitin linkages being added through one of the seven lysine residues within the previously attached substrate bound ubiquitin, forming a chain of several ubiquitin molecules linked together (polyubiquitination). Polyubiquitination through K48 and K29 linkages serves as a targeting mechanism for proteasome-dependent degradation whereas other polyubiquination linkages (e.g. K63) or monoubiquitination can alter substrate protein localization, activity or interactions with other proteins establishing

regulatory functions in DNA damage tolerance, inflammatory response or the endocytic pathway (Pickart & Fushman, 2004).

Survivin expression is highly regulated in cell-cycle dependent manner with levels rapidly falling following successful cell division and entry into G1 phase (Li et al., 1998a). Indeed, survivin is subject to proteasomal degradation via K48 linkage ubiquitination and has a half-life of about 30 minutes (Zhao et al., 2000). Fbxl7, a component of the Skp1_Cul1_F-box (SCF) ubiquitin E3 ligase, has been shown to mediate survivin polyubiquitination on survivin residues Lys90 and Lys91 (Liu et al., 2015). Additionally, survivin is also modified through polyubiquitination via the K63 linkage (Vong et al., 2005). A balance between Ufd1 mediated survivin ubiquitination and the opposing hFAM deubiquitination at mitosis was found to determine the localization and the dynamic turnover of survivin at the centromere, and that of Aurora B (and presumably the other CPC members) (Vong et al., 2005). hFAM knockdown, similarly to survivin knockdown, caused accumulation of misaligned chromosomes but only a mild increase in number of multinucleated cells suggesting such ubiquitination fine tuning is required only at (pro)metaphase and is not essential for survivin function from anaphase onwards. This was accompanied by a slightly diffuse but higher intensity staining of misaligned chromosomes with slower dissociation of survivin from the centromeres. Conversely, Ufd1 knockdown resulted in reduced centromeric survivin. Importantly, enhanced accumulation of survivin and Aurora B at centromeres led to an increase in phosphorylated MCAK, which in turn would have an effect on correction of erroneous kinetochore-microtubule attachments (Andrews et al., 2004; Lan et al., 2004). Thus, K63-linked survivin ubiquitination seems to play an important role in controlling the dynamics of survivin association with the centromeres and so the localization of the entire CPC and its ability to deal with chromosome misalignment. Previous studies also highlighted the importance of such dynamic survivin centromere localization, which was found to depend also on Aurora B kinase activity and microtubule attachment (Beardmore et al., 2004; Delacour-Larose et al., 2004, 2007).

1.4.5.2 PHOSPHORYLATION

Survivin is extensively regulated by phosphorylation events both when part of CPC, but also when in complex with other interacting partners. Cdk1 associates with survivin upon entry into mitosis and phosphorylates it at threonine 34 which has distinct effects on both its mitotic and anti-apoptotic activities, including a positive effect on its stability (O'Connor et al., 2000; Wall et al., 2003). Such phosphorylated survivin complexes with active caspase-9 preventing the onset of apoptosis at cell division (O'Connor et al., 2000). Conversely, overexpression of phosphorylation-defective survivin mutant (Thr34→Ala) or suppression of Cdk1 with broad spectrum Cdk inhibitor flavopiridol induces apoptosis, presumably due to the inability to sequester active caspase-9 (O'Connor et al., 2000; Wall et al., 2003). Transient overexpression or adenoviral transduction of the survivin (T34A) mutant was also able to suppress tumour growth *in vivo* (Grossman et al., 2001; Mesri et al., 2001). Another study with nonphosphorylatable survivin mutant (T34A) and survivin mutant mimicking phosphorylation with glutamic acid (T34E) showed opposing effects of the two mutants on the rate of cell growth and their sensitivity to either extrinsic or intrinsic apoptotic stimuli (Barrett et al., 2009; Jones et al., 2010). Therefore, phosphorylation at this residue has important implications for cytoprotection, but cannot support the mitotic function of survivin, helping to separate the two roles.

Another residue within the BIR domain, threonine 48, is the target of casein kinase 2 (CK2) (Barrett et al., 2011). Regulation of T48 phosphorylation also seems to be play a role both in mitotic and pro-survival roles of survivin, as survivin with substitution of this residue to either alanine or glutamic acid could not support cell proliferation in the absence of endogenous protein or protect against TRAIL-induced apoptosis (Barrett et al., 2011). Polo-like kinase 1 (Plk1) has been implicated in regulation of multiple processes at mitosis including mitotic entry, centrosome separation, spindle assembly checkpoint and cytokinesis (van Vugt & Medema, 2005). Plk1 phosphorylates survivin on serine 20 which does not affect its IAP activity, but seems to play an essential role in survivin involvement in mitotic

spindle checkpoint (Colnaghi & Wheatley, 2010). Mutational analysis with survivin phosphorylation defective S20A mutant showed cells could not correct wrong kinetochore-microtubules attachments yet prematurely proceeded through anaphase and cytokinesis highlighting the importance of this phosphorylation event for the proper activation of SAC and accurate chromosome alignment and segregation (Chu et al., 2011; Colnaghi & Wheatley, 2010). Indeed, phosphorylation of this residue was found to be important for maintaining Aurora B kinase activity at the centromere for accurate chromosome segregation (Chu et al., 2011). Moreover, S20 was reported to be the substrate of PKA which regulates survivin complex formation with XIAP and so its pro-survival function (Dohi et al., 2007).

Survivin is also phosphorylated at threonine 117 by Aurora-B kinase itself, the enzymatic component of the CPC, *in vitro* and *in vivo* at mitosis (Wheatley et al., 2004, 2007). Whereas phosphorylation defective survivin mutant T117A behaved similarly to the overexpressed wildtype survivin, survivin phosphomimetic T117E could not support cell proliferation in the absence of endogenous protein and caused mislocalization of Aurora B and BubR1 (Wheatley et al., 2007). However, another study reported neither of the two mutants could rescue depletion of survivin (Delacour-Larose et al., 2007). Interestingly, whereas T117A mutant stably associated with the centromeres, this was not the case for T117E mutant which was rapidly released from the centromeres (Delacour-Larose et al., 2007; Wheatley et al., 2007). Therefore, Aurora B dependent phosphorylation at this residue might be regulating the dynamics of survivin association with the centromeres.

1.4.5.3 ACETYLATION

Histone acetyltransferase CREB-binding protein (CBP) mediates acetylation of survivin at multiple lysines including lysine K129 (Wang et al., 2010b). Particularly the acetylation of K129 promotes homodimerization of survivin whereas deacetylation by histone deacetylase 6 favours its monomeric form in which survivin can interact with CRM1 and be actively exported from the nucleus (Riolo et

al., 2012; Wang et al., 2010b). As expected, K129E mutant, which cannot be acetylated, preferentially exists as a monomer and so localizes primarily in the cytoplasm where it can still efficiently inhibit apoptosis but does not support correct mitosis progression in the absence of the endogenous survivin (Aljaberi et al., 2014; Wang et al., 2010b). This is in agreement with previous report showing forced nuclear accumulation of survivin sensitized cells to X-irradiation but did not affect its function at mitosis (Colnaghi et al., 2006; Connell et al., 2008). Nuclear survivin was found to exist in survivin/STAT3 complex which was able to repress transcription of STAT3 dependent genes including BCL-X_L and MCL-1 and this was dependent on acetylation of survivin, further supporting the notion nuclear survivin sensitizes cells to death (Wang et al., 2010b).

1.5 PHOSPHOLIPID SYNTHESIS

Cell membranes are composed primarily of phospholipids, but also other lipids such as cholesterol and glycosphingolipids, in different proportions which imparts specific physicochemical properties to the membranes allowing them to modulate the function of embedded proteins (Dowhan, 1997). Phospholipids are amphipathic molecules comprising two hydrophobic hydrocarbon tails and a hydrophilic head-group which allows them to spontaneously form bilayers in aqueous environments. Specifically, the two fatty acid tails connect to a glycerol backbone which links to a phosphate group and a specific head group moiety (an alcohol e.g. choline, ethanolamine, serine) which defines the phospholipid properties (Figure 1-8). The length of fatty acid chains and their degree of unsaturation influence the phospholipid packing ability with other phospholipids and so the overall fluidity of the membrane.

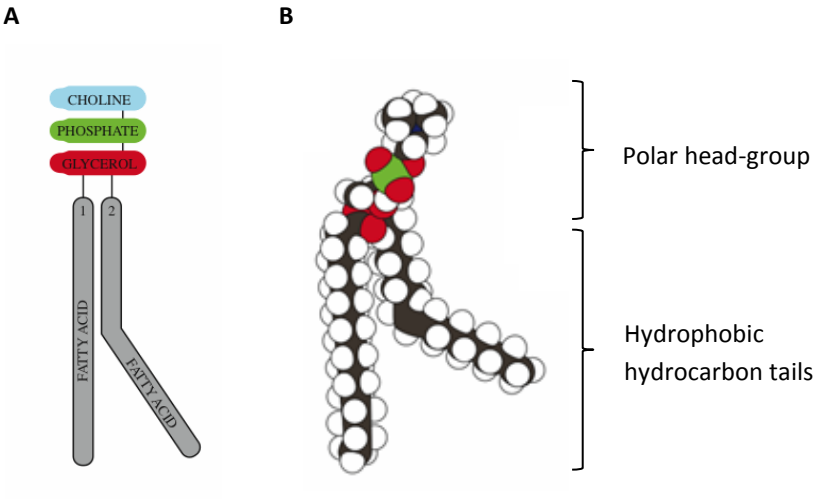


Figure 1-8. Schematic (A) and physical (B) structure of a phospholipid - phosphatidylcholine (PC). (Figure adapted from Alberts et al. 2002).

In mammalian cells, the majority (40-50%) of total phospholipids is accounted for by phosphatidylcholine (PC). Next in line is phosphatidylethanolamine (PE), the content of which is more variable and represents 15-25% of total phospholipids whilst the scarcer phosphatidylserine (PS) accounts for only 5-10%. Sphingomyelin (SM), phosphatidylinositol (PI), phosphatidic acid (PA) and mitochondria-specific cardiolipin (CL) are also important phospholipid constituents of membranes (Table 1-1) (Vance, 2014b). However, the exact phospholipid composition differs across cell types and organelles. For instance, both mitochondrial outer and inner membranes are distinctly enriched in PE comprising 30-40% of total mitochondrial phospholipids as compared to ~15-25% found in other cell membranes (Vance, 2014b). Additionally, the unique phospholipid cardiolipin, which is exclusively found only in mitochondrial membranes, particularly the inner membrane, comprises 10-15% of mitochondrial lipids and plays important roles in supporting the function of electron transport chain proteins (Pfeiffer et al., 2003; Zhang et al., 2005). The distribution of these phospholipids in the membranes is also leaflet-specific (Balasubramanian & Schroit, 2003). In plasma membranes, PC and SM tend to dominate in the external leaflet whereas aminophospholipids PS and PE are most abundant on the inner leaflet

(Schick et al., 1976; Higgins & Evans, 1978). However, as the trans-bilayer movement of phospholipids is energetically unfavourable, this asymmetry is established via specialized enzymes such as flippases, floppases and scramblases (Balasubramanian & Schroit, 2003). Furthermore, this asymmetry is purposely lost during certain physiological processes such as apoptosis.

1.5.1 PHOSPHOLIPID SYNTHESIS PATHWAYS

In mammalian cells, the main sites of phospholipid synthesis are the endoplasmic reticulum (ER), mitochondria and also sites of close apposition between the two, known as the mitochondria-associated membranes (MAM), which regardless of their mitochondrial designation present an extension derived from the ER. The synthesis pathways of individual phospholipids are highly interlinked, generally with more than one way of obtaining a particular phospholipid, which are often spatially separated. As mentioned CL is found only in mitochondrial membranes, hence unsurprisingly, its synthesis is restricted to the mitochondria. Additionally, mitochondria synthesize their own PE, PA and phosphatidylglycerol (PG), although they can also be made in the ER and MAM. PC, PS and PI are formed exclusively in ER and MAM and so require to be imported into the mitochondria. Here, a summary of the main phospholipid biosynthesis pathways will be given, with emphasis on the mitochondria.

	Percentage of total lipids
Phosphatidylcholine	45–55
Phosphatidylethanolamine	15–25
Phosphatidylinositol	10–15
Phosphatidylserine	5–10
Phosphatidic acid	1–2
Sphingomyelin	5–10
Cardiolipin	2–5
Phosphatidylglycerol	<1
Glycosphingolipids	2–5
Cholesterol	10–20

Table 1-1. Typical lipid composition of mammalian cells. (Figure adapted from Vance, 2014b).

1.5.1.1 BIOSYNTHESIS OF PHOSPHATIDIC ACID (PA)

Phosphatidic acid (PA), made either in the ER or the mitochondria is a major substrate for synthesis of other phospholipids either directly or indirectly, even though itself is only a rare component of cell membranes. It is from this phospholipid that the two main precursor molecules, cytidine diphosphate-diacyglycerol (CDP-DAG) or diacylglycerol (DAG) are made via CDP-DAG synthase and phosphatidic acid phosphohydrolase -1 (PAP-1), respectively (Inglis-Broadgate et al., 2005; Donkor et al., 2007). Whereas CDP-DAG is used for the generation of PI and PG, DAG is required for *de novo* synthesis of PC and PE (Vance, 2014b).

1.5.1.2 BIOSYNTHESIS OF PHOSPHATIDYLGLYCEROL (PG) AND CARDIOLIPIN (CL)

PG synthesis takes place both in the ER and the mitochondria. The precursor CDP-DAG is reacted with glycerol-3-phosphate to form PG-phosphate (PG-P) which is catalysed by PG-P synthase, at the inner mitochondrial membrane (Kawasaki et al., 1999). Next, PG-P is dephosphorylated to form PG by PG-P phosphatase (Osman et al., 2010). Such formed PG can then be directly combined with another CDP-DAG molecule to produce CL in a reaction catalysed by CL synthase, an integral protein of the inner mitochondrial membrane (Chen et al., 2006).

1.5.1.3 BIOSYNTHESIS OF PHOSPHATIDYLCHOLINE (PC)

The majority of cellular PC is synthesized by incorporation of extracellular choline via a three step CDP-choline pathway, known as the 'Kennedy pathway' (Kennedy & Weiss, 1956). In the first step, cytosolic choline kinase (CK) generates phosphocholine using ATP. This is followed by CTP:phosphocholine cytidylyltransferase (CT) catalysed addition of CTP to phosphocholine forming CDP-choline which is considered to be the rate-limiting step of the Kennedy pathway. Finally, CDP-choline:1,2-diacylglycerol cholinephosphotransferase (CPT), an ER integral enzyme, generates PC by addition of DAG to CDP-choline (reviewed in Gibellini & Smith, 2010) (Figure 1-9). An alternative pathway for PC synthesis is from PE through three consecutive methylation reactions catalysed by PE *N*-

methyltransferase, which localizes in the ER. The highest activity of this enzyme is in the liver where it can produce up to 30% of total cellular PC (Vance, 2014a). In other tissues its expression is negligible and contributes only marginally to the cellular PC pool.

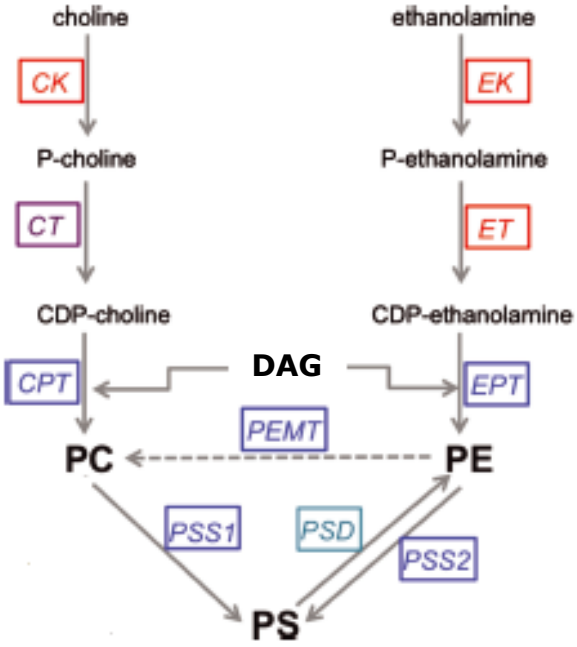


Figure 1-9. Biosynthetic pathways of PC, PE and PS. Both PC and PE can be synthesized *de novo* from choline and ethanolamine, respectively, via the Kennedy pathway. In the PC branch of the pathway, choline is phosphorylated to phosphocholine via choline kinase (CK), which is in turn modified with CTP to CDP-choline by CTP-phosphocholine cytidylyltransferase (CT). Finally, PC is formed through addition of a diacylglycerol (DAG) molecule to CDP-choline via the integral ER membrane enzyme CDP-choline:1,2-diacylglycerol cholinephosphotransferase (CPT). Alternatively, PC can be produced from PE by three consecutive methylation reactions catalysed by PE methyltransferase (PEMT). The PE branch of the Kennedy pathway performs identical reactions to the PC pathway though using ethanolamine as substrate and catalysed by ethanolamine kinase (EK), CTP-phosphoethanolamine cytidylyltransferase (ET) and CDP-ethanolamine:1,2-diacylglycerol ethanolaminephosphotransferase (EPT). PS synthesis relies on a base exchange reaction from from PC via PS synthase-1 (PSS-1) or from PE via PS synthase-2 (PSS-2). (Figure adapted from Vance et al. 2014b).

1.5.1.4 BIOSYNTHESIS OF PHOSPHATIDYLSERINE (PS)

PS can only be synthesized from other pre-existing phospholipids through a Ca^{2+} -dependent exchange of their head-groups for serine. PS synthase-1(PSS1) and PS synthase-2 (PSS2), found exclusively in the MAM, present with distinct substrate specificities (Kuge et al., 1986, 1997; Stone & Vance, 2000). PSS1 preferentially replaces the head-group of PC whereas PSS2 uses PE as the substrate phospholipid for the base-exchange reaction (Figure 1-9).

1.5.1.5 BIOSYNTHESIS OF PHOSPHATIDYLETHANOLAMINE (PE)

The bulk of PE is derived from two spatially separated pathways: the CDP-ethanolamine pathway in the ER, and the PS decarboxylation pathway in the mitochondria (reviewed in (Vance & Tasseva, 2013)). The CDP-ethanolamine pathway parallels the reactions employed for PC synthesis, using ethanolamine as the initial substrate. The first reaction consists of ethanolamine kinase (EK) mediating ATP-dependent phosphorylation of ethanolamine. Next, phosphoethanolamine is activated with CTP giving rise to CDP-ethanolamine via CTP:phosphoethanolamine cytidylyltransferase (ET). The pathway completes with the ER integral enzyme CDP-ethanolamine:1,2-diacylglycerol ethanolaminephosphotransferase (EPT) mediated reaction of CDP-ethanolamine with DAG to produce PE (Figure 1-9). In the PSD pathway, PSD which localizes to the outer leaflet of the inner mitochondrial membrane decarboxylates its substrate PS to PE (Zborowski et al., 1983; Kuge et al., 1991).

Limited amounts of PE can be also made via two additional biosynthetic pathways. The third pathway involves MAM-localized lyso-PE acetyltransferase catalysed acetylation of lyso-PE to PE (Stein & Stein, 1966). The fourth pathway comprises the PSS2 catalysed reverse base-exchange reaction from PS, replacing its serine headgroup for ethanolamine (Leonardi et al., 2009). Though PC is the most abundant phospholipid, its synthesis occurs solely in the ER in contrast to the requirement for mitochondria and ER specific PE production. Indeed, ER and mitochondria produced PE differs in its acyl-chain composition (Bleijerveld et al.,

2007). Stable isotope labelling revealed the CDP-ethanolamine pathway preferentially synthesizes PE with mono- or di-unsaturated fatty acids on the sn-2 position such as 16:0-18:2, and the PSD decarboxylase pathway generates mainly polyunsaturated fatty acid species on the sn-2 position such as 18:0-20:4 and 18:0-20:5 (Bleijerveld et al., 2007). The pathways of PE synthesis are summarized in Figure 1-10.

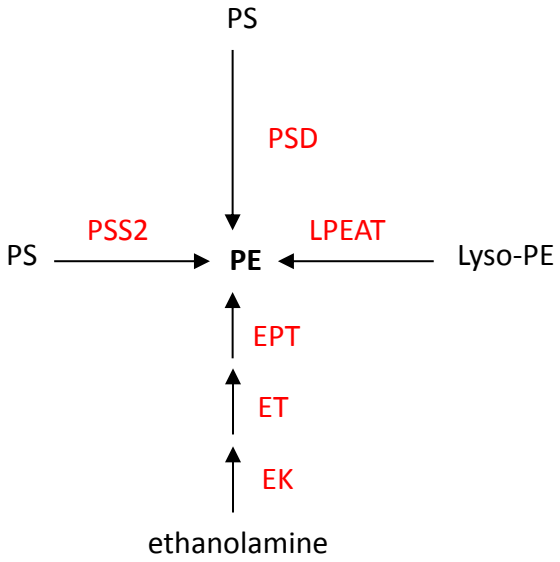


Figure 1-10. Biosynthetic pathways for PE in mammalian cells. Main contributors to the cellular PE pool are the CDP-ethanolamine (Kennedy) pathway from ethanolamine via successive enzymatic reactions catalyzed by ethanolamine kinase (EK), CTP:phosphoethanolamine cytidylyltransferase (ET), CDP-ethanolamine:1,2-diacylglycerol ethanolaminephosphotransferase (EPT), and PS decarboxylation via the enzyme PS decarboxylase (PSD). Small amounts of PE are made by acylation of lyso-PE by lyso-PE acyltransferase (LPEAT), and also by a base-exchange reaction in which the serine of PS is replaced by ethanolamine catalysed by PS synthase-2 (PSS2).

1.5.2 THE PHYSIOLOGICAL ROLES OF PS AND PE IN MAMMALIAN CELLS

As mentioned previously, PS and PE are both restricted to the inner leaflet of the plasma membrane. Since ATP is expended to preserve membrane asymmetry, its disturbance has been postulated to serve a specific purpose. Indeed, the activity of transporter proteins maintaining such lipid distribution alters in response to a rise in intracellular Ca^{2+}, which occurs during specific cellular events such as cell division, apoptosis, malignant transformation, cell injury or cell

activation as a result of which the inner leaflet-restricted aminophospholipids appear on the outer surface (Marconescu & Thorpe, 2008). For example, following platelet activation, PS becomes exposed on platelet plasma membrane which signals a pro-coagulant response to which clotting factors are recruited to promote wound healing (Bevers et al., 1982; Majumder et al., 2008). Exposure of PS can also occur on aged red blood cells which signals macrophages to efficiently remove them from the blood stream (Connor et al., 1994; Boas et al., 1998). Similarly, PS translocates to the outer plasma membrane leaflet during early stages of apoptosis prior to DNA condensation and serves as an engulfment signal for surveying phagocytes to clear the dying cells (Fadok et al., 1992). Indeed, this property is often exploited in cell apoptosis assays via Annexin V labelling which binds to PS on cell surface. In activated T-cells, cell surface density of exposed PS allows distinction between activated apoptotic and non-apoptotic T-cell which is important for tight immune regulation (Tietjen et al., 2014). Further, in Fas stimulated primary macrophages, MOMP mediated AIF release was necessary for PS exposure and efficient cell clearance (Preta & Fadeel, 2012). In addition to PS, PE also appears on the surface of apoptotic cells as well as irradiated tumour or vascular endothelial cells, co-localizing with PS to the membrane blebs as determined by staining cells with PE-specific fluorescence conjugated peptide cinnamycin (Ro09-0198) (Emoto et al., 1997) or duramycin (Iwamoto et al., 2007; Marconescu & Thorpe, 2008).

Accumulation of PS in the inner-leaflet of the plasma membrane has important implications for various cell signalling cascades as it acts as a scaffold onto which different signalling effectors are recruited and also participates in their activation. The negatively charged head-group of PS mediates electrostatic interactions with positively-charged motifs of c-Src non-receptor tyrosine kinase and Rho GTPase Rac1, allowing them to translocate to the plasma membrane (Sigal et al., 1994; Finkielstein et al., 2006). Similarly, the 3-Phosphoinositide dependent kinase-1 contains a pleckstrin homology domain with specific PS binding site necessary for its membrane localization (Lucas & Cho, 2011). On the other hand, both membrane targeting and activation of Akt depend on

phosphatidylinositol-3,4,5-trisphosphate (PIP(3)) and PS binding (Huang et al., 2011). Therefore, though PS is only a minor component of cell membranes, its anionic nature makes a significant difference to membrane properties.

Whereas many PS functions stem from its negative charge, PE has a conical shape due to its small head-group which provides it with the propensity to form non-lamellar membrane structures. In this manner it introduces membrane tension, a characteristic essential for successful membrane fusion where sharp membrane curvature becomes indispensable (Verkleij et al., 1984). Indeed, in yeast vacuoles tethered through protein fusion machinery (SNARE) the rate and extent of fusion are reduced in the absence of PE in the vacuole membrane (Zick et al., 2014). PE has been shown to decorate the cleavage furrow of cells at late telophase during cytokinesis (Emoto et al., 1996). Immobilization of surface exposed PE with the PE-binding peptide (Ro09-0198) effectively inhibited the disassembly of the contractile ring causing the persistence of a cytoplasmic bridge between daughter cells (Emoto et al., 1996; Emoto & Umeda, 2000). Therefore, membrane redistribution of PE during cell division is essential for successful completion of cytokinesis. Interestingly, PE is also covalently attached to LC3 which is then recruited to the nascent autophagosome membranes where it might contribute to cargo degradation via mediating fusion between the autophagosome and the lysosome (Nebauer et al., 2007). PE appears to be important also as a source for ethanolamine containing structural modifications in protein posttranslational processing. Indeed, some proteins are post-translationally modified to contain a glycosylphosphatidylinositol (GPI) anchor which allows them to be tethered to lipid microdomains in the outer leaflet of plasma membrane (Paulick & Bertozzi, 2008). The GPI anchor, composed of a phosphoethanolamine linker,a glycan core, and a phospholipid tail, requires PE as a donor of the phosphoethanolamine moiety (Menon et al., 1993; Paulick & Bertozzi, 2008). Indeed, cellular PE deficiency in yeast caused a defect in GPI-anchor biosynthesis (Birner et al., 2001). PE is also the source of the ethanolamine-phosphoglycerol moiety modifying the eukaryotic elongation factor eEF1A (Signorell et al., 2008).

Consistent with enrichment of PE in the mitochondria, changes in mitochondrial PE levels detrimentally affect mitochondrial morphology and health in all eukaryotes (Steenbergen et al., 2005; Signorell et al., 2009; Joshi et al., 2012; Tasseva et al., 2013). Though the parasite *T. Brucei* suffers alterations of inner mitochondrial cristae, ATP production via oxidative phosphorylation measured in isolated mitochondria is unaffected indicating a greater leeway in mitochondrial morphology (Signorell et al., 2009). However, in mammalian cells fragmented mitochondria due to acute PE deficiency do suffer from decreased ATP production (Tasseva et al., 2013). Developmentally, deletion of mitochondrial PE synthesis in mice via PSD causes gross mitochondrial abnormalities and is embryonically lethal (Steenbergen et al., 2005). Similarly, deletion of the rate limiting enzyme of the CDP-ethanolamine pathway, ET, results in death prior to embryonic day 8.5 (Fullerton et al., 2007). Hence, PE is relevant in a plethora of fundamental cellular processes and its site of synthesis contributes to their regulation.

1.6 HYPOTHESIS AND AIMS

During previous work in the lab, GST-survivin was incubated with whole cell extracts prepared from apoptotic HeLa cells to identify any potential interacting partners via tandem mass spectroscopy analysis. This approach isolated PSD as a potential survivin interactor. As described previously, PSD resides within the mitochondria where it converts PS to PE. PE has been characterized in cellular processes such as cytokinesis, autophagy and apoptosis to name a few. On the other hand, survivin has important roles in cell division, apoptosis suppression and possibly also autophagy, with further roles gradually emerging.

Here, we hypothesize that survivin contributes to these processes by regulating PSD-mediated conversion of PS to PE in the mitochondria. The aim of this thesis was to test this hypothesis, by determining whether interaction between survivin and PSD does occur and if so, how such interaction could impact cell behaviour.

2 MATERIALS AND METHODS

2.1 MOLECULAR BIOLOGY TECHNIQUES

For all molecular biology procedures, products from New England Biolabs (NEB) were used unless otherwise indicated.

2.1.1 PREPARATION OF *E. COLI* COMPETENT CELLS

An aliquot of competent cells glycerol stock was added to 100ml of sterile antibiotic free Luria Bertani (LB) broth and grown with shaking at 37°C until Optical Density (OD) was in the range 0.4 – 0.7. The cells were pelleted at 3,220xg for 10 min at 4°C, the supernatant discarded and the pellet resuspended in 10 ml of ice-cold 0.1M $CaCl_2$ and incubated for 1 h on ice. Cells were centrifuged again, resuspended in 2ml of ice-cold 0.1M $CaCl_2$ and incubated for further 15 minutes on ice, before adding 1ml of 80% glycerol and storing in 100µl aliquots at -80°C.

2.1.2 TRANSFORMATION OF *E. COLI* WITH PLASMID DNA

Approximately 1µg of plasmid was added to 100µl of *E. coli* DH5α competent cells and incubated on ice for 30 minutes. Next, the cells were heat-shocked for 2 minutes and returned to ice for 1 minute. 750µl of sterile LB broth was then added to the cells and they were incubated for 30 – 60 minutes at 37°C. The cells were pelleted at 16,200xg for 1 minute the supernatant discarded and the pellet resuspended in 100 µl of LB, spread on LB agar plates containing the appropriate antibiotic and incubated overnight at 37°C.

2.1.3 PURIFICATION OF PLASMID DNA

A single colony of *E. coli* treated as above was used to inoculate either 8ml or 25ml LB broth containing vector-appropriate antibiotics. The plasmid DNA was subsequently purified from the bacterial cells using the QIAprep Spin Mini or MidiPrep purification kit (Qiagen) according to the manufacturer's instructions. At

the final step, the plasmid DNA was eluted with 40µl (Mini) or 100µl (Midi) of sterile deionized water. The resulting DNA concentration was measured as absorbance at 260 and 280nm by NanoDrop 2000 Spectrophotometer (Thermo Scientific).

2.1.4 Polymerase Chain Reaction (PCR)

A typical PCR reaction was set up for all primer combinations consisting of 1µg of template DNA, 400nM of each forward and reverse primer, 1x ThermoPol Reaction Buffer, 200µM of each dNTP, Vent DNA Polymerase (1U) and sterile deionized water in a final reaction volume of 50µl. The reaction was initiated with a denaturation step at 98°C for 3 min, followed by 35 cycle repeats of denaturation at 98°C for 30 seconds, annealing at 50°C - 60°C for 1 min and elongation at 72°C for 1 minute, finally ending the run with a single further elongation step at 72°C for 5 minutes. The annealing temperature of the reaction was selected depending on the melting temperature of the primer pair used.

2.1.5 Site directed mutagenesis

The mutagenesis PCR reactions were set up similarly to the standard PCR reaction described above, including a negative control with no primers present, with the cycling conditions as follows: initiated with a denaturation step at 95.9°C for 3 min, followed by 12 cycle repeats of denaturation at 95°C for 45 seconds, annealing at 60°C for 1 min and elongation at 72°C for 7 minutes, finally ending the run with a single further elongation step at 72°C for 15 minutes. The resulting whole plasmid PCR products were ethanol precipitated with 1 volume of 4M ammonium acetate and 2 volumes of ice-cold ethanol and incubated at -20°C overnight. The mix was centrifuged at 16,200xg for 10 minutes at room temperature and the supernatant removed. The DNA pellet was then washed with 100µl of 70% ethanol and recentrifuged. After removal of the supernatant, the DNA pellet was air-dried, then resuspended in 30µl sterile deionized water. The entire PCR product was immediately digested with 20U DpnI (6 h at 37°C) to remove the methylated

template plasmid. The reaction was inactivated at 70°C for 20 mins, cooled and used to transform *E. coli* cells (See section 2.1.2).

2.1.6 DNA AGAROSE GEL ELECTROPHORESIS

DNA samples were prepared with 5x DNA loading dye (0.25% (w/v) Bromophenol Blue, 0.25% (w/v) Xylene cyanol and 15% (w/v) Ficoll R 400) and run on 0.8% agarose gels (w/v prepared in 1xTBE buffer (89mM Trizma, 82mM Boric acid, 2.3mM EDTA) with 0.5µg/ml Ethidium Bromide) in TBE buffer at 90-100 V for approximately 1 to 1.5 hours. DNA was visualized using a UV transilluminator.

2.1.7 PCR PURIFICATION

PCR products were run on a DNA agarose gel (See section 2.1.6) and fragments of expected size excised and gel purified using the QIAquick Gel Extraction kit (Qiagen) until final elution with 30µl sterile deionized water.

2.1.8 RESTRICTION DIGESTIONS OF DNA

The reaction conditions for each double digest were found using Double Digest Finder on the NEB website.

A 20µl reaction volume was set up for the destination vectors with 0.5 U of each of the restriction enzymes, the appropriate 1x NEBuffer, 1X BSA where required, approximately 1-2µg of plasmid DNA and sterile deionized water. Similarly, the gel purified PCR products were digested with restriction enzymes (0.5U) complementary to their engineered restriction sites in a 50µl reaction volume. All reactions were incubated at 37°C for up to 3 hours, run on agarose gels and subsequently, the desired fragments were gel excised and purified using the QIAquick Gel Extraction kit (Qiagen).

2.1.9 PHOSPHATASE TREATMENT OF VECTOR DNA

Vectors cut with a single restriction enzyme were phosphatase treated in a 20µl reaction volume with 1x Antarctic Phosphatase Reaction Buffer and 5U of Antarctic

phosphatase at 37°C for 30mins. The enzyme was heat inactivated at 70°C for 5 minutes.

2.1.10 LIGATIONS

All ligations were performed in a 20µl reaction volume containing 15µl of the gel excised PCR product or sterile deionized water only as negative control, approximately 70ng of the appropriate vector, 1xT4 DNA ligase buffer and 400 units of T4 DNA ligase. These were left to incubate at 16°C overnight. Half of the ligation mixture was used to transform 100µl competent *E. coli* DH5α cells and subsequently purify ligated plasmid DNA.

2.1.11 RNA EXTRACTION AND cDNA SYNTHESIS

RNA was extracted from $1x10^6$ cells (Hela, U2OS, SH5YSY) using the Total RNA extraction kit (Norgen Biotek) following manufacturer's instructions. The concentration and purity of purified RNA was measured by NanoDrop. Next, 3µg of RNA was reverse transcribed into cDNA with Superscript II Reverse Transcriptase (Invitrogen) following manufacturer's instructions using 250ng random primers. Due to reoccurrence of contamination, 8µg Hela and SH5YSY RNA were treated with TURBO DNase (2U) (Invitrogen) to remove any genomic contamination prior to cDNA synthesis. The DNase was inactivated with DNase Inactivation Reagent (Invitrogen).

2.1.12 REVERSE TRANSCRIPTION POLYMERASE CHAIN REACTION (RT-PCR)

A typical RT-PCR reaction was set up using 1x Q5 Reaction Buffer, 200 µM of each dNTP, 500nM of each forward and reverse primer, cDNA as template, 1 Unit of Q5 Hot Start High Fidelity Polymerase and sterile deionized water up to 50µl final reaction volume. The reaction was initiated with a denaturation step at 98°C for 30 sec, followed by 35 cycle repeats of denaturation at 98°C for 10 sec, annealing at 70°C for 30 sec and elongation at 72°C for 1 minute, ending the run with a final elongation step at 72°C (2 minutes).

CLONING STRATEGIES FOR INDIVIDUAL PLASMID CONSTRUCTS

All constructs generated via PCR amplification were sequence verified whereas constructs made via subcloning of a previously sequenced insert from one vector to another were checked with a restriction digest for the right sized fragments.

CLONING OF MITOCHONDRIALLY TARGETED SURVIVIN CONSTRUCTS

A mitochondrial targeting signal peptide of cytochrome c oxidase subunit VIIIA was amplified by PCR from U2OS cDNA with EcoRI sites at both termini. The resulting PCR product and destination vectors (pcDNA-GFP and pcDNA-SVN GFP) were digested with EcoRI-HF at 37°C for 30 mins. The vectors were phosphatase treated, and ligations were set up as described. The resulting constructs contain a mitochondrial targeting signal (MTS) at the N-terminus fused to GFP or survivin-GFP. The mitochondrial localization of the constructs was verified by fluorescence microscopy.

CLONING OF FLAG-TAGGED SURVIVIN EXPRESSION CONSTRUCTS

Survivin was amplified by PCR with appropriate primers (see list of primers in Appendix) from pcDNA-survivin to obtain an insert flanked with BglII sites at both termini for cloning with FLAG tag at the N-terminus, or NotI/BamHI sites (without stop codon) for cloning survivin with C-terminal FLAG tag. The resulting PCR products and also the target pCMV Tag 1 vector were digested with their respective enzymes, gel extracted and ligated together. In case of the survivin BglII/BglII PCR product, the pCMV vector was phosphatase treated prior to ligation. The FLAG-Survivin was then digested with BamHI/XhoI, the Survivin-FLAG with NotI/XhoI and subcloned into pcDNA 3.1 (+), where successful expression and detection with the FLAG antibody was attained.

Cloning of His-tagged survivin expression construct

Survivin was 8xHis tagged at the C-terminus using NcoI/XhoI (no stop codon) with pQE-TriSystem His.Strep 1 vector, where only the His tag was used, and the Strep tag was removed by restriction digest.

Cloning of Phosphatidylserine decarboxylase (PSD) expression constructs

Full length PSD isoform1 (GenBank accession no. CAG 30426.1) was amplified by PCR from U2OS cDNA. PSD isoform 2 was cloned from a sequence verified cDNA in pOTB7 vector from the I.M.A.G.E. consortium (cDNA clone MGC: 1308; IMAGE clone ID 3508281; GenBank accession number BC001482.2). Both PSD isoform 1 and 2 were cloned EcoRI/XhoI into pcDNA 3.1 and pGEX4-T1 or using EcoRI/HindII without a stop codon (for C-terminal GFP tagging) into pBlueScript SK (+)as in intermediate step given that pcDNA has an internal HindIII site preventing direct insertion into pcDNA. From pBluescript, the PSD-GFP iso1/2 fusion could be subcloned EcoRI/XhoI into pcDNA 3.1.

Cloning of inactive PSD with the point mutation S378A

Site-directed mutagenesis was performed as described, using pcDNA-PSD isoform 1 and 2 as templates to obtain the S378A mutant. Subsequently, PSD S378A iso1 was also subcloned into pGEX-4T1, using EcoRI/XhoI sites as for wildtype PSD.

Epitope tagging of PSD (FLAG and 8xHis)

PSD isoform 1 wild type and S378A were FLAG-tagged at the C-terminus using NotI/BamHI sites (no stop codon) as used for cloning survivin-FLAG and subsequently subcloned into pcDNA using NotI/XhoI sites.

PSD isoform 1 wild type and S378A were also 8xHis tagged at the C-terminus using NcoI/XhoI (no stop codon) with pQE-TriSystem His.Strep 1 vector, where only the His tag was used, and the Strep tag was removed by restriction digest. Using the

same restriction sites, PSD was also cloned into pET-22b(+) vector for bacterial overexpression as C-terminal His fusion.

2.2 MAMMALIAN CELL CULTURE TECHNIQUES

2.2.1 CELL CULTURE

All cell lines (HeLa, HEK293T, MRC5, U2OS, RPE-1, EJ30) were cultured in DMEM (Dulbecco's Modified Eagle's Medium, Gibco®, Invitrogen) supplemented with 2mM glutamine, 10% HyClone bovine growth serum supplemented calf (Thermo Scientific), with the exception of SH5YSY cells which were grown in EMEM: F12 supplemented the same way. Additionally, HeLa cells lines stably expressing GFP, survivin-GFP or survivin$_{1\text{-}10}$-GFP were maintained under selection with G418. All cells were grown in a humidified incubator at 37°C in 5% CO_2 atmosphere and periodically passaged at 80% confluency at a 1:10 dilution.

2.2.2 CELL TRANSFECTIONS

2.2.2.1 DNA TRANSFECTION

Cells were seeded at an appropriate cell density for the destination culture vessel (24, 6-well plate) in antibiotic free media and left to grow for 12-24 h to reach 50 – 80% confluency prior to transfection. Fugene6 transfection reagent was diluted in reduced serum media OptiMEM (Gibco, Invitrogen) and incubated with DNA at a ratio 3:1 transfection reagent (µl): DNA (µg) for a minimum of 20 minutes at room temperature. The transfection reagent-DNA complex was then directly added to cells in a drop wise manner and cells were returned to incubator for 12-48 hours to allow for protein expression. Alternatively, linear polyethylenimine (PEI) (MW 25,000, Cat# 24765-2, Polysciences) was used in large scale transfections in 10cm dishes. Briefly, PEI was dissolved in water at 6.45 mg/ml and used at a ratio 6:1 PEI (µg): DNA (µg). PEI was diluted in 800µl sterile Mili-Q water and added to DNA

diluted in 800µl PBS, mixed, left to incubate for 20 minutes at room temperature and added to cells in drop-wise manner.

2.2.2.2 siRNA TRANSFECTION

To knock down survivin or PSD, $4x10^4$ cells were seeded immediately prior to siRNA transfection in a 24 well plate or a 4 chamber slide for live imaging (Lab-Tek II). Silencer siRNA (Ambion) (60nM for survivin or 150nM for PSD) was diluted in OptiMEM (Invitrogen) to which 3µl of HiPerFect transfection reagent (Qiagen) was added, the mix was vortexed, left to incubate for 8 minutes at room temperature and then added to cells. A mock transfection was performed with transfection reagent only as control.

2.2.3 CELL COUNTING

HeLa cells in suspension were counted with a haemocytometer and $4x10^4$ cells were seeded for siRNA transfection. An aliquot corresponding to $4x10^4$ cells was pelleted and resuspended in 100µl 1:1 PBS:0.4% Trypan Blue, 10µl taken to count the number of viable cells (i.e. excluding the blue dye) which was to be time 0. Afterwards, at 24, 48 and 72h time points post-siRNA, cells were harvested, resuspended in 40, 80 and 120µl of trypan blue solution, respectively, and counted. Total number of cells for each condition at each time point was plotted to assess the rate of cell growth.

2.2.4 PREPARATION OF WHOLE CELL EXTRACTS

Cells were washed with pre-warmed PBS and harvested with trypsin. The cell suspension was centrifuged at 300xg for 3 minutes and the pellet washed with PBS, centrifuged again until final resuspension in HEPES lysis buffer (20mM HEPES pH 7.5, 250mM NaCl, 0.5% NP40) with freshly added protease and phosphatase inhibitors: 2µg/mL CLAP (Chymostatin, Leupeptin, Antipain, Pepstatin A), 100µM PMSF (Phenylmethylsulfonyl fluoride) and 2mM β-glycerophosphate. The lysates were briefly vortexed and then cleared by centrifugation at 17,200xg for 15 min 4°C. A sample of the supernatant was analysed by Bradford, the remnant was

boiled with 5x sample buffer (250 mM Tris-HCl pH 6.8, 5% (w/v) SDS, 50% (v/v) Glycerol, 500mM β-mercaptoethanol, 0.005% (w/v) Bromophenol Blue) at 95°C for 3 mins and stored at -20°C until analysis.

2.2.5 CELL TREATMENTS

2.2.5.1 CELL CYCLE SYNCHRONIZATION

G1 PHASE

The cells were treated with 0.5mM mimosine (Sigma) overnight and harvested the next day.

S PHASE

To arrest cells in S phase, a double thymidine block was employed. Cells were seeded at 30-40% confluency and allowed to adhere overnight. Cells were treated with 2mM thymidine (Sigma) for 18h overnight, then washed with PBS and incubated with fresh media for 9h. The treatment was repeated for a second 16h/overnight and finally cells were washed with PBS and harvested.

M PHASE

For enrichment of cells in M phase of the cell cycle, cells were treated with 1μM dimethylenastron (DMA) (Alexis) then harvested by shake off.

MUSE CELL CYCLE ANALYSIS

Cells were analysed for successful enrichment in the different phases of the cell cycle with flow cytometry. Approximately $1x10^6$ cells harvested by trypsinization (only M phase arrested cells harvested by mitotic shake-off) were centrifuged at 300xg for 5 minutes and washed with 0.5ml PBS, the majority of supernatant was aspirated. The cells were resuspended in the remnant of PBS and added in a dropwise manner to freshly prepared -20°C cold 70% ethanol whilst vortexing. Cells were then left at -20°C for at least 3 hours before analysis. Such fixed cells were pelleted, washed with PBS, resuspended in MUSE cell cycle reagent and incubated for 30 minutes in the dark prior to analysis on the MUSE cell analyser (Merck Millipore) as per manufacturer's instructions.

2.2.5.2 CYCLOHEXIMIDE AND MG132 TREATMENT

Cells were treated with 50µg/ml Cycloheximide and/or 20µM MG132 diluted in cell culture media for 4, 7 and 16 hours (Cycloheximide only) and subsequently harvested for immunoblotting.

2.3 BIOCHEMICAL ASSAYS

2.3.1 SUBCELLULAR FRACTIONATION

Cells grown in 15cm dishes were washed twice with ice-cold PBS and then harvested into a small volume of ice-cold PBS by scraping with a rubber cell scraper. The cells were pelleted at 300xg for 3 minutes at 4°C, the supernatant was discarded and the cells were resuspended in approximately 2ml of isolation buffer (200mM Mannitol, 70mM Sucrose, 1mM EGTA, 10mM HEPES pH 7.5 with freshly added protease and phosphatase inhibitors) and subsequently homogenized 1ml at a time with 25 gentle strokes in a glass Teflon homogenizer. The lysate was centrifuged at 1,000xg for 5min at 4°C to pellet nuclei and any unlysed cells. The supernatant (cytosol/mitochondria fraction) was transferred to a fresh tube. The cell pellet was then homogenized again in only 1 ml isolation buffer in a smaller homogenizer, repeating the 1,000g spin, and again keeping the supernatant in a fresh tube. In total, cells were homogenized three times in this manner to increase the yield of mitochondria. The nuclear pellet was washed three times with 500µl of Buffer A (10mM HEPES pH7.9, 1.5mM $MgCl_2$, 10mM KCl, 0.5mM DTT, 0.3% NP-40) (with a brief vortex) to remove any unlysed cells, with a spin step at 1,000g 5 min 4°C between each wash until final resuspension in 200µl of isolation buffer. The suspension was given two 10 second sonication pulses to shear genomic DNA and subsequently cleared of any remaining large debris by centrifugation at 17,200g 10 min 4°C. A sample of the supernatant was taken for Bradford, the rest was added to 5x sample buffer, boiled and kept frozen until analysis.

The combined cyto/mito fraction was centrifuged at 1,000xg 5 min 4°C to remove any contaminating traces of nuclei, the supernatant was moved to a fresh tube. This

was then centrifuged at 10,000xg, 15 minutes, 4°C to pellet mitochondria. The supernatant (cytosolic fraction) was transferred to a fresh tube, centrifuged at 17,200g for 20 min 4°C to remove any mitochondrial contaminants, a sample of the supernatant was taken for Bradford and the remnant was concentrated by acetone precipitation. Briefly, 4 sample volumes of -20°C cold acetone were added to the cytosolic fraction, vortexed and incubated at -20°C for 1 hour or overnight. This was then centrifuged 15,000xg 10 min, supernatant was aspirated and the protein pellet left to air dry. The pellet was resuspended in a suitable volume of 1x sample buffer, boiled and kept frozen until analysis. The crude mitochondrial pellet was washed a total of 3 times in 500 µl isolation buffer with a spin at 10,000xg 10 mins 4°C between each wash. However, at last wash, a spin step at 800xg for 4 mins was added and only the supernatant was centrifuged at 10,000xg to obtain the final pellet which was resuspended in a suitable volume of isolation buffer. At this stage, the mitochondria could be used in a number of assays. However, wherever higher purity mitochondria were desired, sucrose density gradient was employed.

2.3.2 DISCONTINUOUS SUCROSE DENSITY GRADIENT

Crude mitochondrial pellet was resuspended in 500µl of isolation buffer and layered on top of a sucrose step gradient in a 5ml ultracentrifuge tube consisting of 1ml each 15%, 23%, 32% and 60% sucrose buffer (15, 23, 32 and 60% Sucrose in 1mM EDTA, 10mM MOPS pH 7.2). Pure mitochondria were collected at the 32-60% sucrose interface after 1hour spin at 33,200 rpm 4°C (SW55Ti rotor, deceleration set to slow). The mitochondria were washed with approximately 6-7 volumes of isolation buffer and centrifuged 10,000xg 10 mins 4°C. The pellet was washed again in 300µl isolation buffer until resuspension in suitable volume of isolation buffer. A sample was taken for Bradford, the remaining sample was incubated with 5x sample buffer (95°C, 3 min), and frozen until further analysis.

2.3.3 EXPERIMENTS WITH ISOLATED MITOCHONDRIA

2.3.3.1 PROTEASE PROTECTION ASSAY

40µg isolated mitochondria were resuspended in 400µl control buffer (10mM HEPES pH 7.5, 250mM Sucrose) or swelling buffer (10mM HEPES pH 7.5) for 30 mins on ice, with periodical pipetting every 6 minutes. Mitochondria were then reisolated at 10,000 g for 10 minutes at 4 °C and subsequently resuspended in 90µl control buffer with or without trypsin at 80 and 300µg/ml final concentration or 1% Triton X-100 in control buffer with or without trypsin for 25 minutes on ice. The digestion was stopped by incubating with 50µg/ml AEBSF for 15 minutes on ice. Whole and swollen mitochondria were then reisolated at 10,000 g for 10 minutes at 4 °C, mixed with 40µl sample buffer, boiled and stored until analysis. Triton X-100 treated mitochondria were acetone precipitated, centrifuged and the pellet also resuspended and boiled in 40µl 1x sample buffer.

2.3.3.2 DIGITONIN FRACTIONATION OF MITOCHONDRIA

100µl aliquots of 0-0.5% digitonin in isolation buffer without EGTA were mixed with a 100µl aliquot of mitochondria (50µg) and incubated on ice for 30 mins with periodical agitation to maintain the mitochondria in suspension. The solubilisation was stopped by adding 800µl of isolation buffer and the mitochondria were reisolated 11,000xg 10 mins 4°C. The pellets were resuspended in 4 volumes of isolation buffer with 250mM KCl, incubated for 5 minutes on ice and then once again reisolated 11,000xg 10 mins 4°C. Finally, the mitochondrial pellets were resuspended in 1x sample buffer, boiled and stored until analysis.

2.3.3.3 *IN VITRO* IMPORT OF UNLABELED GFP-TAGGED OR ^{35}S-LABELED PROTEINS INTO MITOCHONDRIA

In vitro transcription and translation of pcDNA3.1 constructs of proteins of interest was carried out using the T7 polymerase TNT® Quick Coupled Transcription/ Translation system (Promega) according to the manufacturer´s instructions. Proteins were translated to incorporate ^{35}S-methionine to allow detection via

autoradiography; alternatively they were synthesized unlabeled as GFP fusions to allow distinction from endogenous proteins via blotting for GFP. 60 µg freshly isolated HeLa mitochondria were resuspended in 93µl import buffer (20mM HEPES pH 7.5, 3% (w/v) fatty acid free BSA, 250mM Sucrose, 80mM KCl, 5mM $MgCl_2$) supplemented with 2mM ATP and 10mM sodium succinate and preincubated for 5 minutes at 37°C. Next, 7µl of ^{35}S-labeled/unlabeled GFP-tagged precursor proteins were added. The import mix was incubated at 37 °C for 1 hour. Samples were centrifuged at 10,000 g for 5 minutes at 4 °C and supernatants were removed. The pellets were washed with 200µl isolation buffer, centrifuged again and then resuspended in isolation buffer (without EGTA) with or without trypsin at 150µg/ml for 15 mins on ice. As control, a subset of mitochondrial pellets was resuspended in isolation buffer supplemented with 1% Triton X-100 and trypsin. Trypsin was inhibited with AEBSF added to 50µg/ml for 15 mins on ice. Samples were mixed with 5x sample buffer, boiled and stored frozen until analysis by SDS-PAGE and autoradiography.

2.4 SDS POLYACRYLAMIDE GEL ELECTROPHORESIS (SDS-PAGE) AND IMMUNOBLOTTING

2.4.1 SDS-PAGE

Protein samples were prepared with 5x sample buffer boiled for 3 mins at 90°C and analysed on 12 or 15% resolving SDS-PAGE gels. The gels were run at 200V in SDS running buffer (25mM Tris, 192mM Glycine, 0.1% (w/v) SDS) until the dye front reached the bottom of the gel. Gels were stained with Coomassie or carried over to immunoblotting.

2.4.2 IMMUNOBLOTTING

Proteins resolved by SDS-PAGE were blotted onto a 0.22µm nitrocellulose membrane by wet transfer system in transfer buffer (24mM Tris, 195mM Glycine, 0.05% (w/v) SDS, 10% Methanol) employing the BioRad Blotting Module. The

protein transfer was carried out at 350mA for 1.5 hours. Nitrocellulose membranes were blocked in 5% non-fat milk (w/v) in PBS with added 0.1% Tween 20 (PBST) either for 1-2 hours at room temperature or overnight at 4°C. The membranes were incubated with primary antibody (see Table 2-1 for antibodies used in this thesis) diluted in 5% milk for 1 hour at room temperature (or overnight at 4°C), followed by four 5-minute washes in PBST. Next, membranes were incubated with species appropriate horseradish peroxidase conjugated secondary antibody (Dako) diluted 1:2000 in 1% non-fat milk for 1 hour at room temperature. Any unbound antibody was removed with four 5-minute washes with PBST. Finally, the membranes were incubated with Z- ECL chemiluminescence detection reagents (Geneflow) before exposure on the Lumifilm chemiluminescent detection film (Roche).

Antibodies

Primary antibodies

Antibody	Host species	Dilution WB	Source
Cytochrome c	Mouse	1:1000	Abcam (Gift from Dr. L. Bedford)
Cytochrome c oxidase subunit II	Mouse	1:1000	Abcam (Gift from Dr. L. Conforti)
FLAG M2	Mouse	1:1000	Sigma
GST	Rabbit	1:1000	Cell Signaling
Hsp60	Rabbit	1:5000	Gift from Dr. Lynn Bedford
Penta His	Mouse	1:1000	Qiagen (Gift from M. Hardcastle)
PSD	Rabbit	1:500	Sigma (Atlas)
TBP	Rabbit	1:1000	Cell signaling
αTubulin (B512)	Mouse	1:1000	Sigma
Survivin	Rabbit	1:500	In house
VDAC	Rabbit	1:1000	Cell Signaling

Secondary antibodies

Antibody	Host species	Dilution	Source
Anti-Rabbit HRP conjugated	Goat	1:2000	Dako
Anti-Mouse HRP conjugated	Rabbit	1:2000	Dako

Table 2-1. List of antibodies used for immunoblotting

2.5 PROTEIN PURIFICATION

2.5.1 BACTERIAL PROTEIN OVEREXPRESSION

Proteins subcloned in pGEX-4T1 were overexpressed in BL21 (DE3) pLysS cells. For other bacterial expression vectors (pQE and pET-22b(+)), bacterial strains XL-Blue 1, SG13009 (pREP4) and T7 Express were also used. Single colonies were used to inoculate small starter overnight cultures in LB with appropriate antibiotic. Subsequently, these were diluted 1/40-1/100 into larger cultures until OD reached 0.6-0.7 when they were induced with 0.2-1mM isopropyl-β-D-thiogalactopyranoside (IPTG) to initiate desired protein overexpression. After the desired time, bacteria were harvested by centrifugation at 3,220xg for 20 mins 4°C and washed with ice-cold PBS.

The pellets with overexpressed GST tagged proteins were then lysed in GST lysis buffer (10mM EDTA pH 7.5, 0.1% Triton X100 in PBS) supplemented with protease inhibitors 100μM PMSF and 1μg/ml CLAP (containing chymostatin, leupeptin, antipain and pepstatin A) by sonication on ice with 6 x 10 second pulses at half power with 10 second pauses machine (Vibra Cell VC50T). The lysates were cleared of insoluble material by centrifugation at 17,200xg for 15 minutes 4°C. Alternatively, the pellets were resuspended in PBS, sonicated, then supplemented with 1% Triton X-100, incubated for 30 mins at room temperature and then cleared by centrifugation at 17,200xg for 15 minutes 4°C.

2.5.1.1 GST OR GST PSD PURIFICATION

GST-tagged *E. coli* overexpressed proteins were purified using GST SpinTrap columns (max capacity 500μg GST protein) for small scale purification according to the manufacturer's instructions with GST elution buffer (50mM Tris-HCl, 10mM reduced glutathione, pH 8.0). For larger protein prep GSTrap 4B 1ml columns connected to AKTA liquid chromatography system were employed. The columns were equilibrated with 10CV (column volumes) of PBS and the sample applied at a flow rate 0.5ml/min. The column was washed with 10CV of PBS and proteins eluted

with GST elution buffer in 1ml elution fractions. These were pooled together and concentrated/buffer exchanged into 50mM Tris pH7.4 (at 20 °C), 0.1% Triton X-100 using Amicon pro centrifugal filters with 10,000kDa cutoff.

2.5.2 MAMMALIAN PROTEIN OVEREXPRESSION/HIS PURIFICATION

HEK293T cells were PEI transfected with either pQE-PSD-8xHis or pQE-PSD S378A-8xHis, and lysed with MHis lysis buffer (50mM NaH_2PO_4, 300mM NaCl, 10mM Imidazole, 0.5% Triton X-100 pH 7.8) by incubation with rotation at 4°C for 10 minutes. Next, the lysate was cleared by centrifugation at 10,000xg for 10 minutes 4°C. Meanwhile, 100µl of 50% slurry Profinity™ IMAC resin (BioRad) per sample was transferred into a fresh tube, 20% ethanol storage solution removed by centrifugation at 1,000xg for 1 minute (speed used for all subsequent centrifugations). The resin was washed twice with 5x resin bed volume of deionized water, followed by equilibration with 5xbed volumes of the MHis lysis buffer. Cleared lysates were added to the equilibrated resin and left to rotate for 2 hours at 4°C. The resin was washed twice with 5 bed volumes of MHis wash buffer (50mM NaH_2PO_4, 300mM NaCl, 20mM Imidazole, 0.1% Triton X-100 pH 7.8) and bound proteins eluted with 5 rounds of 4xbed volumes of MHis elution buffer of increasing imidazole concentration going from 50mM imidazole to 250mM Imidazole (50mM NaH_2PO_4, 300mM NaCl, 50/100/150/200/250mM Imidazole, 0.1% Triton X-100). The five elution fractions were pooled together and concentrated/buffer exchanged into 50mM Tris pH7.4 (at 20 °C), 0.1% Triton X-100 using Amicon pro centrifugal filters with 10,000Da cutoff.

2.6 BINDING STUDIES

2.6.1 CO-IMMUNOPRECIPITATIONS

HEK293T cells were transfected in 6 well plate at $4x10^5$ cells per well with specified constructs allowing 36-48 hours for protein expression. 3 hours prior to harvest, cells were treated with 10µM MG132 to increase the amount of protein available

by inhibiting proteasomal protein degradation. Cells were washed with ice-cold PBS, and lysed with addition of 700µl co-IP lysis buffer (50mM Tris-HCl, pH 7.4 (at 4°C), 150mM NaCl, 1mM EDTA, 1% Triton X-100). Lysates were cleared of insoluble debris at 12,000xg for 10 min 4°C. A 40µl sample of cleared lysate was taken as "Input", mixed with 5x sample buffer, boiled and kept frozen till analysis. For immunoprecipitation of FLAG proteins, 30µl of Anti-FLAG M2 Affinity Gel (Sigma) per sample was washed twice with 500µl of TBS (50mM Tris-HCl pH 7.5, 150mM NaCl) and centrifuged at 4,000xg 30 seconds 4°C, leaving the tubes undisturbed for 1-2 mins for the gel to fully sediment. Cleared lysates were then added to the washed Anti-FLAG gel and incubated with end-over-end rotation for 2 hours at 4°C. The gel was centrifuged as before and supernatant containing unbound material was aspirated. The gel was then washed for a total of three times with 500µl TBS, gently inverting the tubes each time to mix. Finally, the gel was resuspended with 2x non-reducing sample buffer (125mM Tris-HCl, pH 6.8, 4% SDS, 20% (v/v) glycerol, 0.004% bromophenol blue), boiled and kept at -20°C.

2.6.2 Glutathione S-Transferase Pull-down Assays

Cleared lysates of GST alone or GST survivin were used for binding to approximately 50µl neat glutathione sepharose 4B beads (GE Healthcare) overnight at 4°C with rotation. The beads were then washed three times with 1ml of chilled GST lysis buffer and resuspended in the same buffer. pcDNA3.1 constructs of Borealin and PSD were *in vitro* transcribed and translated (IVT) with the T7 TNT® Coupled Reticulocyte Lysate System (Promega) according to the manufacturer's instructions in 50 or 100µl reactions using 0.04mCi or 0.08mCi [^{35}S]L-methionine as a tracer, incubated at 30°C for 90 minutes. 20µl of IVT products was then added to GST alone and to a GST fusion protein prebound beads and left to incubate for 2 hours at room temperature with rotation. Finally, the beads were washed three times with GST lysis buffer with rotation for 10 minutes, resuspended in SDS loading buffer, boiled and analysed by SDS-PAGE. The gels were stained with Instant Blue gel stain (Expedeon) for 20 minutes, dried, and visualized by PhosphoImager FLA-3000.

2.7 LIPID TECHNIQUES

2.7.1 PSD CONVERSION ASSAY AND LIPID EXTRACTION

Varying amounts of GST-PSD or GST alone either bound to GST beads or already purified in solution were incubated with 10µg of phosphatidylserine (Avanti), dissolved in 4% ethanol, in a final volume of 100µl in reaction buffer (50mM Tris-HCl pH 7.4 (at 20 °C) , 0.1% Triton X-100) and incubated for 1 hour at 37°C. The reaction was stopped by addition of 50µl reaction termination buffer (1M KCl, 0.2M $H_3PO_{4)}$, mixed by inversion and lipids extracted with an equal volume of 100µl chloroform/methanol 2:1. The reaction was then mixed and centrifuged 14000xg 2 minutes. The bottom organic phase was then transferred into a fresh tube, vacuum evaporated and dried lipids resuspended in 20µl of chloroform for thin layer chromatography (TLC).

2.7.2 LIPID EXTRACTION FROM CELLS

Lipids were isolated from HeLa cells as described by Folch et al., (1957). Briefly, cells were washed with PBS and detached from culture vessel by trypsinization and centrifuged at 300xg for 3 min to pellet. Cells were then resuspended in PBS, divided three ways and pelleted. One pellet was lysed in HEPES lysis buffer and protein quantified via Bradford. The remaining two pellets had lipids extracted by addition of 200µl chloroform/methanol 2:1 per $1x10^6$ cells with a brief vortex. The suspension was incubated for 20 min with shaking at room temperature, after which 40µl of 0.9% NaCl was added. The suspension was thoroughly vortexed and centrifuged at 500xg for 10 minutes to separate the upper aqueous phase and the lower organic phase containing the extracted lipids. The organic phase was transferred to a fresh tube, vacuum evaporated and resuspended in 20µl of chloroform for subsequent TLC.

2.7.3 THIN LAYER CHROMATOGRAPHY (TLC)

The extracted lipids from cells were separated on TLC silica gel 60 plates (Merck) in chloroform, methanol, acetic acid and water 50:30:8:3 (v/v) alongside authentic PS, PC (Avanti) and PE (Sigma) standards. The plates were left to dry and the phospholipids were visualized by exposure to iodine vapour.

Lipids extracted from PSD conversion assays were separated on the same plates as above in chloroform: methanol: water 65:25:4 (v/v) solvent mixture.

2.7.4 LIPID QUANTITATION

Silica spots of the desired phospholipids as identified by comparison to authentic standards were scraped from TLC plates into chromic acid cleaned Pyrex tubes. These were then digested with 80µl of 70% perchloric acid at 170°C for 1 hour to liberate the inorganic phosphate. Phosphate release was quantified by malachite green method described by (Itaya & Ui, 1966). Samples were diluted with 400µl of ddH2O (i.e ratio 1:5 perchloric acid:ddH_2O) and subsequently centrifuged down briefly to pellet the silica gel. A standard curve was prepared with a solution of 1mM KH_2PO_4 to obtain 0, 1, 2, 4, 8, 16, 32, 48nmol of phosphate in each tube (duplicate). These were heated at 170°C until evaporated and subsequently diluted the same way as samples with 80µl of 70% perchloric and 400µl of ddH_2O. The malachite colour reagent was prepared on the day of quantitation by mixing 0.2% malachite green solution (w/v in dH_2O vigorously stirred for at least 30 mins at room temperature, then filtered through #2 Whatmann filter paper), 4% ammonium heptamolybdate (w/v in 5M HCl) and 0.5% Tween20 (v/v in dH_2O) at a ratio of 15:5:1. This mixture was stirred vigorously at 4°C for at least 30 mins. A 250µl aliquot of all samples and standards was transferred to fresh Eppendorf tubes, mixed with 1ml of the prepared colour reagent and incubated for 30 minutes at room temperature. The absorbency of the samples was measured at 660nm using water as a blank. Results were expressed as nmol lipid/mg protein.

2.8 IMAGING TECHNIQUES

2.8.1 LIVE CELL FLUORESCENCE IMAGING

HeLa cells treated with siRNA for 48 or 72 hours in live imaging chambers (Lab-Tek II) were stained for mitochondria with 100nM MitoTracker Red CMXRos (Invitrogen) for 15-45 minutes at 37°C in CO_2-independent media (phenol red free) and immediately imaged using an inverted (Olympus Axiophot, Delta Vision Elite) microscope equipped with 63x oil immersion objective as stacks of 0.3µm slices for each channel. All images were deconvolved and saved as TIFF files.

2.8.2 FIXED CELL FLUORESCENCE IMAGING

Cells were cultured on ethanol washed coverslips in 24 well plates. Cells were washed three times with PBS, fixed with 4% prewarmed freshly prepared paraformaldehyde (in PBS from 16% stock (Thermo Scientific) for 5 minutes. Subsequently, the coverslips were thoroughly washed three times for 5 minutes with PBS with mild agitation. At this stage, where no antibody staining was required, the coverslips were left to dry and then mounted on ethanol cleaned slides with a drop of Mowiol, left to dry overnight and then sealed with nailpolish. Alternatively, the cells on coverslips were permeabilized with 0.15% Triton-X for 2 minutes and again washed three times per 5 minutes with PBS. Next, coverslips were blocked with 1% BSA in PBS for 15 minutes and then incubated with primary antibody (Anti-FLAG M2 at 1:1000) in 1%BSA in PBS for 1 hour at room temperature. The coverslips were then washed three times 5 minutes with PBS followed by secondary antibody incubation at 1/200 dilution together with DAPI at 1/500 dilution in 1%BSA in PBS for 1 hour at room temperature in the dark. The coverslips were given final three 5minute washes, left to dry and mounted on glass slides with Mowiol. Slides were imaged as for live imaging.

2.8.3 ELECTRON MICROSCOPY

Cell pellets were resuspended in EM fixative (3% Glutaraldehyde in 0.1M Cacodylate buffer) and subsequently processed by Miss Denise McLean from Advanced Microscopy Unit (AMU) in the School of Life Sciences Imaging (SLIM) facility.

3 MITOCHONDRIAL TARGETING OF SURVIVIN

3.1 PROTEIN IMPORT INTO MITOCHONDRIA

Mitochondria are double membrane organelles most recognized for their energy (ATP) producing capacity through a process known as oxidative phosphorylation, but also the ability to instruct the cell to undergo apoptosis (McBride et al., 2006). Additionally, they orchestrate multiple other events essential for normal functioning of the cell, such as calcium homeostasis, production of iron-sulphur clusters and heme, lipid biosynthesis and control of reactive oxygen species (Keeble & Gilmore, 2007). They are able to integrate with other cell signalling pathways and so respond promptly to the changing physiological conditions.

The structure of the mitochondrion comprises two distinct compartments – the innermost matrix encapsulated by the inner mitochondrial membrane (IMM) with its characteristic invaginations known as cristae, and the intermembrane space (IMS) surrounded by the outer mitochondrial membrane (OMM) (Figure 3-1). This unusual structural arrangement has been attributed to the hypothesized origin of mitochondria from an α-proteobacterium, living in symbiosis with its eukaryotic host, but eventually surrendering most of its primitive genome to the host nucleus and evolving to the current form (Cavalier-Smith, 2006; Dolezal et al., 2006). Therefore, though mitochondria have their own genome and protein synthesis

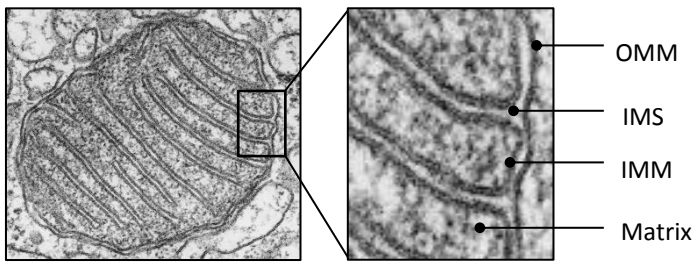


Figure 3-1. Structural features of mitochondria. Electron microscopy image of a mitochondrion. Enlargement of section marked by rectangle with highlighted submitochondrial compartments: OMM, outer mitochondrial membrane, IMS, intermembrane space, IMM, inner mitochondrial membrane and matrix. (Image adapted from Alberts et al. 2002).

machinery, few mitochondrial proteins are actually made *in situ*, with the majority of approximately 1500 mitochondrial proteins (in humans) being encoded by nuclear genes (Chacinska et al., 2009). A set of dedicated multimeric translocation complexes embedded in the OMM and IMM has evolved to guide preprotein entry into the mitochondria and their assembly/folding at the correct destination once inside. Importantly, this import machinery has receptor subunits which allow entry only to proteins that have specialized import signal sequences. The different import complexes have mostly been characterized in yeast and *Neurospora crassa* but are highly conserved across phyla (Hoogenraad et al., 2002). The vast majority of imported proteins traverse the OMM through the TOM (translocase of the mitochondrial outer membrane) complex. The main component of this complex is the integral Tom40 β-barrel protein which, together with Tom22 and small Tom proteins 5,6 and 7, oligomerizes to form a protein conducting pore (Abe et al., 2000; Künkele et al., 1998). Accessory to the Tom40 pore are the mitochondrial preprotein receptors Tom20 and 70 which recognize and interact with distinct subsets of preproteins carrying various import signals (Ahting et al., 1999; Abe et al., 2000; Brix et al., 1997, 1999). β-barrel proteins destined for insertion into the OMM are passed onto the mitochondrial sorting and assembly machinery (SAM) complex, a relic of the protobacterial ancestor (Endo & Yamano, 2010). On the other hand, α-helical transmembrane domain proteins of the OMM are handled by the MIM complex, which currently has no known mammalian homolog (Neupert, 2015). At the inner membrane, the preproteins interact with one of the two TIM (translocase of the mitochondrial inner membrane) complexes – TIM23 or TIM22, which then sort the preproteins to the intermembrane space, the inner membrane or the matrix (Bauer et al., 1999). Successful translocation into the matrix is achieved in an ATP-dependent manner via matrix-localized presequence translocase-associated protein import motor (PAM) comprising among multiple components, the matrix heat shock protein 70 (mHsp70) and Tim44, which is tethered to the TIM23 complex (Bauer et al., 2000). Also at the IMM, the OXA1 complex functions in a retrograde manner, inserting proteins into the IMM which have either been first targeted into the matrix or which have been synthesized by

the mitochondrial translation machinery (Neupert, 2015). A very specialized import pathway is the Mia40-Erv1 (Mia40-ALR in humans) disulphide relay system whose client proteins, containing characteristic cysteine motifs, are oxidatively folded and so are retained in the IMS (Allen et al., 2005; Banci et al., 2009).

3.2 MITOCHONDRIAL TARGETING SEQUENCES

Given the way mitochondria have evolved, most of mitochondrial proteins required for the proper functioning of this organelle need to be delivered from their site of synthesis on cytosolic ribosomes via specialized import machinery. The information required for this import to occur is contained within specialized targeting sequences. To date, three different signal subtypes have been described and are summarized in figure 3-2. The most frequently occurring and so the best described are the N-terminal targeting sequences, also known as presequences. These are characterized by enrichment of positively charged and hydrophobic residues, with a tendency to form amphipathic α-helices (Allison & Schatz, 1986; Roise & Schatz, 1988; von Heijne, 1986). Therefore, it is the amino acid composition i.e. the physicochemical properties of the sequence that are vital for successful import rather than a conserved consensus amino acid sequence. Presequences are typically 10-80 amino acids in length and are preferentially recognized by Tom20, and directed via Tim23 into the matrix (Abe et al., 2000; Marom et al., 2011). A further impetus for matrix translocation across the inner membrane is provided by the electrophoretic pull of the negatively charged membrane potential on the overall positive charge of the presequence (Shariff et al., 2004). Upon entry into the matrix, the presequence is cleaved off by matrix resident processing peptidases (MPP), with a subset of proteins additionally processed by the mitochondrial intermediate peptidase (MIP), and a mature protein is released into the matrix (Gakh et al., 2002). Alternatively, presequence-proteins may contain additional signals which will change the ultimate destination of the protein. For example, an

Targeting and sorting signals of mitochondrial proteins

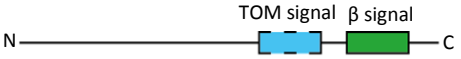
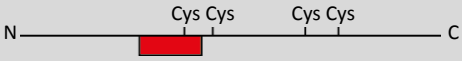
A Presequences		**Destination**	**Example**
Presequence amphipathic α-helix		Matrix	Alcohol dehydrogenase, Hsp60
Presequence+uncleaved hydrophobic domain (sorting signal)		Inner membrane	PSD
Presequence+cleaved hydrophobic sorting signal (bipartite presequence)		Intermembrane space	Cytochrome b_2, Smac/DIABLO
B Noncleavable signals			
β signal		Outer membrane (β-barrel)	VDAC, Tom40
Signal-anchor			Tom70, Tom20
C tail anchor		Outer membrane (α-helical)	Fis1, Bcl-2 family
Internal signal			Mitofusins 1/2
Multiple internal signals		Inner membrane	AAC carrier, PiC carrier
Presequence-like internal signal		Inner membrane	BCS1
C MIA pathway signals			
Cysteine motif		Intermembrane space	Small Tim proteins, Atp23

Figure 3-2. Targeting and sorting signals of mitochondrial precursor proteins. Mitochondrial proteins can contain different targeting information depending on their ultimate destination in the mitochondria. Three different types of targeting signals are shown. (A) Presequences are usually cleaved off by matrix processing peptidases (MPP). Additional neighbouring hydrophobic stretch (blue box) can serve as a "stop transfer" signal, preventing complete translocation into the matrix and releasing the protein laterally into the inner membrane. Alternatively, it can be cleaved as well by inner membrane peptidase (IMP) and the protein released into the IMS. (B) Non-cleavable Internal signals of various membrane associated proteins. The β signal necessary for association of β-barrel proteins with the SAM complex is shown in green, the still uncharacterized signal necessary for docking into TOM complex is shown in light blue. The hydrophobic transmembrane domains of OM α-helical proteins acting as sorting signals are shown in yellow. Multiple import machinery recognition sites of carrier proteins are shown in purple. (C) The mitochondrial intermembrane space sorting (MISS) signal/IMS-targeting signal (ITS) of the MIA pathway, encompassing a cysteine residue of the cysteine twin motif, show in red. (Figure adapted from Chacinska et al., 2009).

extra hydrophobic stretch upstream of the presequence can arrest translocation into the matrix and instead direct the preprotein to insert into the inner membrane, or this hydrophobic stretch cleaved off by inner membrane peptidase (IMP) and the protein released into the IMS such as for example Smac/DIABLO or cytochrome b_2 (Beasley et al., 1993; Burri et al., 2005; Gasser et al., 1982).

The second type of targeting sequences encompass all unusual internal targeting elements which are not cleaved upon import but remain part of the mature protein. The best described examples of internal targeting information are the inner membrane integral carrier proteins such as the phosphate or ADP/ATP (AAC) carriers. These contain several targeting elements each comprising about 13 amino acids recognized by the Tom70 but also Tom20 receptors of the TOM complex (Brix et al., 1999, 2000). Next, they associate with the small Tim protein complexes in the IMS followed by docking at the TIM22 complex for their sorting to the inner membrane in a membrane potential dependent manner (Endres et al. 1999; Koehler et al. 1998; Ryan et al. 1999). An atypical non-cleavable presequence type signal located at the C-terminus of the protein, with dependence on the flanking N-terminal transmembrane domain and a C-terminal neighbouring region, has also been described (Fölsch et al., 1996). A distinct targeting signal group consists of proteins destined for insertion into the OMM which comprises α-helical N or C terminal-anchored or multi-spanning transmembrane proteins and β-barrel proteins. For helical OM proteins, it is the transmembrane segments themselves flanked by additional positively charged residues, which serve as the targeting signal (Dukanovic & Rapaport, 2011). Though a recognition signal of β-barrel proteins for TOM complex remains elusive, the signal important for association with the SAM complex has been identified, and is denoted as a β signal (Dukanovic & Rapaport, 2011).

Finally, the third signal subtype of import signal has been described for small soluble IMS proteins containing conserved twin CX_3C or twin CX_9C motifs imported via the MIA pathway (Banci et al., 2009). Known MIA client proteins – small Tim proteins (9 and 10) and Cox19 (cytochrome c oxidase) were used to identify a

consensus mitochondrial intermembrane space sorting (MISS) signal/IMS-targeting signal (ITS) recognized by this pathway (Milenkovic et al., 2009; Sideris et al., 2009). However, given its recent discovery and the list of known client proteins growing, it is likely that other MISS signals are yet to be identified.

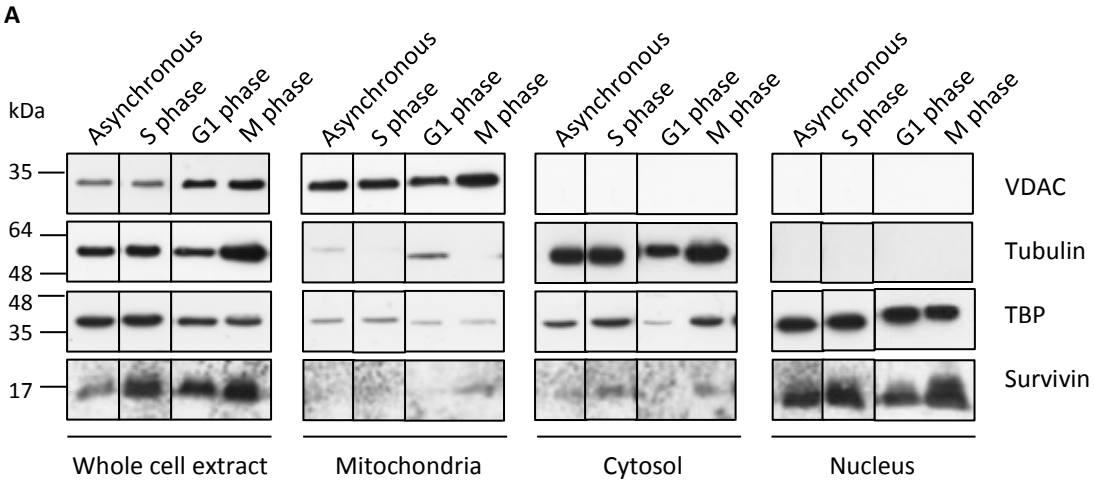
3.3 MITOCHONDRIAL LOCALIZATION OF PSD AND SURVIVIN

Survivin is expressed in the cytoplasm and nucleus during interphase, however, as a chromosomal passenger complex protein during mitosis, it localizes at the centromeres of condensed chromosomes at prophase and the spindle midzone at anaphase, until being eventually discarded in the midbody in late telophase (Skoufias et al., 2000; Uren et al., 2000; Wheatley et al., 2001a). In this study, we focus on previously described mitochondrial pool of survivin thought to mediate protection against apoptosis (Dohi et al., 2004a, 2007). However, novel roles for mitochondrial survivin are beginning to be realized and will be discussed in detail in chapter 4. Indeed, mitochondria have important roles in regulation of energy metabolism but also other processes such as lipid transport and cell cycle progression (McBride et al., 2006). Mitochondria are also the residence of PSD, an enzyme responsible for decarboxylation of the lipid PS into PE, providing them with their very own pool of PE (Shiao et al., 1995). PE is essential for maintenance of normal mitochondrial morphology and function in mammalian cells (Tasseva et al., 2013). This study aimed to consolidate a possible link between survivin and PSD suggested by preliminary data in the Wheatley laboratory (S.P.Wheatley, personal communication). Specifically, this chapter will analyse survivin mitochondrial localization in detail with respect to PSD.

3.4 RESULTS

3.4.1 MITOCHONDRIAL SURVIVIN AT DIFFERENT STAGES OF CELL CYCLE

Survivin expression has been described to go from complete absence at interphase to peaking levels at mitosis (Li et al., 1998a). Therefore, possible cell-cycle regulated changes in survivin levels within mitochondria were assessed by HeLa cell fractionation via differential centrifugation and sucrose gradient purification into mitochondrial, cytosolic and nuclear/chromosomal fractions at different stages of the cell cycle. Prior to fractionation, cells were either left untreated (asynchronous control) or were synchronized at G1 phase by treatment with mimosine by blocking DNA replication fork assembly, S phase with double thymidine block and M phase by treatment with the mitotic kinesin Eg5 inhibitor DMA. All cell synchronizations were verified with FACS analysis (Figure 3-3B). Highest levels of survivin in the mitochondria were seen at mitosis whereas all other conditions analysed showed barely detectable amounts of survivin which could indicate possible functional overlap between survivin at mitosis as part of CPC and survivin in the mitochondria. However, the presence of survivin in the mitochondria did not preclude its localization in the cytosol or in the nuclear/chromosomal fraction of mitotic cells.



B

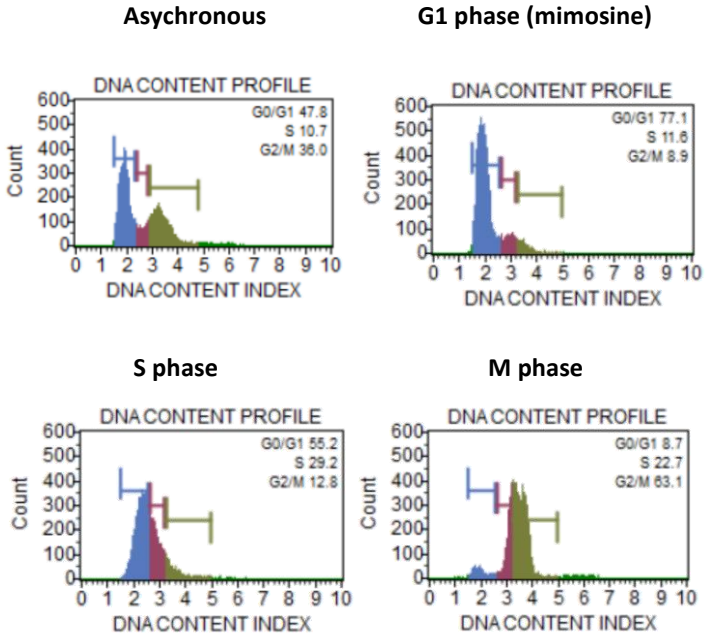


Figure 3-3. Expression of survivin in the mitochondria during the cell cycle. (A) HeLa cells were fractionated to enrich for mitochondria either without synchronisation, or after synchronization in G1 phase by overnight treatment with mimosine, S phase via double thymidine block and in M phase by treatment with the Eg5 inhibitor, DMA. Purity of the fractions was assessed by immunoblotting for markers of each subcellular compartment: VDAC (mitochondria), tubulin (cytosol) and TBP (nucleus). 20µg of protein was loaded for whole cell extract, cytosol and nucleus, 8µg for mitochondria. **(B)** Cell synchronization was confirmed by flow cytometry with a propidium iodide based assay.

Similarly, though only low levels of mitochondrial survivin were detected at S-phase, it was clearly detected in the cytosol and the nucleus as well. In G1 arrested cells, there was complete absence of survivin in the mitochondria or the cytosol, with moderate levels detected in the nucleus. However, given the cell-cycle regulated nature of survivin, it was surprising to see such high levels in the nucleus of cells at phases of the cell cycle other than mitosis which could be due to less efficient nuclear export in this particular cell line analysed.

3.4.2 MITOCHONDRIAL SURVIVIN IN NORMAL VERSUS CANCER CELLS

Next, using the same fractionation procedure the presence of survivin in the mitochondria was compared between asynchronous human normal and cancer cells. As representative of normal cells, the MRC5 lung fibroblast cell line and primary hepatocytes were used. As an intermediate between non-tumour and tumour cells, untransformed but immortalized retinal pigmented epithelium RPE-1 cell line was used. The osteosarcoma U2OS, bladder carcinoma EJ30 and neuroblastoma SH-SY5Y cell lines were selected for the panel of tumour cell lines. Primary hepatocytes lacked survivin in all of the fractions analysed, including the whole cell extract, whereas normal lung fibroblasts MRC5 presented with low survivin levels in the nuclear (and chromosomal) fraction only (Figure 3-4). All cancer cell lines analysed had very high survivin expression overall as seen in the whole cell extract (Figure 3-4). Moreover, they showed some survivin expression also in the mitochondria with U2OS and EJ30 cells showing particularly abundant levels. Interestingly, the immortalized RPE-1 cell line also expressed survivin at whole cell level albeit less than cancer cells, with virtually undetectable amount in the mitochondria.

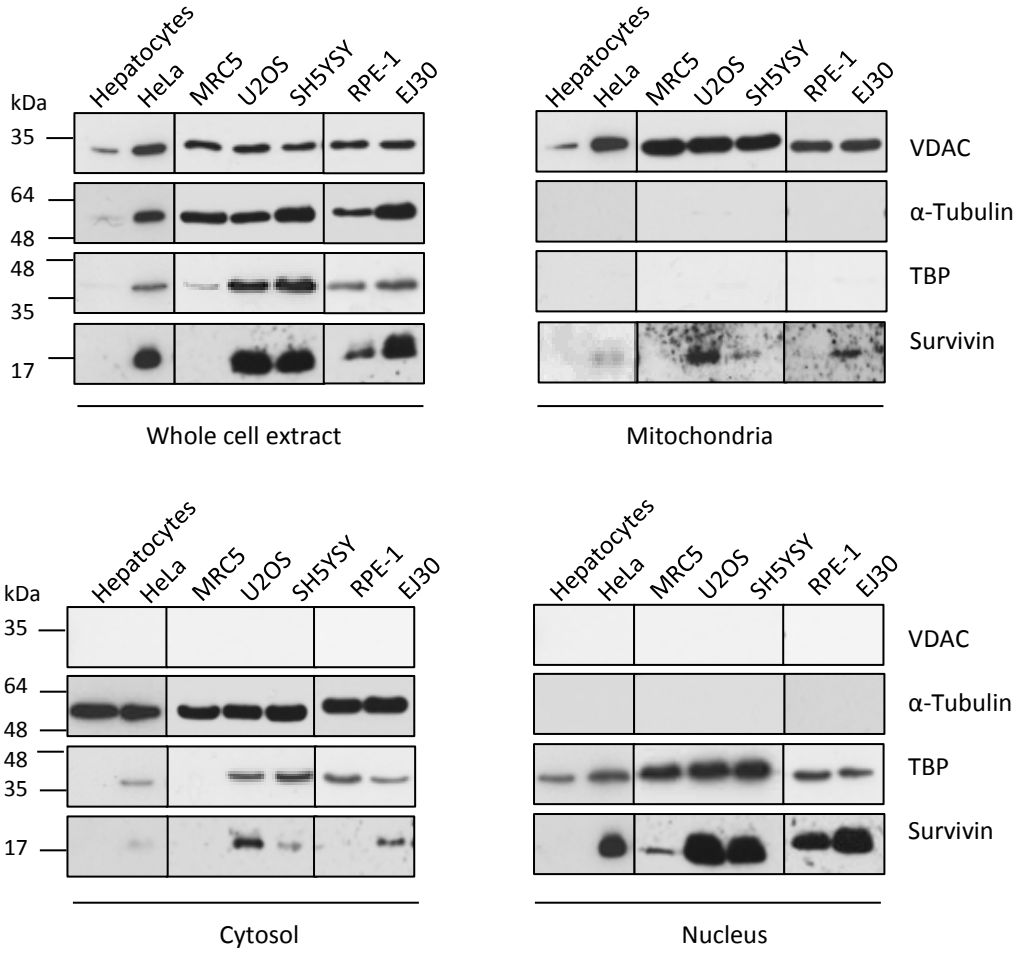


Figure 3-4. Survivin is present in the mitochondria of cancer cells but not normal cells. The presence of survivin in mitochondria was analysed by immunoblotting after fractionation as detailed in the previous figure 3-3. Its expression was compared between the cancer cell lines (Hela, U2OS, SH5YSY and EJ30), immortalized normal epithelial RPE-1 cells, normal lung fibroblasts MRC5 and primary hepatocytes. Purity of fractions was assessed using antibodies to the following: VDAC (mitochondria), tubulin (cytosol) and TBP (nucleus). 20µg of protein was loaded for whole cell extract, cytosol and nucleus, 8µg for mitochondria.

3.4.3 COMPUTATIONAL ANALYSIS OF PSD AND SURVIVIN SUBCELLULAR DISTRIBUTION

Currently, several bioinformatics prediction tools can be used to predict sorting of proteins into the different subcellular compartments including the mitochondria such as Psort or MitoProt II. Given that such tools are designed to distinguish canonical N-terminal presequences based on a defined set of characteristics (amino acid content, hydrophobicity), they can most frequently detect only proteins with obvious canonical targeting sequences, and even so can

be quite unreliable (Emanuelsson & Von Heijne, 2001). Therefore, mitochondrial localization of proteins with internal or otherwise unusual cryptic mitochondrial targeting sequences cannot be predicted through such tools and fully relies on experimental confirmation. For instance, though the enzyme PSD has been previously characterized as a mitochondrial protein that follows the presequence import pathway, it is still wrongly assigned to other compartments by some prediction programs (Table 3-1). Therefore, though survivin was not recognized as mitochondrial by these prediction tools (Table 3-1) does not necessarily mean it is not present in this compartment. On the contrary, its targeting into three distinct compartments, namely cytoplasm, nucleus and mitochondria, seems to indicate an intricate mechanism of survivin localization regulation is in place which might require multiple cryptic signals.

	PSD	Survivin	Reference
iPSORT	No mito presequence	No mito presequence	(Bannai et al., 2002)
PSORTII	Cytoplasmic	Cytoplasmic	(Nakai & Horton, 1999)
MitoProtII	Mitochondrion	Non mitochondrial	(Claros, 1995)
ngLOC	Mitochondrion	Cytoplasm/nucleus	(King & Guda, 2007)
iLoc-Euk	Mitochondrion	Cytoplasm	(Chou et al., 2011)
Hum-mPLoc 2.0	Endoplasmic reticulum	Cytoplasm/Nucleus	(Shen & Chou, 2009)
TargetP	Mitochondrion	Non mitochondrial	(Emanuelsson et al., 2000)
MitoFates	No mito presequence	No mito presequence	(Fukasawa et al., 2015)
Predotar	Possibly mitochondrial	No prediction	(Small et al., 2004)

Table 3-1. Prediction of subcellular localization of PSD and survivin by different prediction programs

The N-terminal portions of the PSD and survivin protein sequence were also analysed manually using Pepwheel to determine whether they possess any presequence characteristics. As expected for PSD, which had been not only predicted (Table 3-1) but experimentally confirmed as a mitochondrial protein, its first 19 residues arranged as an amphipathic α-helix (Figure 3-5). The first secondary structure element, a β-sheet, of survivin BIR domain initiates at residue 15, with the preceding 15 residue segment assuming a relatively extended conformation (Verdecia et al., 2000). Therefore, the amphipathic potential of the first 10 and 15

residues was analysed, with the first 19 residues also tested (Figure 3-5). Interestingly, a tendency for the hydrophobic residues to cluster on one side of the helix could be seen, though the other face contained a mixture of positively and negatively charged residues, and so lacked the characteristic positive charge. Unusually the first ten amino acid stretch is highly enriched in proline residues which might be important for assuming a particular conformation for mitochondrial targeting.

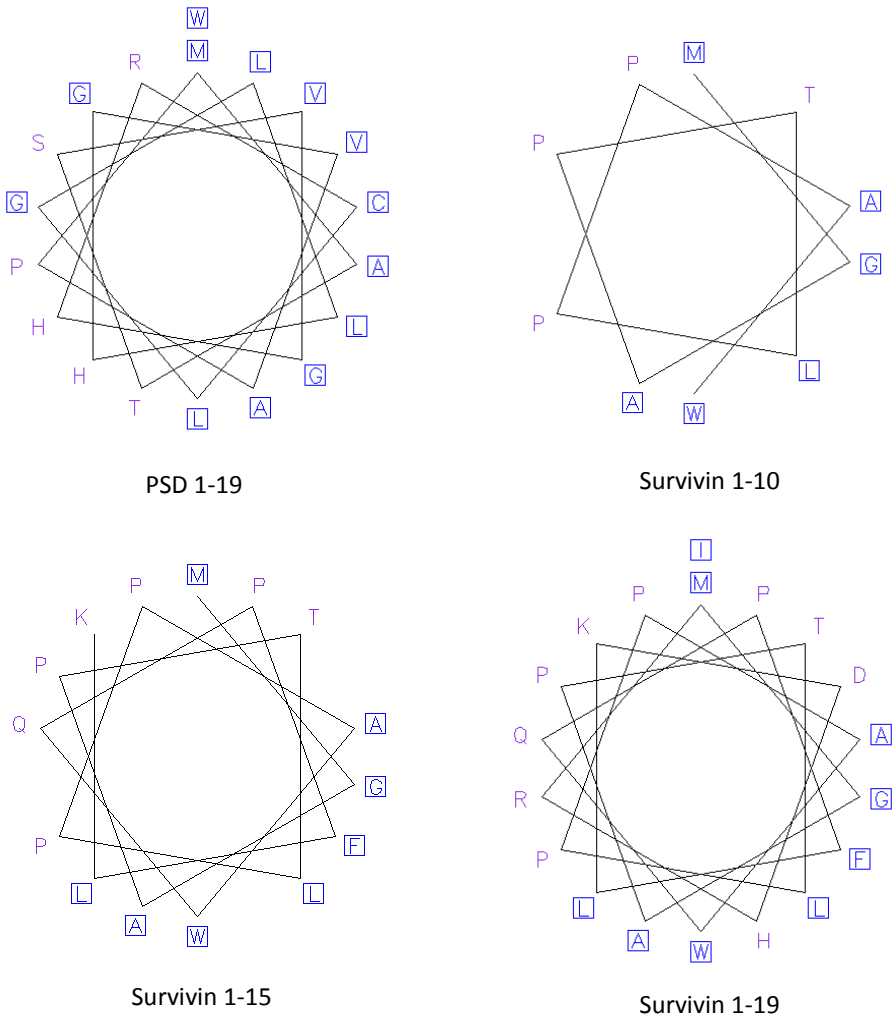


Figure 3-5. *In silico* analysis of human PSD and survivin N-termini to identify potential MTS. N-terminal residues 1-19 of PSD and residues 1-10, 1-15 and 1-19 of survivin were plotted with helical wheel to assess the potential to form amphipathic α-helices and possibly act as presequences for targeting into mitochondria. Hydrophobic residues were marked as squares, polar and charged residues were left unmarked.

3.4.4 Subcellular localization of ectopically expressed Survivin and PSD in HeLa cells

HeLa cells stably expressing GFP alone as a negative control, survivin-GFP or a chimeric protein consisting of only the first ten amino acids of survivin fused to GFP (survivin$_{1-10}$-GFP) were stained for mitochondria and then imaged live to ascertain the localization of said constructs in the cell. As shown in Figure 3-6A, GFP was diffuse throughout the cell, whereas survivin-GFP expression was largely cytoplasmic with less intense and sometimes punctuate expression seen in the nucleus. The survivin puncta observed in the nucleus might be the result of survivin accumulation at sites of DNA damage or at condensing chromosomes preparing to enter mitosis. As a result of this, specific localisation of survivin-GFP to the mitochondria was not observed. However, though survivin$_{1-10}$-GFP was also expressed throughout the cell it was also decorating the mitochondria, stained with Mitotracker CMXRos red, in a very obvious manner. This suggests that the first 10 residues of survivin could be contributing to mitochondrial targeting of survivin. Alongside, the mitochondrial localization of PSD was corroborated with Flag-tagged PSD transiently transfected into HeLa cells together with mitoRFP which is designed to accumulate in the mitochondria only and allow their visualization. Indeed, PSD-FLAG colocalized fully with mitoRFP labelled mitochondria (Figure 3-6B).

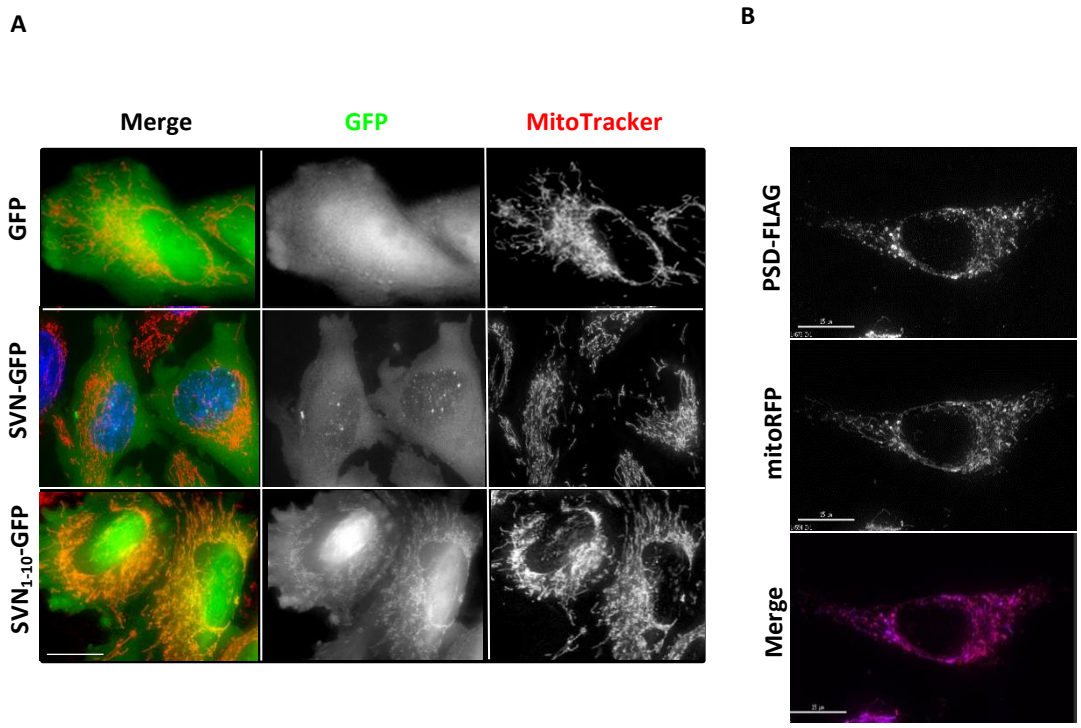


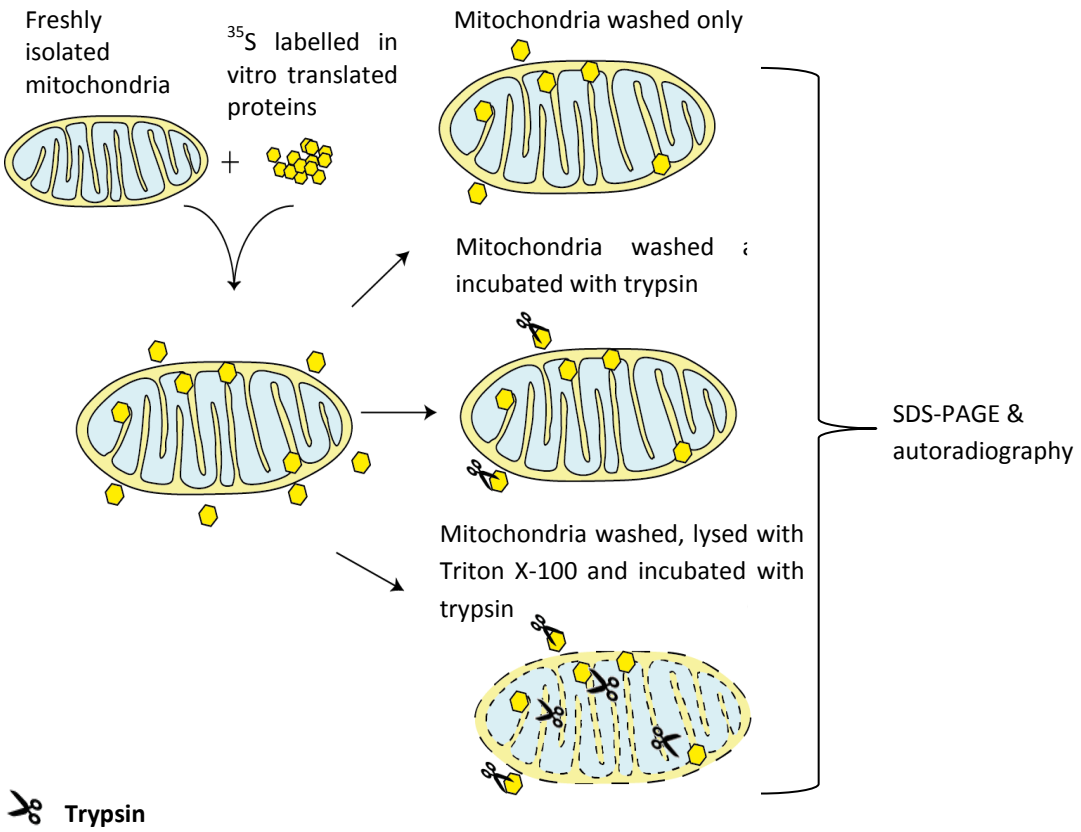
Figure 3-6. Localization of survivin and PSD in HeLa cells. **(A)** HeLa cells overexpressing GFP, survivin-GFP or survivin$_{1\text{-}10}$-GFP were stained for mitochondria with MitoTracker Red and imaged live using an inverted Olympus Axiophot, Delta Vision Elite microscope with 63x oil objective. **(B)** HeLa cells on coverslips were transiently transfected with PSD-FLAG and mitoRFP, fixed and stained with FLAG M2 antibody prior to imaging as in A. Scale bar 15µm.

3.4.5 MITOCHONDRIAL IMPORT OF SURVIVIN AND PSD

The preferred method for elucidating protein import into mitochondria is the *in vitro* mitochondrial import assay of radiolabelled precursor proteins. In this assay, freshly isolated energised mitochondria are incubated with excess protein precursors synthesized in a cell-free system to incorporate a radioactive label. Following an incubation period to allow for the import to take place, removal of non-imported precursors by washing the mitochondria yields information on the precursors that have translocated into the mitochondria but also the ones that remain engaged with the OMM. Additionally, washed mitochondria are treated with the protease trypsin which is excluded from intact mitochondria and so can degrade only precursors present at the OMM. In this manner, only fully imported mitochondrial proteins are detected. As a control, the mitochondria were detergent

solubilized and trypsin treated which was expected to remove all signal as also proteins translocated into the mitochondria would be accessible to protease degradation. Therefore this assay, summarized in the schematic of Figure 3-7A was employed to analyse the import of PSD and survivin. Moreover, given the apparent mitochondrial localization of survivin$_{1-10}$-GFP in fluorescence microscopy in Figure 3-6A, the import of this construct was analysed to ascertain the importance of the first ten residues in survivin mitochondrial import. This was complemented with import analysis of a corresponding survivin construct lacking the first ten amino acids - survivin$_{11-142}$. GFP alone which localizes diffusely in the cytoplasm and nucleus was used as a negative control for mitochondrial import. Conversely, GFP fused at its N-terminus with a mitochondrial targeting signal peptide of cytochrome c oxidase subunit VIIIA amplified from U2OS cDNA was used as a positive control for the import reaction. As expected, MTS-GFP was present in mitochondria both before and after trypsin removal of all non-imported proteins at the OMM, whereas GFP alone was absent in both conditions (Figure 3-7B). PSD was also successfully imported into mitochondria as shown by its continued presence also following trypsin treatment, as was full length survivin (Figure 3-7C). Survivin$_{1-10}$-GFP was clearly engaging with the OMM (mitochondria not treated with trypsin) and could be imported into mitochondria albeit less efficiently than full length survivin (Figure 3-7B). However, survivin lacking the first 10 amino acids (survivin$_{11-142)}$ could also translocate into the mitochondria, suggesting the presence of additional signals in the protein sequence of survivin which guide its mitochondrial entry (Figure 3-7C). Given that only a crude mitochondrial preparation was used for this experiment, some degree of cytosolic contamination might still be present where a cytosolic factor could be acting as a chaperone for survivin import. However, taken together these findings clearly show that survivin can enter mitochondria using the first 10 amino acids in addition to further so far unknown mitochondrial targeting signal/s. PSD, as a previously characterized mitochondrial protein, could also be efficiently imported.

A


Freshly isolated mitochondria
^{35}S labelled in vitro translated proteins
Mitochondria washed only
Mitochondria washed a
incubated with trypsin
SDS-PAGE &
autoradiography
Mitochondria washed, lysed with Triton X-100 and incubated with trypsin
Trypsin

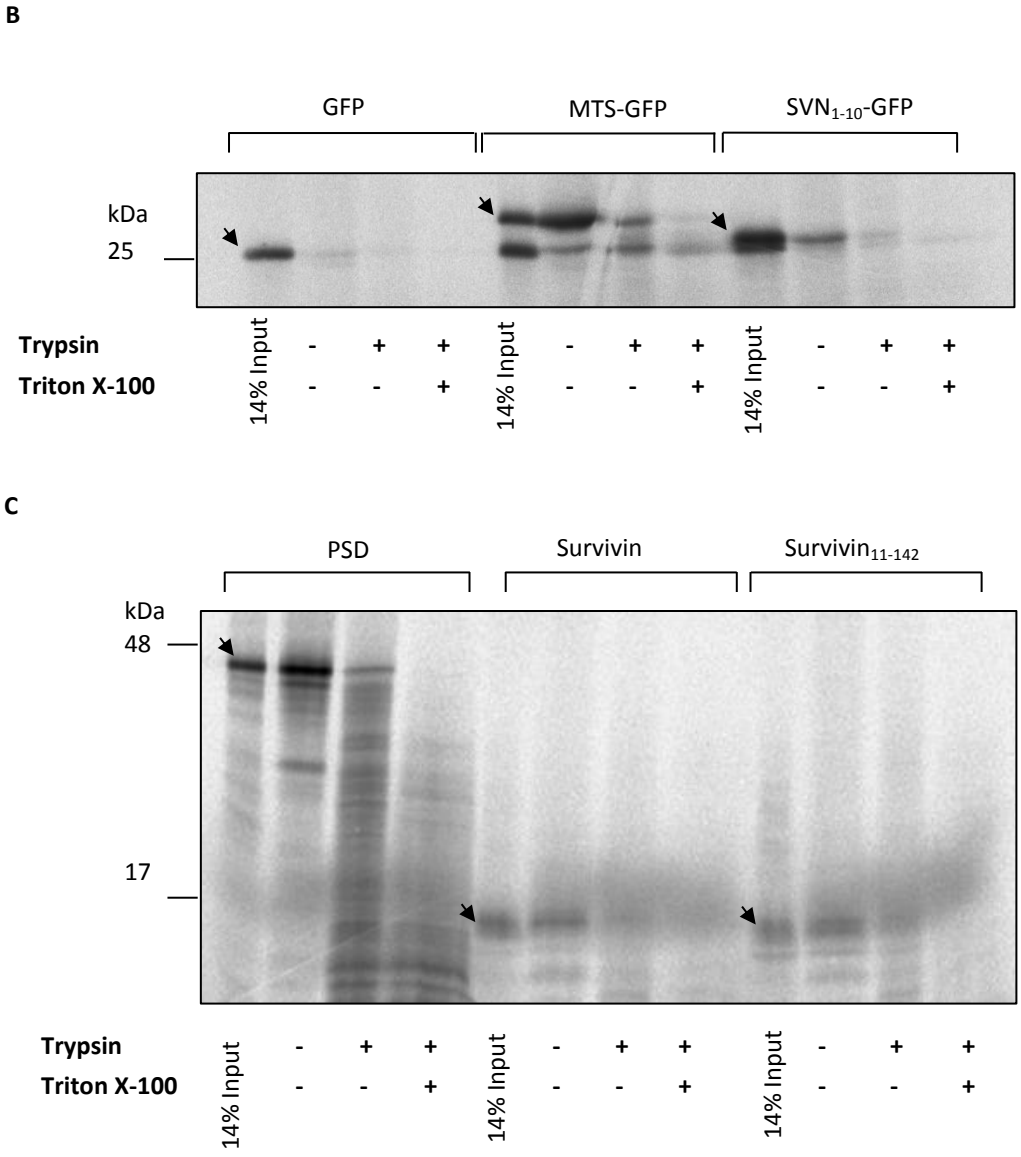


Figure 3-7. *In vitro* import of radiolabelled GFP, MTS-GFP, Survivin$_{1-10}$-GFP, PSD, Survivin$_{wt}$ and Survivin$_{11-142}$ into isolated HeLa mitochondria. (A) Schematic diagram of the import experiment layout (B) GFP, MTS-GFP and Survivin$_{1-10}$-GFP were synthesized from rabbit reticulocyte lysate incorporating ^{35}S-Methionine in 25µl reaction volume. Such radiolabelled lysates were incubated with 60µg isolated Hela mitochondria for 1 hour at 37°C. Following import, samples were washed and reisolated and left untreated, treated with 150µg/ml trypsin alone or in combination with 1% Triton X-100. The protease was inactivated with AEBSF, samples were mixed with 5x sample buffer, boiled and analysed by SDS-PAGE. Alongside, 1µl of the *in vitro* translated products, corresponding to approximately 14% of the lysate used in the import reaction, were also analysed. The translated proteins are indicated with black arrows in their respective Input lanes. (C) PSD, Survivin$_{wt}$ and Survivin$_{11-142}$ were treated as in (B). Apart from GFP alone, all expressed proteins interact with the outer mitochondrial membrane and can be imported into the mitochondria with varying efficiency.

3.4.6 SUBMITOCHONDRIAL LOCALIZATION OF SURVIVIN AND PSD

Submitochondrial localisation of a protein is important when considering potential function and potential interactions with other proteins. Thus, to determine the submitochondrial localisation of survivin, two distinct approaches were undertaken. First, a protease protection assay of mitochondria was employed as shown in schematic (Figure 3-8A). Briefly, isolated HeLa mitochondria were treated when intact with both low and high concentrations of trypsin such that only outer membrane proteins should be accessible to the protease. Next, the mitochondria were swollen with osmotic shock to remove the outer membrane and expose all proteins in or facing the intermembrane space to trypsin degradation. Finally, mitochondria were solubilised with detergent where also matrix components became exposed to protease degradation. The different treatments were monitored via a set of markers for each mitochondrial subcompartment, that is, mitochondrial proteins with well characterized submitochondrial localization. In this experiment, the markers used were Hsp60 for mitochondrial matrix and CoxII for intermembrane space/inner mitochondrial membrane. As would be expected, both mitochondrial markers Hsp60 (matrix) and CoxII (IMS/IMM) were unaffected when intact mitochondria were incubated with trypsin (Figure3-8B). Indicative of also being shielded by the OMM, PSD and Survivin were found to be similarly unaffected by trypsin during this treatment. Therefore, both PSD and survivin are clearly not present in the OMM. However, the IMS/IMM marker CoxII and also PSD and survivin were degraded after the loss of outer mitochondrial membrane indicating a shared mitochondrial subcompartment i.e. intermembrane space. On the other hand, the matrix protein Hsp60 was unaffected: only at higher trypsin concentrations some degradation was seen suggesting that the swelling treatment possibly lysed also the inner mitochondrial membrane of some mitochondria. Finally, as expected, trypsin was able to degrade all proteins after detergent lysis, including the innermost matrix marker Hsp60. Collectively these data suggest that survivin resides in the intermembrane space of mitochondria, which is simultaneously the site of PSD residence.

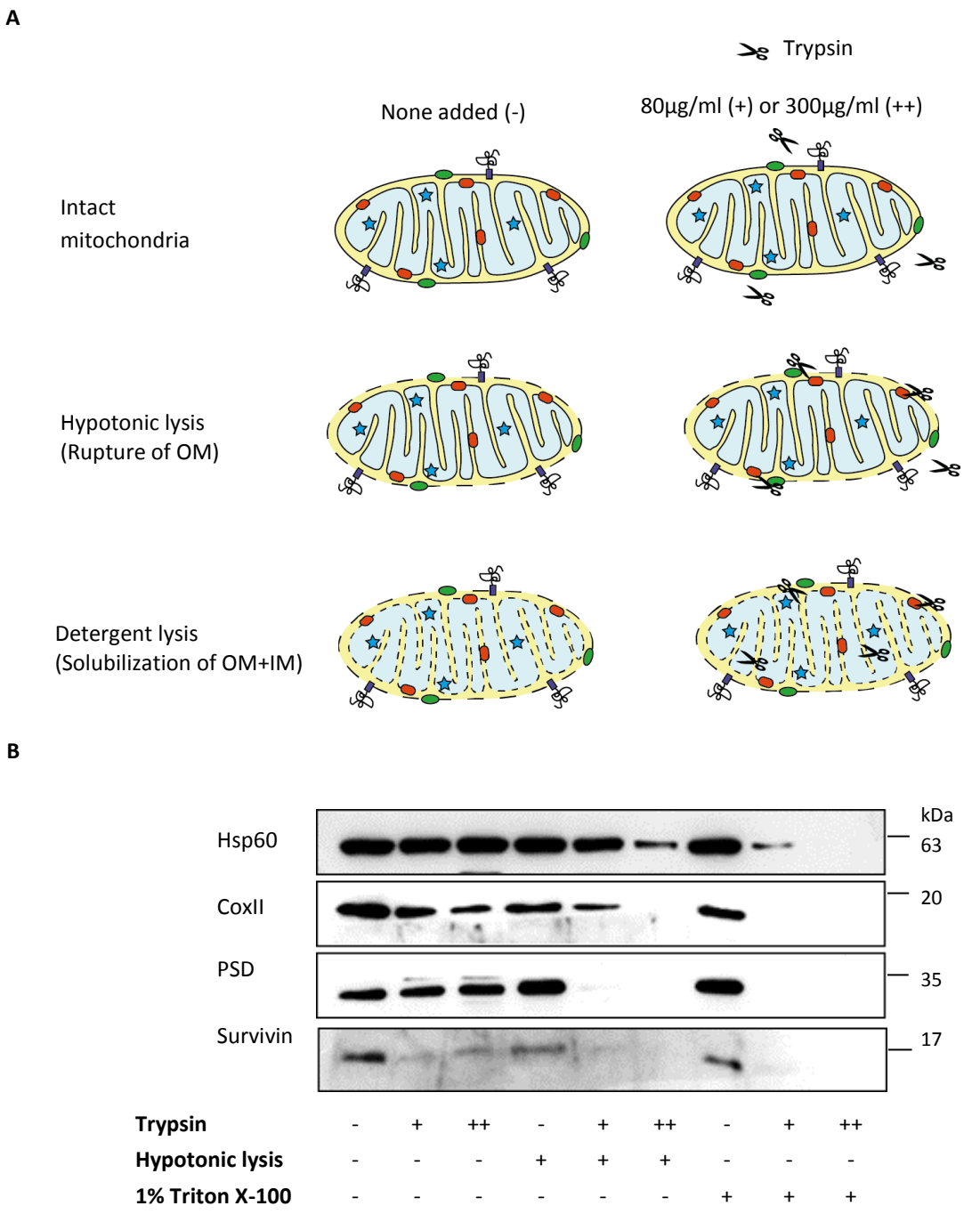


Figure 3-8. Survivin resides in the intermembrane space of the mitochondrion together with PSD. (A) Schematic diagram of the experiment. (A+B) Purified HeLa mitochondria were either used intact, swollen in hypotonic buffer to generate mitoplasts, or solubilized with detergent Triton X-100 and then left untreated (-), treated with 80µg/ml trypsin (+) or 300µg/ml trypsin (++) for 25 minutes on ice, followed by inactivation with AEBSF. The markers used to determine the submitochondrial localization of survivin were Hsp60 for matrix and CoxII for intermembrane space/inner mitochondrial membrane. Both PSD and survivin were localizing in the intermembrane space as previously described. 20µg of mitochondria was loaded.

A second approach for assessing the submitochondrial localization of PSD and survivin consisted of incubating isolated HeLa mitochondria with increasing concentrations of digitonin to progressively permeabilize mitochondrial membranes. Using this method, outer membrane proteins should be extracted first, then intermembrane space proteins, inner membrane proteins, and finally matrix components. To ensure efficacy of this treatment a set of antibodies was used as markers to identify known components of each compartment in immunoblotting: outer mitochondrial membrane (VDAC), intermembrane space (cytochrome c), inner mitochondrial membrane (CoxII) and mitochondrial matrix (Hsp60) (Figure 3-9). Cytochrome c was extracted with relative ease which was expected given it is a soluble protein within the IMS that can leak out of holes in the OMM, with levels steadily declining until essentially full extraction at 0.125% digitonin. In contrast, VDAC proved more resistant to digitonin extraction than cytochrome c even though it is located in the OMM. The reason for this difference is that extraction of VDAC is more challenging as it forms a pore embedded in the membrane though its levels also declined more noticeably by 0.095% digitonin. Next, the IMM marker CoxII was abruptly extracted by 0.125% digitonin whereas the matrix marker Hsp60 levels only moderately declined also at the highest digitonin concentration. PSD was extracted under identical conditions to CoxII, at 0.125% digitonin which further strengthened its allocation to the IMS/IMM. In contrast, the survivin signal in the mitochondria proved highly variable and did not seem to follow the same declining trend of other markers. Nonetheless, given a lot of survivin remained in the mitochondria also after 0.5% digitonin treatment similarly to Hsp60, it could be assigned to the matrix.

Altogether, the two methods for assessment of submitochondrial localization unanimously allocated PSD in the IMS/IMM. Similarly, the protease protection assay revealed survivin also resides in the IMS. However, the second method of digitonin extraction indicated survivin was in the matrix. Therefore, since the focus of this study is the investigation of a possible cross-talk between PSD and

survivin, this proposition has been given further support by survivin at least partially sharing the same submitochondrial compartment, the IMS, as PSD.

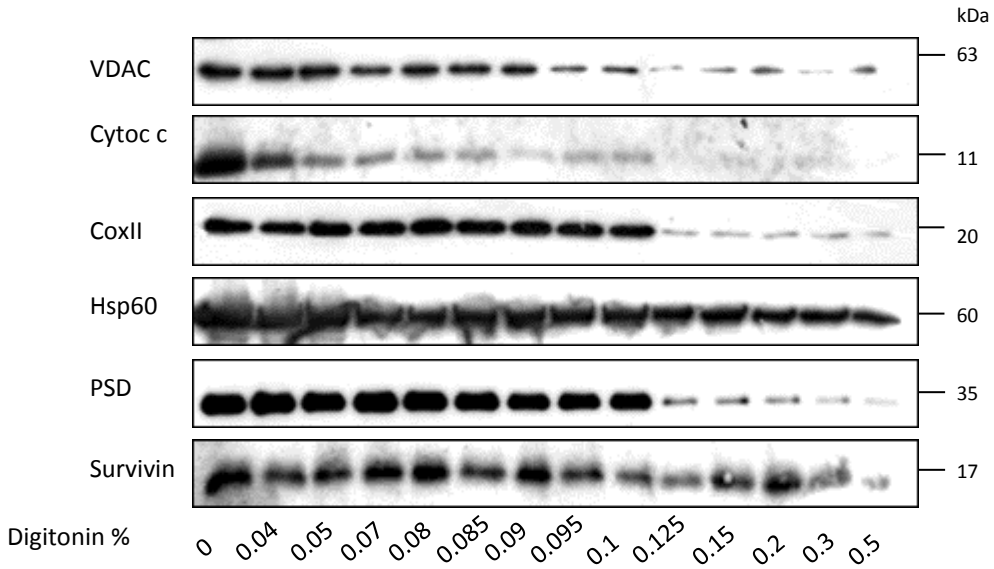
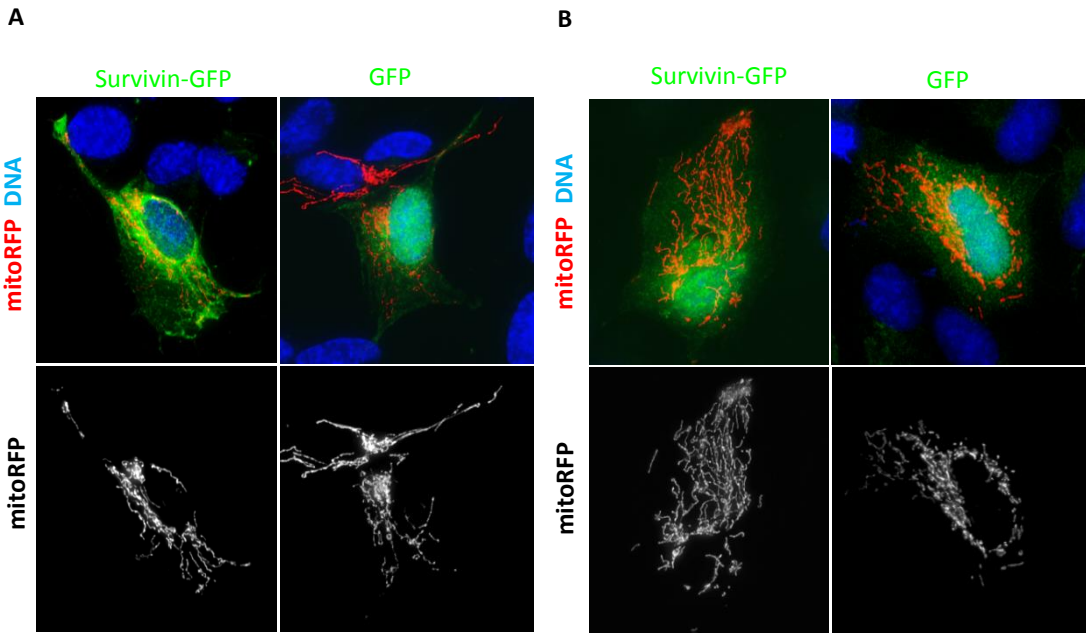


Figure 3-9. Submitochondrial targeting of survivin. Purified HeLa mitochondria were incubated with increasing concentrations of digitonin to selectively permeabilize the mitochondrial membranes. VDAC was used as a marker of outer mitochondrial membrane, cytochrome c for intermembrane space, CoxII for mitochondrial inner membrane and Hsp60 for mitochondrial matrix. PSD was extracted similarly to CoxII which is consistent with PSD being inserted into the inner mitochondrial membrane. 25μg of mitochondria was loaded.

3.4.7 OVEREXPRESSION OF SURVIVIN DOES NOT AFFECT MITOCHONDRIAL MORPHOLOGY

Overexpression of survivin in HeLa cells caused no obvious changes in the tubularity of mitochondrial networks (Figure 3-6A). To determine whether overexpression of survivin could affect mitochondrial morphology or organisation in other cell types distinct from HeLa cells, the neuroblastoma cell line SH5YSY and immortalized retinal pigment epithelial cell line RPE-1 seeded on glass coverslips were both transiently transfected with GFP or survivin-GFP and the mitoRFP construct to label mitochondria, fixed, mounted on glass slides and imaged (Figure 3-10A and B). However, as for HeLa cells, no changes in mitochondrial morphology were observed in these cell lines.

To exacerbate any potential problems that might arise due to survivin expression in the mitochondria, constructs were generated with a mitochondrial targeting signal (MTS) derived from cytochrome c oxidase subunit VIIIA at the N-terminus fused to either GFP, as mentioned previously, or to survivin-GFP. The ability of these constructs to effectively target solely to the mitochondria and not to any other compartment was tested by assessing their colocalisation with MitoTracker red labelling the mitochondria. Indeed, transient transfection of HeLa cells showed both MTS-GFP and MTS-survivin-GFP were successfully expressed only in the mitochondria of HeLa cells. More importantly, presence of such high survivin levels in the mitochondria showed no difference in mitochondrial appearance when compared to MTS-GFP expressing cells (Figure 3-10C).



C

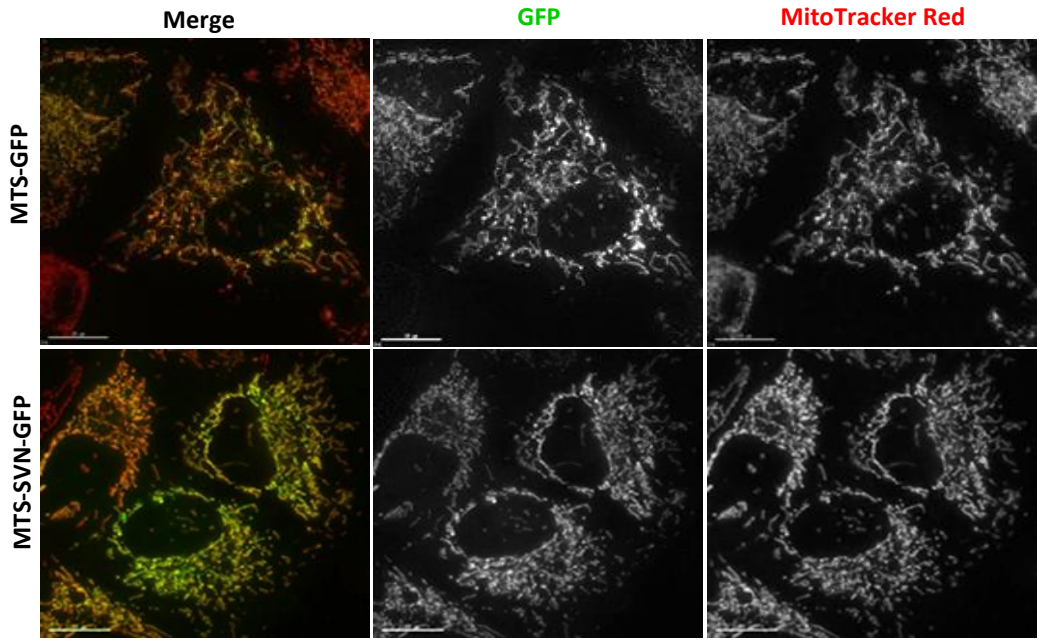


Figure 3-10. Survivin overexpression at whole cell level or restricted into mitochondria does not have any effect on the integrity of mitochondrial networks. (A) SH5YSY cells and **(B)** RPE-1 cells were transiently co-transfected with GFP or survivin-GFP together with mito-RFP and stained with Hoechst 33342 for DNA, fixed and imaged using an inverted Olympus Axiophot, Delta Vision Elite microscope with 63x oil objective. (**C)** HeLa cells were transiently transfected with chimeric proteins consisting of a mitochondrial targeting signal (MTS) fused to either GFP or survivin-GFP, the mitochondria stained with Mitotracker Red and imaged live using an inverted Olympus Axiophot, Delta Vision Elite microscope with 63x oil objective. Scale bar 10µm.

3.5 DISCUSSION

The present study focused on the analysis of the mitochondrial pool of survivin. With respect to the different phases of the cell cycle, this pool was found to be particularly enriched at G_2/M phase. Analysis of tumour versus non-tumour cell lines revealed survivin is more abundant in the mitochondria of tumour cells, though with quantitative differences also across different tumour cell lines. Ectopic expression of survivin-GFP in HeLa, SH5YSY and RPE-1 cells showed no detrimental effects on mitochondrial morphology. In addition, ectopic targeting of survivin-GFP exclusively in the mitochondria of HeLa cells was similarly without any consequences. With regards to PSD and survivin involvement in the mitochondria, both PSD and survivin could be efficiently imported into isolated HeLa mitochondria. Moreover, the first 10 amino acids of survivin were shown to

contribute to survivin mitochondrial targeting though further signals are required as survivin$_{11-142}$ lacking this initial stretch was still imported. Additionally, PSD and survivin were shown in the same submitochondrial compartment, namely the IMS.

3.5.1 CIRCUMSTANCES OF SURVIVIN MITOCHONDRIAL LOCALIZATION

Previous reports have described survivin as subject to cell-cycle dependent regulation with highest expression seen at G_2/M phase (Jiang et al., 2001; Li et al., 1998a; Zhao et al., 2000). In the present study, subfractionation of synchronized HeLa cells also showed an accumulation of mitochondrial survivin at G_2/M phase which could be indicative of a functional coordination between survivin in CPC and mitochondrial survivin. Alternatively, such observation could be due to overall higher survivin levels present at mitosis, providing a larger survivin pool that can be translocated into the mitochondria. A panel of normal and tumour-derived cell line subfractionations showed varying degrees of survivin expression in whole cell extracts and mitochondria of tumour cells to complete absence in normal cells. Therefore, since in the present study only asynchronous normal cells were fractionated, it remains to be ascertained whether possibly a similar accumulation of survivin at M phase occurs also in normal cells. Nonetheless, the presence of survivin in the mitochondria of predominantly cancer cells, with an additional increase at mitosis, suggests its role is to further promote tumorigenesis. Indeed, a previous report established survivin could be imported indistinguishably into mitochondria isolated from normal tissue or a tumour cell line, however, addition of cytosolic extracts from normal liver abolished import into the tumour mitochondria indicating the presence of additional factors in tumour cells which enable survivin import *in vivo* (Kang et al., 2011a). Moreover, it was shown specifically mitochondrial survivin enacted protection against apoptosis (Dohi et al., 2004a, 2007). Survivin mostly functions as an adaptor protein where interacting with other proteins allows it to participate in numerous processes. It is possible the repertoire of its interacting partners and so functions is effectively expanded via mitochondrial targeting, gaining a proliferative advantage for cancer cells.

3.5.2 MITOCHONDRIAL IMPORT OF SURVIVIN

Mitochondrial preproteins can be translocated into the mitochondria only if present in a particular conformation which is achieved via association with cytosolic factors. These bind to nascent mitochondrial polypeptides in the cytosol, maintaining them in an unfolded or partially folded state hence preventing their aggregation. The presequence binding factor (PBF) or mitochondrial import stimulation factor (MSF) have been identified as possible import accessory cytosolic factors (Hachiya et al., 1994; Murakami et al., 1992). The cytosolic chaperones Hsp70 and Hsp90, which oversee cellular protein quality control, also direct preproteins in an import-competent state to the Tom70 receptor of the TOM complex (Fan et al., 2006; Young et al., 2003). A similar chaperone-like activity for the Tom20 receptor might be performed by the immunophilin aryl hydrocarbon receptor-interacting protein (AIP)(Yano et al., 2003). Though survivin has been shown to interact with both Hsp90 and AIP, it is the latter which was postulated to be required for mitochondrial targeting of survivin via the Tom20 receptor as determined in pulldown studies (Fortugno et al., 2003; Kang & Altieri, 2006; Kang et al., 2011a). However, the requirement for AIP for survivin import into mitochondria was uncompelling as data presented showed wild type survivin or survivin$_{1\text{-}141}$ truncation mutant, which can reportedly no longer associate with AIP, being imported into mitochondria with similar efficiency. Indeed, also in the present study survivin was imported into mitochondria in the absence of external factors suggesting sufficient targeting information is present within survivin sequence.

We focused on investigating the potential of survivin N-terminus to act as a mitochondrial targeting sequence given this is the frequent location of targeting sequences. Fluorescence imaging showed the first ten amino acids of survivin fused to GFP diffuse throughout the cell in addition to clearly colocalising with the mitochondrial stain MitoTracker, which prompted testing this construct in import experiments. The first 10 amino acids of survivin (survivin$_{1\text{-}10}$) supported the import

of its fusion GFP partner albeit inefficiently compared to full length survivin. However, survivin lacking these residues was still import-competent which suggested though loss of amino acids 1-10 was insufficient to completely abolish survivin mitochondrial targeting, it might be a contributing factor given the extent of association seen with the OMM. Constructs comprising the first 14, 21, 26 and 30 amino acids of survivin fused to GFP or the full length survivin lacking these residues were made in our laboratory and are yet to be tested in import experiments. Though survivin N-terminus is quite rich in hydrophobic residues which cluster together in a helical conformation, it lacks a high number of positively charged amino acids typical for mitochondrial presequences. Nonetheless, it could still constitute at least a partial mitochondrial targeting signal which is not cleaved upon import.

The finding that survivin resides in the intermembrane space of mitochondria, in agreement with previous studies by Dohi et al. (2004), presents an exciting possibility of survivin as a client protein of the MIA import pathway. The key players of this pathway are Mia40, an oxidoreductase which binds to cysteine-rich substrate proteins ensuring their folding by correct disulphide bridge formation, and ALR (in humans, Erv-1 in yeast), flavin-dependent sulfhydryl oxidase, which reoxidizes Mia40 and itself via transferring electrons to the respiratory chain (Allen et al., 2005; Banci et al., 2009; Bihlmaier et al., 2007; Fischer et al., 2013). Mia40 recognizes substrate proteins of up to 27kDa, with typical twin cysteine motifs CX_9C, CX_3C or CX_2C (ALR) and in possession of a consensus 9 amino acid stretch near one of the motifs, X[R]XX[Hy][Hy]XXC, where particularly the arginine and the two hydrophobic residues are essential and allow docking of a single cysteine residue of the motif into Mia40 (Gabriel et al., 2007; Milenkovic et al., 2009; Sideris et al., 2009). However, other unusual cysteine motifs have been reported as binding to Mia40 in yeast (Vogtle et al., 2012). Though all MIA substrate proteins described to-date are oxidatively folded upon IMS import, the possibility of MIA acting as a folding chaperone only still remains (Neupert, 2015). This is evidenced by Atp23 protease engineered to have all cysteine residues

substituted to serines and still being efficiently imported (Weckbecker et al., 2012). Though survivin does not contain the specified twin motifs or the consensus peptide motif, it has six cysteine residues in total as possible sites for Mia40 docking. Three cysteines (Cys57, 60, 84) are universally conserved across all species as they are involved in coordinating the zinc atom within the BIR domain, however, the remaining three cysteines also show good degree of conservation (Chantalat et al., 2000). Therefore, the possibility that survivin is imported into the IMS via Mia40 still remains to be established.

3.5.3 Effect of ectopic survivin expression at the level of mitochondria in different cell types

A previous report by Hagenbuchner et al. (2012) showed survivin overexpression in neuroblastoma SH-EP cell line caused mitochondrial fragmentation due to increase in the fission driving protein Drp1. Therefore, given that no such defect in mitochondrial fusion was observed in HeLa cells overexpressing survivin, further cell lines, namely the neuroblastoma SH5YSY cell line and retinal pigmented epithelial RPE-1 cell line were also transiently transfected with survivin-GFP. As with HeLa, there was no change in mitochondrial morphology in these cells. Further enhancement of the mitochondrial survivin pool in HeLa cells via transfection of survivin-GFP fused to a mitochondria targeting signal of cytochrome c oxidase subunit VIIIA also did not generate an obvious phenotype. A possible explanation for the discrepancies observed could be the use of GFP-tagged survivin in the present study which could be masking certain domains of the protein necessary for mediating its effects in the mitochondria. Moreover, whereas the present study employed commercially available transfection reagents for expression of desired GFP-tagged proteins either stably via selection with geneticin or transiently (24-48 hours), Hagenbuchner et al. (2012) used retroviral transduction to generate untagged survivin overexpressing stable cell lines.

In conclusion, the present study demonstrated survivin is present in the mitochondria of cancer cells, which suggests a tumour-promoting function rather than a physiologically important role also in normal cells. Moreover, its mitochondrial accumulation specifically at G_2/M phase of the cell cycle could be indicative of a cross-talk between survivin at the CPC and the pool in the mitochondria, possibly directing successful mitochondrial division. Though full mitochondrial targeting signal of survivin is still elusive, this study found the first ten amino acids of survivin are a contributing element. More importantly, survivin was found to colocalize in the intermembrane space of the mitochondria with PSD, the putative survivin interacting partner being investigated in this study (Chapter 4).

4 DOES SURVIVIN HAVE A ROLE IN AMINOPHOSPHOLIPID SYNTHESIS?

4.1 MITOCHONDRIAL SURVIVIN IN CYTOPROTECTION

We (Chapter 3) and others have shown that a small pool of survivin localizes to the intermembrane space of the mitochondria in tumour but not normal cells, pointing to a further possible pro-survival mechanism exploited by cancer (Dohi et al., 2004a). Perhaps the most acknowledged role of mitochondria, beside that of maintaining cellular ATP levels via oxidative phosphorylation, is to respond to various cell damaging stimuli through induction of apoptotic cell death. As indicated by low apoptotic index in a vast array of tumours associated with survivin overexpression, survivin has a known cytoprotective effect which has been investigated in connection to its mitochondrial pool. Indeed, several studies focusing on possible mechanisms of apoptosis evasion orchestrated by mitochondrial survivin have been published to-date and will be discussed. Initial support originated from characterization of mitochondrial survivin deficient rat insulin secreting beta cell derived line (INS-1) with high sensitivity to apoptosis induction, which was abolished by survivin overexpression in the mitochondria (Dohi et al., 2004a). Following apoptosis onset, MOMP causes the release of mitochondrial survivin into the cytosol which is accompanied by attenuation of caspase-9 activation (Dohi et al., 2004a). Differential regulation of cytosolic and mitochondrial pools of survivin is achieved via compartmentalized protein kinase A (PKA)-mediated phosphorylation of survivin on Ser20. Only non-S20-phosphorylated mitochondrial survivin released into the cytosol can bind to and stabilize XIAP enhancing its caspase inhibitory activity (Dohi et al., 2007). Moreover, following DNA damage upregulation of mitochondrial survivin prevents the release of Smac/DIABLO from the mitochondria through direct interaction, intercepting the latter's inhibitory effect on XIAP (Song et al., 2003; Ceballos-Cancino et al., 2007). Conversely, overexpression of mature Smac in ovarian carcinoma cells causes cytochrome c independent caspase-9 activation and apoptosis accompanied by

downregulation of survivin (McNeish et al., 2005). In this instance, survivin-Smac interaction had no effect on Smac-induced apoptosis, and instead survivin was directed for proteasomal degradation (McNeish et al., 2005). The importance of particular survivin subcellular distributions for its different roles is highlighted by the fact that forced confinement of survivin to the nucleus prevents survivin from protecting cells against apoptotic stimuli (X-irradiation, TRAIL) (Colnaghi et al., 2006; Connell et al., 2008).

4.2 AMINOPHOSPHOLIPID SYNTHESIS IN THE MITOCHONDRIA

From the information above it might seem reasonable to hypothesise that survivin resident in the mitochondria might be exerting its anti-apoptotic activity via this organelle. However, besides the aforementioned roles, mitochondria are important for the biosynthesis of various cell components (iron-sulphur clusters, heme, biotin, lipids, etc.), many of which mitochondria are the sole provider of (Herrmann & Riemer, 2010). This chapter focuses on exploring a possible cross-talk between survivin and the enzyme phosphatidylserine decarboxylase, which converts the phospholipid phosphatidylserine into phosphatidylethanolamine. Though phospholipids are often thought of as mere building blocks of cellular membranes, their participation in different processes and signalling pathways is becoming more evident. Different cell types and different organelles within these cells have defined composition of specific phospholipids which is essential for supporting the protein network. Cardiolipin is a unique mitochondrial phospholipid present solely in the mitochondrial membranes, which together with PE represent the non-bilayer phospholipids i.e. their polar headgroup is much smaller than the hydrophobic side chains providing them with a characteristic cone shape. Inclusion of these phospholipids, which do not support formation of bilayers, imposes curvature stress on the membrane (Hui et al., 1981; Verkleij et al., 1984). The specific proportion of bilayer and non-bilayer forming phospholipids within mitochondrial membranes is a requisite for allowing the characteristic membrane curvature of the cristae as well as the constant cycles of fusion and fission which

give rise to a dynamic network of interconnected mitochondria (Verkleij et al., 1984; Martens & McMahon, 2008).The importance of cardiolipin for mitochondrial structure and function has been described in connection to mitochondrial diseases such as Barth syndrome (Yan & Kang, 2011; Lu & Claypool, 2015). However, novel functions of phosphatidylethanolamine (PE) which comprises about 30% of mitochondrial phospholipids have also surfaced and are summarized in Chapter 1.

As mentioned, mammalian cells have several pathways for PE procurement, mainly the PS decarboxylation pathway (via the enzyme phosphatidylserine decarboxylase at the outer surface of mitochondrial inner membrane) and the CDP-ethanolamine pathway, which terminates in the ER (Kennedy & Weiss, 1956; Percy et al., 1983). Other possible but only minor routes involve PS synthase-2 which catalyses the exchange of the serine headgroup of phosphatidylserine (PS) for ethanolamine, and lyso-PE acetyltransferase catalysed acetylation of lyso-PE to PE (in mitochondria associated membranes or MAM) (Sundler et al., 1974; Riekhof & Voelker, 2006). The relative contributions of the individual pathways to cellular PE appear to vary among cell types, however, most of the PE found in mitochondrial membranes originates from PSD which decarboxylates PS imported from the ER into mitochondria-associated membranes (MAM) and then mitochondria (Shiao et al., 1998; Bürgermeister et al., 2004; Kainu et al., 2013). Interestingly, the two main pathways for PE synthesis are non-redundant as knock out of PSD or the rate limiting enzyme of the Kennedy pathway are both embryonically lethal, suggesting compartmentalized PE production has physiological relevance (Steenbergen et al., 2005; Fullerton et al., 2007). Indeed, PSD -/- embryos presented with fragmented, rounded and dispersed mitochondria in contrast to the elongated shape of mitochondria from wild-type embryos even though the CDP-ethanolamine pathway was fully functional (Steenbergen et al., 2005). A screen of potential novel survivin interacting partners via tandem mass spectroscopy analysis with GST-survivin incubated with extracts from HeLa cells revealed the enzyme phosphatidylserine decarboxylase (PSD) as a possible binding candidate (Wheatley, S.P., personal communication). Thus at the outset of this study we sought to determine whether

this putative interaction was in fact real/ bona fide interaction and if so, investigate its physiological relevance.

4.3 RESULTS

4.3.1 SURVIVIN INTERACTS WITH PSD *IN VIVO* AND *IN VITRO*

The interaction between survivin and PSD was investigated with co-immunoprecipitation experiments in HEK293T cells overexpressing FLAG-tagged survivin and PSD. Though small in size, in order to exclude the possibility of FLAG tag interference with complex formation, survivin was tagged at both termini. N-terminally FLAG tagged survivin expressed considerably more efficiently than C-terminally tagged survivin which was virtually undetectable in the input (Figure 4-1A). Correspondingly, following immunoprecipitation with FLAG antibody conjugated resin, substantially higher amounts of FLAG-survivin over the less expressed survivin-FLAG were immunoprecipitated from the transfected cell extracts. As shown in Figure 4-1A, ample amount of PSD was in complex with the more abundant FLAG-survivin, though some PSD was also interacting with the scarcer immunoprecipitated survivin-FLAG but not with FLAG tag vector only control.

Next, we sought to detect endogenous survivin-PSD complexes in untransfected cells. Two sets of protein G beads were conjugated with either IgG control antibody or survivin antibody to immunoprecipitate endogenous survivin from HEK293F cells. Indeed, endogenous PSD was detected where endogenous survivin was immunoprecipitated with survivin antibody but was absent in extracts immunoprecipitated with control IgG (Figure 4-1B).

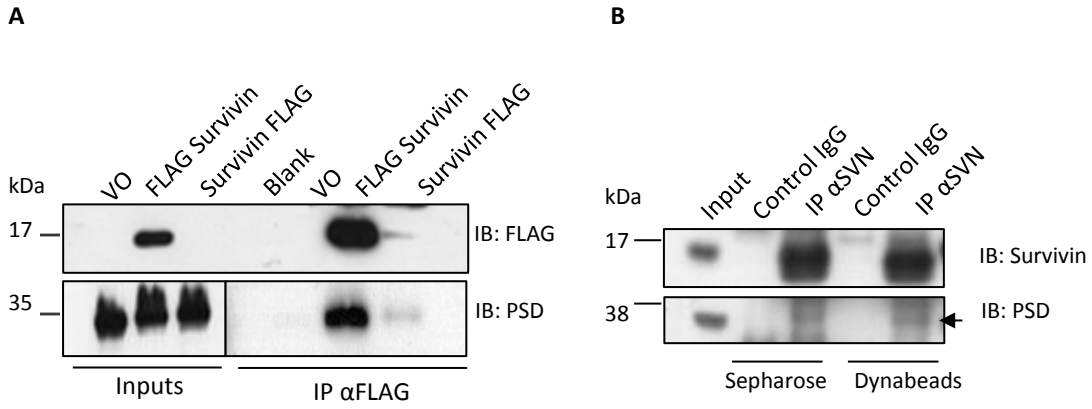


Figure 4-1. Survivin co-immunoprecipitates PSD (A) Vector alone (VO), N- or C-terminally FLAG tagged survivin were co-transfected with PSD into HEK293T cells and FLAG proteins immunoprecipitated using Anti-FLAG gel. 2% Input was loaded to indicate overexpressed protein levels before IP. Samples were analysed by immunoblotting for FLAG and PSD. Anti-FLAG gel with lysis buffer only was used as blank control. **(B)** Endogenous survivin was immunoprecipitated from HEK293F cells with survivin antibody using either sepharose Protein G beads or magnetic Protein G Dynabeads. Control IgG was used as a negative control. Associating PSD is indicated with an arrow.

PSD is synthesized on cytosolic ribosomes as an inactive proenzyme, and is imported into the mitochondria via a mitochondrial targeting sequence which is then cleaved off. The enzyme undergoes a self- cleavage at a conserved LGST motif to give rise to two distinct subunits, the 34kDa β-subunit and the much smaller C-terminal 4kDa α-subunit, which assemble into the active enzyme (Figure 4-2A). In order to prevent this auto-catalytic event and to generate an inactive version of this enzyme, the serine residue (S378) of this conserved motif was substituted with alanine, effectively locking the protein in proenzyme form (Figure 4-2A). Immunoblotting with PSD antibody which detects the middle portion of the protein, showed overexpression of both wildtype and mutant PSD was successful (Figure 4-2B).

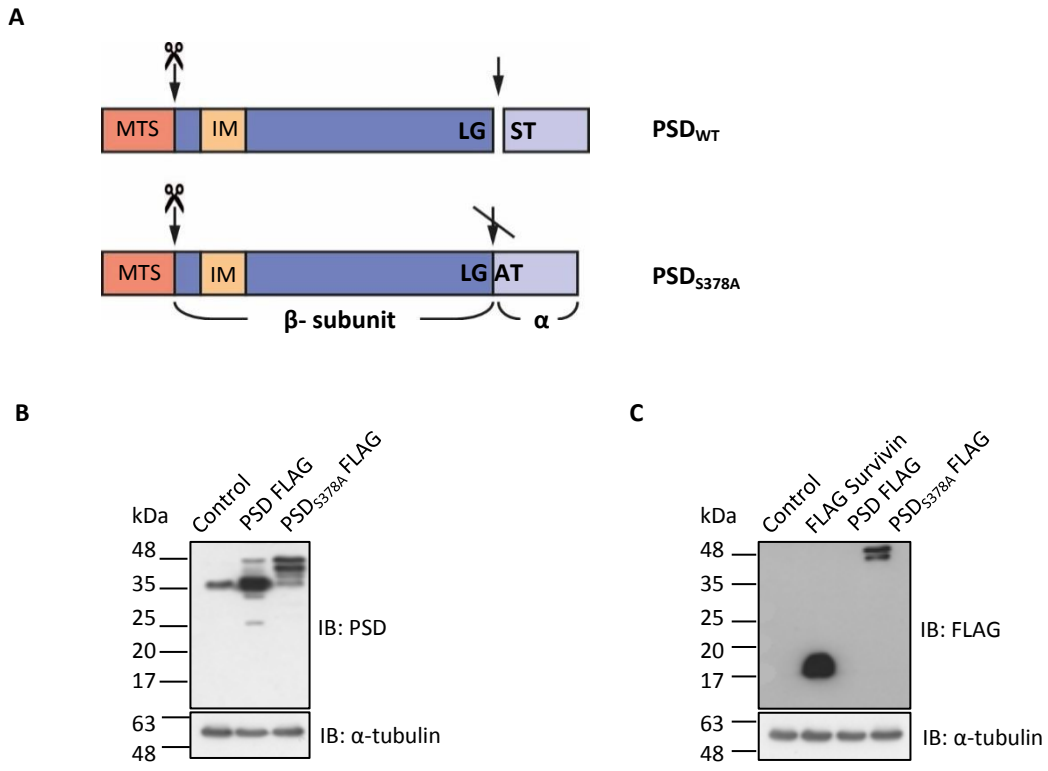


Figure 4-2. Generation of a PSD mutant unable to mature into an active enzyme. (A) Schematic of a wild type PSD proenzyme with a mitochondrial targeting signal (MTS), cleaved off during mitochondrial import, an inner membrane sorting signal (IM) and a highly conserved LGST motif necessary for autocatalytic cleavage to generate two distinct subunits (α and β) which assemble into an active enzyme. Substitution of the conserved serine to alanine within the motif prevents this cleavage and thus inhibits maturation of PSD into its active conformation. **(B+C)** HEK293T cells were untransfected (control) or transfected with FLAG SVN, PSD_{WT} FLAG and PSD_{S378A} FLAG and immublotted with PSD antibody (B) or FLAG antibody (B). Tubulin was used as a loading control.

Levels of β-subunit for PSD_{WT}-FLAG were elevated whereas PSD_{S378A}-FLAG β-subunit levels were indistinguishable from the untransfected control as expected (Figure 4-2B). However, immunoblotting with anti-FLAG antibodies could not detect PSD_{WT}-FLAG as the processing splits the proenzyme into only 4kDa FLAG tagged α-subunit, difficult to resolve on a 15% SDS-PAGE gel (Figure 4-2C). On the other hand, PSDS378A-FLAG mutant can be seen as two bands below the 48kDa marker representing the 46kDa full proenzyme and MPP cleaved protein as it is being imported in the mitochondria (Figure 4-2C). In chapter 3, it was shown that survivin and PSD colocalize together in the intermembrane space of the mitochondria. However, to ascertain whether the association of survivin with PSD can occur prior

to mitochondrial import of both proteins when PSD is still in its proenzyme state, co-immunoprecipitation experiments with PSD_{S378A} mutant were also carried out. Only FLAG-survivin, given its higher expression levels than survivin-FLAG, was immunoprecipitated with anti-FLAG resin. Whereas PSD_{WT} was again in complex with FLAG-survivin, PSD_{S378A} inactive mutant could not form a complex, suggesting that survivin can only associate with PSD in its fully active, correctly assembled state (Figure 4-3).

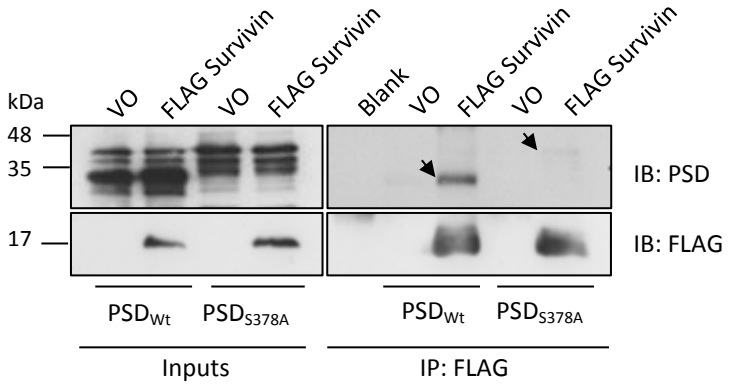


Figure 4-3. Survivin co-immunoprecipitates wild type but not enzymatically inactive PSD Vector alone (VO) or N-terminally FLAG tagged survivin were co-transfected with either wild type PSD or mutant PSD_{S378A} and immunoprecipitated as figure 4-1. 2% Input was loaded to indicate overexpressed protein levels before IP. Anti-FLAG gel with lysis buffer only was used as a blank control.

Next, to determine whether the association between survivin and PSD was direct, *in vitro* GST pull-down experiments were performed. For this purpose recombinant GST or GST-tagged survivin were expressed in *E. coli*. These were then bound to glutathione sepharose beads and incubated with ^{35}S-labelled prey proteins. Synthesis of such labelled proteins was achieved using an *in vitro* cell-free system for transcription and translation (IVT) of pcDNA3.1 constructs incorporating a ^{35}S-tagged methionine during translation. As shown in figure 4-4A, a clear band was detected in the control lane in which IVT ^{35}S-labelled borealin was introduced to GST-survivin, which agrees with borealin being positive control. Incubation of GST-survivin or GST only with IVT ^{35}S-labelled PSD revealed PSD directly bound to

GST-survivin but not to GST (Figure 4-4B). Therefore, survivin and PSD can form a complex in which they can interact directly, without the requirement for an additional adaptor protein. In order to map which regions of survivin mediate binding to PSD, GST-tagged N-terminal region of survivin (residues 1-90), constituting the BIR domain, and GST-tagged C-terminal 90-142 residues of survivin were also recombinantly expressed and used in the pull-down experiments with ^{35}S-labelled PSD as prey. As shown in Figure 4-4B, PSD bound avidly to the N-terminal BIR domain whereas this interaction was seen abolished with C-terminus of survivin which manifested with background binding similar to the one seen with GST alone(Figure 4-4B).

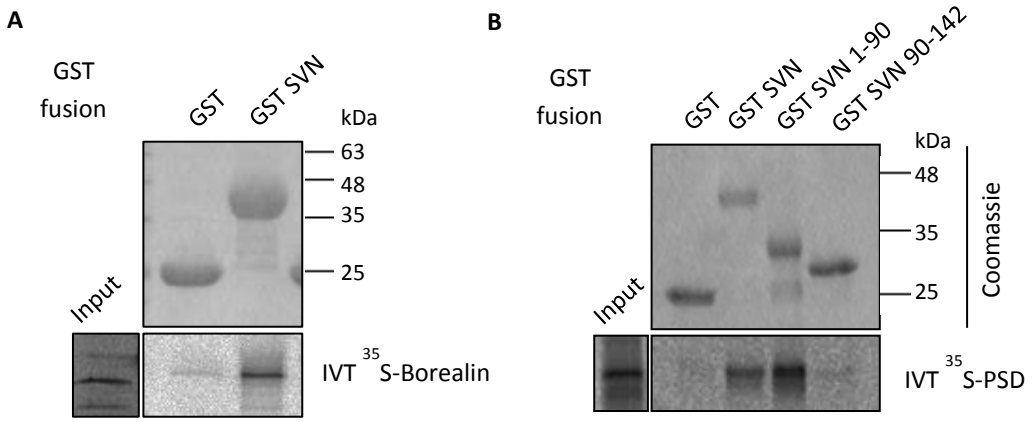


Figure 4-4. Survivin binds directly to PSD *in vitro* through its N-terminus (1-90). (A) GST alone or GST Survivin (SVN) fusion proteins immobilized on glutathione sepharose beads (binding shown with Coomassie stain) were incubated with *in vitro* translated (IVT) [^{35}S]L-methionine labelled borealin as a positive control for binding. **(B)** GST alone, GST-SVN, GST-SVN 1-90 (N-terminus) and 90-142 (C-terminus) fusion proteins immobilized on beads were incubated with radiolabelled IVT PSD. For all pulldowns, 15% Input was loaded as control for success of IVT reaction.

4.3.2 PROBING FOR FUNCTIONAL SIGNIFICANCE OF SURVIVIN – PSD INTERACTION

4.3.2.1 RECOMBINANT EXPRESSION OF PSD

Once the association between survivin and PSD was established, it was desired to describe any functional relevance of this interaction. PSD is an enzyme involved in converting one type of phospholipid into another hence we asked whether this reaction is somehow affected by survivin. To address this first

purification of the membrane integrated protein PSD had to be optimized. PSD was initially cloned with a GST tag on its N-terminus in an *E. coli* pGEX-4Ti vector and the overexpression tested at two different growth temperatures 30°C and 37°C. After 4 hour induction, samples were then lysed and cleared by centrifugation to assess the solubility of the protein. 37°C 4 hour induction of expression was chosen as the more suitable growth condition from the two (Figure 4-5A). Though initial experiments with PSD activity were carried out whilst GST-PSD was still immobilized on the GST beads, eventually greater amounts of PSD were purified using the AKTA purification system connected to a GST 1ml column and the success of the purification verified by SDS-PAGE (Figure 4-5B). The 1 ml elution fractions A11 to B11 were pooled together, buffer exchanged and concentrated to be used in PSD conversion assays. The identity of the purified protein after this step was assessed by SDS-PAGE with direct staining of the gel but also via Western blotting for PSD (Figure 4-5C). Interestingly, Coomassie staining revealed the presence of three protein bands (figure 4-5B), two with size larger than the 63kDa marker, where at least one should have been GST-PSD at the expected size of ~72kDa (46kDa PSD + 26kDa GST tag), and another protein band just below the 63kDa marker. In the A11 fraction on the Western blot, both protein bands cross-reacted with PSD antibody whilst in the final concentrated sample of GST-PSD only one band remains (Figure 4-5D). PSD undergoes an autocatalytic cleavage yielding a bigger N-terminal β-subunit, here fused to a GST tag, and a small 4kDa α-subunit, which could explain at least one of the size shifts observed.

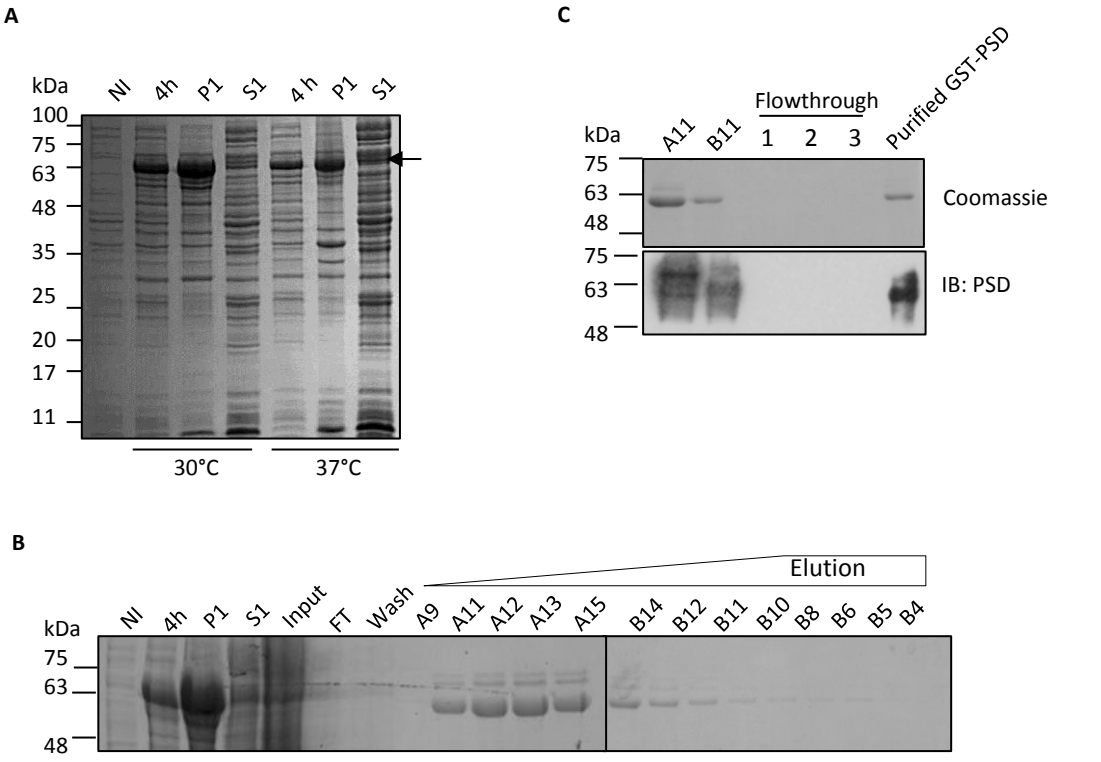


Figure 4-5. Initial purification of GST PSD from *E. coli* cells. (A) Cultures after 4 hour induction at 30 and 37°C were lysed by sonication and subsequently cleared. Samples of pellet (P1) and supernatant-soluble fraction (S1) were analysed by SDS-PAGE. Since more soluble protein was present in S1 at 37°C growth (arrow), this condition was used for subsequent purification. **(B)** GST-PSD purification with GSTtrap 4B 1ml column connected to AKTA liquid chromatography system from 2.4l *E. coli* culture. GST-PSD was eluted in 1ml fractions with linear gradient of elution buffer containing 10mM reduced glutathione. GST tag alone (not shown) was purified using the same system with a single elution step instead. All fractions of the purification were analysed by SDS-PAGE. **(C)** Concentration and buffer exchange of pooled GST-PSD elution fractions (A11-B11) with Amicon centricon plus-20. Samples of fractions A11 and B11, along with flowthrough of the concentrating device and the final purified protein were analysed by SDS-PAGE with Coomassie stain and immunoblotting for PSD.

4.3.2.2 Developing a PS-PE Conversion Assay

Next, an assay which would permit detection of the two phospholipids involved in PSD conversion reaction needed to be established. First, the reaction conditions were tested with an enzyme preparation consisting of PSD-FLAG directly immunoprecipitated from transfected HEK293T cells using an anti-FLAG gel or vector only as a negative control (Figure 4-6A). The lipids were extracted from the reaction mixture with chloroform/methanol and separated by thin layer chromatography (TLC). A clear spot corresponding to PE, as determined by

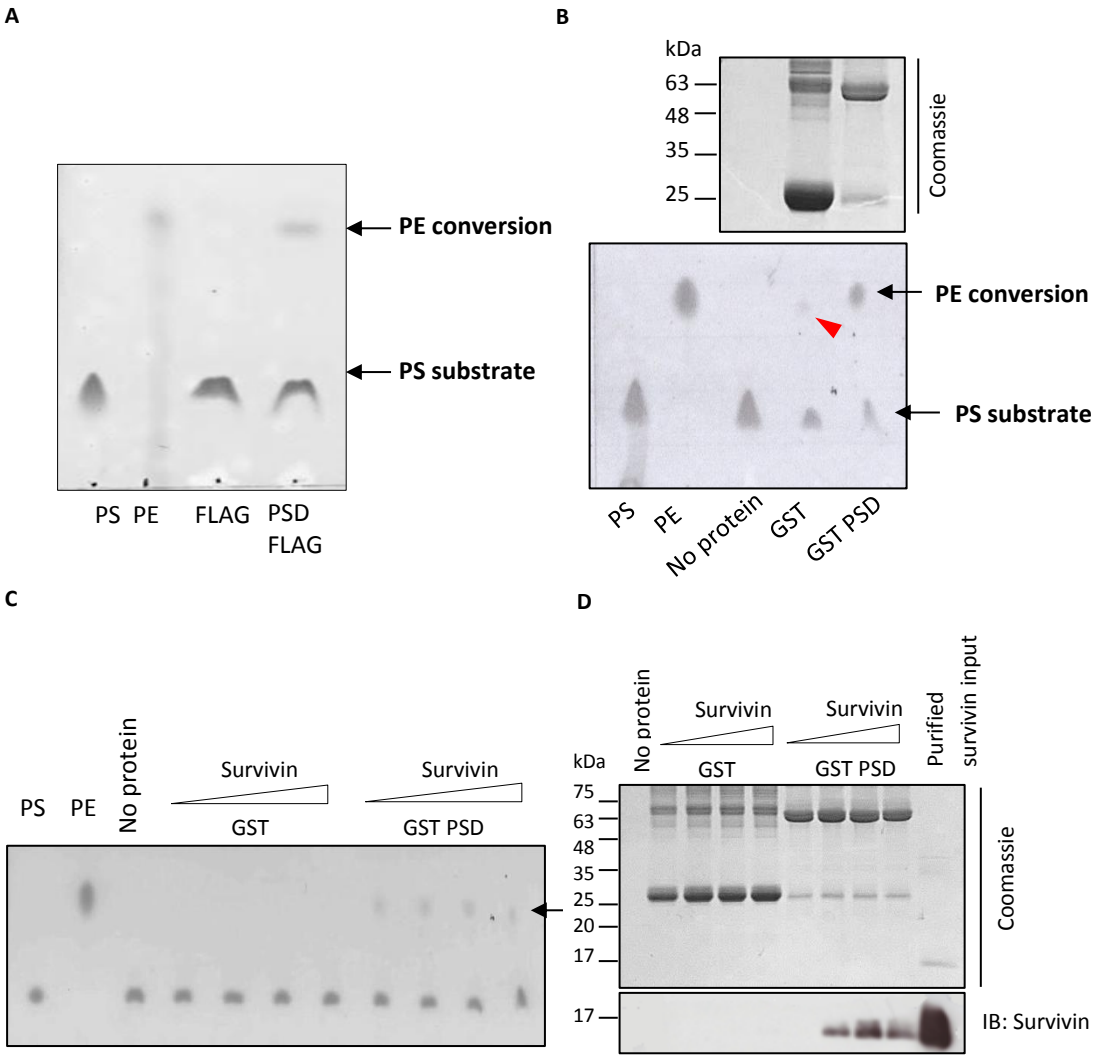


Figure 4-6. Detection of PSD mediated conversion of PS to PE (A) Vector alone (FLAG) or C-terminally FLAG tagged PSD were transfected into HEK293T cells and FLAG proteins immunoprecipitated using Anti-FLAG gel. Washed gel was resuspended in reaction buffer with 10µg PS as substrate and reaction incubated at 37°C for 1 hour. Reaction was terminated by acidification, lipids extracted as described in Methods and then separated by TLC and visualized by exposure to iodine vapour. **(B)** GST beads alone (no protein), with immobilized GST tag only or GST PSD were incubated with PS as in (A) and lipids resolved by TLC. Reaction substrate PS and the reaction product PE are indicated with black arrows. Unknown contaminant corresponding in size to PE in GST lane indicated with red arrow. A fraction of the beads was analysed by SDS-PAGE to ascertain binding, shown with coomassie staining in upper panel. **(C)** GST beads alone (no protein), or a set with immobilized GST tag only or GST PSD were incubated with increasing concentrations of purified survivin (0-15µg) for 2 hours, subsequently washed and incubated with 10µg PS in reaction buffer at 37°C, lipids were extracted and separated by TLC. The converted PE is indicated with a black arrow. No apparent difference in PE conversion can be seen between GST PSD with or without survivin binding **(D)** A fraction of the beads from (C) was analysed by SDS-PAGE via direct staining with Coomassie to ascertain GST protein binding and association with survivin which was however, below the stain detection sensitivity threshold. Subsequent analysis via immunoblotting with survivin antibody showed survivin binding to GST PSD but not GST tag alone.

comparison to authentic PE standard, was observed in PSD-FLAG but not vector alone lane, suggesting the reaction conditions were favourable for the reaction to take place. The same reaction set up was then used with GST tag alone or GST-PSD bound to GST beads. Though again a clear PE spot could be seen in GST PSD lane, a smaller intensity spot was also apparent with GST tag only, whereas beads alone which have not been incubated with any protein did not give any signal (Figure 4-6B). SDS-PAGE analysis revealed more GST bound to the beads than GST-PSD, and also a higher number of contaminants which could possibly be the source of the small PE spot observed on the TLC plate. A preliminary experiment with this set up was then performed incorporating survivin binding to assess any visually apparent differences in the converted PE spot intensity. GST alone or GST-PSD were immobilized on beads and subsequently incubated with increasing amounts of previously purified recombinant survivin to allow for the interaction to occur. After several washes, the binding was assessed by direct staining where survivin was undetectable, however, western blotting with survivin antibody revealed survivin binding to GST-PSD but not GST alone (Figure 4-6D). The conversion reaction yielded a PE spot with similar intensity across all conditions, highlighting the necessity for a quantification method of the spots (Figure 4-6C). Subsequent reactions were done both on beads and also in solution with the attempt to quantify the spots via a colorimetric method of inorganic phosphate measurement. Each phospholipid comprises a phosphate group which can be released via hydrolysis in strong acid heated to very high temperatures. Such released inorganic phosphate group (P_i) can form a coloured complex with malachite green and ammonium molybdate under acidic conditions measured at 660nm. Malachite green complex formation is directly related to the free orthophosphate concentration and so known amounts of inorganic phosphate can be used to construct a standard curve of colour absorbance, a principle commonly used by protein quantification methods. However, such attempts gave highly inconsistent results which often did not reflect the intensity of the spot seen on the TLC plate. Additionally, a test reaction done using excess GST protein resulted in PE spot intensity similar to GST-PSD which cast doubt on the contribution of the co-

purifying contaminants and the actual activity of the purified GST-PSD. Therefore, the GST tag was to be removed and decarboxylase dead mutant PSD_{S378A} described in figure 4-2 used as a negative control for the activity assay instead.

As wild-type PSD, the PSD mutant was also cloned with an N-terminal GST tag in pGEX4-Ti vector. Given the previously used conditions for GST-PSD purification did not yield very high amounts of soluble protein, conditions for both PSD_{WT} and PSD_{S378A} overexpression were re-optimized. Growth temperatures 37°C, 30°C, 27°C and 20°C were all examined for expression for specified time intervals and highest expression conditions selected for solubility screen. Small cultures corresponding to 3 hours induction at 37°C, 5 hours at 30°C and overnight at 27°C and 20°C were lysed by sonication, cleared by centrifugation and both pellet (insoluble material and unlysed cells) and supernatant (soluble fraction) were analysed by SDS-PAGE (Figure 4-7A and B). Induction at 27°C and 20°C overnight proved to give higher amount of soluble protein as compared to the previously used 37°C induction for PSD_{WT}. Supernatants from all four test inductions (i.e. all growth temperatures tested) for PSD_{WT} or PSD_{S378A} were used in small scale

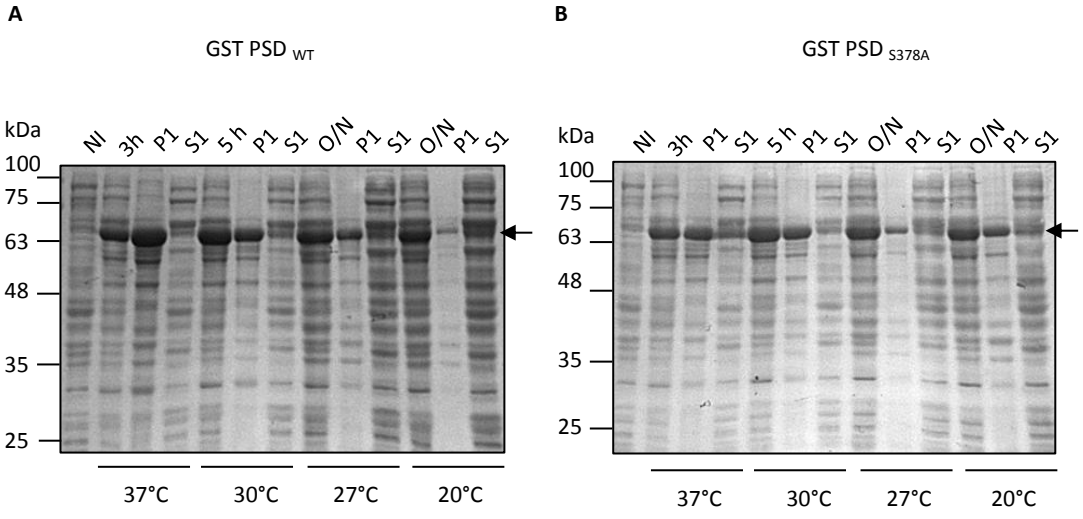
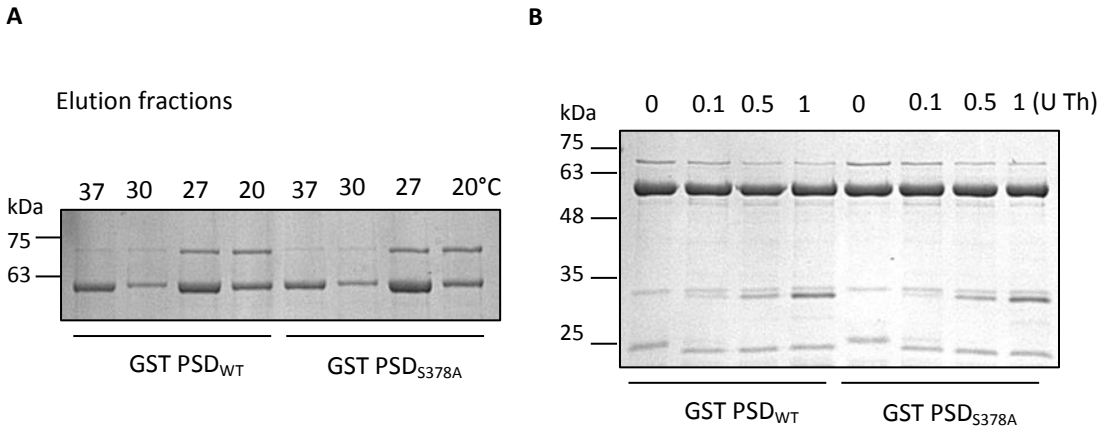


Figure 4-7. Optimization of GST PSD_{WT} and GST PSD_{S378A} mutant overexpression in *E. coli* (A+B) GST-PSD_{WT} (A) and GST-PSD_{S378A} (B) were induced with IPTG for the times and at temperatures indicated that have been established in previous pilot experiments. The pelleted cultures were lysed, solubilized with 1% Triton X-100 cleared of insoluble material by centrifugation and a sample of the pellet (P1) and supernatant (S1) taken for analysis by SDS-PAGE. Most GST fusion protein in soluble form (indicated with black arrow) was produced with induction at 27 and 20°C overnight.

purification using GST SpinTrap columns where first elution fractions were analysed by SDS-PAGE analysis (Figure 4-8A). Two protein bands were observed for both wild type and mutant PSD, as in previous AKTA purification. Next, to obtain a more suitable protein preparation for the *in vitro* PSD activity assay, the GST tag was to be cleaved off with thrombin, from both PSD proteins using a thrombin cleavage site upstream of the protein. As shown in figure 4-8B and C, increasing amounts of thrombin had no apparent effect on PSD (wild type or mutant) in solution even though all GST-survivin was successfully cleaved. The possibility that GST-PSD in solution assumes a conformation which sterically hinders access of thrombin to its cleavage site was next investigated using thrombin cleavage of GST-PSD immobilized on GST beads, together with GST survivin as a positive control for cleavage reaction. However, neither these conditions facilitated removal of the GST tag from PSD as analysed by SDS-PAGE. Whereas GST survivin was successfully cleaved, seen as a band at 17kDa, GST PSD protein band remained unchanged (Figure 4-8D). Given, the inability to remove the GST tag from GST-PSD, an essential requirement for proceeding with the PSD *in vitro* activity assay, a different purification strategy was selected altogether.



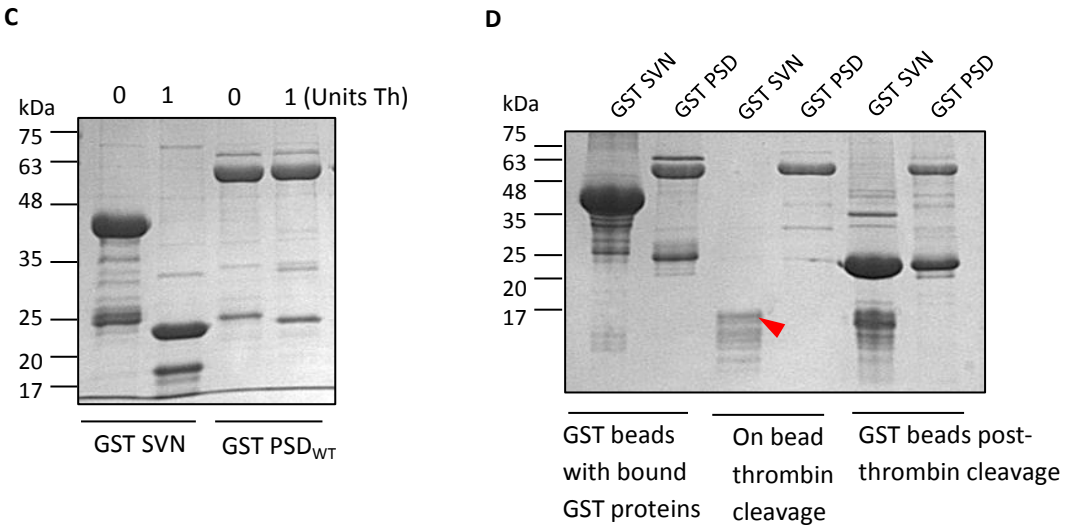


Figure 4-8. Purification of GST-PSD$_{WT}$ and GST-PSD$_{S378A}$ mutant with attempted thrombin cleavage of GST tag. (A) GST-PSD$_{WT}$ and GST-PSD$_{S378A}$ overexpressed at different temperatures and times shown in figure 4-7A and B were purified using GST SpinTrap columns. Samples of elutions were analysed by SDS-PAGE. **(B)** Samples of eluted proteins were incubated with none, 0.1, 0.5 and 1 units of thrombin in thrombin cleavage buffer for ≥16 hours at room temperature to cleave off the GST tag from the recombinant proteins. **(C)** GST-survivin, used as control, or GST-PSD$_{WT}$ were left uncleaved or incubated with 1 unit of thrombin as in B to evaluate efficiency of cleavage conditions used in B. **(D)** GST-survivin or GST-PSD$_{WT}$ were prebound to GST beads and incubated with 1 unit of thrombin in thrombin cleavage buffer as in B. Beads were pelleted, the supernatant (cleaved proteins) and any proteins still bound to beads were analysed by SDS-PAGE. Cleaved survivin indicated with red arrow.

PSD$_{WT}$ and PSD$_{S378A}$ were subsequently cloned with an 8x Histidine tag at its C-terminus in a pQE vector enabling parallel overexpression in mammalian, insect and bacterial cells. As initial overexpression screens were unsuccessful, survivin was cloned in the same way and used as a control. As exemplified in figure 4-9A, survivin was overexpressed at all tested induction temperatures in SG13009 strain. However, no appreciable induction was seen for either wild type or mutant PSD. Further strains tested including T7 Express, XL Blue and BL21 pLysS with a range of different temperatures (25, 30, 37°C) and IPTG concentrations (0.2, 0.5, 1mM) yielded a similar result (data not shown). Next, both PSD proteins were subcloned with a C-terminal 6x Histidine tag into the *E. coli* expression vector pET-22b(+). The same *E. coli* strains as for pQE were tested in overexpression screens with no obvious protein induction as assessed with direct staining of the gel. To account for the possibility of rare codons rendering protein overexpression more challenging in the absence of an N- terminal GST tag providing efficient translation initiation or

the protein being promptly degraded following induction, Rosetta-gami-pLysS was employed. However, samples 15, 30 minutes, 1, 2 and 3 hours post-induction showed no appreciable expression (Figure 4-9B). Nonetheless, immunoblotting of induced BL21 samples revealed possibly very low amount of PSD-His is induced, though this remains to be determined as test purification efforts did not yield sufficient protein for Coomassie stain detection (Figure 4-9C).

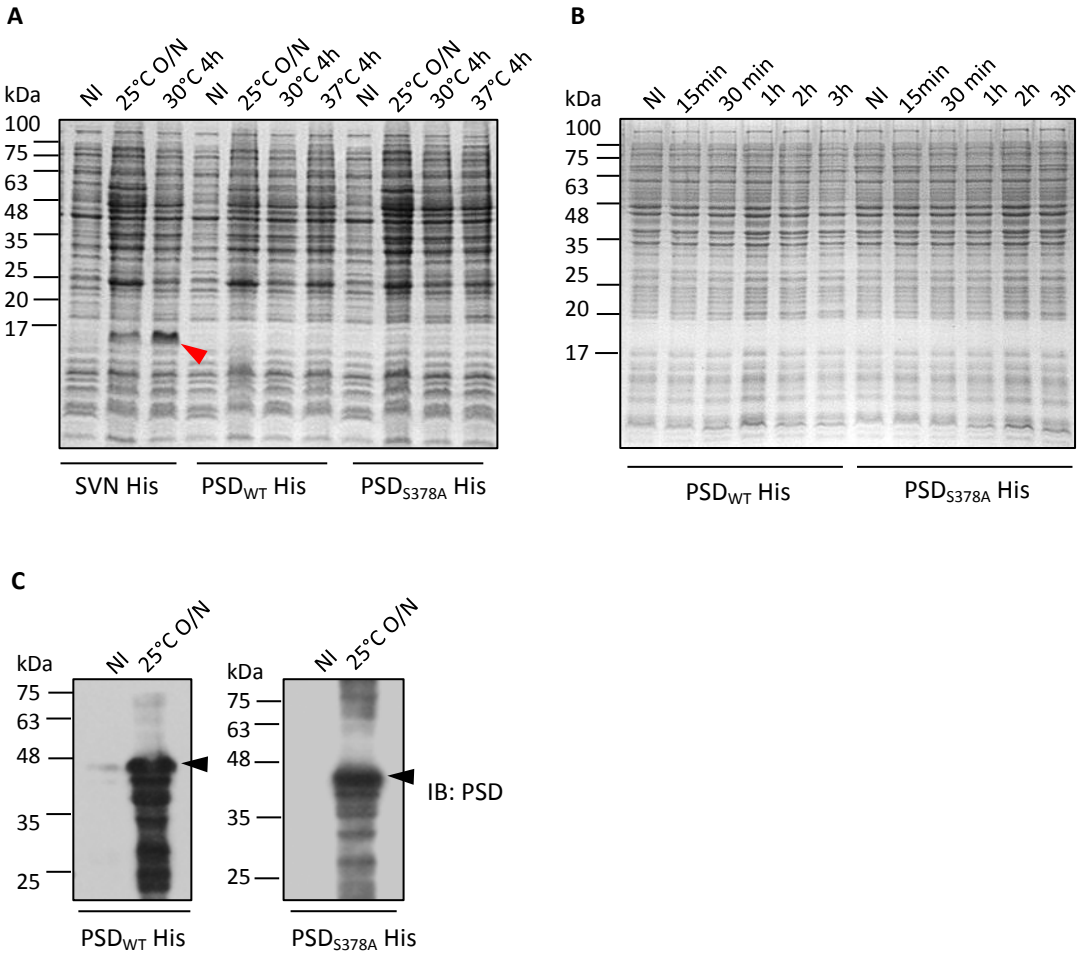


Figure 4-9. Optimization of PSD_{WT} and PSD_{S378A} His expression in *E. coli*. **(A)** Samples of *E. coli* SG13009 strain (with pREP4 repressor plasmid) harbouring either pQE Survivin-His, pQE PSD_{WT}-His or pQE PSD_{S378A}-His either non-induced or induced with IPTG for the times and at temperatures indicated were analysed by SDS-PAGE. Only overexpression of His-tagged survivin was detectable (red arrowhead), no discernible change was observed between the non-induced and either of the induced conditions for both PSD-His proteins. **(B)** Cultures of Rosetta-gami-pLysS cells harbouring either pET-22b(+) PSD_{WT} His or pET-22b(+) PSD_{S378A} His were induced with IPTG at 37°C and samples for SDS-PAGE analysis taken at time points indicated. There was no detectable protein overexpression at either of the time points. **(C)** Cultures of BL21 pLysS cells harbouring either pET-22b (+) PSD_{WT} His or pET-22b(+) PSD_{S378A} were sampled before and after induction with IPTG at 25°C overnight and analysed by immunoblotting for PSD. PSD His is denoted with black arrowhead.

PSD-His in the universal pQE vector was also tested for expression in HEK293T cells. In these cells, overexpression of both PSD forms was successful (Figure 4-10A) as detected by both His tag and PSD antibodies. Therefore, small scale IMAC purification was carried out from two 10 cm plates of transfected HEK293T cells for wild type, and one plate for mutant PSD. Though purified PSD could not be detected by SDS-PAGE Coomassie stain analysis, figure 4-10B shows immunoblotting of the purified fractions with PSD antibody revealed that both wild type and mutant PSD were in fact successfully purified (indicated by arrow). However, the overall yield was very low – approximately 15µg for wild type and 7µg for mutant PSD. This purified PSD was tested in the established conversion assay for assessment whether decarboxylase activity had been retained through the purification procedure. However, perhaps due to low enzyme content in the reaction no PE conversion could be detected in the *in vitro* activity assay.

Next, mitochondria were isolated from twenty 10cm plates of transfected HEK293T cells with the aim of increasing the yield of active protein and possibly limiting the amount of contaminants. PSD_{WT}-His was also successfully purified using this strategy, with particular enrichment in active form rather than the initial inactive proenzyme, however, the yield remained quite low (Figure 4-10C). Nonetheless, this purification procedure is more likely to yield active protein than overexpression in *E. coli.*

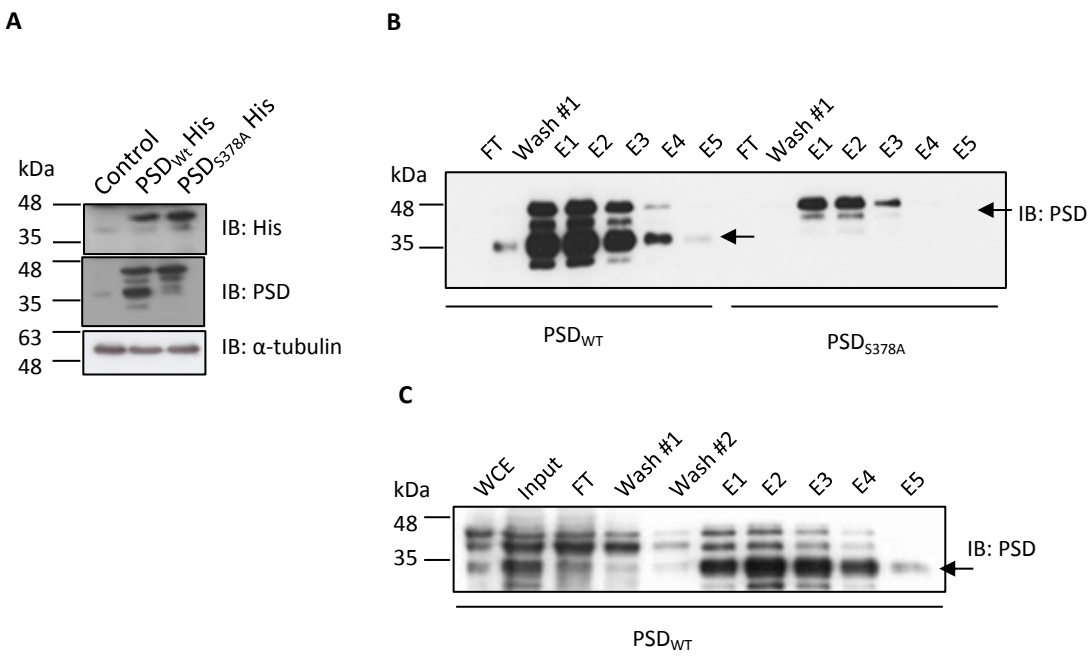


Figure 4-10. Optimization of PSD_{WT}-His and PSD_{S378A}-His mutant overexpression in HEK293T cells. **(A)** HEK293T cells were left untreated (control) or transfected with pQE PSD_{WT}-His or pQE PSD_{S378A}-His, lysed and immunoblotted for His tag or PSD. Both PSD (wild type and mutant) proteins were successfully detected in HEK whole cell extracts. **(B)** Two 10 cm plates of HEK293T cells were transfected with pQE PSD_{WT}-His and one plate with pQE PSD_{S378A}-His, lysed and His tagged proteins purified with IMAC. Immunoblotting analysis of Input, flowthrough (FT), two washes of the IMAC resin and five elution fractions with increasing concentrations of imidazole of PSD_{WT}-His and PSD_{S378A}-His to assess the success of IMAC purification. Purified PSD proteins were indicated with arrows. **(C)** IMAC purification of PSD_{WT} His from isolated mitochondria from twenty 10cm HEK293T transfected plates. Samples of whole cell lysates (WCE), isolated mitochondrial lysate (Input), flowthrough (FT), two washes of the IMAC resin and five elution fractions with increasing concentrations of imidazole of PSD_{WT} His only were analysed by immunoblotting for PSD. PSD, indicated with arrow, was successfully purified from HEK293T cells.

4.3.3 Assessment of cell behaviour after Survivin and PSD depletion

Survivin RNA interference has previously been used to study the effects of loss of survivin expression on cell behaviour in terms of cell division and apoptosis. Here, this was partially recapitulated with assessment of cell growth following survivin silencing as control and PSD interference, tested with increasing concentrations of siRNA. Both survivin and PSD expression was successfully knocked-down with all concentrations of siRNA when analysed at 48 and 72 hour time points post-transfection (Figure 4-11A). As expected, given its essential role at

mitosis, decreasing survivin protein levels had detrimental effects on cell proliferation with cell growth cessation after 48 hours in culture and higher number of apoptotic floating cells in the culture media (Figure 4-11B and visual inspection). Though not as pronounced as for survivin knockdown, depleting PSD presented with a trend of slower cell proliferation with increasing concentrations of siRNA and with more apoptotic cells when compared to mock controls (Figure 4-11B and visual inspection). In particular the growth rate of the highest concentration of PSD siRNA 150nM after 72 h treatment was found to be significantly different from mock control growth, hence this concentration was employed in all subsequent siRNA experiments.

In some instances survivin silencing at 72 and 96 hour time point caused decrease in PSD expression (Figure 4-12A). This was investigated further in case survivin had a stabilising role for PSD. HeLa cells were treated with cycloheximide to inhibit protein synthesis, MG132 to inhibit proteasomal degradation and with the combination of both drugs. Whereas survivin was rapidly degraded following inhibition of protein translation at all assessed time points, PSD levels were only affected after 16h inhibition (Figure 4-12B). On the other hand, survivin protein turnover was arrested following inhibition of the proteasome whereas PSD levels were again largely unchanged, suggesting the protein has a long half-life.

As PSD localizes exclusively in the mitochondria, the possibility that the mitochondrial mass of survivin treated cells was lower was examined. Equal amounts of mock treated, survivin or PSD siRNA treated cells for 72 hours were immunoblotted for mitochondrial marker VDAC and tubulin as a loading control. Though in this particular experiment, lower amount of VDAC in survivin treated cells as compared to either mock or PSD treated cells can be seen, this could not be consistently replicated suggesting there is no difference in mitochondrial mass following survivin silencing (Figure 4-12C). In parallel, equal amounts of protein for mock treated or borealin siRNA treated cells for 72 hours were also immunoblotted for VDAC and tubulin. Immunoblotting for survivin revealed complete depletion of survivin which implied successful knockdown of borealin, given the mutual

interdependence of chromosomal passenger complex proteins (Honda et al., 2003). Also in this experiment, VDAC was lower than in mock treated controls (Figure 4-12D). In summary, considering when apoptotic cells were included in the siRNA harvest, lower PSD expression after prolonged survivin silencing was more likely due to onset of overall cell destruction rather than specific decrease in mitochondrial mass.

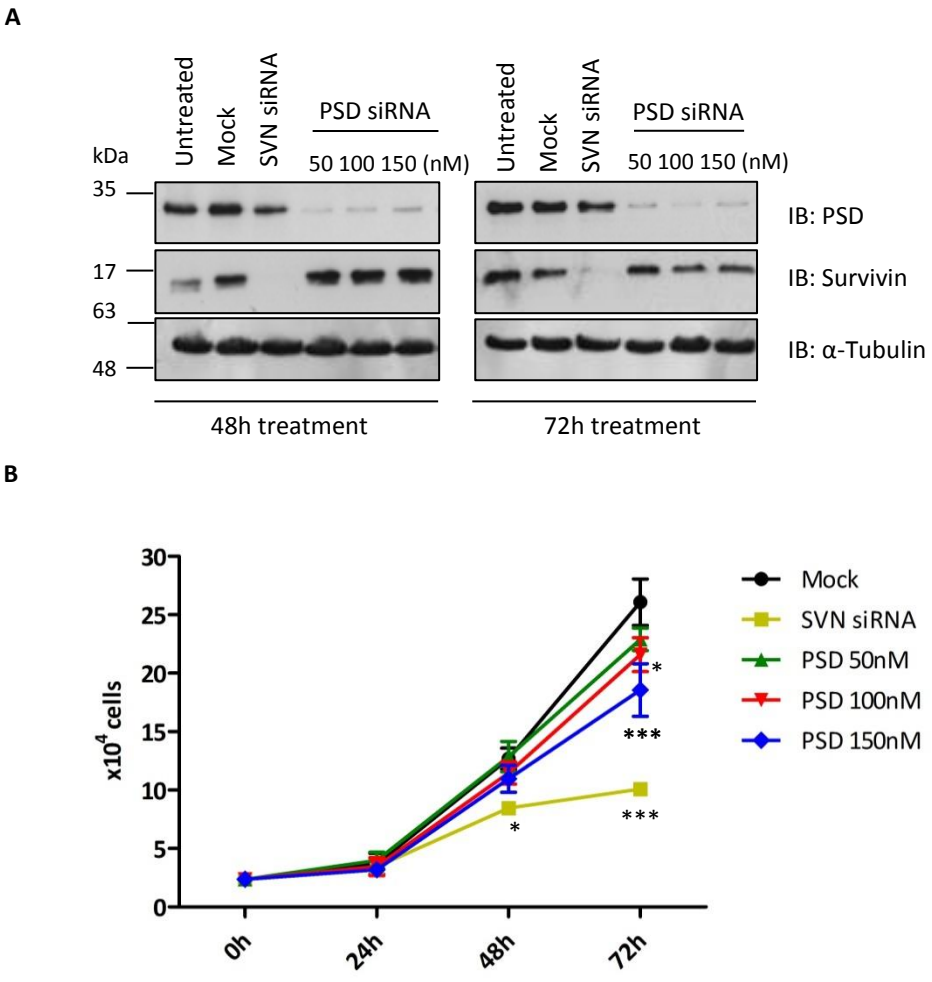


Figure 4-11. Cell growth of HeLa cells treated with siRNA to survivin and PSD. (A) HeLa cells were left untreated, treated with transfection reagent only (mock), with 60nM survivin siRNA or a range of PSD siRNA concentrations 50, 100 and 150nM, harvested at 48 and 72 hour time points and immublotted for survivin and PSD to verify successful knockdown. α-tubulin was used as a loading control. 50µg protein/lane was loaded. **(B)** Cell number at 0, 24, 48 and 72hours post siRNA treatment was determined by trypan blue exclusion and expressed as mean ± SEM from three independent experiments. (*P<0.05, *** P<0.001 versus mock as determined by two-way ANOVA).

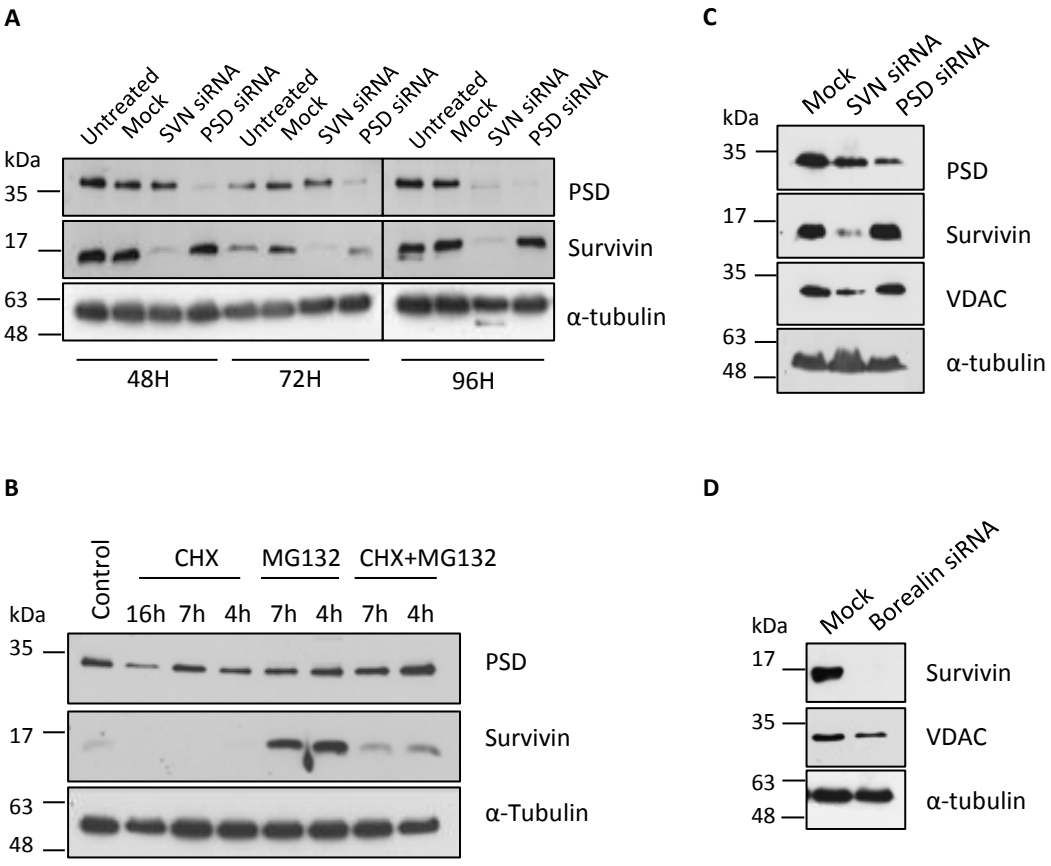


Figure 4-12. Assessment of PSD stability. (A) HeLa cells were left untreated, treated with transfection reagent only (mock), with 60nM survivin siRNA or 150nM PSD siRNA, harvested at 48, 72 and 96 hour time points and immunoblotted for survivin and PSD, α-tubulin was used as a loading control. 50µg protein/lane was loaded. Knockdown of survivin led to decrease in PSD protein levels at 72 and 96h time points. **(B)** Immunoblot of HeLa cells treated with cycloheximide (CHX) (new protein synthesis inhibitor), MG132 (proteasome inhibitor) or both, blotted for PSD and survivin to assess the stability of the two proteins. 30µg protein/lane was loaded. **(C)** Immunoblot of equal amounts of cells after 72H siRNA treatment, blotted for PSD and survivin to confirm successful knockdown, and VDAC (mitochondrial marker) and α-tubulin (loading control) for mitochondrial mass assessment. **(D)** Immunoblot of HeLa cells treated with transfection reagent only (Mock) or 60nM Borealin siRNA for 72 hours, blotted for survivin, VDAC (mitochondrial marker) and α-tubulin (loading control) for mitochondrial mass assessment 50µg protein/lane was loaded.

Next, in order to indirectly assess effects of survivin on PSD activity, HeLa cells were untreated, mock treated or treated with survivin, PSD or BubR1 siRNA for 72 hours. Given that survivin has an important role at mitosis, BubR1, which functions in mitotic checkpoint for spindle assembly, was also silenced to help distinguish from any changes seen due to interference with mitosis rather than loss of mitochondrial survivin expression. The cells were harvested and the lipids were extracted and resolved on thin layer chromatography into the individual phospholipid classes and then scraped from the TLC plates for analysis. For the

purpose of this study, phosphatidylcholine (PC) as the most abundant membrane phospholipid, the PSD decarboxylase reaction substrate PS and reaction product PE were quantified by malachite green assay. Preliminary assessment of whole cell lipids showed no substantial differences in the lipids analysed (Figure 4-13 A). However, in PSD silenced cells where alterations in lipid content are to be expected, only a modest decrease in PE content could be seen (Figure 4-13A). Of note, the efficiency of siRNA knockdown was incomplete in this experiment (Figure 4-13B).

Therefore, since PSD resides in the mitochondria and most of the converted PE remains incorporated in the mitochondrial membranes, the lipid composition of isolated mitochondria from siRNA treated cells was assessed (Figure 4-14). Apart from a very slight decrease in mitochondrial PE following PSD siRNA treatment, no changes either in PE, PS or PC were detected in any of the conditions (Figure 4-14A-C). The knockdown was assessed via western blot from the two independent experiments, scanned, the intensity of bands quantified by densitometry, normalized against tubulin and expressed as fold change compared to untreated control (Figure 4-14D). As can be seen in figure 4-14D, though the silencing worked for all targets, it was not particularly efficient as substantial amounts of residual protein remained.

A

	nmol lipid/mg protein		
	PE	**PS**	**PC**
Untreated	59.27	27.57	105.00
Mock siRNA	68.02	30.41	115.61
SVN siRNA	73.08	36.12	119.96
PSD siRNA	53.75	34.04	131.97
BubR1 siRNA	54.34	29.64	88.74

B

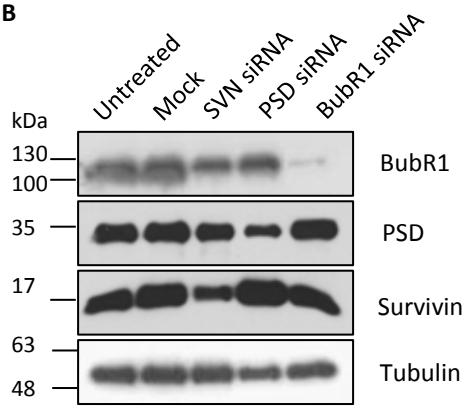


Figure 4-13. Lipid quantitation from HeLa cells treated with siRNA (A and B) HeLa cells were untreated or transfected with transfection reagent only (Mock), 60nM survivin siRNA, 150nM PSD siRNA or 60nM BubR1 siRNA for 72 hours. A fraction of the cells was used for protein quantification and confirmation of knockdown by western blotting **(B)**, the remnant was used for lipid extraction. Lipids were separated by TLC, scraped, hydrolysed through heating with strong acid and their inorganic phosphate content quantified via a malachite green based reagent. Results were expressed as nmol lipid/mg protein.

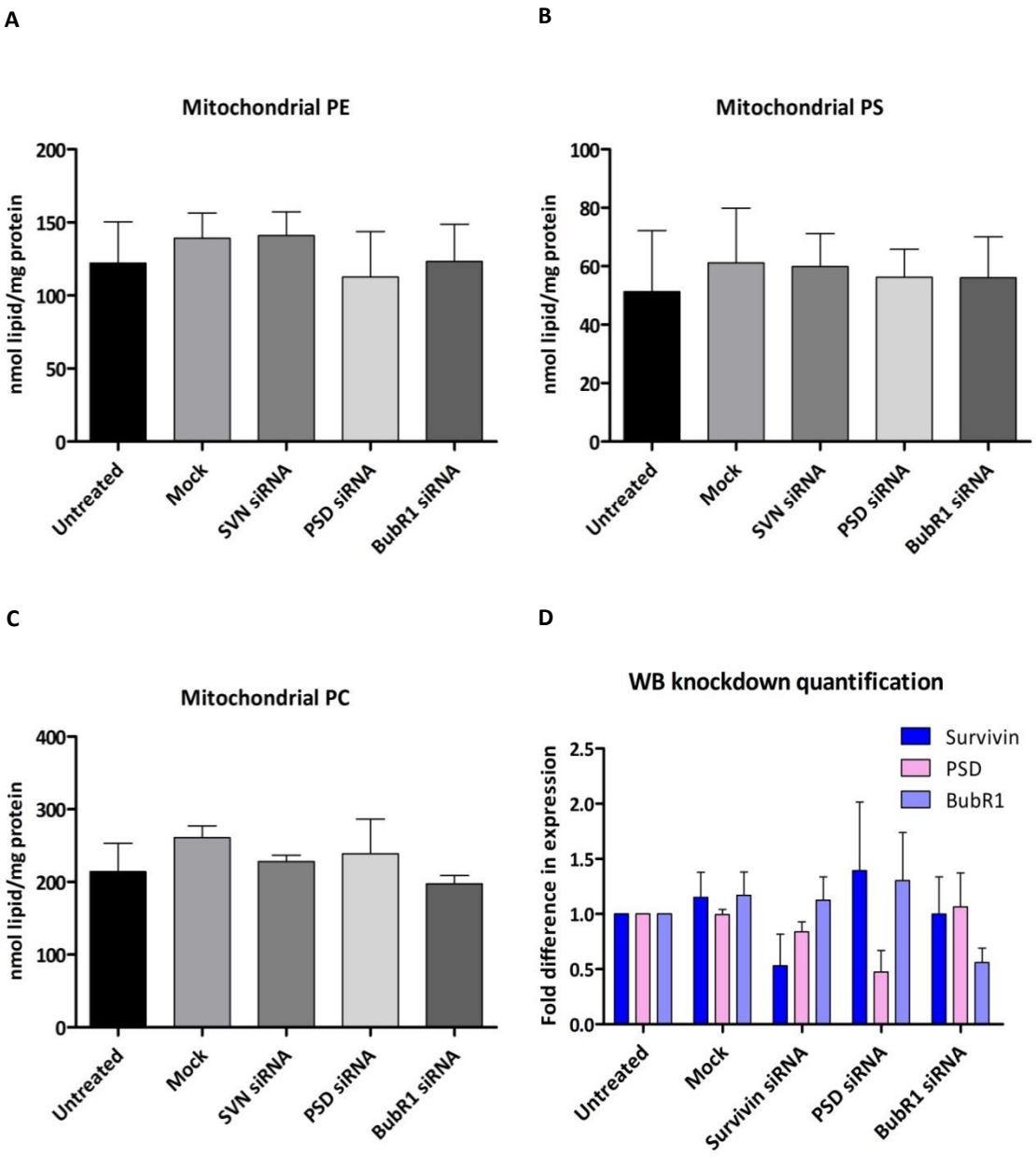
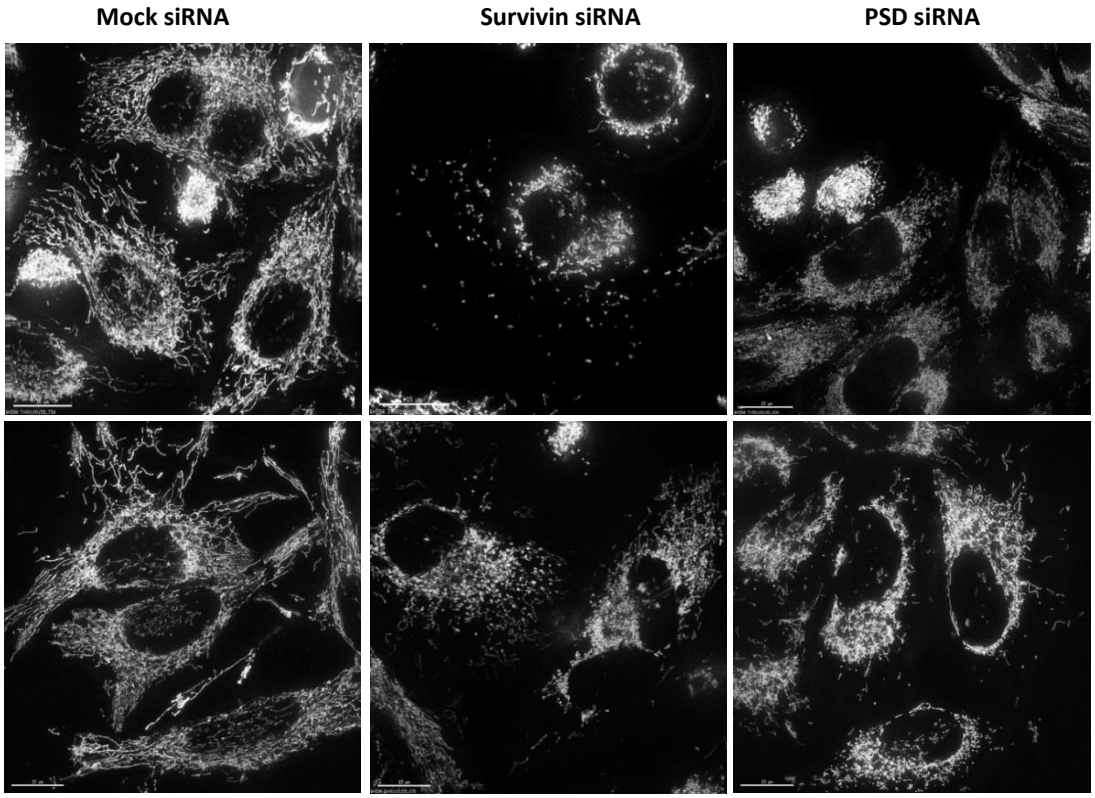


Figure 4-14. Lipid quantitation of mitochondria isolated from siRNA treated HeLa cells (A-D) HeLa cells were left untreated or transfected with transfection reagent only (Mock), 60nM survivin siRNA, 150nM PSD siRNA or 60nM BubR1 siRNA for 72 hours. Cells were harvested, a fraction was taken for western blot verification of the target knockdowns (D) and the remnants subfractionated as described in Methods to obtain a crude mitochondrial preparation. For each condition, a fraction of the mitochondrial suspension was assessed for protein by Bradford and then subdivided into replicates from which lipids were extracted and then separated by TLC. Lipids of interest were scraped, hydrolysed by heating with strong acid and their inorganic phosphate content quantified via a malachite green based reagent. Results were expressed as nmol lipid/mg protein with error bars showing SEM. Lipids quantified were phosphatidylethanolamine (PE) (A), phosphatidylserine (PS) (B) and phosphatidylcholine (PC) (C), (n=2). Western blot signals of siRNA targets survivin, PSD and BubR1 from two individual experiments were quantified by densitometry using ImageJ and normalized against the tubulin loading control. Results were expressed as fold difference compared to untreated control which was set at 1, with error bars are showing SEM.

Lastly, the mitochondrial morphology of siRNA treated cells was examined both by fluorescence microscopy of mitochondria stained with MitoTracker red and by electron microscopy for any ultrastructural changes. Whereas mock treated cells presented with highly interconnected mitochondria, both survivin and PSD silenced cells deviated from such mitochondrial appearance by having higher amount of fragmented mitochondria (Figure 4-15A). Particularly, in survivin siRNA treated cells with larger size, mitochondria appeared as distinct puncta, whereas other cells showed a mixture of punctate mitochondria with some fused mitochondrial tubules. On the other hand, the phenotype of PSD silenced cells was not visibly affected, however, also here the mitochondrial network is no longer as continuous as in mock treated cells. EM imaging of siRNA treated cells revealed no changes in survivin silenced cells as compared to mock treated controls (Figure 4-15B). PSD siRNA treated cells potentially had some swollen mitochondria but also here a distinct phenotype was not obvious.

A



B

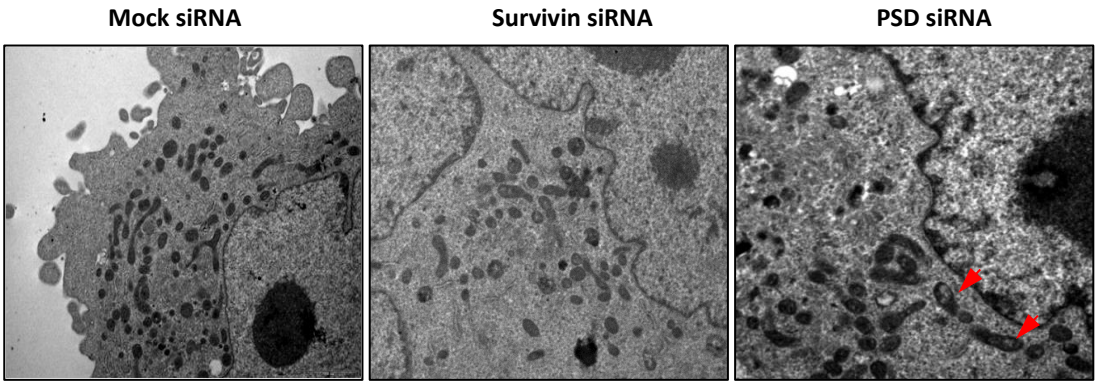


Figure 4-15. Evaluation of mitochondrial morphology of siRNA treated HeLa cells (A&B) HeLa cells were transfected with transfection reagent only (Mock), 60nM survivin siRNA or 150nM PSD siRNA 72 hours. **(A)** Mitochondria of siRNA treated cells were stained with Mitotracker Red prior to imaging with an inverted Olympus Axiophot, Delta Vision Elite microscope with 63x oil objective. Scale bar 15 µm **(B)** siRNA treated cells were fixed and subjected to electron microscopy at x8200 magnification. Swollen mitochondria indicated with red arrows.

4.4 DISCUSSION

This chapter verified the existence of an interaction between survivin and the enzyme PSD both *in vivo* and *in vitro*. This interaction was direct and was mediated by the N-terminus of survivin. However, complex formation was precluded when a proenzyme-locked PSD mutant was used in the co-immunoprecipitation assays indicating that survivin only interacts with the active enzyme. Knockdown of survivin decreased the rate of cell growth, as did PSD knockdown. Interestingly, diminished expression of survivin also manifested with mitochondrial fragmentation which was to a much lesser extent recapitulated in PSD silenced cells. However, ultrastructural analysis of isolated mitochondria from siRNA treated cells by electron microscopy showed no differences from mock treated controls. Also, lipid content analysis of siRNA treated whole cells or mitochondria isolated from equally treated cells did not reveal major alterations. An *in vitro* assay of PSD decarboxylase activity was developed and initially tested with GST-tagged PSD preparations. As such preparations were deemed unsuitable, further optimization of PSD-His expression was performed. Whereas PSD-His purification in *E. coli* was not achieved, HEK293T overexpressed PSD-His was successfully purified and holds promise for future activity assays.

4.4.1 SURVIVIN INTERACTS WITH PSD *IN VITRO* AND *IN VIVO*

This study found, phosphatidylserine decarboxylase (PSD) which is involved in mitochondrial phospholipid biosynthesis, to be a novel survivin interacting partner. Importantly, this interaction was direct and complexes of both proteins were detected by immunoprecipitation. Further *in vitro* mapping revealed the NH_2 (BIR) domain of survivin mediates the interaction with PSD. The survivin monomer is known to consist of two main domains–the N-terminal globular BIR domain (M1-S88) and an amphipathic C-terminal helix (L98-D142) interspersed by a connecting linker segment (V89-T97) (Chantalat et al., 2000). Interestingly, both domains have been implicated in protein-protein interactions. Whereas the C-terminal helix is involved in associating with borealin and INCENP in the CPC at mitosis, the BIR

domain mediates binding to other protein factors, including some involved in apoptosis regulation such as Smac (Sun et al., 2005; Jeyaprakash et al., 2007). Although PSD was first purified from *E. coli* by Dowhan et al. in 1974, as of yet the crystal structure of this protein is still lacking which precluded the design of PSD truncations to further map the interaction site within PSD. Mammalian PSD is translated as an inactive proenzyme of 46kDa which undergoes an autocatalytic cleavage at a conserved LGST motif, between the glycine and serine residues, to release the mitochondrial inner membrane anchored 34 kDa β subunit and the C-terminal ~ 4kDa α-subunit, where the serine residue becomes the pyruvoyl prosthetic group within the active site of the mature enzyme (Kuge et al., 1996; Schuiki & Daum, 2009). Introducing a point mutation at the conserved LGST motif, S378A, should completely inhibit formation of the active enzyme (Onguka et al., 2015). We found survivin could not form a complex with catalytically inactive proenzyme form of PSD in cells, suggesting a possible involvement of survivin in the regulation of enzymatic activity of PSD. To date not much is known about regulation of mammalian phosphatidylserine decarboxylases (Schuiki & Daum, 2009). The only information of their regulation comes from studies in yeast and plants which have pointed to transcriptional regulation of the protein (Rontein et al., 2003; Iwanyshyn et al., 2004). However, no mechanism of a direct modulation of their activity has been described.

4.4.2 RECOMBINANT EXPRESSION SYSTEMS FOR PSD

For the purpose of understanding whether survivin affects PSD activity, this enzyme first needed to be cloned into a suitable expression vector and subsequently purified to be used in *in vitro* decarboxylase activity assay. As mentioned, so far PSD has been purified and characterized only in *E. coli*, with further studies on PSD performed mostly in yeast. The initial approach used here involved cloning, expression and purification of PSD with the glutathione S-transferase (GST)-tag at the N-terminus in *E. coli*, to allow single-step affinity purification using glutathione coupled to a sepharose matrix. Since PSD requires a

self-cleavage maturation step to become active, this could pose an obstacle to its overexpression in a non-mammalian system. However, previous reports suggested PSD can undergo this autocatalysis event also prior to mitochondrial import, in the absence of mitochondrial potential or when mistargeted into a different organelle (ER) altogether (Horvath et al., 2012; Onguka et al., 2015). Therefore, overexpressed GST-PSD should be able to form the mature enzyme also in this system. Nonetheless, given PSD has a transmembrane domain through which it is embedded in the IMM, such expressed protein has limited solubility and may not fold correctly in solution. Moreover, the GST tag interfered with the *in vitro* assay of enzyme activity, prompting the cleavage of the tag which was not successful. As expression of PSD His-tagged at its C-terminus in *E. coli* did no yield useable results, a mammalian system for PSD-His expression, HEK293T cells, was selected for purification. The clear advantage of this system is that it provides a native environment for PSD maturation where it can be targeted into mitochondria to embed into the IMM. In this manner, membranes with embedded PSD are simply solubilized with detergent. This approach proved successful and PSD-His was successfully purified from both whole cell extracts and from isolated mitochondria of transfected HEK293T cells. The activity of the purified PSD-His was below detection limit which suggests higher number of cells will be required for more consistent protein yields. This can be achieved by using suspension instead of adherent cells, HEK293F cells, whereby high levels of proteins can be obtained from 30 -100 ml cultures (Portolano et al., 2014). However, *in vitro* assessment of whether survivin in fact modulates PSD activity might require the presence of additional co-factors otherwise present in cells.

4.4.3 Assay systems for measurement of PSD activity

Current approaches employed to study decarboxylase activity rely on using either whole cell or mitochondrial extracts as a source of PSD and monitor product (PE) formation from labelled PS substrate. Using Ptd[1'-^{14}C]Ser, released $^{14}CO_2$ is captured on KOH-saturated filter paper, and the radioactivity subsequently counted

by liquid scintillation spectrometry (Trotter et al., 1993). This quantification method is used also for substrates with radiolabel present elsewhere in the phospholipid headgroup, such as Ptd[3'-^{3}H]Ser or Ptd[U'-^{14}C]Ser, however, prior separation of the two phospholipid species (PS and PE) by thin layer chromatography and scraping of the silica gel containing radiolabelled PE is required (Choi et al., 2005). An non-radioactive alternative is the use of fluorescent lipid analogs which contain 7-Nitrobenz-2-oxa-1,3-diazol-4-yl (NBD) fluorescent moiety attached to the headgroup or acyl chains. Such labelled phospholipids, NBD-PS and NBD-PE, are again separated via TLC and detected by fluorescence scanning the TLC plates, analogously to Licor Odyssey scanning of western blots. The use of labelled substrate provides the advantage of its distinction from endogenous PS in membranes. Therefore, alternatively to an *in vitro* assessment, PSD activity could be tested in whole cell extracts, or even isolated mitochondria of cells overexpressing mitochondrially targeted survivin generated in this thesis to assess any potential effects of survivin on PSD function in its native environment.

4.4.4 Effect of Survivin and PSD silencing on cell growth

Indirect assessment of survivin – PSD relationship was performed employing siRNA knockdown. Survivin knockdown had a detrimental effect on cell proliferation and induced apoptosis in accordance with previous studies where interference with survivin function using a variety of techniques (antisense oligonucleotides, dominant-negative survivin mutant (C84A), siRNA) manifested as defects in chromosome segregation and failure in cytokinesis with concomitant increase in ploidy and enhanced apoptosis (Carvalho et al., 2003; Lens et al., 2003; Li et al., 1999). Silencing PSD also significantly affected cell growth which was in line with recent evidence supporting acute mitochondrial depletion of PE following PSD knockdown as the causative factor of reduced proliferation in CHO cells (Tasseva et al., 2013). We have found only a slight decrease in both whole cell and mitochondrial PE levels, most likely due to reduction in siRNA efficiency overtime which meant high residual protein levels precluded observing a more consistent

decrease in PE levels. Interestingly, decreasing survivin levels reflected in reduction of PSD, however, it was determined that PSD is a stable protein with slow turnover, whereas survivin turns over rapidly, hence, it is unlikely that survivin regulates PSD stability. Moreover, neither mitochondrial mass was affected therefore the PSD reduction seen, was likely due to overall increase in apoptosis and so destruction of the cell components by caspases rather than a direct effect of survivin interacting with PSD.

4.4.5 MITOCHONDRIAL MORPHOLOGY IN PSD SILENCED CELLS

Mitochondria exist in dynamic interconnected networks undergoing constant fusion/fission events controlled by a set of dynamin-related GTPases modulating their function in response to different stimuli (van der Bliek et al., 2013). Analysis of mitochondria of PSD silenced HeLa cells via fluorescence microscopy revealed minor disruptions of mitochondrial networks with larger amount of unfused, punctate mitochondria compared to untreated or mock treated controls, in agreement with studies in PSD silenced CHO cells and embryonic fibroblasts isolated from PSD knockout mice (Steenbergen et al., 2005; Tasseva et al., 2013). However, as opposed to the study by Tasseva et al. (2013) only small amounts of mitochondrial swelling was observed by electron microscopy. Though this remains to be determined in our system, PSD knockdown in CHO cells led to lower O_2 consumption, lower ATP levels and decline in Complex I and IV activities, with concomitant reduction in complex IV protein (Tasseva et al., 2013). In yeast, loss of mitochondrial Psd1 also leads to defects in mitochondrial fusion, apparent as fragmented or aggregated mitochondria, which cannot be compensated by the CDP-ethanolamine pathway through ethanolamine supplementation, suggesting Psd1 generated PE is essential for maintaining normal mitochondrial morphology (Chan & McQuibban, 2012; Joshi et al., 2012). Indeed, though CDP-ethanolamine pathway synthesized PE is also imported into the mitochondria, and conversely PSD-generated PE is exported into the ER, most of the mitochondrial PE derives from PSD (Shiao et al., 1998; Kainu et al., 2013). PSD depletion was also

accompanied by slower growth, lower oxygen consumption, lower ATP levels and interestingly, impaired biogenesis of the yeast mitochondrial fusion factor s-Mgm1 (Opa1 in mammals), whereas no changes in fusion/fission machinery proteins were detected in CHO cells (Chan & McQuibban, 2012; Tasseva et al., 2013). Together with cardiolipin, which has essential roles in electron transport chain (ETC) complex assembly and stability, adequate levels of PE are important for catalytic activity of ETC complexes (Gebert et al., 2009; Böttinger et al., 2012). Specifically, bovine heart complex IV crystal structure contained associating PE molecules and complex I preparations activity depended on bound PE (Sharpley et al., 2006; Shinzawa-Itoh et al., 2007).

Therefore, though the present study did not detect major changes in PE levels due to inconsistent gene silencing effect, the impairment in cell growth together with mitochondrial fragmentation observed are still most likely due to reduction of mitochondrial PE content.

4.4.6 Survivin as PE regulator in autophagy and mitochondrial bioenergetics

As mentioned previously, survivin has also been implicated in autophagy via its interactions with autophagic modulators Beclin-1 and LC-3, which is coincidentally modified by a covalent PE attachment (Niu et al., 2010; Roca et al., 2008). Indeed, PE, particularly from PS decarboxylation by PSD, was deemed limiting for autophagy as yeast Psd1 and Psd2 deletion mutants manifested with impaired autophagy induction, also with ethanolamine supplementation (Nebauer et al., 2007). This is further demonstrated by eye-specific knockdown of PSD in Drosophila which caused light-dependent retinal degeneration as a result of impaired autophagy driven clearance of activated Rhodopsin 1 (Midorikawa et al., 2010). Conversely, increasing total PE levels with overexpression of Psd1 enhanced yeast survival and upregulated autophagy, which could be also achieved with ethanolamine addition (Rockenfeller et al., 2015). Interestingly, downregulation of survivin, either by siRNA or using the compound YM155 known to suppress survivin

expression, lead to induction of autophagy which might be in part a result of PSD regulation, determining the amount of PE available (Wang et al., 2011b, 2014).

As highlighted, PE is essential for mitochondrial health and activity and indeed, novel pathways involving modulation of mitochondrial bioenergetics have been proposed for mitochondrial survivin in promoting tumour progression. Hagenbuchner et al. (2012) reported survivin overexpression caused mitochondrial fragmentation in neuroblastoma (NB) cell lines, which was in contrast to our own observations where survivin did not affect mitochondrial network integrity in three different cell lines tested, including an NB cell line (Chapter 3). One mechanism of survivin function involved repression of oxidative phosphorylation with concomitant enhancement of aerobic glycolysis to meet the energy requirement (Hagenbuchner et al., 2012). Therefore, pharmacological inhibition of glycolysis causing mitochondrial survivin repression can sensitize tumour cells to cell death (Hagenbuchner et al., 2015). Rivadeneira et al., (2015) showed survivin localized to the inner membrane and the matrix of mitochondria in androgen-independent prostate cancer PC3 cells. This is somewhat puzzling as survivin is a soluble protein and to current knowledge, does not possess any transmembrane domains for membrane anchoring. In this report, survivin silencing (siRNA or YM155) caused wide changes in mitochondrial metabolism which comprised accumulation of different oxidative phosphorylation metabolites, glutamine reduction, decreased O_2 consumption and lower ATP levels probably due to Complex II inhibition, whose components were found to be misfolded and subsequently degraded. However, rather than causing mitochondrial fragmentation, survivin silencing inhibited mitochondrial trafficking to the cell cortex which could be rescued by mitochondrial overexpression of survivin. Therefore, it is possible that metabolic changes occur also in our system though this remains to be determined.

The current study, and also other studies cited, employed overall survivin silencing which also affected survivin function during mitosis, arresting cell division and causing cell death. Therefore, in order to better study the role of mitochondrial survivin, understanding how it is targeted into mitochondria through specialized

sequence motifs required for import machinery recognition is essential. Interference with this process may help dissect the specific roles of survivin in the mitochondria.

In conclusion, this study provided clear evidence for interaction of survivin with PSD both *in vivo* and *in vitro*, which occurs through the N-terminus of survivin. Though the modulation of PSD activity by survivin could not be directly assessed, individual knockdowns of PSD and survivin showed some degree of involvement in the mitochondria. Therefore, ours and studies of others point to novel roles of mitochondrial survivin, which might be a more specific target of anti-cancer therapy without detrimental side effects of interfering with the mitotic function of survivin.

5 INVESTIGATION OF A PUTATIVE PSD SPLICE VARIANT

5.1 TYPES OF PSD

Phosphatidylethanolamine (PE) is an essential phospholipid for correct functioning of the cell, as it participates in processes beyond simply maintaining the integrity of cellular membranes. Different organisms have different ways of obtaining this phospholipid, tailoring PE synthesis to their specific needs. As introduced in chapter 1, in mammalian cells four distinct pathways of PE synthesis exist. The two predominant routes constitute the *de novo* PE synthesis from ethanolamine or ethanolamine-phosphate via the CDP-ethanolamine (Kennedy) pathway in the ER and the PSD mediated decarboxylation of PS at the inner membrane of mitochondria (Vance & Tasseva, 2013). The contribution of these pathways to the cellular PE pool appears to vary among different cell types. In McA-RH7777, Chinese hamster ovary (CHO) K1 cells and isolated rat hepatocytes the CDP-ethanolamine pathway provides the bulk of PE (Tijburg et al., 1989; Bleijerveld et al., 2007). On the other hand, baby hamster kidney (BHK-21) cells and in conflict with another study, CHO cells derive most of their PE from PS decarboxylation, even in the presence of CDP-ethanolamine substrate ethanolamine (Voelker, 1984; Miller & Kent, 1986). However, many of these studies are dated and warrant further attention. Nonetheless, PSD is an important source of PE for mitochondrial membranes (Shiao et al., 1995; Kainu et al., 2013). Interestingly, the two pathways produce different molecular species of PE, which can be recognised by the composition of their hydrocarbon tails (Bleijerveld et al., 2007). Therefore, not only is PE production compartmentalized, it also produces PE species with different physicochemical characteristics. Additional minor contributors to cellular PE in mammalian cells include head-group exchange between PS and ethanolamine by PSS2 and acetylation of lyso-PE to PE (Stein & Stein, 1966; Sundler et al., 1974).

Bacteria rely solely on PE originating from decarboxylation of the precursor phosphatidylserine (PS), and this lipid makes up the bulk of bacterial membranes

(Kanfer & Kennedy, 1964). Both plants and yeast also use the CDP-ethanolamine and PSD pathways for PE synthesis (Clancey et al., 1993; Bessoule & Moreau, 2004; Gibellini & Smith, 2010). Additional pathways for PE synthesis are the base exchange reaction in plants and lyso-PE to PE conversion in yeast (Bessoule & Moreau, 2004; Riekhof & Voelker, 2006).

Some organisms such as yeast and plants have evolved to have more than one gene coding for PSD with different subcellular distribution presumably to compartmentalize the supply of PE. As a result of this divergence, PSDs can be classed as type I, encompassing mitochondrially localized and bacterial enzymes, or type II, which comprise PSD enzymes residing in the Golgi, ER or vacuolar compartment/tonoplast (Schuiki & Daum, 2009). Both types contain a conserved GST motif where self-catalysed cleavage converts the serine residue into the active site associated pyruvoyl group yielding two non-covalently associated non-identical subunits. However, whereas type I enzymes contain mitochondrial targeting signals (MTS) and an inner membrane sorting sequence (IM), type II PSDs have additional domains in the N-terminus (Schuiki & Daum, 2009). In yeast *Saccharomyces cerevisae*, two different gene products with PSD activity have been described, Type I Psd1 in the mitochondria and Type II Psd2 in the Golgi and vacuolar compartments (Clancey et al., 1993; Trotter & Voelker, 1995). On the other hand, in *Arabidopsis thaliana*, three PSD genes have been described comprising the mitochondrial type I Psd1p, and type II Psd2p and Psd3p resident in the tonoplast and the ER, respectively (Rontein et al., 2003; Nerlich et al., 2007). The N-terminus of plant type II PSDs comprises long sequence extensions that are absent from Psd1p and which have not been extensively studied (Nerlich et al., 2007). However, in yeast the N-terminus of Psd2 has a C2 homology domain (Trotter et al., 1995). Originally identified as a Ca^{2+}-binding motif in protein kinase C, this domain can mediate associations with phospholipids and proteins and so Psd2 may be specialised to facilitate PS transport (Nalefski & Falke, 1996). Indeed, in Psd2 this domain was not required for its enzymatic activity *per se*, however, an engineered Psd2 lacking this domain could not complement Psd1 and Psd2 deleted strain *in vivo* (Kitamura et al.,

2002). Therefore, whereas type I PSDs are mostly characterized by the presence of an MTS, type II PSDs can contain additional N-terminal domains with further functions. However, no additional PSD isoforms stemming from the same gene by alternative splicing have been found in these organisms.

To date only a single gene for PSD has been described in mammalian cells, PSD, which was originally identified in complementation studies in CHO cells (Kuge et al. 1991). Mammalian PSD encodes a proenzyme of 409 amino acids with an apparent molecular mass of 46kDa which is processed through sequential steps of proteolysis into 42 and 38kDa forms as it is imported into the mitochondria, until finally undergoing the self-cleavage into 4kDa α and 34kDa β subunits (Kuge et al., 1996). A portion of the β subunit remains anchored in the inner mitochondrial membrane and the associated α subunit remains exposed to solvent in IMS (Zborowski et al., 1983). Interestingly, the UniProtKB entry for the human PSD protein contains an additional sequence of 375 amino acids with no prior experimental confirmation available, suggesting the possible existence of a second isoform. As shown in Figure 5-1A, sequence alignment showed a portion of the N-terminus of the canonical PSD (hereafter referred to as isoform 1) (residues 1-108) has no similarity to isoform 2 but the remaining sequence is identical between the two isoforms (Figure 5-1 A and B). In order to shed light on the existence of a bona fide isoform in humans, analysis of isoform 2 was carried out at the transcript and protein level.

A

```
ISO1      1 MATSVGHRCLGLLHGVAPWRSSLHPCEITALSQSLQPLRKLPFRAFRTDARKIHTAPART
ISO2      1 MMCQSEARQGPEL-RAAKWLH---FPQ-LALRRRLG-----QLSCMSRPALKLRSWPLTV

ISO1     61 MFLLRPLPILLVTGGGYAGYRQYEKYRERELEKLGLEIPPKLAGHWEVALYKSVPTRLLS
ISO2     51 LYYLLPFGAL------------------RPLSRVGWRP------VSRVALYKSVPTRLLS

ISO1    121 RAWGRLNQVELPHWLRRPVYSLYIWTFGVNMKEAAVEDLHHYRNLSEFFRRKLKPQARPV
ISO2     87 RAWGRLNQVELPHWLRRPVYSLYIWTFGVNMKEAAVEDLHHYRNLSEFFRRKLKPQARPV

ISO1    181 CGLHSVISPSDGRILNFGQVKNCEVEQVKGVTYSLESFLGPRMCTEDLPFPPAASCDSFK
ISO2    147 CGLHSVISPSDGRILNFGQVKNCEVEQVKGVTYSLESFLGPRMCTEDLPFPPAASCDSFK

ISO1    241 NQLVTREGNELYHCVIYLAPGDYHCFHSPTDWTVSHRRHFPGSLMSVNPGMARWIKELFC
ISO2    207 NQLVTREGNELYHCVIYLAPGDYHCFHSPTDWTVSHRRHFPGSLMSVNPGMARWIKELFC

ISO1    301 HNERVVLTGDWKHGFFSLTAVGATNVGSIRIYFDRDLHTNSPRHSKGSYNDFSFVTHTNR
ISO2    267 HNERVVLTGDWKHGFFSLTAVGATNVGSIRIYFDRDLHTNSPRHSKGSYNDFSFVTHTNR

ISO1    361 EGVPMRKGEHLGEFNLGSTIVLIFEAPKDFNFQLKTGQKIRFGEALGSI  409
ISO2    327 EGVPMRKGEHLGEFNLGSTIVLIFEAPKDFNFQLKTGQKIRFGEALGSI  375
```

IDENTICAL RESIDUES

SIMILAR RESIDUES

B

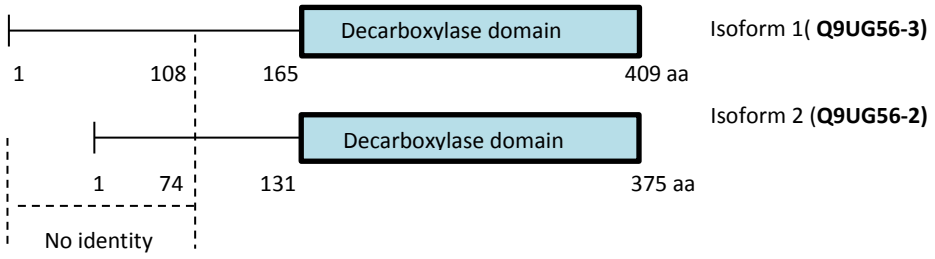
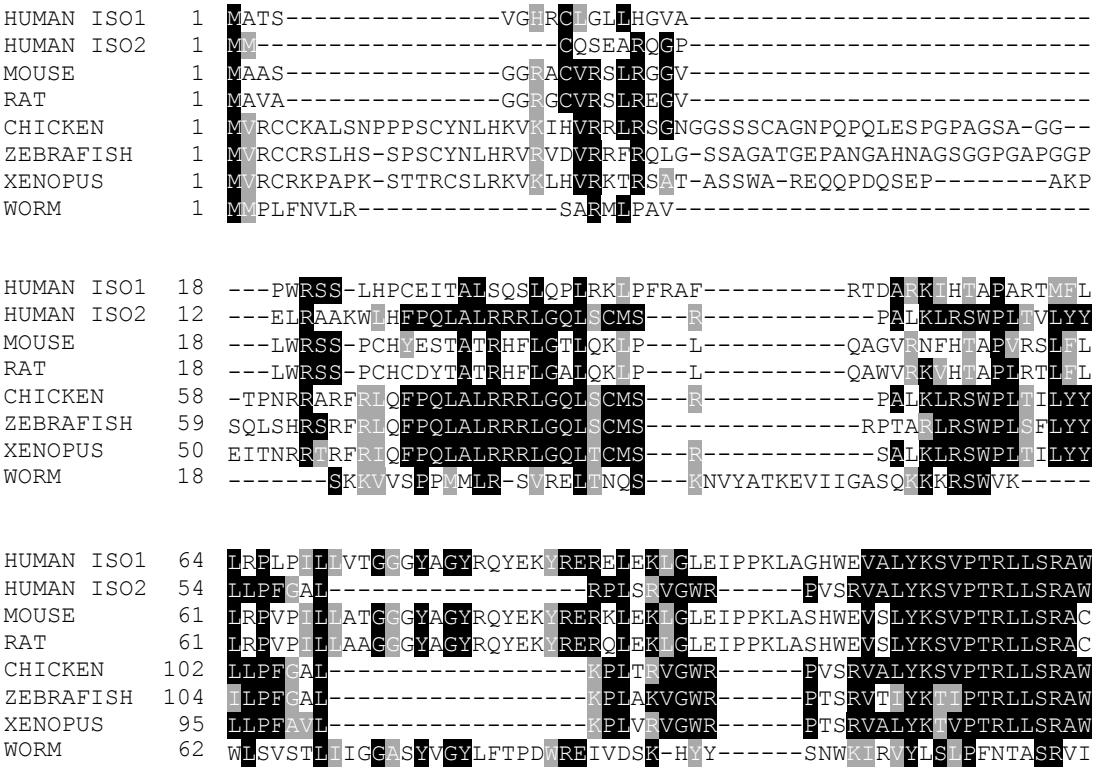


Figure 5-1. Comparison of the canonical PSD sequence (isoform 1) and the putative PSD splice variant (isoform2) (A) Protein sequence alignment of PSD isoform 1 (Q9UG56-3) and isoform 2 (Q9UG56-2) was performed with T-Coffee, and the output subsequently visualized with BoxShade. Identical residues are highlighted in black, similar residues in grey. **(B)** Diagram of the similarity and differences between the two isoforms.

5.2 RESULTS

5.2.1 ANALYSIS OF THE PUTATIVE PSD ISOFORM 2

As opposed to the type II PSDs found in lower organisms which are coded for by a different gene altogether, here the focus was on a putative isoform arising through alternative splicing of the human PSD gene. Multiple sequence alignment from several different organisms revealed a higher degree of conservation of the isoform 2 N-terminus with N-termini of chicken, zebrafish and *Xenopus* PSD than isoform 1 (Figure 5-2). On the other hand, the canonical PSD N-terminus appeared more similar to other mammalian PSDs, in this case mouse and rat sequences. Despite similarities in the N-terminus, this region of the protein seems to be less conserved among the decarboxylases from different species when compared to the highly conserved C-terminus which comprises the active site signature GST motif.



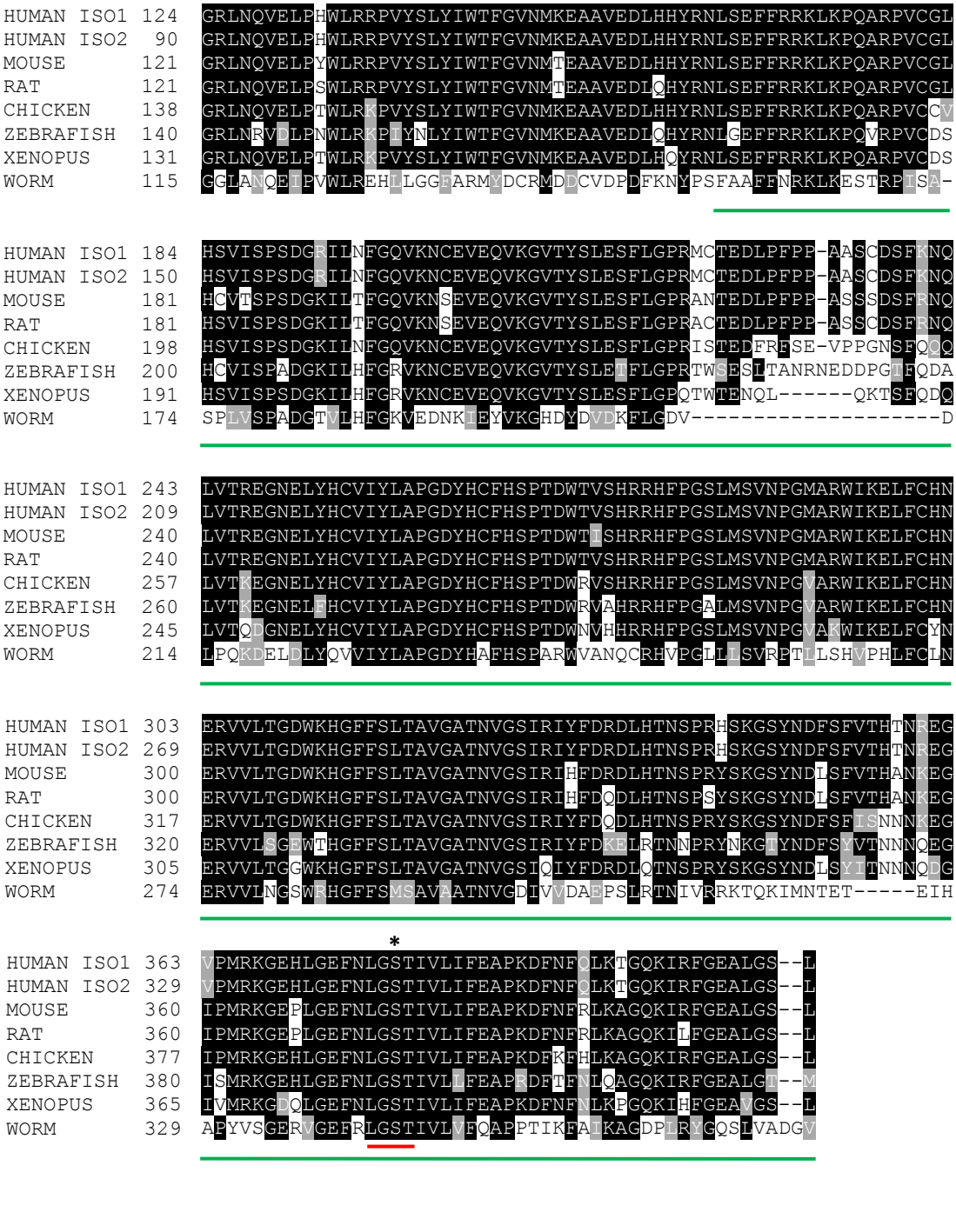


Figure 5-2. Alignment of human PSD isoform1 and the putative isoform2 against PSD enzymes from various species. Protein sequence alignment was performed with T-Coffee, and the output subsequently visualized with BoxShade. Identical residues are highlighted in black, similar residues in grey. Decarboxylase domain underlined in green. The conserved LGST motif at which cleavage into the two nonidentical subunits β and α occurs are underlined with red, with the essential serine residue which becomes the pyruvoyl prosthetic group marked with a star.

5.2.2 TRANSCRIPTIONAL EXPRESSION OF PSD ISOFORM 1 AND PUTATIVE ISOFORM 2 IN DIFFERENT TUMOUR CELL LINES

Since the existence of this second PSD isoform has not been experimentally validated we sought to determine whether it is being actively transcribed in the cell. For this purpose, total RNA from three cancer cell lines – HeLa, SH-SY5Y and U2OS cells, was extracted and reverse transcribed into cDNA using random primers. Subsequently, this cDNA was used as a template in a PCR reaction with either the canonical isoform 1 primers as a positive control or putative isoform 2 primers. As expected, PSD isoform 1 (1230bp) showed amplification in all three cell lines tested (Figure 5-3A and B). A slightly smaller band corresponding to PSD isoform2 (1128bp) was also present in the three cell lines analysed, which was corroborated by comparison to a control reaction where pcDNA3.1- PSD isoform 2 template (VO Iso2), cloned from an IMAGE consortium provided sequence, was used as a positive control. Therefore, this suggests at least in the tumour cell lines tested, PSD isoform 2 is indeed transcribed.

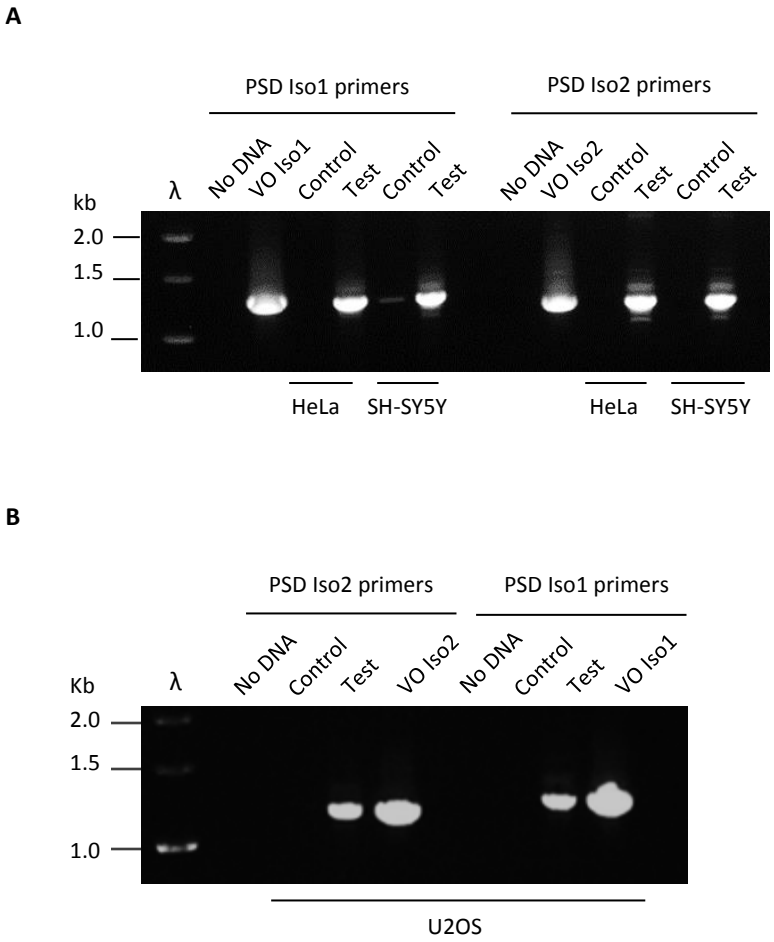


Figure 5-3.Transcription of PSD isoform 2 in human tumour cell lines. (A and B) Reverse-transcriptase PCR performed on cDNA (test) obtained from HeLa cells, SH-SY5Y cells (A) and U2OS cells (B) using primers for the canonical PSD isoform 1 and primers specic for PSD isoform 2. No DNA and cDNA control (reverse transcriptase was excluded so no cDNA should have been made) were used as a negative control with both primer sets. Cloned PSD isoform 1 and 2 pcDNA constructs were used as a positive control, VO Iso1 and VO Iso2.

5.2.3 GENERATION OF A PSD ISOFORM 2 SPECIFIC ANTIBODY

Given that PSD isoform 2 could be detected at the transcript level in all three lines tested, we next sought to assess whether it is also translated in these cells. The available commercial PSD antibody recognizes the middle portion of the protein, corresponding to a sequence within the β-subunit, which is present in both PSD isoforms and so cannot distinguish between them. Therefore, generation of a PSD isoform 2 specific antibody was commissioned against the unique N-terminus of PSD isoform 2. An antigenic peptide (residues 3-14) at the beginning of the

sequence was selected for immunization of two male rabbits as it was the most dissimilar to the host rabbit sequences (Figure 5-4A). The pre-immune serum of four different rabbits was screened by immunoblotting either as neat or at dilutions 1:10 and 1:100 in 5% non-fat milk in PBST (Figure 5-4B - only 1:100 shown) to check for the presence of non-specifically reacting components of the rabbit serum with proteins of the same size as our protein of interest. Particularly rabbit number 1 serum was deemed unsuitable as it cross-reacted with proteins just below 48kDa and another one at 35kDa, protein sizes close to the expected unprocessed and mature forms of both PSD isoforms, respectively. Therefore, rabbits number 2 and 4 were selected for the immunization programme which would provide antigen peptide-affinity purified antibody. The resulting affinity purified antibody was then tested against whole cell extracts from cells transfected with both wild type and the processing mutant of isoform 1 and 2.

The specificity of the generated PSD isoform 2 specific antibody was assayed in immunoblotting with extracts from HEK293T cells transfected with PSD isoform 1 and 2, both wild-type and proenzyme locked-mutant (LGST→LGAT) unable to form an active heterodimer. First, the commercial pan-PSD antibody was used to identify transfected proteins to subsequently allow comparison with proteins detected by isoform 2-specific antibody. The pan-PSD antibody recognized a band at ~46 and ~42kDa corresponding to unprocessed and presumably the mitochondria imported and cleaved forms, respectively, in the isoform 1 (wild type and mutant) transfected lanes (Figure 5-4C). In contrast, in the untransfected lane, these processing intermediate forms were not detectable given that probably most of PSD has successfully translocated into mitochondria and processed into an active heterodimer comprising the 34kDa β-subunit, shown by immunoblotting in Figure 5-4C and the 4kDa α-subunit. As expected, this same band was upregulated in isoform 1 wild type but not mutant transfected lanes. Interrogation of transfected PSD isoform 2 species with pan-PSD antibody revealed overexpressed β-subunit of wild-type PSD isoform 2 had a higher molecular weight than the isoform 1 subunit (Figure 5-4C). However, since the isoform 2 processing mutant appeared at the

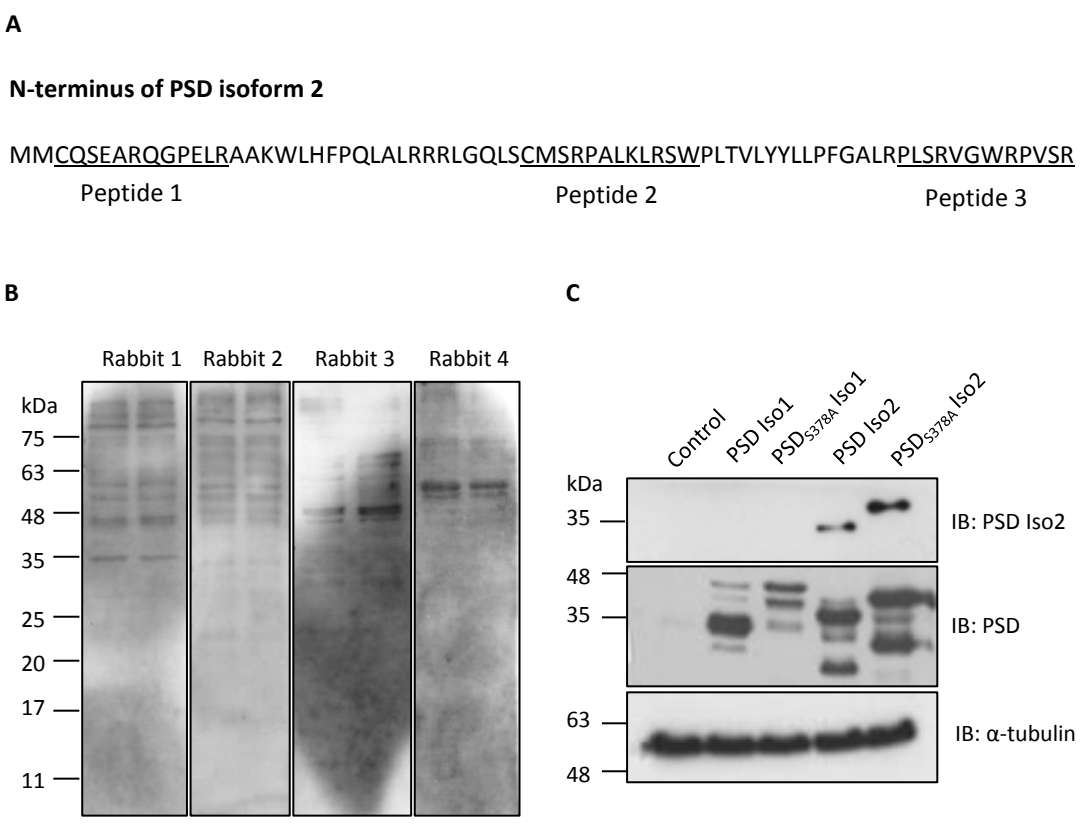


Figure 5-4. Generation of a PSD isoform 2 specific antibody. (A) N-terminus of PSD isoform 2 with no homology to PSD isoform1 with three possibilites of antigenic peptides for antibody production. Peptide 1 was selected for its highest foreigness to the host animal. **(B)** The immunoreactivity of pre-immune bleeds (from rabbits 1-4) against whole cell extracts from HeLa cells (20µg protein loaded) was tested by immunoblotting at 1:100 dilution **(C)** Affinity purified antibody raised against PSD isoform 2 specific peptide was tested against whole cell extracts made from untrasfected HEK293T cells, HEK293T cells transfected wild type PSD or the processing inactive mutant PSD_{S378A} of either isoform 1 or isoform 2. The same extracts were also blotted with PSD antibody recognizing both isoforms and α-tubulin as loading control. 30µg protein loaded per lane.

predicted ~43kDa with no intermediate cleaved forms during mitochondrial import, this suggested that unlike isoform 1, the N-terminus of isoform 2 does not undergo proteolytic cleavage. Next, the isoform 2 specific antibody was tested on these same extracts and revealed two bands in the isoform 2 transfected lanes only – a band corresponding in size to the isoform 2 β-subunit and in the next lane, a band for the unprocessed isoform 2 proenzyme identified by comparison with bands obtained with the general PSD antibody. Therefore, the generated PSD isoform 2 antibody specifically recognised the overexpressed PSD2 but not PSD1, although additional non-specific bands were also detected in whole cell extracts. However,

no endogenous PSD2 was detected in these asynchronous whole cell extracts, which could be due to low expression.

5.2.4 Ectopically expressed PSD isoform 2 localizes in the mitochondria

Since PSD contains a mitochondrial targeting sequence within its N-terminus that is subsequently cleaved off upon import, and isoform 2 differs precisely in this part of the sequence, we sought to determine where the ectopically expressed PSD2 protein localizes in the cell. Computational analysis suggested cytoplasmic localization of isoform 2 with the exception of one prediction program assigning it to the mitochondrial compartment. HeLa cells transiently transfected with pcDNA3.1 PSD iso2-GFP were stained with MitoTracker Red to reveal the mitochondria and imaged live. As shown in figure 5-4, PSD isoform 1 GFP fusion and isoform 2 GFP fusion localized in the mitochondria. Therefore, the distinct N-terminus of isoform 2 also appears to contain signals for efficient mitochondrial delivery, suggesting a cryptic signal could be present also within the decarboxylase domain of the protein.

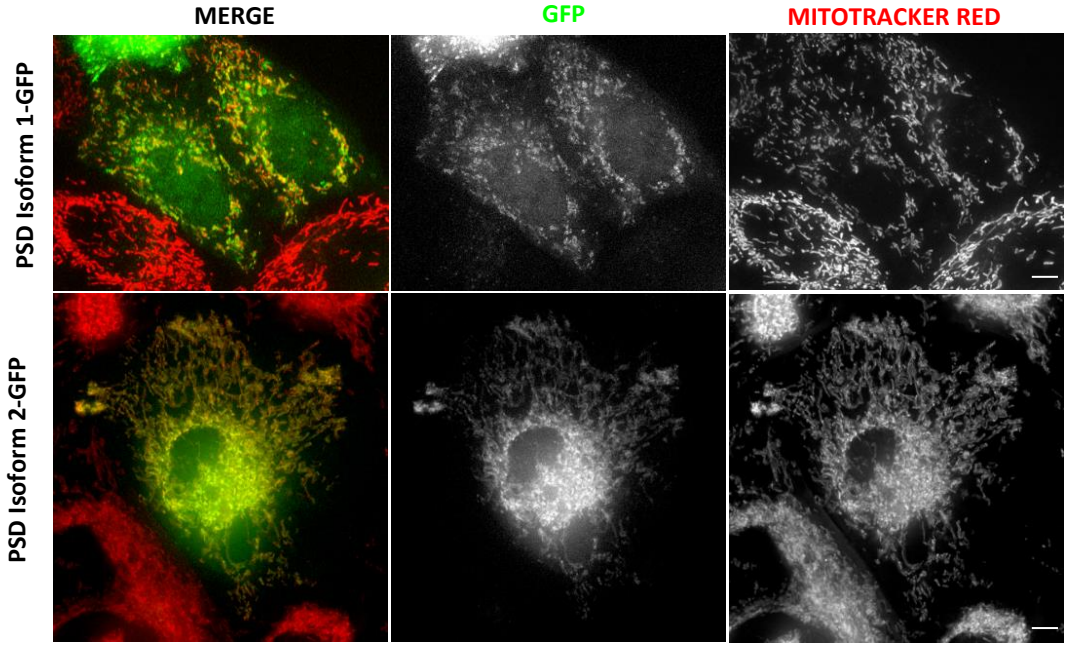


Figure 5-5. Subcellular localization of PSD GFP isoform 1 and 2. (A and B) HeLa cells were transiently transfected with either pcDNA3.1 PSD-GFP isoform 1 (A) or isoform 2 (B). Mitochondria were stained with MitoTracker Red CMXRos just prior to live cell imaging using an inverted Olympus Axiophot, Delta Vision Elite microscope with 63x oil objective. Scale bar 10µm.

5.2.5 PSD ISOFORM 2 BINDS DIRECTLY TO SURVIVIN *IN VITRO*

In chapter 4, we found PSD isoform 1 interacted directly with survivin *in vitro* and could only immunoprecipitate with mature PSD in heterodimer conformation and not with the processing mutant PSD_{S378A} permanently held in the proenzyme form. Since this observation suggested the decarboxylase domain of PSD mediates the interaction with survivin, we sought to evaluate whether PSD isoform 2 which shares this portion of the protein but has a different N-terminus can recapitulate this interaction. Therefore, a GST pull-down assay was performed during which immobilized GST or GST-survivin was incubated with ^{35}S-labelled IVT PSD isoform 2 or Borealin as positive control (see chapter 4). As shown in figure 5-6, ^{35}S-labelled PSD isoform 2 could efficiently bind to GST-survivin but not to GST alone.

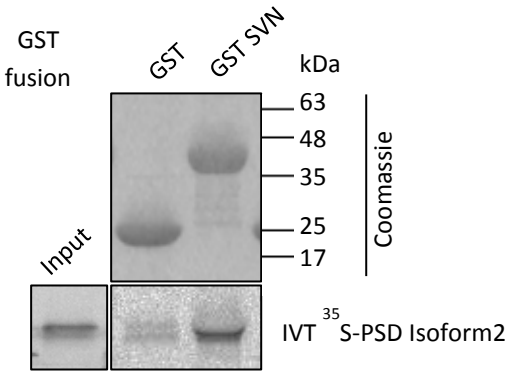


Figure 5-6. PSD isoform2 interacts directly with survivin *in vitro.* (Top panel) GST alone and GST SVN proteins immobilized on glutathione sepharose beads (binding shown with Coomassie stain) were incubated with *in vitro* translated radioactively ([^{35}S]L-methionine) labelled PSD isoform 2. 15% Input was loaded as control for success of IVT reaction.

5.3 DISCUSSION

PSD is a conserved enzyme that accommodates the cellular demands for PE. However, to date not much is known about how these enzymes are regulated in the cell. Yeast and plants have more than one PSD coded by different genes, the products of which localize within different organelles to provide site-specific PE

synthesis. By contrast, mammalian cells are thought to rely on a single mitochondrial PSD with other PE producing pathways in place elsewhere in the cell. However, although only one PSD has been described in humans to date, UniprotKB annotation suggested the possibility of a second PSD splice variant, thus the expression of this putative isoform was investigated.

Comparison between the isoform sequences revealed the putative isoform only differs in the first 108 amino acids of isoform 1, after which the two proteins are fully identical. Moreover, multiple sequence alignment demonstrated some degree of conservation of this unique N-terminus at least in half of the organisms examined, namely chicken, zebrafish and *Xenopus*. Importantly, this splice variant is actively transcribed in three tumour cell lines tested. Given the commercial PSD antibody could not distinguish between the two PSD isoforms, an isoform 2 specific antibody was commissioned and successfully raised against an isoform 2 specific N-terminal peptide. As designed, this antibody specifically recognized overexpressed PSD isoform 2 but not isoform 1. However, endogenous PSD isoform 2 levels were possibly too low and to date, have not been detected by this antibody. One reason for this could be that isoform 2 is rapidly degraded following translation and only be stabilized under specific conditions. Alternatively, as ectopically expressed isoform 2 localized to the mitochondria as isoform 1, it is possible the levels of this isoform become upregulated to contribute to mitochondrial PE production under conditions of higher PE demand. Of note, since the antibody cross reacted with a minimum of 3 other proteins with higher affinity, depleting the amount of antibody available to cross-react with our protein of interest could have hindered its detection. Indeed, the isoform 2 specific antibody was less sensitive than the pan-PSD antibody. However, even though endogenous isoform 2 was not detected in the present study, an essential tool for its specific detection has been generated as part of this thesis and will provide an important reagent for PSD isoform 2 protein validation.

Alternative splicing is an important regulatory pathway of gene expression in eukaryotic cells which allows a single gene to give rise to several messenger RNAs by joining of different exon combinations. These can then be translated into distinct

protein products with different biological function leading to a substantial enrichment of the proteome. Some estimates argue for ~40–60% of human genes to be alternatively spliced (Modrek & Lee, 2002), while genome-wide splice-sensitive microarray studies suggest approximately 74% of human genes with multiple exons are alternatively spliced (Johnson et al., 2003). These splicing events can be tissue specific, occur at a particular stage of development or play a role in disease pathogenesis. High-density array analysis of chromosomes 21 and 22 indicated that 12-21% of the genes have only one isoform, whereas the remaining 79 – 88% can have several (Kampa et al., 2004). Coincidentally, the PSD gene is indeed located on chromosome 22 and given the results of the present study could fall in the multiple isoform category. This study found the PSD isoform 2 is transcribed in cancer cell lines but it remains to be determined whether this is a cancer specific phenomenon or also pertains to normal healthy cells. Indeed, changes in the splicing regulatory factors could contribute to malignancy and this isoform could be only active in tumours (David & Manley, 2010; Faustino et al., 2003). While detection of PSD isoform 2 transcripts in cells does not provide evidence as to whether it exists as a functional protein in cells, preliminary experiments with purified GST-tagged PSD isoform 2 suggest its decarboxylase activity is intact.

An alternative reason why endogenous PSD2 has evaded detection at the protein level is that the isoform 2 transcript is the product of a pseudogene. Pseudogenes are copies of genes which have lost their protein-coding ability due to incomplete duplication or mutations giving rise to premature stop codons and frameshifts, or due to loss of important regulatory elements required for efficient transcription, splicing and translation (Torrents et al., 2003). Whereas non-processed pseudogenes arise from duplication events with high incidence of mutations resulting in non-functional truncation products, processed pseudogenes arise through retro-transposition of mRNA back into the genome (Torrents et al., 2003). The latter, even though disabled, can then be transcribed such that the resulting RNA molecule resembles a messenger RNA with a long open reading

frame. Database mining did not show any other location in the genome with sequences homologous to PSD isoform 2, therefore this theory seems unlikely.

In conclusion, PSD isoform 2 is transcribed across a panel of tumour cell lines but it remains to be established whether it is also translated as a functional protein. However, since PSD isoform 2 specific antibody has been successfully raised which recognizes isoform 2 specifically, the answer to this question is imminent.

6 FINAL CONCLUSIONS AND OUTLOOK

The main focus of this thesis has been the multifaceted protein survivin which is involved in a plethora of processes including cell division, apoptosis suppression, autophagy and even mitochondrial ATP production and metabolism. In most adult differentiated cells, survivin expression is tightly regulated and only elevates at the onset of mitosis when it functions as part of the CPC ensuring successful cell division (Ambrosini et al., 1997). Importantly, survivin is highly upregulated in most human cancers where it is associated with resistance to radiation and chemotherapy (Rödel et al., 2005; Colnaghi et al., 2006; Athanasoula et al., 2014), thus understanding its roles in these various pathways has clear medical implications. When overexpressed, survivin localizes predominantly in the cytoplasm, however a small mitochondrial pool of survivin has been described (Dohi et al., 2004a). Given that mitochondria orchestrate the MOMP and the subsequent release of pro-apoptotic factors, it is perhaps not surprising that mitochondrial survivin has been investigated mainly in connection to a cytoprotective role. The focus of this thesis was to investigate mitochondrial survivin and its functions in the mitochondria distinct from apoptosis suppression. Specifically, a putative link between survivin and the mitochondrial enzyme phosphatidylserine decarboxylase (PSD), suggested by preliminary data in the Wheatley laboratory, was examined. PSD mediates the conversion of the phospholipid phosphatidylserine (PS) into phosphatidylethanolamine (PE), which is an essential component of cell membranes and so is required for maintaining normal mitochondrial morphology and multiple other functions.

This study determined that mitochondrial survivin was indeed present exclusively in tumour and not normal healthy cells. Moreover, its levels were enhanced in the mitochondria isolated from cells arrested in M-phase of the cell cycle. Both survivin and PSD shared the same sub-mitochondrial localization, the intermembrane space reinforcing the possibility of a link between them. Though mitochondrial import of survivin has been studied previously, the signal/s required

for successful translocation were not identified. This study established the initial ten amino acid stretch of survivin could target its fusion partner GFP into mitochondria. Although this decapeptide is not a canonical mitochondrial targeting sequence, these data nevertheless demonstrate that it is sufficient to direct mitochondrial import, and therefore is, at least a contributing element that directs survivin to the mitochondrion. However, as a truncation mutant lacking these ten amino acids was also able to enter the mitochondrion, further studies should address any contributions of longer survivin N-terminal sequences on mitochondrial import, or perhaps also examine how the C-terminus of survivin participates in this process, and whether any cofactors are engaged in mitochondrial targeting in the intact cell.

Surprisingly, neither ectopic expression of survivin at a whole cell level, nor mitochondrial confinement of survivin expression manifests with any morphological mitochondrial abnormalities. However, it would be interesting to test the functional competence of such mitochondria in terms of respiration to better understand the role of mitochondrial survivin, particularly given its association with PSD.

The main finding of this thesis was the corroboration of a putative interaction between survivin and the enzyme PSD. Further mapping revealed that the N-terminus (1-90) of survivin, that is the BIR domain, is the domain responsible for PSD interaction. Additional mutational analysis of the BIR domain could help unravel the precise interaction interface required for docking onto PSD. Similar study in PSD was precluded by the lack of an available PSD structure, and further confounded by the self-processing event which takes place to generate two distinct subunits of the mature enzyme. However, interestingly, interaction with survivin was dependent upon PSD being in an active conformation, which suggests that the decarboxylase domain may be engaged in the interaction, and lends weight to the notion that survivin is a direct regulator of PSD.

In this thesis, extensive purification efforts were undertaken to obtain an active PSD preparation, with the aim of assessing the impact of survivin on its

activity *in vitro*. The most successful preparation came from purification of His-tagged PSD from transiently transfected HEK293T cells, presumably as this system provided a native environment for PSD folding. Therefore, future experiments with protein preparations obtained from this purification strategy should be used for *in vitro* activity assays with titrated amounts of survivin binding to PSD. As no regulatory mechanisms of this enzyme in mammalian cells have been described to date, any potential effects unravelled by this approach will be an exciting advancement in this field.

Finally, this thesis also addressed the existence of a novel human PSD isoform (Isoform 2), which differed from the canonical protein solely in its N-terminus, with the remaining sequence encompassing the decarboxylase domain fully identical. Therefore, this second isoform would be predicted to be functionally competent. Importantly, this isoform was detectable at the transcript level in a panel of three tumour cell lines. Given that commercial PSD antibody does not allow distinction between the two isoforms, an isoform 2 N-terminus specific antibody was successfully raised. This antibody effectively distinguished between PSD isoform 1 and PSD isoform 2, however, the presence of endogenous PSD isoform 2 has yet to be achieved. Therefore, future studies employing this isoform-2 specific tool generated in this thesis will be essential in proving the existence and function of this second isoform.

In conclusion, this thesis unveiled a novel survivin interacting partner, the lipid biosynthetic enzyme PSD, which is specifically relevant to the pool of survivin localizing in the mitochondria. Given that this interaction was exclusive to the active form of PSD, it is tempting to speculate that survivin regulates PSD activity, thereby regulating PE availability in cells. As PE is an essential phospholipid which is required for maintenance of mitochondrial integrity, successful cytokinesis and lipidation of autophagosomes during autophagy, the identification of mitochondrial survivin as a regulator of PSD activity can be expected to have a significant impact on cellular health. Therefore, this thesis identified a completely novel mechanism by which mitochondrial survivin could be further fuelling tumorigenesis *in vivo*.

7 REFERENCES

Abe, Y., Shodai, T., Muto, T., Mihara, K., Torii, H., Nishikawa, S., Endo, T. & Kohda, D. (2000). Structural basis of presequence recognition by the mitochondrial protein import receptor Tom20. *Cell*. 100 (5). p.pp. 551–560.

Adams, R.R., Eckley, D.M., Vagnarelli, P., Wheatley, S.P., Gerloff, D.L., Mackay, a M., Svingen, P. a, Kaufmann, S.H. & Earnshaw, W.C. (2001). Human INCENP colocalizes with the Aurora-B/AIRK2 kinase on chromosomes and is overexpressed in tumour cells. *Chromosoma*. 110 (2). p.pp. 65–74.

Adams, R.R., Wheatleya, S.P., Gouldsworthy, a. M., Kandels-Lewis, S.E., Carmena, M., Smythe, C., Gerloff, D.L. & Earnshaw, W.C. (2000). INCENP binds the Aurora-related kinase AIRK2 and is required to target it to chromosomes, the central spindle and cleavege furrow. *Current Biology*. 10 (17). p.pp. 1075–1078.

Ahting, U., Thun, C., Hegerl, R., Typke, D., Nargang, F.E., Neupert, W. & Nussberger, S. (1999). The TOM core complex: The general protein import pore of the outer membrane of mitochondria. *Journal of Cell Biology*. 147 (5). p.pp. 959–968.

Alberts, Bruce; Johnson, Alexander; Lewis, Julian, Raff, Martin; Roberts, Keith; Walter, Peter. 2002. Molecular Biology of the Cell, 4th edition. New York: Garland Science. ISBN-10: 0-8153-3218-1

Alberts, Bruce; Bray, Dennis; Hopkin, Karen;Johnson, Alexander; Lewis, Julian. 2013. Essential Cell Biology, 4th edition. New York: Garland Science

Aljaberi, A.M., Webster, J. & Wheatley, S.P. (2014). Analysis of the functional repertoire of a mutant form of survivin, K129E, which has been linked to lung cancer. *Cancer Cell International*. [Online]. 14 (1). p.p. 78.

Allen, S., Balabanidou, V., Sideris, D.P., Lisowsky, T. & Tokatlidis, K. (2005). Erv1 mediates the Mia40-dependent protein import pathway and provides a functional link to the respiratory chain by shuttling electrons to cytochrome c. *Journal of Molecular Biology*. 353 (5). p.pp. 937–944.

Allison, D.S. & Schatz, G. (1986). Artificial mitochondrial presequences. *Proceedings of the National Academy of Sciences of the United States of America*. 83 (23). p.pp. 9011–9015.

Altieri, D.C. (2010). Survivin and IAP proteins in cell-death mechanisms. *The Biochemical journal*. 430 (2). p.pp. 199–205.

Ambrosini, G., Adida, C. & Altieri, D.C. (1997). A novel anti-apoptosis gene, survivin, expressed in cancer and lymphoma. *Nature medicine*. 3 (8). p.pp. 917–921.

Andrews, P.D., Ovechkina, Y., Morrice, N., Wagenbach, M., Duncan, K., Wordeman, L. & Swedlow, J.R. (2004). Aurora B regulates MCAK at the mitotic centromere.

Developmental Cell. 6 (2). p.pp. 253–268.

Ashkenazi, A. & Dixit, V.M. (2015). Receptors : Signaling and Modulation. *Science*. 281 (5381). p.pp. 1305–1308.

Athanasoula, K.C., Gogas, H., Polonifi, K., Vaiopoulos, A.G., Polyzos, A. & Mantzourani, M. (2014). Survivin beyond physiology: Orchestration of multistep carcinogenesis and therapeutic potentials. *Cancer Letters*. [Online]. 347 (2). p.pp. 175–182.

Badran, A., Yoshida, A., Ishikawa, K., Goi, T., Yamaguchi, A., Ueda, T. & Inuzuka, M. (2004). Identification of a novel splice variant of the human anti-apoptopsis gene survivin. *Biochemical and Biophysical Research Communications*. 314 (3). p.pp. 902–907.

Balasubramanian, K. & Schroit, A.J. (2003). Aminophospholipid asymmetry: A matter of life and death. *Annual review of physiology*. 65. p.pp. 701–734.

Banci, L., Bertini, I., Cefaro, C., Ciofi-Baffoni, S., Gallo, A., Martinelli, M., Sideris, D.P., Katrakili, N. & Tokatlidis, K. (2009). MIA40 is an oxidoreductase that catalyzes oxidative protein folding in mitochondria. *Nature structural & molecular biology*. 16 (2). p.pp. 198–206.

Banks, D.P., Plescia, J., Altieri, D.C., Chen, J., Rosenberg, S.H., Zhang, H. & Ng, S.C. (2000). Survivin does not inhibit caspase-3 activity. *Blood*. 96 (12). p.pp. 4002–4003.

Bannai, H., Tamada, Y., Maruyama, O., Nakai, K. & Miyano, S. (2002). Extensive feature detection of N-terminal protein sorting signals. *Bioinformatics (Oxford, England)*. 18 (2). p.pp. 298–305.

Barrett, R.M. a, Colnaghi, R. & Wheatley, S.P. (2011). Threonine 48 in the BIR domain of survivin is critical to its mitotic and anti-apoptotic activities and can be phosphorylated by CK2 in vitro. *Cell Cycle*. 10 (3). p.pp. 538–548.

Barrett, R.M.A., Osborne, T.P. & Wheatley, S.P. (2009). Phosphorylation of survivin at threonine 34 inhibits its mitotic function and enhances its cytoprotective activity. *Cell Cycle*. [Online]. 8 (2). p.pp. 278–283.

Bauer, M.F., Gempel, K., Reichert, a S., Rappold, G. a, Lichtner, P., Gerbitz, K.D., Neupert, W., Brunner, M. & Hofmann, S. (1999). Genetic and structural characterization of the human mitochondrial inner membrane translocase. *Journal of molecular biology*. 289 (1). p.pp. 69–82.

Bauer, M.F., Hofmann, S., Neupert, W. & Brunner, M. (2000). Protein translocation into mitochondria: The role of TIM complexes. *Trends in Cell Biology*. 10 (1). p.pp. 25–31.

Beardmore, V. a, Ahonen, L.J., Gorbsky, G.J. & Kallio, M.J. (2004). Survivin dynamics increases at centromeres during G2/M phase transition and is regulated by microtubule-attachment and Aurora B kinase activity. *Journal of cell science*. 117 (Pt 18). p.pp. 4033–4042.

Beasley, E.M., Muller, S. & Schatz, G. (1993). *cytochrome b2*. 1 (6). p.pp. 2303–2311.

Bekier, M.E., Mazur, T., Rashid, M.S. & Taylor, W.R. (2015). Borealin dimerization mediates optimal CPC checkpoint function by enhancing localization to centromeres and kinetochores. *Nature Communications*. [Online]. 6. p.p. 6775.

Bessoule, J. & Moreau, P. (2004). 2 Phospholipid synthesis and dynamics in plant cells. In: *Lipid Metabolism and Membrane Biogenesis*. pp. 89–124.

Bevers, E.M., Comfurius, P., van Rijn, J.L.M.L., Hemker, H.C. & Zwaal, R.F. (1982). Generation of prothrombin-converting activity and the exposure of phosphatidylserine at the outer surface of platelets. *European Journal of Biochemistry*. 122 (2). p.pp. 429–436.

Bihlmaier, K., Mesecke, N., Terziyska, N., Bien, M., Hell, K. & Herrmann, J.M. (2007). The disulfide relay system of mitochondria is connected to the respiratory chain. *Journal of Cell Biology*. 179 (3). p.pp. 389–395.

Birner, R., Bürgermeister, M., Schneiter, R. & Daum, G. (2001). Roles of phosphatidylethanolamine and of its several biosynthetic pathways in Saccharomyces cerevisiae. *Molecular biology of the cell*. 12 (4). p.pp. 997–1007.

Bishop, J.D. & Schumacher, J.M. (2002). Phosphorylation of the carboxyl terminus of inner centromere protein (INCENP) by the Aurora B Kinase stimulates Aurora B kinase activity. *The Journal of biological chemistry*. 277 (31). p.pp. 27577–27580.

Bleijerveld, O.B., Brouwers, J.F.H.M., Vaandrager, A.B., Helms, J.B. & Houweling, M. (2007). The CDP-ethanolamine pathway and phosphatidylserine decarboxylation generate different phosphatidylethanolamine molecular species. *Journal of Biological Chemistry*. 282 (39). p.pp. 28362–28372.

van der Bliek, A.M., Shen, Q. & Kawajiri, S. (2013). Mechanisms of mitochondrial fission and fusion. *Cold Spring Harbor perspectives in biology*. 5 (6).

Boas, F.E., Forman, L. & Beutler, E. (1998). Phosphatidylserine exposure and red cell viability in red cell aging and in hemolytic anemia. *Proceedings of the National Academy of Sciences of the United States of America*. 95 (6). p.pp. 3077–3081.

Boidot, R., Végran, F. & Lizard-Nacol, S. (2014). Transcriptional regulation of the survivin gene. *Molecular Biology Reports*. 41 (1). p.pp. 233–240.

Bolton, M.A., Lan, W., Powers, S.E., McCleland, M.L., Kuang, J. & Stukenberg, P.T. (2002). Aurora B kinase exists in a complex with survivin and INCENP and its kinase activity is stimulated by survivin binding and phosphorylation. *Molecular biology of the cell*. 13 (9). p.pp. 3064–3077.

Böttinger, L., Horvath, S.E., Kleinschroth, T., Hunte, C., Daum, G., Pfanner, N. & Becker, T. (2012). Phosphatidylethanolamine and cardiolipin differentially affect the stability of mitochondrial respiratory chain supercomplexes. *Journal of Molecular Biology*. [Online]. 423 (5). p.pp. 677–686.

Brix, J., Dietmeier, K. & Pfanner, N. (1997). Differential recognition of preproteins by the purified cytosolic domains of the mitochondrial import receptors Tom20, Tom22, and Tom70. *Journal of Biological Chemistry*. 272 (33). p.pp. 20730–

20735.

Brix, J., Rüdiger, S., Bukau, B., Schneider-Mergener, J. & Pfanner, N. (1999). Distribution of binding sequences for the mitochondrial import receptors Tom20, Tom22, and Tom70 in a presequence-carrying preprotein and a non-cleavable preprotein. *Journal of Biological Chemistry*. 274 (23). p.pp. 16522–16530.

Brix, J., Ziegler, G. a, Dietmeier, K., Schneider-Mergener, J., Schulz, G.E. & Pfanner, N. (2000). The mitochondrial import receptor Tom70: identification of a 25 kDa core domain with a specific binding site for preproteins. *Journal of molecular biology*. 303 (4). p.pp. 479–488.

Bürgermeister, M., Birner-Grünberger, R., Nebauer, R. & Daum, G. (2004). Contribution of different pathways to the supply of phosphatidylethanolamine and phosphatidylcholine to mitochondrial membranes of the yeast Saccharomyces cerevisiae. *Biochimica et Biophysica Acta - Molecular and Cell Biology of Lipids*. 1686 (1-2). p.pp. 161–168.

Burri, L., Strahm, Y., Hawkins, C.J., Gentle, I.E., Puryer, M.A., Verhagen, A., Callus, B., Vaux, D. & Lithgow, T. (2005). Mature DIABLO/Smac Is produced by the IMP protease complex on the mitochondrial inner membrane. *Molecular Biology of the Cell*. [Online]. 16 (6). p.pp. 2926–2933.

Caldas, H., Honsey, L.E. & Altura, R. a (2005). Survivin 2alpha: a novel Survivin splice variant expressed in human malignancies. *Molecular cancer*. 4 (1). p.p. 11.

Carmena, M., Wheelock, M., Funabiki, H. & Earnshaw, W.C. (2012). The chromosomal passenger complex (CPC): from easy rider to the godfather of mitosis. *Nature reviews. Molecular cell biology*. [Online]. 13 (12). p.pp. 789–803.

Carvalho, A., Carmena, M., Sambade, C., Earnshaw, W.C. & Wheatley, S.P. (2003). Survivin is required for stable checkpoint activation in taxol-treated HeLa cells. *Journal of cell science*. 116 (Pt 14). p.pp. 2987–2998.

Cavalier-Smith, T. (2006). Origin of mitochondria by intracellular enslavement of a photosynthetic purple bacterium. *Proceedings. Biological sciences / The Royal Society*. 273 (1596). p.pp. 1943–1952.

Ceballos-Cancino, G., Espinosa, M., Maldonado, V. & Melendez-Zajgla, J. (2007). Regulation of mitochondrial Smac/DIABLO-selective release by survivin. *Oncogene*. 26 (54). p.pp. 7569–7575.

Certo, M., Moore, V.D.G., Nishino, M., Wei, G., Korsmeyer, S., Armstrong, S. a. & Letai, A. (2006). Mitochondria primed by death signals determine cellular addiction to antiapoptotic BCL-2 family members. *Cancer Cell*. 9 (5). p.pp. 351–365.

Chacinska, A., Koehler, C.M., Milenkovic, D., Lithgow, T. & Pfanner, N. (2009). Importing Mitochondrial Proteins: Machineries and Mechanisms. *Cell*. 138 (4). p.pp. 628–644.

Chan, E.Y.L. & McQuibban, G.A. (2012). Phosphatidylserine decarboxylase 1 (Psd1)

promotes mitochondrial fusion by regulating the biophysical properties of the mitochondrial membrane and alternative topogenesis of mitochondrial genome maintenance protein 1 (Mgm1). *Journal of Biological Chemistry*. 287 (48). p.pp. 40131–40139.

Chan, Y.W., Jeyaprakash, a. A., Nigg, E. a. & Santamaria, A. (2012). Aurora B controls kinetochore-microtubule attachments by inhibiting Ska complex-KMN network interaction. *Journal of Cell Biology*. 196 (5). p.pp. 563–571.

Chantalat, L., Skoufias, D. a, Kleman, J.P., Jung, B., Dideberg, O. & Margolis, R.L. (2000). Crystal structure of human survivin reveals a bow tie-shaped dimer with two unusual alpha-helical extensions. *Molecular cell*. 6 (1). p.pp. 183–189.

Cheeseman, I.M., Chappie, J.S., Wilson-Kubalek, E.M. & Desai, A. (2006). The Conserved KMN Network Constitutes the Core Microtubule-Binding Site of the Kinetochore. *Cell*. 127 (5). p.pp. 983–997.

Chen, D., Zhang, X.-Y. & Shi, Y. (2006). Identification and functional characterization of hCLS1, a human cardiolipin synthase localized in mitochondria. *The Biochemical journal*. 398 (2). p.pp. 169–176.

Chinnaiyan, a M., O'Rourke, K., Tewari, M. & Dixit, V.M. (1995). FADD, a novel death domain-containing protein, interacts with the death domain of Fas and initiates apoptosis. *Cell*. 81 (4). p.pp. 505–512.

Choi, J.S., Park, B.C., Chi, S.W., Bae, K., Kim, S., Cho, S., Son, W., Myung, P.K., Kim, J. & Park, S.G. (2014). HAX1 regulates E3 ubiquitin ligase activity of cIAPs by promoting their dimerization. *OncoTarget*. 5 (20).

Choi, J.Y., Wu, W.I. & Voelker, D.R. (2005). Phosphatidylserine decarboxylases as genetic and biochemical tools for studying phospholipid traffic. *Analytical Biochemistry*. 347 (2). p.pp. 165–175.

Chou, K.-C., Wu, Z.-C. & Xiao, X. (2011). iLoc-Euk: A Multi-Label Classifier for Predicting the Subcellular Localization of Singleplex and Multiplex Eukaryotic Proteins. *PLoS ONE*. [Online]. 6 (3). p.p. e18258. Available from: http://dx.doi.org/10.1371%2Fjournal.pone.0018258.

Chu, Y., Yao, P.Y., Wang, W., Wang, D., Wang, Z., Zhang, L., Huang, Y., Ke, Y., Ding, X. & Yao, X. (2011). Aurora B kinase activation requires survivin priming phosphorylation by PLK1. *Journal of Molecular Cell Biology*. 3 (4). p.pp. 260–267.

Cimini, D., Wan, X., Hirel, C.B. & Salmon, E.D. (2006). Aurora Kinase Promotes Turnover of Kinetochore Microtubules to Reduce Chromosome Segregation Errors. *Current Biology*. 16 (17). p.pp. 1711–1718.

Clancey, C.J., Chang, S.C. & Dowhan, W. (1993). Cloning of a gene (PSD1) encoding phosphatidylserine decarboxylase from Saccharomyces cerevisiae by complementation of an Escherichia coli mutant. *Journal of Biological Chemistry*. 268 (33). p.pp. 24580–24590.

Claros, M.G. (1995). MitoProt, a Macintosh application for studying mitochondrial proteins. *Computer applications in the biosciences : CABIOS*. 11 (4). p.pp. 441–

447.

Colnaghi, R., Connell, C.M., Barrett, R.M. a & Wheatley, S.P. (2006). Separating the anti-apoptotic and mitotic roles of survivin. *Journal of Biological Chemistry*. 281 (44). p.pp. 33450–33456.

Colnaghi, R. & Wheatley, S.P. (2010). Liaisons between survivin and Plk1 during cell division and cell death. *Journal of Biological Chemistry*. 285 (29). p.pp. 22592–22604.

Connell, C.M., Colnaghi, R. & Wheatley, S.P. (2008). Nuclear survivin has reduced stability and is not cytoprotective. *Journal of Biological Chemistry*. 283 (6). p.pp. 3289–3296.

Connor, J., Pak, C.C. & Schroit, A.J. (1994). Exposure of Phosphatidylserine in the Outer Leaflet of Human Red Blood Cells: Relationship to Cell Density, Cell Age, and Clearance by Mononuclear Cells. *Journal of Biological Chemistry*. 269 (4). p.pp. 2399–2404.

Conway, E.M., Pollefeyt, S., Cornelissen, J., DeBaere, I., Steiner-Mosonyi, M., Ong, K., Baens, M., Collen, D. & Schuh, a C. (2000). Three differentially expressed survivin cDNA variants encode proteins with distinct antiapoptotic functions. *Blood*. 95 (4). p.pp. 1435–1442.

Creagh, E.M., Murphy, B.M., Duriez, P.J., Duckett, C.S. & Martin, S.J. (2004). Smac/Diablo antagonizes ubiquitin ligase activity of inhibitor of apoptosis proteins. *Journal of Biological Chemistry*. 279 (26). p.pp. 26906–26914.

Crook, N.E., Clem, R.J. & Miller, L.K. (1993). An apoptosis-inhibiting baculovirus gene with a zinc finger-like motif. *Journal of virology*. 67 (4). p.pp. 2168–2174.

Czabotar, P.E., Lessene, G., Strasser, A. & Adams, J.M. (2014). Control of apoptosis by the BCL-2 protein family: implications for physiology and therapy. *Nature reviews. Molecular cell biology*. [Online]. 15 (1). p.pp. 49–63.

Danial, N.N., Danial, N.N., Korsmeyer, S.J. & Korsmeyer, S.J. (2004). Cell death: critical control points. *Cell*. [Online]. 116 (2). p.pp. 205–19.

David, C.J. & Manley, J.L. (2010). Alternative pre-mRNA splicing regulation in cancer: Pathways and programs unhinged. *Genes and Development*. 24 (21). p.pp. 2343–2364.

Davoodi, J., Lin, L., Kelly, J., Liston, P. & MacKenzie, A.E. (2004). Neuronal apoptosis-inhibitory protein does not interact with Smac and requires ATP to bind caspase-9. *Journal of Biological Chemistry*. 279 (39). p.pp. 40622–40628.

Degterev, A., Boyce, M. & Yuan, J. (2003). A decade of caspases. *Oncogene*. 22 (53). p.pp. 8543–8567.

Delacour-Larose, M., Molla, A., Skoufias, D.A., Margolis, R.L. & Dimitrov, S. (2004). Distinct Dynamics of Aurora B and Survivin During Mitosis. *Cell Cycle*. [Online]. 3 (11). p.pp. 1418–1426.

Delacour-Larose, M., Thi, M.N.H., Dimitrov, S. & Molla, A. (2007). Role of survivin phosphorylation by Aurora B in mitosis. *Cell Cycle*. 6 (15). p.pp. 1878–1885.

Denton, D., Nicolson, S. & Kumar, S. (2012). Cell death by autophagy: facts and apparent artefacts. *Cell Death and Differentiation*. [Online]. 19 (1). p.pp. 87–95.

Deveraux, Q.L., Roy, N., Stennicke, H.R., Van Arsdale, T., Zhou, Q., Srinivasula, S.M., Alnemri, E.S., Salvesen, G.S. & Reed, J.C. (1998). IAPs block apoptotic events induced by caspase-8 and cytochrome c by direct inhibition of distinct caspases. *The EMBO journal*. 17 (8). p.pp. 2215–2223.

Deveraux, Q.L., Takahashi, R., Salvesen, G.S. & Reed, J.C. (1997). X-linked IAP is a direct inhibitor of cell-death proteases. *Nature*. 388 (6639). p.pp. 300–304.

Ditchfield, C., Johnson, V.L., Tighe, A., Ellston, R., Haworth, C., Johnson, T., Mortlock, A., Keen, N. & Taylor, S.S. (2003). Aurora B couples chromosome alignment with anaphase by targeting BubR1, Mad2, and Cenp-E to kinetochores. *Journal of Cell Biology*. 161 (2). p.pp. 267–280.

Dohi, T., Beltrami, E., Wall, N.R., Plescia, J. & Altieri, D.C. (2004a). Mitochondrial survivin inhibits apoptosis and promotes tumorigenesis. *Journal of Clinical Investigation*. 114 (8). p.pp. 1117–1127.

Dohi, T., Okada, K., Xia, F., Wilford, C.E., Samuel, T., Welsh, K., Marusawa, H., Zou, H., Armstrong, R., Matsuzawa, S.I., Salvesen, G.S., Reed, J.C. & Altieri, D.C. (2004b). An IAP-IAP complex inhibits apoptosis. *Journal of Biological Chemistry*. 279 (33). p.pp. 34087–34090.

Dohi, T., Xia, F. & Altieri, D.C. (2007). Compartmentalized Phosphorylation of IAP by Protein Kinase A Regulates Cytoprotection. *Molecular Cell*. 27 (1). p.pp. 17–28.

Dolezal, P., Likic, V., Tachezy, J. & Lithgow, T. (2006). Evolution of the molecular machines for protein import into mitochondria. *Science (New York, N.Y.)*. 313 (5785). p.pp. 314–318.

Donkor, J., Sariahmetoglu, M., Dewald, J., Brindley, D.N. & Reue, K. (2007). Three mammalian lipins act as phosphatidate phosphatases with distinct tissue expression patterns. *Journal of Biological Chemistry*. 282 (6). p.pp. 3450–3457.

Dowhan, W. (1997). Molecular basis for membrane phospholipid diversity: why are there so many lipids? *Annual review of biochemistry*. 66. p.pp. 199–232.

Du, C., Fang, M., Li, Y., Li, L. & Wang, X. (2000). Smac, a mitochondrial protein that promotes cytochrome c-dependent caspase activation by eliminating IAP inhibition. *Cell*. 102 (1). p.pp. 33–42.

Dukanovic, J. & Rapaport, D. (2011). Multiple pathways in the integration of proteins into the mitochondrial outer membrane. *Biochimica et Biophysica Acta - Biomembranes*. [Online]. 1808 (3). p.pp. 971–980.

Emanuelsson, O. & Von Heijne, G. (2001). Prediction of organellar targeting signals. *Biochimica et Biophysica Acta - Molecular Cell Research*. 1541 (1-2). p.pp. 114–119.

Emanuelsson, O., Nielsen, H., Brunak, S. & von Heijne, G. (2000). Predicting subcellular localization of proteins based on their N-terminal amino acid

sequence. *Journal of molecular biology*. 300 (4). p.pp. 1005–1016.

Emoto, K., Kobayashi, T., Yamaji, a, Aizawa, H., Yahara, I., Inoue, K. & Umeda, M. (1996). Redistribution of phosphatidylethanolamine at the cleavage furrow of dividing cells during cytokinesis. *Proceedings of the National Academy of Sciences of the United States of America*. 93 (23). p.pp. 12867–12872.

Emoto, K., Toyama-Sorimachi, N., Karasuyama, H., Inoue, K. & Umeda, M. (1997). Exposure of phosphatidylethanolamine on the surface of apoptotic cells. *Experimental cell research*. 232 (2). p.pp. 430–434.

Emoto, K. & Umeda, M. (2000). An Essential Role for a Membrane Lipid in Cytokinesis. *The Journal of cell biology*. 149 (6). p.pp. 1215–1224.

Ems-Mcclung, S.C., Hainline, S.G., Devare, J., Zong, H., Cai, S., Carnes, S.K., Shaw, S.L. & Walczak, C.E. (2013). Aurora B inhibits MCAK activity through a phosphoconformational switch that reduces microtubule association. *Current Biology*. [Online]. 23 (24). p.pp. 2491–2499.

Endo, T. & Yamano, K. (2010). Transport of proteins across or into the mitochondrial outer membrane. *Biochimica et biophysica acta*. [Online]. 1803 (6). p.pp. 706–714.

Endres, M., Neupert, W. & Brunner, M. (1999). *Transport of the ADP / ATP carrier of mitochondria from the TOM complex to the TIM22 · 54 complex*. 18 (12). p.pp. 3214–3221.

Engelsma, D., Rodriguez, J. a., Fish, A., Giaccone, G. & Fornerod, M. (2007). Homodimerization antagonizes nuclear export of Survivin. *Traffic*. 8 (11). p.pp. 1495–1502.

Eskes, R., Desagher, S., Antonsson, B. & Martinou, J.C. (2000). Bid induces the oligomerization and insertion of Bax into the outer mitochondrial membrane. *Molecular and cellular biology*. 20 (3). p.pp. 929–935.

Fadok, V. a, Voelker, D.R., Campbell, P. a, Cohen, J.J., Bratton, D.L. & Henson, P.M. (1992). Exposure of phosphatidylserine on the surface of apoptotic lymphocytes triggers specific recognition and removal by macrophages. *Journal of immunology*. 148 (7). p.pp. 2207–2216.

Fan, A.C.Y., Bhangoo, M.K. & Young, J.C. (2006). Hsp90 functions in the targeting and outer membrane translocation steps of Tom70-mediated mitochondrial import. *Journal of Biological Chemistry*. 281 (44). p.pp. 33313–33324.

Faustino, N.A., Cooper, T. a & Andre, N. (2003). Pre-mRNA splicing and human disease. *Genes & Development*. [Online]. 17 (4). p.pp. 419–437.

Fimia, G.M., Stoykova, A., Romagnoli, A., Giunta, L., Di Bartolomeo, S., Nardacci, R., Corazzari, M., Fuoco, C., Ucar, A., Schwartz, P., Gruss, P., Piacentini, M., Chowdhury, K. & Cecconi, F. (2007). Ambra1 regulates autophagy and development of the nervous system. *Nature*. 447 (7148). p.pp. 1121–1125.

Finkielstein, C. V., Overduin, M. & Capelluto, D.G.S. (2006). Cell migration and signaling specificity is determined by the phosphatidylserine recognition motif

of Rac1. *Journal of Biological Chemistry*. 281 (37). p.pp. 27317–27326.

Fischer, M., Horn, S., Belkacemi, A., Kojer, K., Petrungaro, C., Habich, M., Ali, M., Küttner, V., Bien, M., Kauff, F., Dengjel, J., Herrmann, J.M. & Riemer, J. (2013). Protein import and oxidative folding in the mitochondrial intermembrane space of intact mammalian cells. *Molecular biology of the cell*. [Online]. 24 (14). p.pp. 2160–70.

Fischle, W., Tseng, B.S., Dormann, H.L., Ueberheide, B.M., Garcia, B. a., Shabanowitz, J., Hunt, D.F., Funabiki, H. & Allis, C.D. (2005). Regulation of HP1–chromatin binding by histone H3 methylation and phosphorylation. *Nature*. [Online]. 438 (7071). p.pp. 1116–1122.

Fleming, A., Noda, T., Yoshimori, T. & Rubinsztein, D.C. (2011). Chemical modulators of autophagy as biological probes and potential therapeutics. *Nat Chem Biol*. [Online]. 7 (1). p.pp. 9–17.

Folch, J., Lees, M. & Slone Stanley, G.H. (1957). A simple method for the isolation and purification of total lipides from animal tissues. *The Journal of biological chemistry*. [Online]. 226 (1). p.pp. 497–509.

Fölsch, H., Guiard, B., Neupert, W. & Stuart, R. a (1996). Internal targeting signal of the BCS1 protein: a novel mechanism of import into mitochondria. *The EMBO journal*. 15 (3). p.pp. 479–487.

Fortugno, P., Beltrami, E., Plescia, J., Fontana, J., Pradhan, D., Marchisio, P.C., Sessa, W.C. & Altieri, D.C. (2003). Regulation of survivin function by Hsp90. *Proceedings of the National Academy of Sciences of the United States of America*. 100 (24). p.pp. 13791–13796.

Fujita, N., Itoh, T., Omori, H., Fukuda, M., Noda, T. & Yoshimori, T. (2008). The Atg16L complex specifies the site of LC3 lipidation for membrane biogenesis in autophagy. *Molecular biology of the cell*. 19 (5). p.pp. 2092–2100.

Fukasawa, Y., Tsuji, J., Fu, S.-C., Tomii, K., Horton, P. & Imai, K. (2015). MitoFates: improved prediction of mitochondrial targeting sequences and their cleavage sites. *Molecular & cellular proteomics : MCP*. 14 (4). p.pp. 1113–1126.

Fullerton, M.D., Hakimuddin, F. & Bakovic, M. (2007). Developmental and metabolic effects of disruption of the mouse CTP:phosphoethanolamine cytidylyltransferase gene (Pcyt2). *Molecular and cellular biology*. 27 (9). p.pp. 3327–3336.

Gabriel, K., Milenkovic, D., Chacinska, A., Müller, J., Guiard, B., Pfanner, N. & Meisinger, C. (2007). Novel Mitochondrial Intermembrane Space Proteins as Substrates of the MIA Import Pathway. *Journal of Molecular Biology*. 365 (3). p.pp. 612–620.

Gakh, O., Cavadini, P. & Isaya, G. (2002). Mitochondrial processing peptidases. *Biochimica et Biophysica Acta - Molecular Cell Research*. 1592 (1). p.pp. 63–77.

Gasser, S.M., Ohashi, a, Daum, G., Böhni, P.C., Gibson, J., Reid, G. a, Yonetani, T. & Schatz, G. (1982). Imported mitochondrial proteins cytochrome b2 and cytochrome c1 are processed in two steps. *Proceedings of the National*

Academy of Sciences of the United States of America. 79 (2). p.pp. 267–271.

Gassmann, R., Carvalho, A., Henzing, A.J., Ruchaud, S., Hudson, D.F., Honda, R., Nigg, E. a., Gerloff, D.L. & Earnshaw, W.C. (2004). Borealin: A novel chromosomal passenger required for stability of the bipolar mitotic spindle. *Journal of Cell Biology*. 166 (2). p.pp. 179–191.

Gebert, N., Joshi, A.S., Kutik, S., Becker, T., McKenzie, M., Guan, X.L., Mooga, V.P., Stroud, D.A., Kulkarni, G., Wenk, M.R., Rehling, P., Meisinger, C., Ryan, M.T., Wiedemann, N., Greenberg, M.L. & Pfanner, N. (2009). Mitochondrial cardiolipin involved in outer-membrane protein biogenesis: implications for Barth syndrome. *Current biology : CB*. 19 (24). p.pp. 2133–2139.

Geng, J. & Klionsky, D.J. (2008). The Atg8 and Atg12 ubiquitin-like conjugation systems in macroautophagy. 'Protein modifications: beyond the usual suspects' review series. *EMBO reports*. 9 (9). p.pp. 859–864.

Gibellini, F. & Smith, T.K. (2010). The Kennedy pathway-de novo synthesis of phosphatidylethanolamine and phosphatidylcholine. *IUBMB Life*. 62 (6). p.pp. 414–428.

Giodini, A., Kallio, M.J., Wall, N.R., Gorbsky, G.J., Tognin, S., Marchisio, P.C., Symons, M. & Altieri, D.C. (2002). Regulation of microtubule stability and mitotic progression by survivin. *Cancer Research*. 62 (9). p.pp. 2462–2467.

Gleason, C.E., Lu, D., Witters, L. a., Newgard, C.B. & Birnbaum, M.J. (2007). The role of AMPK and mTOR in nutrient sensing in pancreatic β-cells. *Journal of Biological Chemistry*. 282 (14). p.pp. 10341–10351.

Grossman, D., Kim, P.J., Schechner, J.S. & Altieri, D.C. (2001). Inhibition of melanoma tumor growth in vivo by survivin targeting. *Proceedings of the National Academy of Sciences of the United States of America*. 98 (2). p.pp. 635–640.

Gruneberg, U., Neef, R., Honda, R., Nigg, E. a. & Barr, F. a. (2004). Relocation of Aurora B from centromeres to the central spindle at the metaphase to anaphase transition requires MKlp2. *Journal of Cell Biology*. 166 (2). p.pp. 167–172.

Hachiya, N., Komiya, T., Alam, R., Iwahashi, J., Sakaguchi, M., Omura, T. & Mihara, K. (1994). MSF, a novel cytoplasmic chaperone which functions in precursor targeting to mitochondria. *The EMBO journal*. 13 (21). p.pp. 5146–5154.

Hagenbuchner, J., Kiechl-Kohlendorfer, U., Obexer, P. & Ausserlechner, M.J. (2015). BIRC5/Survivin as a target for glycolysis inhibition in high-stage neuroblastoma. *Oncogene*. [Online]. (February). p.pp. 1–10.

Hagenbuchner, J., Kuznetsov, a V, Obexer, P. & Ausserlechner, M.J. (2012). BIRC5/Survivin enhances aerobic glycolysis and drug resistance by altered regulation of the mitochondrial fusion/fission machinery. *Oncogene*. [Online]. 32 (40). p.pp. 4748–57.

Hanahan, D. & Weinberg, R.A. (2011). Hallmarks of Cancer: The Next Generation. *Cell*. [Online]. 144 (5). p.pp. 646–674.

Hao, Y., Sekine, K., Kawabata, A., Nakamura, H., Ishioka, T., Ohata, H., Katayama, R., Hashimoto, C., Zhang, X., Noda, T., Tsuruo, T. & Naito, M. (2004). Apollon ubiquitinates SMAC and caspase-9, and has an essential cytoprotection function. *Nature cell biology*. 6 (9). p.pp. 849–860.

Hauf, S., Cole, R.W., LaTerra, S., Zimmer, C., Schnapp, G., Walter, R., Heckel, A., Van Meel, J., Rieder, C.L. & Peters, J.M. (2003). The small molecule Hesperadin reveals a role for Aurora B in correcting kinetochore-microtubule attachment and in maintaining the spindle assembly checkpoint. *Journal of Cell Biology*. 161 (2). p.pp. 281–294.

Hayashi-Takanaka, Y., Yamagata, K., Nozaki, N. & Kimura, H. (2009). Visualizing histone modifications in living cells: Spatiotemporal dynamics of H3 phosphorylation during interphase. *Journal of Cell Biology*. [Online]. 187 (6). p.pp. 781–790.

von Heijne, G. (1986). Mitochondrial targeting sequences may form amphiphilic helices. *The EMBO journal*. 5 (6). p.pp. 1335–1342.

Herrmann, J.M. & Riemer, J. (2010). The intermembrane space of mitochondria. *Antioxidants & redox signaling*. 13 (9). p.pp. 1341–1358.

Higgins, J. a & Evans, W.H. (1978). Transverse organization of phospholipids across the bilayer of plasma-membrane subfractions of rat hepatocytes. *The Biochemical journal*. 174 (2). p.pp. 563–567.

Hoffman, W.H., Biade, S., Zilfou, J.T., Chen, J. & Murphy, M. (2002). Transcriptional repression of the anti-apoptotic survivin gene by wild type p53. *Journal of Biological Chemistry*. 277 (5). p.pp. 3247–3257.

Honda, R., Korner, R. & Nigg, E.A. (2003). Exploring the functional interactions between Aurora B, INCENP, and survivin in mitosis. *Molecular biology of the cell*. 14 (8). p.pp. 3325–3341.

Hoogenraad, N.J., Ward, L. a. & Ryan, M.T. (2002). Import and assembly of proteins into mitochondria of mammalian cells. *Biochimica et Biophysica Acta - Molecular Cell Research*. 1592 (1). p.pp. 97–105.

Horvath, S.E., Böttinger, L., Vögtle, F.N., Wiedemann, N., Meisinger, C., Becker, T. & Daum, G. (2012). Processing and topology of the yeast mitochondrial phosphatidylserine decarboxylase. *Journal of Biological Chemistry*. 287 (44). p.pp. 36744–36755.

Hotchkiss, R., Strasser, a, McDunn, J. & Swanson, P. (2009). Cell Death. *New England Journal of Medicine*. 361 (16). p.pp. 1570–83.

Hsu, H., Huang, J., Shu, H.B., Baichwal, V. & Goeddel, D. V. (1996a). TNF-dependent recruitment of the protein kinase RIP to the TNF receptor-1 signaling complex. *Immunity*. 4 (4). p.pp. 387–396.

Hsu, H., Shu, H.B., Pan, M.G. & Goeddel, D. V. (1996b). TRADD-TRAF2 and TRADD-FADD interactions define two distinct TNF receptor 1 signal transduction pathways. *Cell*. 84 (2). p.pp. 299–308.

Huang, B.X., Akbar, M., Kevala, K. & Kim, H.Y. (2011). Phosphatidylserine is a critical modulator for Akt activation. *Journal of Cell Biology*. 192 (6). p.pp. 979–992.

Huang, Y., Park, Y.C., Rich, R.L., Segal, D., Myszka, D.G. & Wu, H. (2001). Structural basis of caspase inhibition by XIAP: differential roles of the linker versus the BIR domain. *Cell*. 104 (5). p.pp. 781–790.

Hui, S.W., Stewart, T.P., Yeagle, P.L. & Albert, A.D. (1981). *Bilayer to Non-bilayer Transition in Mixtures of Phosphatidylethanolamine and Phosphatidylcholine : Implications for Membrane Properties It is generally believed that phospho- lipids for-m a bilayer in all biological mem- tween membranes , the bilayer is* . 20 (2). p.pp. 227–240.

Hümmer, S. & Mayer, T.U. (2009). Cdk1 Negatively Regulates Midzone Localization of the Mitotic Kinesin Mklp2 and the Chromosomal Passenger Complex. *Current Biology*. 19 (7). p.pp. 607–612.

Inglis-Broadgate, S.L., Ocaka, L., Banerjee, R., Gaasenbeek, M., Chapple, J.P., Cheetham, M.E., Clark, B.J., Hunt, D.M. & Halford, S. (2005). Isolation and characterization of murine Cds (CDP-diacylglycerol synthase) 1 and 2. *Gene*. 356 (1-2). p.pp. 19–31.

Itakura, E., Kishi, C., Inoue, K. & Mizushima, N. (2008). Beclin 1 forms two distinct phosphatidylinositol 3-kinase complexes with mammalian Atg14 and UVRAG. *Molecular biology of the cell*. 19 (12). p.pp. 5360–5372.

Itaya, K. & Ui, M. (1966). A new micromethod for the colorimetric determination of inorganic phosphate. *Clinica Chimica Acta*. [Online]. 14 (3). p.pp. 361–366.

Itoh, N. & Nagata, S. (1993). A Novel Protein Domain Required for Apoptosis. Mutational analysis of human Fas antigen. *The Journal of Biological Chemistry*. [Online]. 268 (15). p.pp. 10932–10937.

Iwamoto, K., Hayakawa, T., Murate, M., Makino, A., Ito, K., Fujisawa, T. & Kobayashi, T. (2007). Curvature-dependent recognition of ethanolamine phospholipids by duramycin and cinnamycin. *Biophysical journal*. 93 (5). p.pp. 1608–1619.

Iwanyshyn, W.M., Han, G.-S. & Carman, G.M. (2004). Regulation of Phospholipid Synthesis in *Saccharomyces cerevisiae* by Zinc. *Journal of Biological Chemistry*. [Online]. 279 (21). p.pp. 21976–21983.

Jeyaprakash, a. A., Klein, U.R., Lindner, D., Ebert, J., Nigg, E. a. & Conti, E. (2007). Structure of a Survivin-Borealin-INCENP Core Complex Reveals How Chromosomal Passengers Travel Together. *Cell*. 131 (2). p.pp. 271–285.

Jiang, X., Wilford, C., Duensing, S., Munger, K., Jones, G. & Jones, D. (2001). Participation of survivin in mitotic and apoptotic activities of normal and tumor-derived cells. *Journal of Cellular Biochemistry*. 83 (2). p.pp. 342–354.

Jiang, Y., Saavedra, H.I., Holloway, M.P., Leone, G. & Altura, R. a. (2004). Aberrant regulation of survivin by the RB/E2F family of proteins. *Journal of Biological Chemistry*. 279 (39). p.pp. 40511–40520.

Johnson, J.M., Castle, J., Garrett-Engele, P., Kan, Z., Loerch, P.M., Armour, C.D., Santos, R., Schadt, E.E., Stoughton, R. & Shoemaker, D.D. (2003). Genome-wide survey of human alternative pre-mRNA splicing with exon junction microarrays. *Science (New York, N.Y.)*. 302 (5653). p.pp. 2141–2144.

Jones, M.K., Padilla, O.R. & Zhu, E. (2010). Survivin is a key factor in the differential susceptibility of gastric endothelial and epithelial cells to alcohol-induced injury. *Journal of Physiology and Pharmacology*. 61 (3). p.pp. 253–264.

Joshi, A.S., Thompson, M.N., Fei, N., Ttemann, M.H. & Greenberg, M.L. (2012). Cardiolipin and mitochondrial phosphatidylethanolamine have overlapping functions in mitochondrial fusion in Saccharomyces cerevisiae. *Journal of Biological Chemistry*. 287 (21). p.pp. 17589–17597.

Kainu, V., Hermansson, M., Hänninen, S., Hokynar, K. & Somerharju, P. (2013). Import of phosphatidylserine to and export of phosphatidylethanolamine molecular species from mitochondria. *Biochimica et Biophysica Acta - Molecular and Cell Biology of Lipids*. [Online]. 1831 (2). p.pp. 429–437.

Kampa, D., Cheng, J., Kapranov, P., Yamanaka, M., Brubaker, S., Cawley, S., Drenkow, J., Piccolboni, A., Bekiranov, S., Helt, G., Tammana, H. & Gingeras, T.R. (2004). Novel RNAs identified from a in-depth analysis of the transcriptome of human chromosomes 21 and 22. *Genome Research*. 14 (3). p.pp. 331–342.

Kanfer, J. & Kennedy, E.P. (1964). METABOLISM AND FUNCTION OF BACTERIAL LIPIDS. II. BIOSYNTHESIS OF PHOSPHOLIPIDS IN ESCHERICHIA COLI. *The Journal of biological chemistry*. 239. p.pp. 1720–1726.

Kang, B.H. & Altieri, D.C. (2006). Regulation of survivin stability by the aryl hydrocarbon receptor-interacting protein. *Journal of Biological Chemistry*. 281 (34). p.pp. 24721–24727.

Kang, B.H., Xia, F., Pop, R., Dohi, T., Socolovsky, M. & Altieri, D.C. (2011a). Developmental control of apoptosis by the immunophilin aryl hydrocarbon receptor-interacting protein (AIP) involves mitochondrial import of the survivin protein. *Journal of Biological Chemistry*. 286 (19). p.pp. 16758–16767.

Kang, J., Chaudhary, J., Dong, H., Kim, S., Brautigam, C. a. & Yu, H. (2011b). Mitotic centromeric targeting of HP1 and its binding to Sgo1 are dispensable for sister-chromatid cohesion in human cells. *Molecular Biology of the Cell*. [Online]. 22 (8). p.pp. 1181–1190.

Kaufmann, T., Tai, L., Ekert, P.G., Huang, D.C.S., Norris, F., Lindemann, R.K., Johnstone, R.W., Dixit, V.M. & Strasser, A. (2007). The BH3-Only Protein Bid Is Dispensable for DNA Damage- and Replicative Stress-Induced Apoptosis or Cell-Cycle Arrest. *Cell*. 129 (2). p.pp. 423–433.

Kawasaki, K., Kuge, O., Chang, S.C., Heacock, P.N., Rho, M., Suzuki, K., Nishijima, M. & Dowhan, W. (1999). Isolation of a Chinese hamster ovary (CHO) cDNA encoding phosphatidylglycerophosphate (PGP) synthase, expression of which corrects the mitochondrial abnormalities of a PGP synthase-defective mutant

of CHO-K1 cells. *Journal of Biological Chemistry*. 274 (3). p.pp. 1828–1834.

Kawashima, S. a, Yamagishi, Y., Honda, T., Ishiguro, K. & Watanabe, Y. (2010). Phosphorylation of H2A by Bub1 prevents chromosomal instability through localizing shugoshin. *Science*. 327 (5962). p.pp. 172–177.

Kawashima, S. a., Tsukahara, T., Langegger, M., Hauf, S., Kitajima, T.S. & Watanabe, Y. (2007). Shugoshin enables tension-generating attachment of kinetochores by loading Aurora to centromeres. *Genes and Development*. 21 (4). p.pp. 420–435.

Keeble, J. a & Gilmore, A.P. (2007). Apoptosis commitment--translating survival signals into decisions on mitochondria. *Cell research*. 17 (12). p.pp. 976–984.

Kelly, A.E., Ghenoiu, C., Xue, J.Z., Zierhut, C., Kimura, H. & Funabiki, H. (2010). Survivin Reads Phosphorylated Histone H3 Threonine 3 to Activate the Mitotic Kinase Aurora B. *Science* . [Online]. 330 (6001). p.pp. 235–239.

Kennedy, E.P. & Weiss, S.B. (1956). The function of cytidine coenzymes in the biosynthesis of phospholipides. *The Journal of biological chemistry*. 222 (1). p.pp. 193–214.

Kerr, J.F., Wyllie, A.H. & Currie, A.R. (1972). Apoptosis: a basic biological phenomenon with wide-ranging implications in tissue kinetics. *British journal of cancer*. 26 (4). p.pp. 239–257.

King, B.R. & Guda, C. (2007). ngLOC: an n-gram-based Bayesian method for estimating the subcellular proteomes of eukaryotes. *Genome biology*. 8 (5). p.p. R68.

Kirisako, T., Ichimura, Y., Okada, H., Kabeya, Y., Mizushima, N., Yoshimori, T., Ohsumi, M., Takao, T., Noda, T. & Ohsumi, Y. (2000). The reversible modification regulates the membrane-binding state of Apg8/Aut7 essential for autophagy and the cytoplasm to vacuole targeting pathway. *Journal of Cell Biology*. 151 (2). p.pp. 263–275.

Kitamura, H., Wu, W.I. & Voelker, D.R. (2002). The C2 domain of phosphatidylserine decarboxylase 2 is not required for catalysis but is essential for in vivo function. *Journal of Biological Chemistry*. 277 (37). p.pp. 33720–33726.

Knauer, S.K., Krämer, O.H., Knösel, T., Engels, K., Rödel, F., Kovács, A.F., Dietmaier, W., Klein-Hitpass, L., Habtemichael, N., Schweitzer, A., Brieger, J., Rödel, C., Mann, W., Petersen, I., Heinzel, T. & Stauber, R.H. (2007). Nuclear export is essential for the tumor-promoting activity of survivin. *The FASEB journal : official publication of the Federation of American Societies for Experimental Biology*. 21 (1). p.pp. 207–216.

Koehler, C.M., Jarosch, E., Tokatlidis, K., Schmid, K., Schweyen, R.J. & Schatz, G. (1998). Import of mitochondrial carriers mediated by essential proteins of the intermembrane space. *Science (New York, N.Y.)*. 279 (5349). p.pp. 369–373.

Kuge, O., Nishijima, M. & Akamatsu, Y. (1991). A cloned gene encoding phosphatidylserine decarboxylase complements the phosphatidylserine biosynthetic defect of a chinese hamster ovary cell mutant. *Journal of*

Biological Chemistry. 266 (10). p.pp. 6370–6376.

Kuge, O., Nishijima, M. & Akamatsu, Y. (1986). Phosphatidylserine biosynthesis in cultured Chinese hamster ovary cells. II. Isolation and characterization of phosphatidylserine auxotrophs. *The Journal of biological chemistry*. 261 (13). p.pp. 5790–5794.

Kuge, O., Saito, K., Kojima, M., Akamatsu, Y. & Nishijima, M. (1996). Post-translational processing of the phosphatidylserine decarboxylase gene product in Chinese hamster ovary cells. *The Biochemical journal*. 319 (Pt 1. p.pp. 33–38.

Kuge, O., Saito, K. & Nishijima, M. (1997). Cloning of a Chinese hamster ovary (CHO) cDNA encoding phosphatidylserine synthase (PSS) II, overexpression of which suppresses the phosphatidylserine biosynthetic defect of a PSS I-lacking mutant of CHO-K1 cells. *Journal of Biological Chemistry*. 272 (31). p.pp. 19133–19139.

Künkele, K.P., Heins, S., Dembowski, M., Nargang, F.E., Benz, R., Thieffry, M., Walz, J., Lill, R., Nussberger, S. & Neupert, W. (1998). The preprotein translocation channel of the outer membrane of mitochondria. *Cell*. 93 (6). p.pp. 1009–1019.

Kuwana, T., Bouchier-Hayes, L., Chipuk, J.E., Bonzon, C., Sullivan, B. a., Green, D.R. & Newmeyer, D.D. (2005). BH3 domains of BH3-only proteins differentially regulate Bax-mediated mitochondrial membrane permeabilization both directly and indirectly. *Molecular Cell*. 17 (4). p.pp. 525–535.

Lan, W., Zhang, X., Kline-Smith, S.L., Rosasco, S.E., Barrett-Wilt, G. a., Shabanowitz, J., Hunt, D.F., Walczak, C.E. & Stukenberg, P.T. (2004). Aurora B phosphorylates centromeric MCAK and regulates its localization and microtubule depolymerization activity. *Current Biology*. 14 (4). p.pp. 273–286.

Lara-Gonzalez, P., Westhorpe, F.G. & Taylor, S.S. (2012). The spindle assembly checkpoint. *Current Biology*. [Online]. 22 (22). p.pp. R966–R980.

Lens, S.M. a, Wolthuis, R.M.F., Klompmaker, R., Kauw, J., Agami, R., Brummelkamp, T., Kops, G. & Medema, R.H. (2003). Survivin is required for a sustained spindle checkpoint arrest in response to lack of tension. *EMBO Journal*. 22 (12). p.pp. 2934–2947.

Leonardi, R., Frank, M.W., Jackson, P.D., Rock, C.O. & Jackowski, S. (2009). Elimination of the CDP-ethanolamine pathway disrupts hepatic lipid homeostasis. *Journal of Biological Chemistry*. 284 (40). p.pp. 27077–27089.

Levine, B. & Kroemer, G. (2008). Autophagy in the Pathogenesis of Disease. *Cell*. 132 (1). p.pp. 27–42.

Li, C., Wu, Z., Liu, M., Pazgier, M. & Lu, W. (2008). Chemically synthesized human survivin does not inhibit caspase-3. *Protein science : a publication of the Protein Society*. 17 (9). p.pp. 1624–1629.

Li, F., Ackermann, E.J., Bennett, C.F., Rothermel, a L., Plescia, J., Tognin, S., Villa, a, Marchisio, P.C. & Altieri, D.C. (1999). Pleiotropic cell-division defects and apoptosis induced by interference with survivin function. *Nature cell biology*. 1

(8). p.pp. 461–466.

Li, F., Ambrosini, G., Chu, E.Y., Plescia, J., Tognin, S., Marchisio, P.C. & Altieri, D.C. (1998a). Control of apoptosis and mitotic spindle checkpoint by survivin. *Nature*. 396 (6711). p.pp. 580–584.

Li, H., Zhu, H., Xu, C.J. & Yuan, J. (1998b). Cleavage of BID by caspase 8 mediates the mitochondrial damage in the Fas pathway of apoptosis. *Cell*. 94 (4). p.pp. 491–501.

Li, L.Y., Luo, X. & Wang, X. (2001). Endonuclease G is an apoptotic DNase when released from mitochondria. *Nature*. 412 (6842). p.pp. 95–99.

Li, P., Nijhawan, D., Budihardjo, I., Srinivasula, S.M., Ahmad, M., Alnemri, E.S. & Wang, X. (1997). Cytochrome c and dATP-dependent formation of Apaf-1/caspase-9 complex initiates an apoptotic protease cascade. *Cell*. 91 (4). p.pp. 479–489.

Liu, D., Vader, G., Vromans, M.J.M., Lampson, M.A. & Lens, S.M.A. (2009). Sensing chromosome bi-orientation by spatial separation of aurora B kinase from kinetochore substrates. *Science (New York, N.Y.)*. 323 (5919). p.pp. 1350–1353.

Liu, T., Biddle, D., Hanks, A.N., Brouha, B., Yan, H., Lee, R.M., Leachman, S. a & Grossman, D. (2006). Activation of dual apoptotic pathways in human melanocytes and protection by survivin. *The Journal of investigative dermatology*. 126 (10). p.pp. 2247–2256.

Liu, Y., Lear, T., Iannone, O., Shiva, S., Corey, C., Rajbhandari, S., Jerome, J., Chen, B.B. & Mallampalli, R.K. (2015). Pro-apoptotic F-box protein Fbxl7 regulates mitochondrial function by mediating the ubiquitylation and proteasomal degradation of survivin. *Journal of Biological Chemistry*. [Online]. 290 (19). p.p. jbc.M114.629931.

Liu, Y. & Levine, B. (2014). Autosis and autophagic cell death: the dark side of autophagy. *Cell Death and Differentiation*. [Online]. 22 (3). p.pp. 367–376.

Lu, Y.-W. & Claypool, S.M. (2015). Disorders of phospholipid metabolism: an emerging class of mitochondrial disease due to defects in nuclear genes. *Frontiers in Genetics*. [Online]. 6 (February). p.pp. 1–27.

Lucas, N. & Cho, W. (2011). Phosphatidylserine binding is essential for plasma membrane recruitment and signaling function of 3-phosphoinositide-dependent kinase-1. *Journal of Biological Chemistry*. 286 (48). p.pp. 41265–41272.

Luo, X., Budihardjo, I., Zou, H., Slaughter, C. & Wang, X. (1998). Bid, a Bcl2 interacting protein, mediates cytochrome c release from mitochondria in response to activation of cell surface death receptors. *Cell*. 94 (4). p.pp. 481–490.

Mahotka, C., Wenzel, M., Springer, E., Gabbert, H.E. & Gerharz, C.D. (1999). Survivin-??Ex3 and survivin-2B: Two novel splice variants of the apoptosis inhibitor survivin with different antiapoptotic properties. *Cancer Research*. 59 (24). p.pp. 6097–6102.

Maiuri, M.C., Le Toumelin, G., Criollo, A., Rain, J.-C., Gautier, F., Juin, P., Tasdemir, E., Pierron, G., Troulinaki, K., Tavernarakis, N., Hickman, J. a, Geneste, O. & Kroemer, G. (2007). Functional and physical interaction between Bcl-X(L) and a BH3-like domain in Beclin-1. *The EMBO journal*. 26 (10). p.pp. 2527–2539.

Majumder, R., Quinn-Allen, M.A., Kane, W.H. & Lentz, B.R. (2008). A phosphatidylserine binding site in factor Va C1 domain regulates both assembly and activity of the prothrombinase complex. *Blood*. 112 (7). p.pp. 2795–2802.

Marconescu, A. & Thorpe, P.E. (2008). Coincident exposure of phosphatidylethanolamine and anionic phospholipids on the surface of irradiated cells. *Biochimica et Biophysica Acta - Biomembranes*. 1778 (10). p.pp. 2217–2224.

Marom, M., Dayan, D., Demishtein-Zohary, K., Mokranjac, D., Neupert, W. & Azem, A. (2011). Direct interaction of mitochondrial targeting presequences with purified components of the TIM23 protein complex. *Journal of Biological Chemistry*. 286 (51). p.pp. 43809–43815.

Martens, S. & McMahon, H.T. (2008). Mechanisms of membrane fusion: disparate players and common principles. *Nature reviews. Molecular cell biology*. 9 (7). p.pp. 543–556.

Marusawa, H., Matsuzawa, S.I., Welsh, K., Zou, H., Armstrong, R., Tamm, I. & Reed, J.C. (2003). HBXIP functions as a cofactor of survivin in apoptosis suppression. *EMBO Journal*. 22 (11). p.pp. 2729–2740.

Maskey, D., Yousefi, S., Schmid, I., Zlobec, I., Perren, A., Friis, R. & Simon, H. (2013). ATG5 is induced by DNA-damaging agents and promotes mitotic catastrophe independent of autophagy. *Nature communications*. [Online]. 4. p.p. 2130.

Matsunaga, K., Saitoh, T., Tabata, K., Omori, H., Satoh, T., Kurotori, N., Maejima, I., Shirahama-Noda, K., Ichimura, T., Isobe, T., Akira, S., Noda, T. & Yoshimori, T. (2009). Two Beclin 1-binding proteins, Atg14L and Rubicon, reciprocally regulate autophagy at different stages. *Nature cell biology*. 11 (4). p.pp. 385–396.

McBride, H.M., Neuspiel, M. & Wasiak, S. (2006). Mitochondria: More Than Just a Powerhouse. *Current Biology*. 16 (14). p.pp. 551–560.

McNeish, I. a., Lopes, R., Bell, S.J., McKay, T.R., Fernandez, M., Lockley, M., Wheatley, S.P. & Lemoine, N.R. (2005). Survivin interacts with Smac/DIABLO in ovarian carcinoma cells but is redundant in Smac-mediated apoptosis. *Experimental Cell Research*. 302 (1). p.pp. 69–82.

Meergans, T., Hildebrandt, a K., Horak, D., Haenisch, C. & Wendel, a (2000). The short prodomain influences caspase-3 activation in HeLa cells. *The Biochemical journal*. 349 (Pt 1). p.pp. 135–140.

Menon, a K., Eppinger, M., Mayor, S. & Schwarz, R.T. (1993). Phosphatidylethanolamine is the donor of the terminal phosphoethanolamine group in trypanosome glycosylphosphatidylinositols. *The EMBO journal*. 12 (5).

p.pp. 1907–1914.

Mesri, M., Wall, N.R., Li, J., Kim, R.W. & Altieri, D.C. (2001). Cancer gene therapy using survivin mutant adenovirus. *Journal of Clinical Investigation*. 108 (7). p.pp. 981–990.

Midorikawa, R., Yamamoto-Hino, M., Awano, W., Hinohara, Y., Suzuki, E., Ueda, R. & Goto, S. (2010). Autophagy-dependent rhodopsin degradation prevents retinal degeneration in Drosophila. *The Journal of neuroscience : the official journal of the Society for Neuroscience*. 30 (32). p.pp. 10703–10719.

Milenkovic, D., Ramming, T., Muller, J.M., Wenz, L.-S., Gebert, N., Schulze-Specking, A., Stojanovski, D., Rospert, S. & Chacinska, A. (2009). Identification of the signal directing Tim9 and Tim10 into the intermembrane space of mitochondria. *Molecular biology of the cell*. 20 (10). p.pp. 2530–2539.

Miller, M. a. & Kent, C. (1986). Characterization of the pathways for phosphatidylethanolamine biosynthesis in Chinese hamster ovary mutant and parental cell lines. *Journal of Biological Chemistry*. 261 (21). p.pp. 9753–9761.

Modrek, B. & Lee, C. (2002). A genomic view of alternative splicing. *Nature genetics*. 30 (1). p.pp. 13–19.

Mollinari, C., Reynaud, C., Martineau-Thuillier, S., Monier, S., Kieffer, S., Garin, J., Andreassen, P.R., Boulet, A., Goud, B., Kleman, J.P. & Margolis, R.L. (2003). The mammalian passenger protein TD-60 is an RCC1 family member with an essential role in prometaphase to metaphase progression. *Developmental Cell*. 5 (2). p.pp. 295–307.

Mootha, V.K., Wei, M.C., Buttle, K.F., Scorrano, L., Panoutsakopoulou, V., Mannella, C. a. & Korsmeyer, S.J. (2001). A reversible component of mitochondrial respiratory dysfunction in apoptosis can be rescued by exogenous cytochrome c. *EMBO Journal*. 20 (4). p.pp. 661–671.

Muchmore, S.W., Chen, J., Jakob, C., Zakula, D., Matayoshi, E.D., Wu, W., Zhang, H., Li, F., Ng, S.C. & Altieri, D.C. (2000). Crystal structure and mutagenic analysis of the inhibitor-of-apoptosis protein survivin. *Molecular cell*. 6 (1). p.pp. 173–182.

Munoz-Barrera, M. & Monje-Casas, F. (2014). Increased Aurora B activity causes continuous disruption of kinetochore-microtubule attachments and spindle instability. *Proceedings of the National Academy of Sciences*. [Online]. 111 (38). p.pp. E3996–E4005.

Murakami, K., Tanase, S., Morino, Y. & Mori, M. (1992). Presequence binding factor-dependent and -independent import of proteins into mitochondria. *Journal of Biological Chemistry*. 267 (19). p.pp. 13119–13122.

Muzio, M., Chinnaiyan, A.M., Kischkel, F.C., O'Rourke, K., Shevchenko, A., Ni, J., Scaffidi, C., Bretz, J.D., Zhang, M., Gentz, R., Mann, M., Krammer, P.H., Peter, M.E. & Dixit, V.M. (1996). FLICE, a novel FADD-homologous ICE/CED-3-like protease, is recruited to the CD95 (Fas/APO-1) death-inducing signaling complex. *Cell*. 85 (6). p.pp. 817–827.

Nakai, K. & Horton, P. (1999). PSORT: a program for detecting sorting signals in

proteins and predicting their subcellular localization. *Trends in biochemical sciences*. 24 (1). p.pp. 34–36.

Nalefski, E.A. & Falke, J.J. (1996). The C2 domain calcium-binding motif: structural and functional diversity. *Protein science : a publication of the Protein Society*. 5 (12). p.pp. 2375–2390.

Nebauer, R., Rosenberger, S. & Daum, G. (2007). Phosphatidylethanolamine, a limiting factor of autophagy in yeast strains bearing a defect in the carboxypeptidase Y pathway of vacuolar targeting. *Journal of Biological Chemistry*. 282 (23). p.pp. 16736–16743.

Nerlich, A., von Orlow, M., Rontein, D., Hanson, A.D. & Dörmann, P. (2007). Deficiency in phosphatidylserine decarboxylase activity in the psd1 psd2 psd3 triple mutant of Arabidopsis affects phosphatidylethanolamine accumulation in mitochondria. *Plant physiology*. 144 (2). p.pp. 904–914.

Neupert, W. (2015). A perspective on transport of proteins into mitochondria: a myriad of open questions. *Journal of Molecular Biology*. [Online]. 427 (6). p.pp. 1135–1158.

Niu, T.K., Cheng, Y., Ren, X. & Yang, J.M. (2010). Interaction of Beclin 1 with survivin regulates sensitivity of human glioma cells to TRAIL-induced apoptosis. *FEBS Letters*. [Online]. 584 (16). p.pp. 3519–3524. Available from: http://dx.doi.org/10.1016/j.febslet.2010.07.018.

Norden, C., Mendoza, M., Dobbelaere, J., Kotwaliwale, C. V., Biggins, S. & Barral, Y. (2006). The NoCut Pathway Links Completion of Cytokinesis to Spindle Midzone Function to Prevent Chromosome Breakage. *Cell*. 125 (1). p.pp. 85–98.

O'Connor, D.S., Grossman, D., Plescia, J., Li, F., Zhang, H., Villa, a, Tognin, S., Marchisio, P.C. & Altieri, D.C. (2000). Regulation of apoptosis at cell division by p34cdc2 phosphorylation of survivin. *Proceedings of the National Academy of Sciences of the United States of America*. 97 (24). p.pp. 13103–13107.

Onguka, O., Calzada, E., Ogunbona, O.B. & Claypool, S.M. (2015). Phosphatidylserine Decarboxylase 1 Autocatalysis and Function Does Not Require a Mitochondrial-specific Factor. *Journal of Biological Chemistry*. [Online]. p.p. jbc.M115.641118. Osman, C., Haag, M., Wieland, F.T., Brügger, B. & Langer, T. (2010). A mitochondrial phosphatase required for cardiolipin biosynthesis: the PGP phosphatase Gep4. *The EMBO journal*. 29 (12). p.pp. 1976–1987.

Papini, D., Langemeyer, L., Abad, M. a., Kerr, A., Samejima, I., Eyers, P. a., Jeyaprakash, a. A., Higgins, J.M.G., Barr, F. a. & Earnshaw, W.C. (2015). TD-60 links RalA GTPase function to the CPC in mitosis. *Nature Communications*. [Online]. 6 (May). p.p. 7678.

Pasparakis, M. & Vandenabeele, P., 2015. Necroptosis and its role in inflammation. *Nature*, 517(7534), pp.311–320.

Pattingre, S., Tassa, A., Qu, X., Garuti, R., Xiao, H.L., Mizushima, N., Packer, M.,

Schneider, M.D. & Levine, B. (2005). Bcl-2 antiapoptotic proteins inhibit Beclin 1-dependent autophagy. *Cell*. 122 (6). p.pp. 927–939.

Paulick, M.G. & Bertozzi, C.R. (2008). The glycosylphosphatidylinositol anchor: A complex membrane-anchoring structure for proteins. *Biochemistry*. 47 (27). p.pp. 6991–7000.

Pavlyukov, M.S., Antipova, N. V., Balashova, M. V., Vinogradova, T. V., Kopantzev, E.P. & Shakhparonov, M.I. (2011). Survivin monomer plays an essential role in apoptosis regulation. *Journal of Biological Chemistry*. 286 (26). p.pp. 23296–23307.

Percy, A.K., Moore, J.F., Carson, M.A. & Waechter, C.J. (1983). Characterization of brain phosphatidylserine decarboxylase: localization in the mitochondrial inner membrane. *Archives of biochemistry and biophysics*. 223 (2). p.pp. 484–494.

Peters, J.-M. (2006). The anaphase promoting complex/cyclosome: a machine designed to destroy. *Nature reviews. Molecular cell biology*. 7 (9). p.pp. 644–656.

Pfeiffer, K., Gohil, V., Stuart, R. a., Hunte, C., Brandt, U., Greenberg, M.L. & Schägger, H. (2003). Cardiolipin Stabilizes Respiratory Chain Supercomplexes. *Journal of Biological Chemistry*. 278 (52). p.pp. 52873–52880.

Pickart, C.M. & Fushman, D. (2004). Polyubiquitin chains: Polymeric protein signals. *Current Opinion in Chemical Biology*. 8 (6). p.pp. 610–616.

Pinsky, B. a, Kung, C., Shokat, K.M. & Biggins, S. (2006). The Ipl1-Aurora protein kinase activates the spindle checkpoint by creating unattached kinetochores. *Nature cell biology*. 8 (1). p.pp. 78–83.

Pinsky, B. a., Nelson, C.R. & Biggins, S. (2009). Protein Phosphatase 1 Regulates Exit from the Spindle Checkpoint in Budding Yeast. *Current Biology*. [Online]. 19 (14). p.pp. 1182–1187.

Portolano, N., Watson, P.J., Fairall, L., Millard, C.J., Milano, C.P., Song, Y., Cowley, S.M. & Schwabe, J.W.R. (2014). Recombinant Protein Expression for Structural Biology in HEK 293F Suspension Cells: A Novel and Accessible Approach. *Journal of Visualized Experiments*. [Online]. 1 (92). p.pp. 1–8.

Preta, G. & Fadeel, B. (2012). AIF and Scythe (Bat3) Regulate Phosphatidylserine Exposure and Macrophage Clearance of Cells Undergoing Fas (APO-1)-Mediated Apoptosis. *PLoS ONE*. 7 (10).

Ramage, P., Cheneval, D., Chvei, M., Graff, P., Hemmig, R., Heng, R., Kocher, H.P., Mackenzie, A., Memmert, K. & Revesz, L. (1995). Expression, refolding, and autocatalytic proteolytic processing of the interleukin-1 beta-converting enzyme precursor. *The Journal of biological chemistry*. 270 (16). p.pp. 9378–9383.

Riedl, S.J., Renatus, M., Schwarzenbacher, R., Zhou, Q., Sun, C., Fesik, S.W., Liddington, R.C. & Salvesen, G.S. (2001). Structural basis for the inhibition of caspase-3 by XIAP. *Cell*. 104 (5). p.pp. 791–800.

Riekhof, W.R. & Voelker, D.R. (2006). Uptake and utilization of lyso-phosphatidylethanolamine by Saccharomyces cerevisiae. *Journal of Biological Chemistry*. 281 (48). p.pp. 36588–36596.

Riolo, M.T., Cooper, Z. a., Holloway, M.P., Cheng, Y., Bianchi, C., Yakirevich, E., Ma, L., Chin, Y.E. & Altura, R. a. (2012). Histone deacetylase 6 (HDAC6) deacetylates survivin for its nuclear export in breast cancer. *Journal of Biological Chemistry*. 287 (14). p.pp. 10885–10893.

Rivadeneira, D.B., Caino, M.C., Seo, J.H., Angelin, A., Wallace, D.C., Languino, L.R. & Altieri, D.C. (2015). Survivin promotes oxidative phosphorylation , subcellular mitochondrial repositioning , and tumor cell invasion. *Science signaling*. 8 (389). p.pp. 1–12.

Roca, H., Varsos, Z. & Pienta, K.J. (2008). CCL2 protects prostate cancer PC3 cells from autophagic death via phosphatidylinositol 3-kinase/AKT-dependent survivin Up-regulation. *Journal of Biological Chemistry*. 283 (36). p.pp. 25057–25073.

Rockenfeller, P., Koska, M., Pietrocola, F., Minois, N., Knittelfelder, O., Sica, V., Franz, J., Carmona-Gutierrez, D., Kroemer, G. & Madeo, F. (2015). Phosphatidylethanolamine positively regulates autophagy and longevity. *Cell Death and Differentiation*. [Online]. 22 (3). p.pp. 499–508.

Rödel, F., Hoffmann, J., Distel, L., Herrmann, M., Noisternig, T., Papadopoulos, T., Sauer, R. & Rödel, C. (2005). Survivin as a radioresistance factor, and prognostic and therapeutic target for radiotherapy in rectal cancer. *Cancer Research*. 65 (11). p.pp. 4881–4887.

Rodríguez, J. a, Span, S.W., Ferreira, C.G.M., Kruyt, F. a E. & Giaccone, G. (2002). CRM1-mediated nuclear export determines the cytoplasmic localization of the antiapoptotic protein Survivin. *Experimental cell research*. 275 (1). p.pp. 44–53.

Roise, D. & Schatz, G. (1988). Mitochondrial presequences. *Journal of Biological Chemistry*. 263 (10). p.pp. 4509–4511.

Rontein, D., Wu, W.-I., Voelker, D.R. & Hanson, A.D. (2003). Mitochondrial phosphatidylserine decarboxylase from higher plants. Functional complementation in yeast, localization in plants, and overexpression in Arabidopsis. *Plant physiology*. 132 (3). p.pp. 1678–1687.

Rosa, J., Canovas, P., Islam, A., Altieri, D.C. & Doxsey, S.J. (2006). Survivin modulates microtubule dynamics and nucleation throughout the cell cycle. *Molecular biology of the cell*. 17 (3). p.pp. 1483–1493.

Rosasco-Nitcher, S.E., Lan, W., Khorasanizadeh, S. & Stukenberg, P.T. (2008). Centromeric Aurora-B activation requires TD-60, microtubules, and substrate priming phosphorylation. *Science*. 319 (5862). p.pp. 469–472.

Roy, N., Deveraux, Q.L., Takahashi, R., Salvesen, G.S. & Reed, J.C. (1997). The c-IAP-1 and c-IAP-2 proteins are direct inhibitors of specific caspases. *The EMBO journal*. 16 (23). p.pp. 6914–6925.

Ruchaud, S., Carmena, M. & Earnshaw, W.C. (2007). Chromosomal passengers:

conducting cell division. *Nature reviews. Molecular cell biology*. 8 (10). p.pp. 798–812.

Russell, R.C., Tian, Y., Yuan, H., Park, H.W., Chang, Y.-Y., Kim, J., Kim, H., Neufeld, T.P., Dillin, A. & Guan, K.-L. (2013). ULK1 induces autophagy by phosphorylating Beclin-1 and activating VPS34 lipid kinase. *Nature cell biology*. [Online]. 15 (7). p.pp. 741–50.

Ryan, M.T., Muller, H. & Pfanner, N. (1999). Functional staging of ADP/ ATP carrier translocation across the outer mitochondrial membrane, J. *Biol. Chem.* 274 (29). p.pp. 9–20627.

Saurin, A.T., van der Waal, M.S., Medema, R.H., Lens, S.M. a & Kops, G.J.P.L. (2011). Aurora B potentiates Mps1 activation to ensure rapid checkpoint establishment at the onset of mitosis. *Nature communications*. 2 (May). p.p. 316.

Scaffidi, C., Fulda, S., Srinivasan, a, Friesen, C., Li, F., Tomaselli, K.J., Debatin, K.M., Krammer, P.H. & Peter, M.E. (1998). Two CD95 (APO-1/Fas) signalling pathways. *Embo J*. 17 (6). p.pp. 1675–1687.

Scaffidi, G., Schmitz, I., Zha, J., Korsmeyer, S.J., Krammer, P.H. & Peter, M.E. (1999). Differential modulation of apoptosis sensitivity in CD95 type I and type II cells. *Journal of Biological Chemistry*. 274 (32). p.pp. 22532–22538.

Schick, P.K., Kurica, K.B. & Chacko, G.K. (1976). Location of phosphatidylethanolamine and phosphatidylserine in the human platelet plasma membrane. *Journal of Clinical Investigation*. 57 (5). p.pp. 1221–1226.

Schuiki, I. & Daum, G. (2009). Phosphatidylserine decarboxylases, key enzymes of lipid metabolism. *IUBMB Life*. 61 (2). p.pp. 151–162.

Sengupta, S., Peterson, T.R. & Sabatini, D.M. (2010). Regulation of the mTOR Complex 1 Pathway by Nutrients, Growth Factors, and Stress. *Molecular Cell*. [Online]. 40 (2). p.pp. 310–322.

Shao, H., Huang, Y., Zhang, L., Yuan, K., Chu, Y., Dou, Z., Jin, C., Garcia-Barrio, M., Liu, X. & Yao, X. (2015). Spatiotemporal dynamics of Aurora B-PLK1-MCAK signaling axis orchestrates kinetochore bi-orientation and faithful chromosome segregation. *Scientific Reports*. [Online]. 5 (October 2014). p.p. 12204.

Shariff, K., Ghosal, S. & Matouschek, A. (2004). The force exerted by the membrane potential during protein import into the mitochondrial matrix. *Biophysical journal*. [Online]. 86 (6). p.pp. 3647–3652.

Sharpley, M.S., Shannon, R.J., Draghi, F. & Hirst, J. (2006). *Interactions between Phospholipids and NADH : Ubiquinone Oxidoreductase*. (Complex I). p.pp. 241–248.

Shen, H.-B. & Chou, K.-C. (2009). A top-down approach to enhance the power of predicting human protein subcellular localization: Hum-mPLoc 2.0. *Analytical biochemistry*. 394 (2). p.pp. 269–274.

Shiao, Y.J., Balcerzak, B. & Vance, J.E. (1998). A mitochondrial membrane protein is

required for translocation of phosphatidylserine from mitochondria-associated membranes to mitochondria. *The Biochemical journal*. 331 (Pt 1. p.pp. 217–223.

Shiao, Y.J., Lupo, G. & Vance, J.E. (1995). Evidence that phosphatidylserine is imported into mitochondria via a mitochondria-associated membrane and that the majority of mitochondrial phosphatidylethanolamine is derived from decarboxylation of phosphatidylserine. *The Journal of Biological Chemistry*. 270 (19). p.pp. 11190–11198.

Shin, S., Sung, B.J., Cho, Y.S., Kim, H.J., Ha, N.C., Hwang, J.I., Chung, C.W., Jung, Y.K. & Oh, B.H. (2001). An anti-apoptotic protein human survivin is a direct inhibitor of caspase-3 and -7. *Biochemistry*. 40 (4). p.pp. 1117–1123.

Shinzawa-Itoh, K., Aoyama, H., Muramoto, K., Terada, H., Kurauchi, T., Tadehara, Y., Yamasaki, A., Sugimura, T., Kurono, S., Tsujimoto, K., Mizushima, T., Yamashita, E., Tsukihara, T. & Yoshikawa, S. (2007). Structures and physiological roles of 13 integral lipids of bovine heart cytochrome c oxidase. *The EMBO journal*. 26 (6). p.pp. 1713–1725.

Shiozaki, E.N., Chai, J., Rigotti, D.J., Riedl, S.J., Li, P., Srinivasula, S.M., Alnemri, E.S., Fairman, R. & Shi, Y. (2003). Mechanism of XIAP-Mediated Inhibition of Caspase-9. *Molecular Cell*. 11. p.pp. 519–527.

Sideris, D.P., Petrakis, N., Katrakili, N., Mikropoulou, D., Gallo, A., Ciofi-Baffoni, S., Banci, L., Bertini, I. & Tokatlidis, K. (2009). A novel intermembrane space-targeting signal docks cysteines onto Mia40 during mitochondrial oxidative folding. *Journal of Cell Biology*. 187 (7). p.pp. 1007–1022.

Sigal, C.T., Zhou, W., Buser, C. a, McLaughlin, S. & Resh, M.D. (1994). Amino-terminal basic residues of Src mediate membrane binding through electrostatic interaction with acidic phospholipids. *Proceedings of the National Academy of Sciences of the United States of America*. 91 (25). p.pp. 12253–12257.

Signorell, A., Gluenz, E., Rettig, J., Schneider, A., Shaw, M.K., Gull, K. & Bütikofer, P. (2009). Perturbation of phosphatidylethanolamine synthesis affects mitochondrial morphology and cell-cycle progression in procyclic-form Trypanosoma brucei. *Molecular Microbiology*. 72 (4). p.pp. 1068–1079.

Signorell, A., Jelk, J., Rauch, M. & Bütikofer, P. (2008). Phosphatidylethanolamine is the precursor of the ethanolamine phosphoglycerol moiety bound to eukaryotic elongation factor 1A. *Journal of Biological Chemistry*. 283 (29). p.pp. 20320–20329.

Skoufias, D. a., Mollinari, C., Lacroix, F.B. & Margolis, R.L. (2000). Human survivin is a kinetochore-associated passenger protein. *Journal of Cell Biology*. 151 (7). p.pp. 1575–1581.

Small, I., Peeters, N., Legeai, F. & Lurin, C. (2004). Predotar: A tool for rapidly screening proteomes for N-terminal targeting sequences. *Proteomics*. 4 (6). p.pp. 1581–1590.

Song, Z., Yao, X. & Wu, M. (2003). Direct interaction between Survivin and Smac/DIABLO is essential for the anti-apoptotic activity of Survivin during Taxol-induced apoptosis. *Journal of Biological Chemistry*. 278 (25). p.pp. 23130–23140.

Srinivasula, S.M., Ahmad, M., Fernandes-Alnemri, T. & Alnemri, E.S. (1998). Autoactivation of procaspase-9 by Apaf-1-mediated oligomerization. *Molecular cell*. 1 (7). p.pp. 949–957.

Srinivasula, S.M. & Ashwell, J.D. (2008). IAPs: What's in a Name? *Molecular Cell*. 30 (2). p.pp. 123–135.

Stauber, R.H., Rabenhorst, U., Rekik, A., Engels, K., Bier, C. & Knauer, S.K. (2006). Nucleocytoplasmic shuttling and the biological activity of mouse survivin are regulated by an active nuclear export signal. *Traffic*. 7 (11). p.pp. 1461–1472.

Steenbergen, R., Nanowski, T.S., Beigneux, A., Kulinski, A., Young, S.G. & Vance, J.E. (2005). Disruption of the phosphatidylserine decarboxylase gene in mice causes embryonic lethality and mitochondrial defects. *Journal of Biological Chemistry*. 280 (48). p.pp. 40032–40040.

Stein, Y. & Stein, O. (1966). Metabolism of labeled lysolecithin, lysophosphatidyl ethanolamine and lecithin in the rat. *Biochimica et Biophysica Acta (BBA) - Lipids and Lipid Metabolism*. [Online]. 116 (1). p.pp. 95–107.

Stone, S.J. & Vance, J.E. (2000). Phosphatidylserine synthase-1 and -2 are localized to mitochondria-associated membranes. *Journal of Biological Chemistry*. 275 (44). p.pp. 34534–34540.

Sun, C., Cai, M., Gunasekera, a H., Meadows, R.P., Wang, H., Chen, J., Zhang, H., Wu, W., Xu, N., Ng, S.C. & Fesik, S.W. (1999). NMR structure and mutagenesis of the inhibitor-of-apoptosis protein XIAP. *Nature*. 401 (6755). p.pp. 818–822.

Sun, C., Nettesheim, D., Liu, Z. & Olejniczak, E.T. (2005). Solution structure of human survivin and its binding interface with Smac/Diablo. *Biochemistry*. 44 (1). p.pp. 11–17.

Sundler, R., Akesson, B. & Nilsson, A. (1974). Quantitative role of base exchange in phosphatidylethanolamine synthesis in isolated rat hepatocytes. *FEBS letters*. 43 (3). p.pp. 303–307.

Susin, S. a, Lorenzo, H.K., Zamzami, N., Marzo, I., Snow, B.E., Brothers, G.M., Mangion, J., Jacotot, E., Costantini, P., Loeffler, M., Larochette, N., Goodlett, D.R., Aebersold, R., Siderovski, D.P., Penninger, J.M. & Kroemer, G. (1999). Molecular characterization of mitochondrial apoptosis-inducing factor. *Nature*. 397 (6718). p.pp. 441–446.

Suzuki, Y., Imai, Y., Nakayama, H., Takahashi, K., Takio, K. & Takahashi, R. (2001). A serine protease, HtrA2, is released from the mitochondria and interacts with XIAP, inducing cell death. *Molecular Cell*. 8 (3). p.pp. 613–621.

Tamm, I., Wang, Y., Sausville, E., Scudiero, D. a., Vigna, N., Oltersdorf, T. & Reed, J.C. (1998). IAP-family protein Survivin inhibits caspase activity and apoptosis induced by Fas (CD95), bax, caspases, and anticancer drugs. *Cancer Research*.

58 (23). p.pp. 5315–5320.

Tanaka, T.U., Rachidi, N., Janke, C., Pereira, G., Galova, M., Schiebel, E., Stark, M.J.R. & Nasmyth, K. (2002). Evidence that the Ipl1-Sli15 (Aurora Kinase-INCENP) complex promotes chromosome bi-orientation by altering kinetochore-spindle pole connections. *Cell*. 108 (3). p.pp. 317–329.

Tartaglia, L. a., Ayres, T.M., Wong, G.H.W. & Goeddel, D. V. (1993). A novel domain within the 55 kd TNF receptor signals cell death. *Cell*. 74 (5). p.pp. 845–853.

Tasseva, G., Bai, H.D., Davidescu, M., Haromy, A., Michelakis, E. & Vance, J.E. (2013). Phosphatidylethanolamine deficiency in mammalian mitochondria impairs oxidative phosphorylation and alters mitochondrial morphology. *Journal of Biological Chemistry*. 288 (6). p.pp. 4158–4173.

Tietjen, G.T., Gong, Z., Chen, C.-H., Vargas, E., Crooks, J.E., Cao, K.D., Heffern, C.T.R., Henderson, J.M., Meron, M., Lin, B., Roux, B., Schlossman, M.L., Steck, T.L., Lee, K.Y.C. & Adams, E.J. (2014). Molecular mechanism for differential recognition of membrane phosphatidylserine by the immune regulatory receptor Tim4. *Proceedings of the National Academy of Sciences of the United States of America*. [Online]. 111 (15). p.pp. E1463–72.

Tijburg, L.B., Geelen, M.J. & Van Golde, L.M. (1989). Biosynthesis of phosphatidylethanolamine via the CDP-ethanolamine route is an important pathway in isolated rat hepatocytes. *Biochemical and biophysical research communications*. 160 (3). p.pp. 1275–1280.

Torrents, D., Suyama, M., Zdobnov, E. & Bork, P. (2003). *A Genome-Wide Survey of Human Pseudogenes A Genome-Wide Survey of Human Pseudogenes*. 7. p.pp. 2559–2567.

Trotter, P.J., Pedretti, J. & Voelker, D.R. (1993). Phosphatidylserine decarboxylase from Saccharomyces cerevisiae. Isolation of mutants, cloning of the gene, and creation of a null allele. *Journal of Biological Chemistry*. 268 (28). p.pp. 21416–21424.

Trotter, P.J., Pedretti, J., Yates, R. & Voelker, D.R. (1995). Phosphatidylserine decarboxylase 2 of Saccharomyces cerevisiae. Cloning and mapping of the gene, heterologous expression, and creation of the null allele. *The Journal of biological chemistry*. 270 (11). p.pp. 6071–6080.

Trotter, P.J. & Voelker, D.R. (1995). Identification of a non-mitochondrial phosphatidylserine decarboxylase activity (PSD2) in the yeast Saccharomyces cerevisiae. *The Journal of biological chemistry*. 270 (11). p.pp. 6062–6070.

Tsukahara, T., Tanno, Y. & Watanabe, Y. (2010). Phosphorylation of the CPC by Cdk1 promotes chromosome bi-orientation. *Nature*. [Online]. 467 (7316). p.pp. 719–723.

Uhlmann, F., Wernic, D., Poupart, M. a, Koonin, E. V & Nasmyth, K. (2000). Cleavage of cohesin by the CD clan protease separin triggers anaphase in yeast. *Cell*. 103 (3). p.pp. 375–386.

Uren, A.G., Wong, L., Pakusch, M., Fowler, K.J., Burrows, F.J., Vaux, D.L. & Choo,

K.H.A. (2000). Survivin and the inner centromere protein INCENP show similar cell-cycle localization and gene knockout phenotype. *Current Biology*. 10 (21). p.pp. 1319–1328.

Vance, D.E. (2014a). Phospholipid methylation in mammals: From biochemistry to physiological function. *Biochimica et Biophysica Acta - Biomembranes*. [Online]. 1838 (6). p.pp. 1477–1487.

Vance, J.E. (2014b). Phospholipid Synthesis and Transport in Mammalian Cells. *Traffic*. [Online]. 16 (1). p.pp. 1–18.

Vance, J.E. & Tasseva, G. (2013). Formation and function of phosphatidylserine and phosphatidylethanolamine in mammalian cells. *Biochimica et Biophysica Acta - Molecular and Cell Biology of Lipids*. [Online]. 1831 (3). p.pp. 543–554.

Varma, D. & Salmon, E.D. (2012). The KMN protein network–chief conductors of the kinetochore orchestra. *Journal of cell science*. [Online]. 125 (Pt 24). p.pp. 5927–36.

Verdecia, M. a, Huang, H., Dutil, E., Kaiser, D. a, Hunter, T. & Noel, J.P. (2000). Structure of the human anti-apoptotic protein survivin reveals a dimeric arrangement. *Nature structural biology*. 7 (7). p.pp. 602–608.

Verkleij, A.J., Leunissen-Bijvelt, J., de Kruijff, B., Hope, M. & Cullis, P.R. (1984). Non-bilayer structures in membrane fusion. *Ciba Foundation symposium*. 103. p.pp. 45–59.

Voelker, D.R. (1984). Phosphatidylserine functions as the major precursor of phosphatidylethanolamine in cultured BHK-21 cells. *Proceedings of the National Academy of Sciences of the United States of America*. 81 (9). p.pp. 2669–2673.

Vogtle, F.-N., Burkhart, J.M., Rao, S., Gerbeth, C., Hinrichs, J., Martinou, J.-C., Chacinska, A., Sickmann, A., Zahedi, R.P. & Meisinger, C. (2012). Intermembrane space proteome of yeast mitochondria. *Molecular & cellular proteomics : MCP*. 11 (12). p.pp. 1840–1852.

Vong, Q.P., Cao, K., Li, H.Y., Iglesias, P. a & Zheng, Y. (2005). Chromosome alignment and segregation regulated by ubiquitination of survivin. *Science*. 310 (5753). p.pp. 1499–1504.

van Vugt, M. a T.M. & Medema, R.H. (2005). Getting in and out of mitosis with Polo-like kinase-1. *Oncogene*. 24 (17). p.pp. 2844–2859.

Wall, N.R., O'Connor, D.S., Plescia, J., Pommier, Y. & Altieri, D.C. (2003). Suppression of survivin phosphorylation on Thr34 by flavopiridol enhances tumor cell apoptosis. *Cancer research*. 63 (1). p.pp. 230–235.

Wang, E., Ballister, E.R. & Lampson, M. a. (2011a). Aurora B dynamics at centromeres create a diffusion-based phosphorylation gradient. *Journal of Cell Biology*. 194 (4). p.pp. 539–549.

Wang, F., Dai, J., Daum, J.R., Niedzialkowska, E., Banerjee, B., Stukenberg, P.T., Gorbsky, G.J. & Higgins, J.M.G. (2010a). Histone H3 Thr-3 Phosphorylation by

Haspin Positions Aurora B at Centromeres in Mitosis. *Science* . [Online]. 330 (6001). p.pp. 231–235.

Wang, H., Holloway, M.P., Ma, L., Cooper, Z. a., Riolo, M., Samkari, A., Elenitoba-Johnson, K.S.J., Chin, Y.E. & Altura, R. a. (2010b). Acetylation directs survivin nuclear localization to repress STAT3 oncogenic activity. *Journal of Biological Chemistry*. 285 (46). p.pp. 36129–36137.

Wang, K. & Lin, B. (2013). Inhibitor of apoptosis proteins (IAPs) as regulatory factors of hepatic apoptosis. *Cellular Signalling*. [Online]. 25 (10). p.pp. 1970–1980.

Wang, Q., Chen, Z., Diao, X. & Huang, S. (2011b). Induction of autophagy-dependent apoptosis by the survivin suppressant YM155 in prostate cancer cells. *Cancer letters*. 302 (1). p.pp. 29–36.

Wang, Y.-F., Zhang, W., He, K.-F., Liu, B., Zhang, L., Zhang, W.-F., Kulkarni, A.B., Zhao, Y.-F. & Sun, Z.-J. (2014). Induction of autophagy-dependent cell death by the survivin suppressant YM155 in salivary adenoid cystic carcinoma. *Apoptosis*. [Online]. 19 (4). p.pp. 748–758.

Weckbecker, D., Longen, S., Riemer, J. & Herrmann, J.M. (2012). Atp23 biogenesis reveals a chaperone-like folding activity of Mia40 in the IMS of mitochondria. *The EMBO Journal*. [Online]. 31 (22). p.pp. 4348–4358.

Wei, M.C., Lindsten, T., Mootha, V.K., Weiler, S., Gross, A., Ashiya, M., Thompson, C.B. & Korsmeyer, S.J. (2000). tBID, a membrane-targeted death ligand, oligomerizes BAK to release cytochrome c. *Genes and Development*. 14 (16). p.pp. 2060–2071.

Wei, M.C., Zong, W.X., Cheng, E.H., Lindsten, T., Panoutsakopoulou, V., Ross, A.J., Roth, K.A., MacGregor, G.R., Thompson, C.B. & Korsmeyer, S.J. (2001). Proapoptotic BAX and BAK: a requisite gateway to mitochondrial dysfunction and death. *Science*. 292 (5517). p.pp. 727–730.

Wheatley, S.P., Barrett, R.M., Andrews, P.D., Medema, R.H., Morley, S.J., Swedlow, J.R. & Lens, S.M.A. (2007). Phosphorylation by aurora-B negatively regulates survivin function during mitosis. *Cell cycle*. 6 (10). p.pp. 1220–1230.

Wheatley, S.P., Carvalho, A., Vagnarelli, P. & Earnshaw, W.C. (2001a). INCENP is required for proper targeting of Survivin to the centromeres and the anaphase spindle during mitosis. *Current Biology*. 11 (11). p.pp. 886–890.

Wheatley, S.P., Henzing, A.J., Dodson, H., Khaled, W. & Earnshaw, W.C. (2004). Aurora-B Phosphorylation in Vitro Identifies a Residue of Survivin That Is Essential for Its Localization and Binding to Inner Centromere Protein (INCENP) in Vivo. *Journal of Biological Chemistry*. 279 (7). p.pp. 5655–5660.

Wheatley, S.P., Kandels-Lewis, S.E., Adams, R.R., Ainsztein, a M. & Earnshaw, W.C. (2001b). INCENP binds directly to tubulin and requires dynamic microtubules to target to the cleavage furrow. *Experimental cell research*. 262 (2). p.pp. 122–127.

Willis, S.N., Chen, L., Dewson, G., Wei, A., Naik, E., Fletcher, J.I., Adams, J.M. & Huang, D.C.S. (2005). Proapoptotic Bak is sequestered by Mcl-1 and Bcl-xL, but

not Bcl-2, until displaced by BH3-only proteins. *Genes and Development*. 19 (11). p.pp. 1294–1305.

Yamagishi, Y., Honda, T., Tanno, Y. & Watanabe, Y. (2010). Two Histone Marks Establish the Inner Centromere and Chromosome Bi-Orientation. *Science* . [Online]. 330 (6001). p.pp. 239–243.

Yamin, T.T., Ayala, J.M. & Miller, D.K. (1996). Activation of the native 45-kDa precursor form of interleukin-1-converting enzyme. *Journal of Biological Chemistry*. 271 (22). p.pp. 13273–13282.

Yan, Y. & Kang, B. (2011). The Role of Cardiolipin Remodeling in Mitochondrial Function and Human Diseases. *Journal of Molecular Biology Research*. 1 (1). p.pp. 1–11.

Yang, Q.H., Church-Hajduk, R., Ren, J., Newton, M.L. & Du, C. (2003). Omi/HtrA2 catalytic cleavage of inhibitor of apoptosis (IAP) irreversibly inactivates IAPs and facilitates caspase activity in apoptosis. *Genes and Development*. 17 (12). p.pp. 1487–1496.

Yang, Z. & Klionsky, D.J. (2010). Mammalian autophagy: Core molecular machinery and signaling regulation. *Current Opinion in Cell Biology*. [Online]. 22 (2). p.pp. 124–131.

Yano, M., Terada, K. & Mori, M. (2003). AIP is a mitochondrial import mediator that binds to both import receptor Tom20 and preproteins. *Journal of Cell Biology*. 163 (1). p.pp. 45–56.

Yasui, Y., Urano, T., Kawajiri, A., Nagata, K.I., Tatsuka, M., Saya, H., Furukawa, K., Takahashi, T., Izawa, I. & Inagaki, M. (2004). Autophosphorylation of a Newly Identified Site of Aurora-B Is Indispensable for Cytokinesis. *Journal of Biological Chemistry*. 279 (13). p.pp. 12997–13003.

Yin, X.M., Wang, K., Gross, a, Zhao, Y., Zinkel, S., Klocke, B., Roth, K. a & Korsmeyer, S.J. (1999). Bid-deficient mice are resistant to Fas-induced hepatocellular apoptosis. *Nature*. 400 (6747). p.pp. 886–891.

Young, J.C., Hoogenraad, N.J. & Hartl, F.U. (2003). Molecular chaperones Hsp90 and Hsp70 deliver preproteins to the mitochondrial import receptor Tom70. *Cell*. 112 (1). p.pp. 41–50.

Zborowski, J., Dygas, a. & Wojtczak, L. (1983). Phosphatidylserine decarboxylase is located on the external side of the inner mitochondrial membrane. *FEBS Letters*. 157 (1). p.pp. 179–182.

Zhang, M., Mileykovskaya, E. & Dowhan, W. (2005). Cardiolipin is essential for organization of complexes III and IV into a supercomplex in intact yeast mitochondria. *Journal of Biological Chemistry*. 280 (33). p.pp. 29403–29408.

Zhao, J., Tenev, T., Martins, L.M., Downward, J. & Lemoine, N.R. (2000). The ubiquitin-proteasome pathway regulates survivin degradation in a cell cycle-dependent manner. *Journal of Cell Science*. 4371. p.pp. 4363–4371.

Zhong, Y., Wang, Q.J., Li, X., Yan, Y., Backer, J.M., Chait, B.T., Heintz, N. & Yue, Z.

(2009). Distinct regulation of autophagic activity by Atg14L and Rubicon associated with Beclin 1-phosphatidylinositol-3-kinase complex. *Nature cell biology*. 11 (4). p.pp. 468–476.

Zick, M., Stroupe, C., Orr, A., Douville, D. & Wickner, W.T. (2014). Membranes linked by trans-SNARE complexes require lipids prone to non-bilayer structure for progression to fusion. *eLife*. [Online]. 3 (1). p.p. e01879.

8 APPENDIX

Cell lines

Name	Description
HeLa	Human cervix adenocarcinoma, ATCC CCL-2
HeLa GFP, Survivin GFP or Survivin$_{1-10}$-GFP	HeLa cells stably transfected with said GFP fusion proteins
HEK293T	Immortalized human embryonic kidney
MRC5	Human lung fibroblast
U2OS	Human bone osteosarcoma
RPE-1	hTERT-immortalized retinal pigment epithelium
EJ30	Human bladder carcinoma
SH5YSY	Human neuroblastoma

Bacterial (*E. coli*) strains

Strain	Genotype
DH5α	F'/endAl hsdR17 (r_K^- m_K^+) sup E44 thi-1 recA1 gyrA (Nal^R) relA1 (lacZYA-argF) U169 (80dlac(lacZ) M15)
XL-Blue 1	F´ ::Tn10 proA+B+ lacIq Δ(lacZ)M15/ recA1 endA1 gyrA96 (NalR) thi hsdR17 (rK– mK+) glnV44 relA1 lac
BL21 (DE3) pLysS	F- ompT gal dcm lon hsdSB(rB- mB-) λ(DE3) pLysS(cmR)
SG13009 (pREP4)	Nals Strs Rifs Thi- Lac- Ara- Gal+ Mtl- F- RecA+ Uvr+ Lon+ [pREP4 KanR]
T7 Express	fhuA2 lacZ::T7 gene1 [lon] ompT gal sulA11 R(mcr-73::miniTn10--TetS)2 [dcm] R(zgb-210::Tn10--TetS) endA1 Δ(mcrC-mrr)114::IS10
Rosetta-gami(DE3)pLysS	Δ(ara-leu)7697 ΔlacX74 ΔphoA PvuII phoR araD139 ahpC galE galK rpsL (DE3) F'[lac+ lacIq pro] gor522::Tn10 trxB pLysSRARE (CamR, StrR, TetR)

Vectors

Name	Antibiotic resistance	Description
pcDNA 3.1 (+)	Ampicillin	T7 promoter (used for in vitro translation), mammalian expression
pBlueScript (SK+)	Ampicillin	Used as a shuttle vector for subcloning with GFP tag
pCMV-Tag 1	Kanamycin	FLAG Tagging, Mammalian Expression
pGEX-4Ti	Ampicillin	GST Tagging, Bacterial expression
pQE-TriSystem His.Strep 1	Kanamycin	(8x)His Tagging, Parallel *E. coli* and mammalian-cell expression
pET-22b(+)	Ampicillin	(6x) His tagging, *E. coli* expression

Cloning primers

Survivin	Primer sequence
pCMV-Survivin FLAG	5'GTAGCGGCCGCATGGGTGCCCCGACGTTG 3'
	5' TTAGGATCCATCCATGGCAGCCAGCTGCTC 3
pCMV-FLAG Survivin	5'ACTTAGAGATCTTGGGTGCCCCGACGTTGCCC 3'
	5'GGTTGTAGATCTTCAATCCATG GCAGCCAGC 3'
Phosphatidylserine decarboxylase (PSD)	
pcDNA/pGEX-PSD iso1	5'GGTAGAATTC ATGGCGACGTCCGTGGGGC 3'
	5'GGGCTCGAGCTAGAGCGAGCCCAGGGC TTC 3'
pcDNA/pGEX-PSD iso2	5' GGGGAATTCATGATGTGTCAGTCAGAGGC 3'
pcDNA PSD iso1/2 S378A	5'GTTCAACCTGGGCGCCACCATCGTGCT 3'
	5'AGCACGATGGTGGCGCCCAGGTTGAAC 5'
pCMV PSD iso1 WT/S378A-Flag	5'ATAGCGGCCGCATGGCGACGTCCGT 3'
	5'TTAGGATCCGGAGAGCGAGCCCAGGG 3'
pQE-TriSystem PSD iso1-8xHis	5'TAACCATGGCGACGT CCGTGGGGCACC 3'
	5' GGATCTCGAGGAGCGAGCCCAGGGCTTCC 3'
Various	
Mitochondrial targeting signal	5'CTAAGAATTCATGTCCGTCCTGAC 3'
	5' GTCCGAATTCCAACGAATGGATCT 3'

siRNA oligonucleotides

siSurvivin (Custom Ambion)	5' UGUAGAGAUGCGGUGGUCCTT 3'
siPSD (ID 118780 Ambion)	Undisclosed

Antibodies

Primary antibodies

Antibody	Host species	Dilution	Source
Cytochrome c	Mouse	1:1000	Abcam (Gift from Dr. Lynn Bedford)
Cytochrome c oxidase subunit II	Mouse	1:1000	Abcam (Gift from Dr. Laura Conforti)
FLAG M2	Mouse	1:1000 (+IFF)	Sigma
GST	Rabbit	1:1000	Cell Signaling
GFP	Mouse	1:2000	Roche
Hsp60	Rabbit	1:5000	Gift from Dr. Lynn Bedford
INCENP	Rabbit	1:4000	Sigma
Penta His	Mouse	1:1000	Qiagen (Gift from Matthew Hardcastle)
PSD	Rabbit	1:500	Sigma (Atlas)
TBP	Rabbit	1:1000	Cell signaling
αTubulin (B512)	Mouse	1:1000	Sigma
Survivin	Rabbit	1:500	In house
VDAC	Rabbit	1:1000	Cell Signaling

Secondary antibodies

Antibody	Host species	Dilution	Source
Anti-Rabbit HRP conjugated	Goat	1:2000	Dako
Anti-Mouse HRP conjugated	Rabbit	1:2000	Dako
Anti-Mouse FITC conjugated	Rabbit	1:200	Vector

Buffers and solutions

GST fusion protein purification	
GST lysis buffer	10mM EDTA pH 7.5, 0.1% Triton X-100 in PBS
His fusion protein purification	
Mammalian His (MHis) lysis buffer	50mM NaH_2PO_4, 300mM NaCl, 10mM Imidazole, 0.5% Triton X-100
Mammalian His (MHis) wash buffer	50mM NaH_2PO_4, 300mM NaCl, 20mM Imidazole, 0.1% Triton X-100
Mammalian His (MHis) elution buffer	50mM NaH_2PO_4, 300mM NaCl, 50/100/150/200/250mM Imidazole, 0.1% Triton X-100
Mammalian cell lysis	
co-IP lysis buffer	50mM Tris HCl, pH 7.4 (at 4°C), 150mM NaCl, 1mM EDTA, 1% TRITON X-100

Experiments with mitochondria	
Isolation buffer	200mM Mannitol, 70mM Sucrose, 1mM EGTA, 10mM HEPES pH 7.5
Buffer A	10mM HEPES pH7.9, 1.5mM $MgCl_2$, 10mM KCl, 0.5mM DTT, 0.3% NP-40
Import buffer	20mM HEPES pH 7.5, 3% (w/v) fatty acid free BSA, 250mM Sucrose, 80mM KCl, 5mM $MgCl_2$
Swelling buffer	10mM HEPES pH 7.5
Control buffer	10mM HEPES pH 7.5, 250mM Sucrose
Density gradient	60,32,23 and 15% Sucrose in 1mM EDTA, 10mM MOPS pH 7.2
SDS-PAGE	
5x Sample buffer	250mM Tris-HCl pH 6.8, 5% (w/v) SDS, 50% (v/v) Glycerol, 500mM β-mercaptoethanol, 0.005% (w/v) Bromophenol Blue
2x Sample buffer (Non-reducing)	125mM Tris-HCl, pH 6.8, with 4% SDS, 20% (v/v) glycerol, 0.004% bromphenol blue
SDS running buffer	25mM Tris, 192 mM Glycine, 0.1% (w/v) SDS
12/15% SDS running gel	12/15% Acrylamide:Bisacrylamide (37.5:1), 375mM Tris-HCl pH 8.8, 0.1% (w/v) SDS, 0.1% (w/v) APS, 0.04 % TEMED
6% SDS stacking gel	6% Acrylamide:Bisacrylamide (37.5:1), 125mM Tris-HCl pH 6.8, 0.1% (w/v) SDS, 0.1% (w/v) APS, 0.08% TEMED
Western blot	
Transfer buffer	24mM Tris, 195mM Glycine, 0.05 % (w/v) SDS, 10% Methanol
PBS-T	137mM NaCl, 3mM KCl, 8mM Na_2HPO_4, 1.5mM KH_2PO_4 pH 7.3, 0.1% Tween 20
Coomassie stain	40% Methanol, 10% Glacial Acetic Acid, 0.07% (w/v) Coomassie R-250
Coomassie destain	20% Methanol, 7% Glacial Acetic Acid
Indirect Immunofluorescence	
Blocking buffer/ Antibody dilution solution	1%BSA in PBS
DNA gel electrophoresis	
5x DNA loading dye	0.25% (w/v) Bromophenol Blue, 0.25% (w/v) Xylene cyanol and 15% (w/v) Ficoll R 400
1x TBE buffer	89mM Trizma, 82mM Boric acid, 2.3mM EDTA
PSD conversion assay	
Reaction buffer	50mM Tris pH7.4 (at 20 °C) , 0.1% Triton X-100
Reaction termination	1M KCl, 0.2M H_3PO_4
Lipid quantitation	
Malachite colour reagent	15:5:1 0.2% Malachite green: 4% ammonium heptamolybdate in 5M HCl: 0.5% Tween20

ABBREVIATIONS

AIF	Apoptosis-Inducing Factor
AIP	Aryl hydrocarbon receptor-Interacting Protein
AMPK	AMP-activated Protein Kinase
Apaf-1	Apoptotic protease activating factor 1
APC/C	Anaphase Promoting Complex/Cyclosome
Atg	Autophagy-related genes
BH domain	BCL-2 Homology domain
BIR domain	Baculovirus Inhibitor of apoptosis Repeat domain
CARD	Caspase Activation and Recruitment Domain
CBP	CREB-binding protein
CCT	Phosphocholine Cytidylyltransferase
CDE	Cell-cycle Dependent Element
Cdk1	Cyclin-dependent kinase 1
CDP	Cytidine diphosphate
CDP-DAG	Cytidine diphosphate-diacyglycerol
CHO	Chinese Hamster Ovary
CHR	Cell-cycle gene Homology Region
cIAP	Cellular Inhibitor of Apoptosis Protein
CL	Cardiolipin
CK	Choline Kinase
CK2	Casein Kinase 2
CPC	Chromosomal Passenger Complex
CPP	Chromosomal Passenger Protein
CPT	CDP-choline:1,2-diacylglycerol cholinephosphotransferase
CT	CTP:phosphocholine cytidylyltransferase
CV	Column Volume

DAG	Diacylglycerol
DD	Death Domain
DED	Death Effector Domain
DISC	Death-Inducing Signalling Complex
DMA	Dimethylenastron
DMEM	Dulbecco's Modified Eagle's Medium
EK	Ethanolamine Kinase
EPT	CDP-ethanolamine:1,2-diacylglycerol ethanolaminephosphotransferase
ER	Endoplasmic Reticulum
ET	CTP-phosphoethanolamine cytidylyltransferase
ETC	Electron Transport Chain
G1 phase	Gap 1 phase
G2 phase	Gap 2 phase
GPI	Glycosylphosphatidylinositol
H3	Histone 3
HBXIP	Hepatitis B X-Interacting Protein
HDAC	Histone Deacetylase
HP1	Heterochromatin Protein 1
IAP	Inhibitor of Apoptosis Protein
ILP-2	IAP-Like Protein 2
IM	Inner Membrane sorting sequence
IMM	Inner Mitochondrial Membrane
IMP	Inner Membrane Peptidase
IMS	Intermembrane Space
ITS	IMS-Targeting Signal
IVT	*in Vitro* Translation
LRR domain	Leucine-Rich Repeat domain
M phase	Mitosis phase

MAM	Mitochondria-Associated Membranes
MCC	Mitotic Checkpoint Complex
mHsp70	matrix Heat shock protein 70
MIP	Mitochondrial Intermediate Peptidase
MISS	Mitochondrial Intermembrane Space Sorting
MOMP	Mitochondrial Outer Membrane Permeabilization
MPP	Matrix resident Processing Peptidases
MPT	Mitochondrial Permeability Transition
mTORC1	mammalian-Target Of Rapamycin Complex 1
MSF	Mitochondrial import Stimulation Factor
MTS	Mitochondrial Targeting Signal
NAIP	Neuronal Apoptosis Inhibitory Protein
NB	Neuroblastoma
NBD	7-Nitrobenz-2-oxa-1,3-diazol-4-yl
NES	Nuclear Export Sequence
NOD	Nucleotide-binding and Oligomerization Domain
OD	Optical Density
OMM	Outer Mitochondrial Membrane
PA	Phosphatidic Acid
PAM	Presequence translocase-Associated protein import Motor
PAP-1	Phosphatidic Acid Phosphohydrolase -1
PAS	Phagophore Assembly Site/Pre-Autophagosomal Structure
PBF	Presequence Binding Factor
PC	Phosphatidylcholine
PCD	Programmed Cell Death
PCR	Polymerase Chain Reaction
PE	Phosphatidylethanolamine
PG	Phosphatidylglycerol

PI	Phosphatidylinositol
P_i	Inorganic Phosphate
PI3K	Phosphatidylinositol 3-Kinase
PI3P	Phosphatidylinositol 3-Phosphate
PIP(3)	Phosphatidylinositol-3,4,5-trisphosphate
PKB	Protein Kinase B
Plk1	Polo-like kinase 1
PS	Phosphatidylcholine
PSD	Phosphatidylserine Decarboxylase
PSS1-2	PS Synthase-1 and 2
RT-PCR	Reverse transcription polymerase chain reaction
S phase	Synthesis phase
SAC	Spindle Assembly Checkpoint
SAM	Sorting and Assembly Machinery complex
Sgo2	Shugoshin2
SKA complex	Spindle and Kinetochore-Associated complex
SCF	Skp1_Cul1_F-box
SM	Sphingomyelin
TIM	Translocase of the mitochondrial inner membrane
TLC	Thin layer chromatography
TNF	Tumour Necrosis Factor
TNFR1-2	Tumour Necrosis Factor Receptor 1 and 2
TOM	Translocase of the mitochondrial Outer Membrane
TRADD	TNFR-Associated Death Domain protein
UBC enzyme domain	Ubiquitin Conjugating enzyme domain
ULK1	Unc-51-Like Kinase 1
UVC	Ultraviolet radiation
VMP1	Vacuole Membrane Protein 1

Vps34	Vacuolar protein sorting 34
XIAP	X-linked Inhibitor of Apoptosis